Carla Alexandra dos Santos Figueira Bento

WHAT HIF?

A NEW BREATH FOR CELL DYSFUNCTION IN DIABETES

Universidade de Coimbra
2009

Dissertação apresentada à Faculdade de Medicina da Universidade de Coimbra para prestação de provas de Doutoramento em Ciências Biomédicas

O trabalho apresentado nesta tese foi realizado no Centro de Oftalmologia e Ciências da Visão, Instituto Biomédico de Investigação da Luz e Imagem (IBILI) da Faculdade de Medicina da Universidade de Coimbra, sob a orientação do Doutor Paulo de Carvalho Pereira, ao abrigo da bolsa de Doutoramento SFRH/BD/15229/2004 (Fundação para a Ciência e a Tecnologia - FCT), no âmbito do Programa Doutoral em Biologia Experimental e Biomedicina (BEB) do Centro de Neurociências e Biologia Celular (CNC) da Universidade de Coimbra. Trabalhos complementares de Doutoramento foram realizados no "Oncology, Membrane Traffic and Signalling Group of the Physiology Department of the School of Biomedical Sciences, University of Liverpool, UK".

Agradecimentos / Acknowledgements

Paulo, pelo apoio, orientação, discussão aberta de ideias, companheirismo, confidencialidade na hora de algumas lágrimas, *horas felizes* e inebriantes, capacidade invulgar de expressão e de ensinamento, um grande Obrigada. O Paulo fez parte de um momento que é e será uma fonte de preparação e referência para a vida.

Agradeço à Fundação para a Ciência e a Tecnologia (FCT) e ao Programa Doutoral em Biologia Experimental e Biomedicina (BEB) do Centro de Neurociências e Biologia Celular (CNC) da Universidade de Coimbra pelo financiamento e pela oportunidade, que me foi dada, em fazer parte de um programa de doutoramento de elevado mérito científico.

Sylvie and Michael thank you for promptly accepting me in your lab, for the help, enthusiasm and guidance.

Alex, Ana, Carla Lopes, Carla Marques, Henrique, Jas, João, Rosa, Sandra, Steve e Zé, o que não falta no nosso quotidiano são momentos de partilha, admiração, amizade, compreensão, ajuda, alento e respeito mútuos, os quais tenho apenas de vos agradecer, profundamente. Obrigada a todos! Esta tese também é vossa.

A todos os outros colegas e amigos de laboratório e piso, Alda, Andreia, Áurea, Celita, Eliana, Ermelindo, Filipa Baptista, Filipa Marques, Francisco, Hugo, Joana Galvão, Joana Gaspar, Joana Liberal, Murat, Paulo Matafome e Raquel um grande obrigada, por me terem ajudado em tantas pequenas/grandes coisas nestes últimos anos.

À voz da razão, ao génio da paciência, ao amigo que nunca falta, ao coração que nunca pára, à sabedoria que nunca esgota e à inteligência que tanto me fascina, um obrigada imenso. Obrigada por me fazeres sentir sempre tão especial!

Du, agradeço a tua amizade incondicional, ternura e dedicação. Contigo, sei que tenho sempre alguém com quem contar. Com grande admiração e amizade… *1, 2, 3… Smile! Light up your face with gladness!*

Mãe e Pai, obrigada por tudo! Obrigada por me fazerem sentir sempre próxima, mesmo que longe. Por nunca termos abdicado dos nossos breves minutos diários, mas que concentram tudo o que uma vida tem. Sem vocês, esta meta teria sido impossível de alcançar. Obrigada por sempre me ouvirem, ajudarem e terem uma palavra de incentivo e sensatez para me dar. Espero nunca vos desapontar.

The results presented in this thesis and obtained in the scope of the SFRH/BD/15229/2004 PhD fellowship (FCT) are under submission or in preparation of manuscripts for future submission to international peer-review scientific journals:

Carla Bento, Rosa Fernandes, José Ramalho, Carla Marques, Fu Shang, Allen Taylor, Paulo Pereira. *The chaperone-dependent ubiquitin ligase CHIP targets HIF-1α for degradation in the presence of methylglyoxal.* (Manuscript under review)

Carla Bento, Filipa Marques, Rosa Fernandes, Paulo Pereira. *Methylglyoxal disrupts the ubiquitin-proteasome system and critical components of the protein quality control.* (Manuscript under review)

Carla Bento, Rosa Fernandes, Raquel Seiça, Paulo Pereira. *Methylglyoxal promotes endothelial dysfunction by disrupting the balance between VEGF and Ang-2.* (Manuscript submitted)

Han Liu, Carla Bento, Monica Faronato, Sebastian Hayes, Sara Cadeco, Michael Clague, Sylvie Urbe. *USP21, a centrosome and microtubule associated deubiquitinase, controls microtubule nucleation.* (Manuscript under preparation)

Cristina Sena, Carla Bento, Paulo Pereira, Raquel Seiça. *Diabetes mellitus: new challenges and innovative therapies*. ("The EPMA Journal" *In press*)

Note: The data presented in this dissertation is formatted according to the style of the journal where the papers are submitted for publication, with minor modifications.

Table of contents

Index of Figures

Index of Tables

Abbreviations

AGEs	Advanced Glycation End products
Ang-2	Angiopoietin-2
ANOVA	Analysis of Variance
AR	Aldose Reductase
ARD1	Arrest Defective-1 protein
ATP	Adenosine Triphosphate
bHLH/PAS	basic helix-loop-helix/Per-Arnt-Sim
BrdU	5-bromo-2'-deoxyuridine
cDNA	complementary DNA
CBP	CREB-Binding Protein
CHIP	Carboxy terminus of Hsp70-Interacting Protein
CMA	Nω-carboxymethylarginine
CML	Nε-carboxymethyllysine
CP	Core Particle
CREB	cAMP Response Element Binding
C-TAD	C-terminal Transactivation Domain
Cul2	Cullin 2
DAG	Diacylglycerol
DDB	1,2-diamino-4,5-dimethoxybenzene
DMEM	Dulbecco's Modified Eagle Medium
DMSO	Dimethyl Sulfoxide
DNA	Deoxyribonucleic Acid
DNPH	2,4-dinitrophenylhydrazine
DR	Diabetic Retinopathy
DTT	Dithiothreitol
DUB	Deubiquitinating Enzyme
E1	Ubiquitin-Activating Enzyme
E2	Ubiquitin-Conjugating Enzyme
E3	Ubiquitin-Protein Ligase
EB	Ethidium bromide
EDTA	Ethylenediaminetetraacetic Acid
EGFR	Epidermal Growth Factor Receptor
EGTA	Ethylene Glycol Tetraacetic Acid
ELISA	Enzyme-Linked Immunosorbent Assay
EPC	Endothelial Progenitor Cell

F6P	Fructose-6-Phosphate
$FADH_2$	Reduced Flavin Adenine Dinocluotide
FIH-1	Factor-Inhibiting HIF-1
FBS	Fetal Bovine Serum
G3P	Glyceraldehyde-3-Phosphate
GADPH	Glyceraldehyde-3-Phosphate Dehydrogenase
GCL	Ganglion Cell Layer
GFP	Green Fluorescent Protein
GK	Goto-Kakizaki
GLO I	Glyoxalase I
GR	Glucocorticoid Receptor
GSH	Reduced Glutathione
GSSH	Oxidized Glutathione
GST	Glutathione-S-Transferase
HAF	Hypoxia-Associated Factor
HDAC	Histone Deacetylase
HDACI	Histone Deacetylase Inhibitor
HECT	Homologous to the E6-AP Carboxyl Terminus
HIF	Hypoxia-Inducible Factor
HPLC	High-Performance Liquid Chromatography
HRE	Hypoxia-Responsive Element
HRP	Horseradish Peroxidase Enzyme
HSF-1	Heat-Shock Factor-1
HSP	Heat-Shock Protein
IGF1-R	Insulin-like Growth Factor 1-Receptor
IgG	Immunoglobulin G
IM	Intramuscular
INL	Inner Nuclear Layer
IOD	Iodoacetamide
IPAS	Inhibitory PAS Domain Protein
MAPK	Mitogen-Activated Protein Kinase
Mdm2	Murine double minute 2
MCA	Methylcoumarinyl-7-Amide
MG-H1	Nδ-(5-hydro-5-methyl-4-imidazolon-2-yl)-ornithine
MGO	Methylglyoxal
mSin3A	mammalian Sin3 homolog A
MTT	3-(4,5-dimethylthiazol-2-yl)-2,5-diphenyltetrazolium bromide
NADH	Nicotinamide Adenine Dinucleotide

NADP	Nicotinamide Adenine Dinucleotide Phosphate
NF-κB	Nuclear Factor-κB
NLS	Nuclear Localization Signal
ODD	Oxygen-Dependent Degradation Domain
2-OG	2-Oxoglutarate
OPL	Outer Plexiform Layer
P4H-TM	Prolyl 4-Hydroxylase, Transmembrane
PBS	Phosphate-Buffered Saline
PCR	Polymerase Chain Reaction
PDK	Pyruvate Dehydrogenase Kinase
PHD	Prolyl Hydroxylase Domain
PI3K	Phosphoinositol 3-Kinase
PKC	Protein Kinase C
PMSF	Phenylmethanesulphonylfluoride
PPi	Pyrophosphate
PVDF	Polyvinylidene Fluoride
RBX	RING-Box protein
RING	Really Interesting New Gene
iRNA	interference RNA
mRNA	messenger RNA
shRNA	short-hairpin RNA
RNA	Ribonucleic acid
RP	Regulatory Particle
RPE	Retinal Pigment Epithelium
RT	Reverse Transcriptase
RT-PCR	Real time-PCR
SDS	Sodium Dodecyl Sulfate
SDS-PAGE	SDS-Polyacrylamide Gel Electrophoresis
STZ	Streptozotocin
STUB-1	STIP1 homology and U-Box containing Protein-1
SUMO	Small Ubiquitin-related Modifier
TCA	Trycarboxylic Acid Cycle
TFA	Trifluoroacetic Acid
TGF	Transforming Growth Factor
TMB	Tetramethylbenzidine
TPR	Tetratricopeptide
UB	Ubiquitin
UBC	Ubiquitin-Conjugating enzyme

UBL	Ubiquitin-Like protein
UDP	Uridine Diphosphate
UPS	Ubiquitin-Proteasome System
UPP	Ubiquitin-Proteasome Pathway
USP	Ubiquitin Specific Protease
VDU	VHL-Interacting Deubiquitinating Enzyme
VBC	VHL-Elongin B-Elongin C complex
VEGF	Vascular Endothelial Growth Factor
VEGFR	Vascular Endothelial Growth Factor Receptor
VHL	Von Hippel Lindau
VWF	Von Willebrand Factor
WB	Western Blot
WHO	World Health Organization

RESUMO

Resumo

A disfunção vascular é uma das principais características da diabetes, contribuindo para o desenvolvimento de uma variedade de complicações, como retinopatia, nefropatia e doenças cardiovasculares, e está, em larga medida, associada a alterações na resposta celular e tecidular a situações de isquemia.

A resposta celular face a situações de isquemia é regulada, principalmente, pelo factor de transcrição HIF-1 (*hypoxia inducible factor-1*). Este factor é um heterodímero composto por uma isoforma nuclear estável, o HIF-1β, e uma forma citosólica lábil, o HIF-1α. Em condições de normoxia, dois resíduos de prolina presentes no HIF-1α (P402 e P564) são hidroxilados, o que permite o seu reconhecimento por uma ligase de ubiquitina, designada por VHL (Von Hippel Lindau). Esta interacção induz poliubiquitinação do HIF-1α e subsequente degradação pelo proteassoma. Em condições de hipoxia, o HIF-1α não é hidroxilado e, como consequência, não é degradado, acumulando-se no núcleo, onde activa mais de 70 genes envolvidos na resposta celular à hipoxia.

Alguns estudos recentes sugerem que os níveis elevados de glicose na diabetes comprometem a estabilidade e actividade do HIF-1α. Os mecanismos moleculares associados à destabilização deste factor de transcrição, em condições de hiperglicemia, são ainda desconhecidos. No entanto, este trabalho mostra que níveis elevados de glicose conduzem a um aumento da produção e acumulação intracelular de metilglioxal (MGO) que, por sua vez, induz uma rápida degradação do HIF-1α, em condições de hipoxia (capítulo 4). Os resultados obtidos mostram que essa degradação não envolve a hidroxilação das prolinas P402/P564, nem o recrutamento da proteína VHL. Neste trabalho é identificada a CHIP (*carboxy terminus of Hsp70-interacting protein*) como sendo a ligase de ubiquitina envolvida no processo de degradação do HIF-1α na presença de MGO. Os resultados mostram que o MGO aumenta a interacção do HIF-1α com os chaperones moleculares Hsp40/70, que por sua vez induzem recrutamento da CHIP, que poliubiquitina e promove degradação do HIF-1α pelo proteassoma. Neste trabalho, demonstra-se ainda que a degradação do HIF-1α é inibida pela sobreexpressão de glioxalase I (GLO I), a enzima envolvida na destoxificação do MGO nas células. As implicações da degradação do HIF-1α incluem uma diminuição acentuada da actividade de transcrição do HIF-1 e da expressão de VEGF (*vascular endothelial growth factor*), um gene alvo do HIF-1 crucial na adaptação celular e tecidular a condições de baixa pressão de O_2.

Dados independentes mostram que o MGO se pode ligar ao co-repressor mSin3A (*mammalian Sin3 homolog A*), levando a um aumento da expressão de Ang-2 (*Angiopoietin-2*). Alguns estudos envolvendo modelos de tumores sólidos, demonstraram que a Ang-2 é um factor de crescimento que induz destabilização dos capilares e vasos sanguíneos, levando à sua regressão na ausência de factores pró-angiogénicos, como o VEGF. Tendo como base esses estudos, este trabalho mostra que o aumento da produção de Ang-2 e a diminuição dos níveis de

VEGF, ambas induzidas pelo MGO, levam a um desequilíbrio da relação VEGF/Ang-2 secretada pelas células do epitélio pigmentado da retina para o meio extracelular. Os resultados obtidos mostram que este desequilíbrio induz apoptose e inibe a proliferação de células endoteliais da retina (capítulo 5), duas características importantes das complicações vasculares da diabetes e que podem, pelo menos em parte, explicar a regressão vascular e as complicações microvasculares associadas à doença.

Uma outra característica fisiopatológica da diabetes induzida pelo MGO é a modificação de proteínas por processos de glicação e oxidação. Alguns estudos parecem indicar que o MGO pode comprometer os mecanismos de controlo de qualidade proteica, levando à acumulação de proteínas obsoletas e, potencialmente, tóxicas na célula. No entanto, os mecanismos moleculares subjacentes aos efeitos do MGO na via da ubiquitina-proteassoma e na estabilidade de chaperones moleculares, envolvidos no controlo de qualidade proteica, continuam ainda por esclarecer. Neste trabalho, mostra-se que o MGO compromete a actividade da via da ubiquitina-proteassoma e induz alteração do eixo CHIP/chaperones moleculares, o que compromete o controlo de qualidade proteico. Essas alterações são acompanhadas por uma acumulação de proteínas modificadas e diminuição da viabilidade celular, o que pode contribuir para o desenvolvimento de algumas alterações patológicas associadas à diabetes e que se caracterizam pela acumulação de proteínas obsoletas e potencialmente tóxicas para a célula. No entanto, o stress celular e algumas das alterações induzidas pelo MGO parecem ser parcialmente compensadas pela activação do factor de transcrição Hsf-1 (*heat-shock factor*-1), crucial na resposta e sobrevivência celular em situações de stress (capítulo 6).

Em resumo, este trabalho identifica dois novos mecanismos moleculares que podem contribuir para uma melhor compreensão de duas das principais características fisiopatológicas da diabetes: a perda de resposta celular à hipoxia e a acumulação de proteínas modificadas nas células. Este estudo cria, ainda, as condições para o desenvolvimento de novas estratégias de prevenção e terapia das complicações celulares associadas à diabetes, baseadas na entrega direccionada de material genético, através de vectores adenovirais, para silenciamento da CHIP ou sobreexpressão da GLO I.

SUMMARY

Summary

Vascular dysfunction is a main feature of diabetes, contributing to the development of a variety of complications, such as retinopathy, nephropathy and cardiovascular diseases. Diabetes-related vascular complications can be caused by micro and macroangiopathy, display a significant inflammatory and oxidative stress component and are, to a large extent, associated with deregulation of cell and tissue response to ischemia.

Cell proliferation under hypoxia is, primarily, regulated by the transcription factor hypoxia-inducible factor-1 (HIF-1). HIF-1 is a heterodimer that consists of a stable nuclear isoform HIF-1β and a cytosolic labile isoform HIF-1α. Under normoxia, two proline residues on HIF-1α (P402/P564) are hydroxylated. This leads to recruitment of the ubiquitin ligase von Hippel Lindau protein (pVHL), which induces HIF-1α polyubiquitination and its subsequent degradation by the proteasome. Under hypoxia, HIF-1α is neither hydroxylated nor degraded and accumulates in the nucleus, where it dimerizes with HIF-1β and activates the transcription of more than 70 genes involved in the cell response to hypoxia.

Several data from the literature suggest that regulation of HIF-1α stability and activity may be impaired in diabetes and that hyperglycaemia is likely to be the leading cause of such deregulation. The molecular mechanisms associated with HIF-1α destabilization under high glucose remain elusive. However, in this work it was found that high glucose leads to increased production of methylglyoxal (MGO) by the cells and that increased levels of MGO are able to induce a rapid and dramatic proteasome-dependent degradation of HIF-1α, even under hypoxic conditions (chapter 4). Significantly, data indicates that this degradation does not require the recruitment of pVHL protein nor does it require hydroxylation of the proline residues P402/P564 on HIF-1α. More importantly, carboxy terminus of Hsp70-interacting protein (CHIP) was identified as the E3 ligase that ubiquitinates HIF-1α in the presence of MGO. Data shows that increased association of Hsp40/70 with HIF-1α induces CHIP recruitment, which promotes polyubiquitination and subsequent degradation of HIF-1α. Moreover, MGO-induced degradation of HIF-1α can be prevented by overexpression of glyoxalase I (GLO I), which is the rate-limiting enzyme of MGO catabolism and responsible for the MGO detoxification in cells. Consistently, MGO-induced destabilization of HIF-1α leads to a dramatic decrease both in HIF-1 transcriptional activity and expression of vascular endothelial growth factor (VEGF), a target gene of HIF-1 that is crucial for the cellular adaptation to low oxygen levels.

Recently, independent data further indicates that MGO can bind and modify the co-repressor mammalian Sin3 homolog A (mSin3A), leading to increased expression of angiopoietin-2 (Ang-2). Based on models of solid tumours, Ang-2 is known to provide a key destabilizing signal for vessels, leading to regression in the absence of pro-angiogenic factors, such as VEGF. Indeed, data of this thesis show that increased production of Ang-2 and decreased levels of VEGF, induced by MGO, lead to an imbalance on the VEGF/Ang-2 ratio secreted by retinal pigment epithelium

cells. This imbalance was shown to induce apoptosis and decreased proliferation of retinal endothelial cells (chapter 5), which are cardinal features of diabetes and are likely to be responsible for the formation of acellular capillaries and microvascular abnormalities in diabetes.

Increased modification of proteins by MGO is another main feature of diabetes. MGO is likely to account for impairment of the protein quality control, leading to accumulation of non-functional, potentially toxic proteins. However, the effect of MGO in the function of the ubiquitin-proteasome system and on molecular chaperones, involved in the protein quality control, remains elusive. In this work it is provided evidence that MGO may exert noxious effects in cells by impairing the ubiquitin-proteasome system, as well as the CHIP/chaperones-mediated protein quality control axis. Consistently, this impairment is followed by the accumulation of obsolete proteins and cell injury, which are cardinal features of many diabetic complications. However, some of these MGO-induced changes appear to elicit a response from the heat shock factor-1 (Hsf-1) system and seem to be partially compensated by the activation of this transcription factor, which is a critical player in the cell adaptation and survival under stress conditions (chapter 6).

In summary, this work highlights two different and new molecular mechanisms that help to elucidate and integrate in a common model two main features of diabetes: the loss of cell response to hypoxia and the accumulation of obsolete and toxic proteins in affected cells. Moreover, this work helps to envision new strategies for prevention and therapy of vascular diseases in diabetes, based on the delivery of genetic material through adenoviral vectors, for example to silence CHIP or overexpress GLO I.

CHAPTER 1

Chapter 1. Introduction

1.1 Diabetes

Diabetes mellitus, often referred simply as diabetes, is a syndrome of dysfunctional metabolism, resulting in hyperglycaemia or abnormal high blood glucose levels. When glucose is ingested and reaches bloodstream, pancreas should produce the right amount of insulin that will induce most of the body cells to take up glucose from the blood. However, diabetes is characterized by a disturbance on the insulin secretion and/or action in the body. Basically, diabetes develops due to a diminished production of insulin in the β-cells of the islets of Langerhans located in the pancreas (type 1 diabetes), resistance to the insulin action (type 2 diabetes) or the combination of both (Rother, 2007). In patients with type 1, diabetes is due primarily to an autoimmune reaction that mediates destruction of pancreatic islet β-cells, resulting in dramatic insulin deficiency. Its frequency is very low in comparison with type 2 diabetes. Indeed, type 2 diabetes comprises 90% of people with diabetes around the world, and is mainly the result of obesity, physical inactivity, high blood pressure and elevated cholesterol levels.

The World Health Organization (WHO) estimates that more than 180 million people worldwide have diabetes and this number is likely to more than double by 2030. Diabetes is known to cause about 5% of all deaths globally each year, meaning that approximately 2.9 million deaths *per year* are attributed to diabetes.

Acute complications (hypoglycaemia, ketoacidosis or nonketotic hyperosmolar coma) may occur if the disease is not adequately controlled. Serious long-term complications include cardiovascular disease, chronic renal failure, retinal damage, nerve damage and vascular damage, which may cause erectile dysfunction and poor wound healing. Poor healing of wounds, particularly of the feet, can lead to gangrene, and possibly to amputation. According to WHO statistics, diabetic retinopathy (DR) affects up to 80% of all patients who have had diabetes for 10 years or more, while 50% of patients further develop diabetic neuropathy. Moreover, 10-20% of people with diabetes die of kidney failure and 50% of diabetic patients die of cardiovascular disease (heart disease or stroke).

Although the intensive research on the field, the molecular mechanisms that underlie cell and tissue dysfunction on diabetes remain largely unclear. However, hyperglycaemia appears to be the most critical factor in the aetiology of diabetes. The major complications of diabetes are associated with macro and microangiopathies and high levels of glucose appear to be a driving force in the development of such vascular complications. Multiple biochemical pathways have been proposed to explain the pathogenesis of diabetes, all starting initially from hyperglycaemia. These include increased polyol pathway, activation of protein kinase C (PKC), increased hexosamine pathway flux and increased advanced glycation end products (AGEs) formation (Brownlee, 2005).

1.1.1 Polyol pathway

The polyol pathway is characterized by the NADPH-dependent enzymatic reduction of glucose to an acyclic polyol, such as sorbitol, by the aldose reductase (AR) enzyme. AR is characterized by high enzymatic capacity, but low affinity (high Km) with respect to glucose; therefore, at high glucose concentrations, the enzyme can be activated, resulting in intracellular accumulation of sorbitol, with a concomitant decrease in the NADPH levels.

Activation of AR in hyperglycaemia has a number of detrimental effects, including sorbitol-induced osmotic stress, decreased cytosolic NADPH levels and increased reduction of NAD^+ to NADH, the last one being due to increased conversion of sorbitol to fructose by the sorbitol dehydrogenase (SDH) enzyme. Consumption of NADPH depletes the intracellular reducing potential leading to accumulation of oxidized glutathione (GSSG) and decreased levels of reduced glutathione (GSH) (Brownlee, 2001), which is an important cellular antioxidant. On the other hand, increased levels of NADH inhibits the activity of the enzyme glyceraldehyde-3-phosphate dehydrogenase (GADPH), thus leading to an accumulation of triose phosphate (Williamson et al, 1993), which in turn may lead to increased production of methylglyoxal (MGO) and diacylglycerol (DAG). Both MGO and DAG may induce typical diabetic cell damage.

1.1.2 Protein kinase C activation

Accumulation of intracellular glucose stimulates glycolysis, leading to accumulation of glycolytic intermediates, including glyceraldehyde-3-phosphate (G3P). Accumulation of G3P stimulates synthesis of DAG, which in turn activates PKC, through phosphorylation by the phosphoinositide-dependent kinase 1. Through a variety of direct and indirect mechanisms, activation of PKC contributes to the pathophysiology of several diabetic complications, such as DR (Donnelly et al, 2004). PKC mediates changes in endothelial permeability, blood flow, leukocyte adhesion to endothelial cells, capillary tonus and in the response to angiogenic growth factors (Huang & Yuan, 1997; Park et al, 2000; Williams et al, 1997). Indeed, transcription of *vegf* (vascular endothelial growth factor) gene is, in part, induced by PKC activation (Aiello et al, 1995; Williams et al, 1997).

1.1.3 Hexosamine pathway

The inhibition of the GAPDH activity, by increased levels of NADH and hyperglycaemia-induced mitochondrial superoxide overproduction, activates the hexosamine pathway by diverting the upstream metabolite fructose-6-phosphate (F6P) from glycolysis to glucosamine formation (Du et al, 2000). Through the hexosamine pathway, it is catalyzed the conversion of F6P to glucoseamine-6-phosphate, which is subsequently converted to UDP N-acetylglucosamine

(GlcNAc). This compound is known to induce O-GlcNAcylation of serine and threonine residues of several transcription factors, changing the gene expression profile. For example, increased modification of the transcription factor Sp1 results in increased expression of transforming growth factor-β1 (TGF-β1), involved in the regulation of cell cycle and apoptosis.

1.1.4 Advanced glycation end products formation

Glucose can react spontaneously with amino groups of a wide range of proteins to form Schiff bases that, through multiple rearrangements, are transformed into irreversibly bound reactive adducts. Indeed, the chemical and conformational modifications that follow glucose binding to proteins appear to be sufficient to expose -SH groups. Oxidation of -SH residues can lead to protein cross-linking and aggregation, as well as to inactivation of various enzymes (Stevens et al, 1978; Swamy & Abraham, 1987). Subsequent reactions, following glucose binding to amino groups on proteins, result in the formation of the Amadori products. The Amadori products can also be oxidized and undergo further reactions to produce α-ketoaldehydes, like 1- and 3-deoxyglucosones. These products are usually more reactive than the initial monosaccharide and can further react with proteins, yielding a heterogeneous mixture of fluorescent and coloured compounds that can crosslink proteins (Brownlee et al, 1984). These compounds are known as Maillard products or AGEs (Monnier, 1989).

The rate of AGEs formation from glucose is orders of magnitude slower than the rate of AGEs formation from intracellular generated glucose-derived dicarbonyl precursors (Degenhardt et al, 1998). It thus appears that hyperglycaemia is the primary initiating event in the formation of AGEs. Indeed, AGEs can be originated from a number of pathways, including auto-oxidation of glucose to glyoxal, decomposition of the Amadori products to 3-deoxyglucosone and fragmentation of G3P and dihydroxyacetone-phosphate to MGO (Thornalley et al, 1999). These reactive intracellular dicarbonyls (glyoxal, 3-deoxyglucosone and MGO) react with amino groups of proteins to form AGEs (Thornalley, 1990). For example, MGO is known to modify arginine and lysine residues leading to the formation of several adducts (Figure 1), such as *N*δ-(5-hydro-5-methyl-4-imidazolon-2-yl)-ornithine (MG-H1), *N*ε-carboxymethyl-lysine (CML), *N*ε-carboxyethyl-lysine (CEL), *N*ω-carboxymethylarginine (CMA) and argpyrimidine (Kalapos, 1999; Kalapos, 2008; Thornalley, 2008). MGO may also modify nucleotides and phospholipids.

MGO-derived AGEs can be detoxified through the glyoxalase (GLO) system. The GLO system catalyzes the conversion of reactive acyclic α-oxoaldehydes into the corresponding α-hydroxyacids. It is composed of two enzymes, GLO I and GLO II, and a catalytic amount of GSH. GLO I enzyme catalyzes the isomerization of the hemithioacetal, formed spontaneously, from α-oxoaldehyde and GSH, into *S*-2-hydroxyacylglutathione derivatives. GLO II catalyzes the conversion of *S*-2-hydroxyacylglutathione derivatives into α-hydroxyacids and re-forms GSH consumed in the GLO I-catalyzed reaction step. The major physiological substrate for GLO I is

MGO, and this one markedly accumulates when GLO I is inhibited by cell-permeable GLO I inhibitors or by depletion of GSH (Thornalley, 2003a; Thornalley, 2003b).

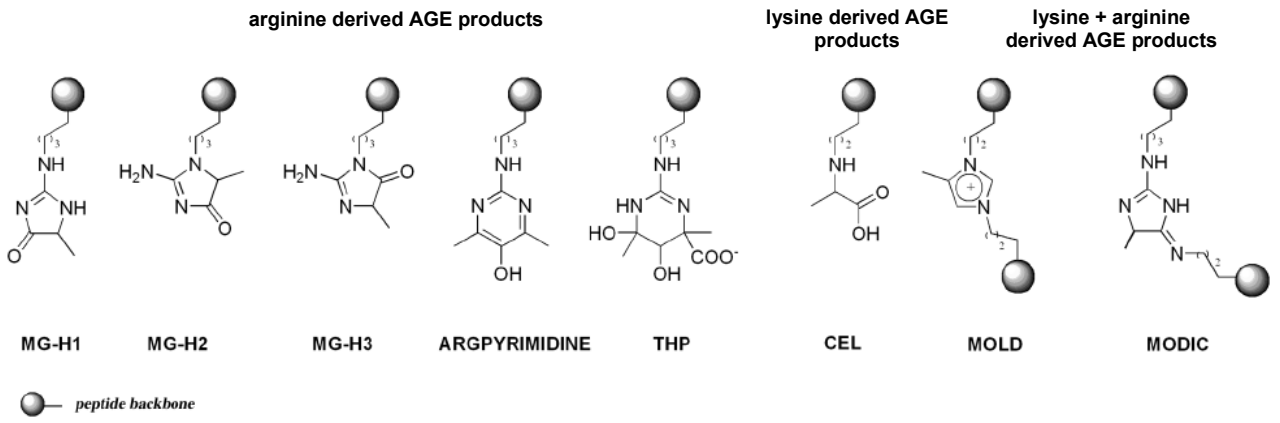

Figure 1. Schematic representation of AGEs formed from the reaction between MGO and lysine or arginine residues. Adapted from (Nemet et al, 2006).

AGEs formed from dicarbonyls (such as MGO) were shown to accumulate in cells and tissues from diabetic patients or animal models of diabetes (McLellan et al, 1994; Oya et al, 1999; Phillips et al, 1993). Indeed, in endothelial cells cultured under high glucose, it was demonstrated that MGO is the major precursor of AGEs (Shinohara et al, 1998).

MGO irreversibly modifies a variety of proteins (Thornalley, 1990), which is closely associated with cell toxicity. MGO selectively inhibits mitochondrial respiratory complexes, as well as inactivates a number of other enzymes, such as membrane ATPases (Biswas et al, 1997; Halder et al, 1993). Of significance for this thesis, MGO also modifies the corepressor mammalian Sin3 homolog A (mSin3A), which increases the recruitment of O-GlcNAc-transferase, with consequent increased modification of the Sp3 transcription factor (SP3) by O-linked N-acetylglucosamine. This modification is known to decrease the binding of SP3 to a glucose-responsive GC-box in the angiopoietin-2 (Ang-2) gene promoter, resulting in increased expression of Ang-2 (Yao et al, 2007). In diabetic retinal and kidney capillaries, increased Ang-2 is associated with pericytes loss and acellular capillary formation, accounting for an impairment of the angiogenic response. Another recent study also shows that hypoxia-induced VEGF expression in fibroblasts is reduced in hyperglycaemia conditions, through a mechanism that involves modification of the hypoxia-inducible factor 1α (HIF-1α) by MGO, which inhibits its interaction with HIF-1β and impairs the formation of a functional HIF-1 heterodimer (Ceradini et al, 2008).

In addition to direct modification of protein and enzymes, AGE-precursors may induce further damage to cells by other mechanisms. For example, AGE-precursors are known to disrupt interaction between extracellular matrix components and integrins. They also bind to AGE receptors (RAGEs) in endothelial cells, inducing activation of the nuclear factor-κB (NF-κB), followed by alteration of the gene expression profile. Moreover, MGO is known to induce vascular

dysfunction and increased cell death of pericytes and endothelial cells in diabetes, by Ang-2-dependent and -independent mechanisms, which is ameliorated by the advanced glycation inhibitor (±)-2-Isopropylidenehydrazono-4-oxo-thiazolidin-5-ylacetanilide (OPB 9195). Increased levels of MGO have also been reported to have direct deleterious effects in a number of essential signalling pathways implicated on diabetes, such as the epidermal growth factor receptor (EGFR), the insulin-like growth factor 1 receptor (IGF1-R) and the protein serine/threonine kinase Raf-1 pathways. For example, in the case of Raf-1, MGO-mediated intracellular oxidation and UPP-dependent proteolysis are involved in downregulation of Raf-1, which is a central switchboard kinase in the transmission of many growth signals (Du et al, 2006).

The potential importance of AGEs in the pathogenesis of diabetic complications is indicated by the observation that two structurally unrelated AGE inhibitors (aminoguanidine and OPB 9195) partially prevent various functional and structural manifestations of diabetic microvascular disease in retina, kidney and nerves (Du et al, 2002; Hammes et al, 1991; Nakamura et al, 1997). Pyridoxine, an inhibitor of AGEs formation, has been further shown to induce protection against many retinal vascular lesions in experimental models of diabetes (Stitt et al, 2002).

1.1.5 Production of superoxide by the mitochondrial electron-chain

For many years, the previously described mechanisms were considered independently to explain modifications associated with pathogenesis of diabetes. However, during the last decade it was found a common link, which can explain the cell damage in diabetes. The hyperglycaemia-induced overproduction of superoxide by the mitochondrial electron transport chain is most likely the crosstalk event between all the other mechanisms (Brownlee, 2001; Du et al, 2000; Nishikawa et al, 2000) (Figure 2).

The mechanism whereby hyperglycaemia induces increased production of superoxide by mitochondria appears to be related to the excessive production of electron donors (NADH and $FADH_2$) from the trycarboxylic acid cycle (TCA) (Du et al, 2001). Indeed, high glucose increases by about 2.2 fold the flux through the TCA cycle in endothelial cells (Nishikawa et al, 2000), leading to increased production of NADH and $FADH_2$. These compounds enter the mitochondrial electron-transport chain, which increases the electron flux and proton gradient, resulting in a significant increase in the production of superoxide.

A number of experimental data appear to support this hypothesis. For example, overexpression of manganese superoxide dismutase, the mitochondrial enzyme that dismutates superoxide (Nishikawa et al, 2000), completely prevents increased activity of the polyol and hexosamine pathways, increased intracellular AGEs formation and increased PKC activation in endothelial cells (Brownlee, 2001). This effect is mainly due to the recovery of GAPDH activity, which inhibits the accumulation of upstream glycolytic metabolites (F6P or G3P) and the activity of the polyol pathway.

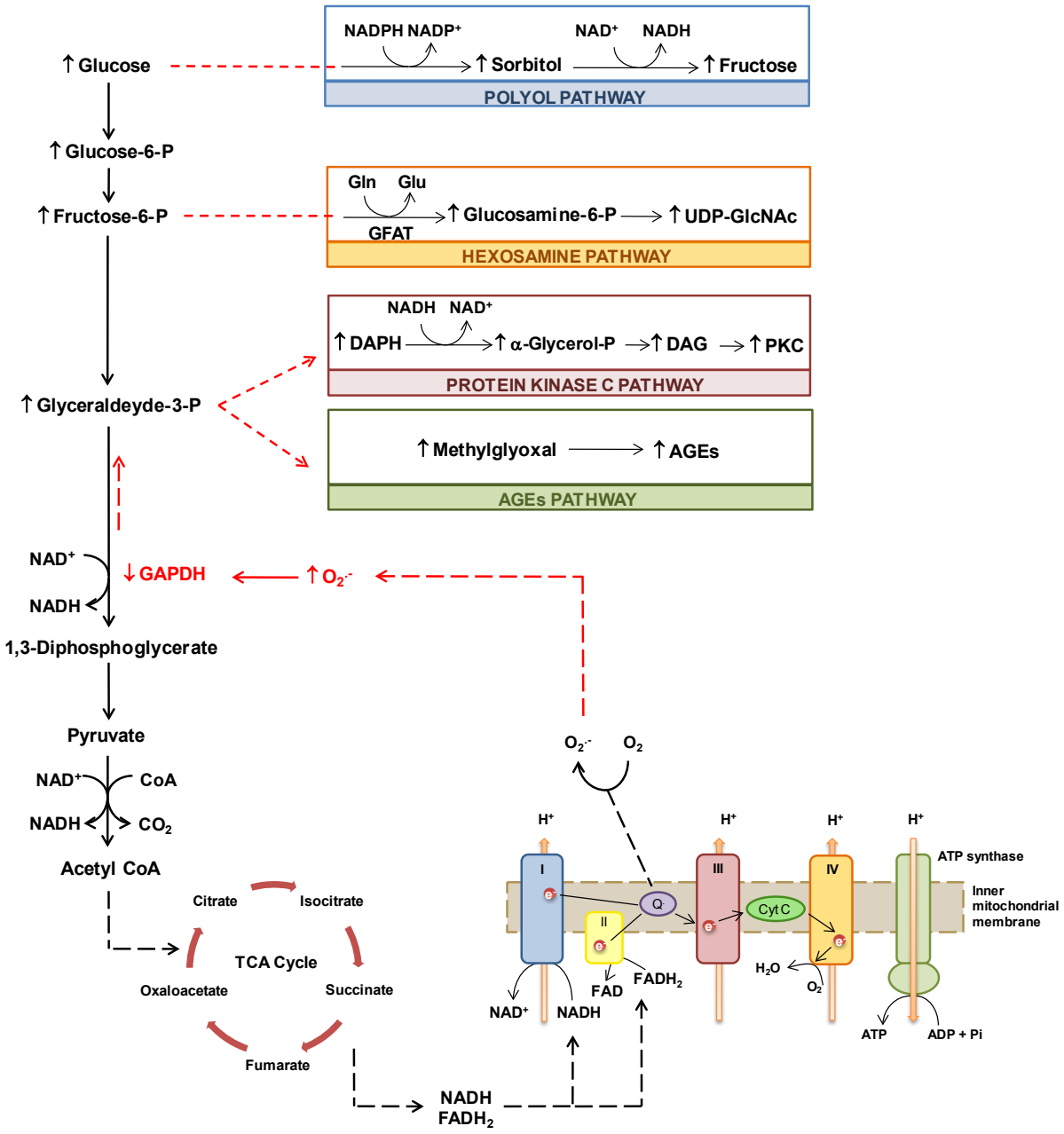

Figure 2. Unifying hypothesis linking the four mechanisms of high glucose-induced cell damage. Adapted from (Brownlee, 2001)

1.1.6 The VEGF paradox and cell response to hypoxia on diabetes

Diabetes is characterized by an “angiogenic paradox”, since both pro and antiangiogenic conditions coexist in chronic diabetes. In some microvascular tissues, increased expression of growth factors result in neovascularization and increased blood vessel permeability. This response has a significant role in advanced stages of diabetic retinopathy, nephropathy and neuropathy complications, which seem to be ameliorated upon angiogenesis inhibition. Conversely, decreased expression of growth factors is associated with impairment of new blood vessels formation leading

to poor wound healing and manifestation of diabetic skin ulcers. Moreover, impairment of the arteriogenesis response in diabetes further results in reduced collateral artery growth and maturation, which in turn leads to reduced myocardial perfusion and enhanced mortality. Indeed, induction of growth factors release reduces clinical symptoms and tissue damage in coronary artery and peripheral limb disease and ameliorates the wound healing process in diabetic patients. Thus, two apparently diametric angiogenic responses occur in diabetes and generate an intriguing paradox (Duh & Aiello, 1999).

Several reports suggest that VEGF plays a central role in mediating diabetic vascular complications and is likely to be at the basis of the angiogenic paradox on diabetes. VEGF is a sub-family of the growth factors family platelet-derived growth factor or PDGF. The most important member is VEGF-A. Other members are VEGF-B, VEGF-C, VEGF-D and placenta growth factor or PlGF (Figure 3).

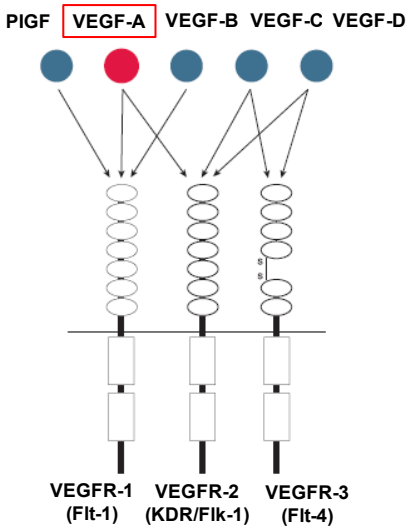

Figure 3. Schematic representation of the VEGF family and their receptor interactions. Adapted from (Yancopoulos et al, 2000).

VEGF-A has been shown to stimulate endothelial cell mitogenesis and cell migration. It is also a well known vasodilator factor, stimulates monocyte/macrophage migration and increases microvascular permeability. The term 'VEGF' covers a number of proteins from two different groups that result from alternative mRNA splicing from a single *vegf* gene composed by 8 exons. The two groups are referred according to their terminal exon splice site - the proximal splice site ($VEGF_{xxx}$) or distal splice site ($VEGF_{xxx}b$). The type of exon 8 splicing determines whether the proteins are pro-angiogenic (proximal splice site) or anti-angiogenic (distal splice site). In addition, alternate splicing of exon 6 and 7 alters their heparin binding affinity and amino acid number (in humans: $VEGF_{121}$, $VEGF_{121}b$, $VEGF_{145}$, $VEGF_{165}$, $VEGF_{165}b$, $VEGF_{189}$, $VEGF_{206}$). All members of the VEGF family bind to tyrosine kinase receptors (the VEGFRs). VEGF binding induces receptor dimerization, which become activated through *trans*-phosphorylation. VEGF-A is known to bind to

VEGFR-1 (Flt-1) and VEGFR-2 (KDR/Flk-1) (Figure 3). VEGFR-2 appears to mediate almost all of the known cellular responses of VEGF (Yancopoulos et al, 2000).

On advanced stages of DR, it is clearly known that VEGF is a major mediator of intraocular neovascularization, serving a pivotal role in the aetiology of DR. Many cell types within the eye produce VEGF, including retinal pigment epithelium cells, retinal pericytes, Müller cells, ganglion cells, glial cells and endothelial cells (Duh & Aiello, 1999). Furthermore, retinal microvascular endothelial cells express large numbers of high-affinity VEGF receptors (Duh & Aiello, 1999; Thieme et al, 1995). VEFG concentrations are markedly elevated in both vitreous and ocular aqueous fluids of patients with active proliferative diabetic retinopathy compared with samples from patients without diabetes, with nonproliferative DR or with quiescent proliferative DR (Aiello et al, 1994; Duh & Aiello, 1999).

Despite all the advances in the understanding of diabetic retinopathy, the nature and time course of molecular changes in the diabetic retina are poorly characterized. Particularly, studies on VEGF mRNA have produced conflicting results. For example, retinal VEGF mRNA levels have been reported by independent studies to be unchanged at 3 months, increased at 6 months and decreased at 6 months duration of streptozotocin (STZ)-induced diabetic rats (Brucklacher et al, 2008). However, a recent study, based on a gene expression profile, showed a consistent decrease in VEGF mRNA expression at the retina of 1 and 3 month-aged STZ-induced diabetic rats (Brucklacher et al, 2008). This work also shows that the decrease of the VEGF mRNA levels is accompanied by increased vascular permeability and caspase-3 activity, two main features of the early stages of DR, which are classically associated with high expression of VEGF, a fact that was not corroborated by this study. Thus, it seems that there are multiple phases in the regulation of *vegf* gene expression in DR and it seems imprudent to generalize its upregulation for all the stages of DR.

The evidence that VEGF is involved in diabetic nephropathy and neuropathy is less extensive and is, also, very controversial. In the case of nephropathy, it was shown that elevated levels of VEGF increase glomerular permeability and contribute to diabetic proteinuria (Lee et al, 2006), while VEGF antibodies (that decrease available VEGF) improve renal function (Nakagawa et al, 2006; Wirostko et al, 2008). However, other clinical studies have reported low levels of VEGF at the renal glomeruli, contributing to podocyte cell death, diminished tissue repair and progression of renal disease in diabetes (Baelde et al, 2007; Hohenstein et al, 2006). This controversy is also common between several studies on diabetic neuropathy. For example, neural damage due to ischemia typically results in increased VEGF levels in the plasma of diabetic animals, with increased VEGF expression in axons and dorsal root glia. However, other studies showed that supply of VEGF reverses diabetic peripheral neuropathy and preserve vascularity, blood flow and nerve function (Carmeliet & Storkebaum, 2002; Wirostko et al, 2008).

VEGF also has a key role in the development of coronary heart disease in diabetic patients. In preclinical diabetic studies, researchers observed diminished endothelial progenitor cell (EPC)

mobilization following ischemia-reperfusion myocardium injury and lower VEGF levels compared to controls (Fadini et al, 2006). mRNA levels and protein expression of VEGF and its receptors, VEGFR1 and VEGFR2, in the myocardium were shown to be significantly decreased by 40% to 70% in both diabetic and insulin-resistant non-diabetic rats. Moreover, a two-fold reduction in VEGF and VEGFR2 was observed in ventricles from diabetic patients compared with nondiabetic donors (Chou et al, 2002). Additionally, VEGF supply via a plasmid vector was shown to decrease apoptosis, as well as to improve EPC function, migration and capillary density (Yoon et al, 2005). Therefore, progressive attenuation of myocardial VEGF expression seems to be a determining event in diabetic cardiomyopathy.

Lymphatic and vascular aspects of defective wound healing in diabetic patients are also associated with impaired VEGF production. Fibroblasts from diabetic mice exhibit a seven-fold impairment in VEGF production compared with wild-type fibroblasts. Moreover, production of VEGF, in wild-type fibroblasts, was shown to be increased three-fold in response to hypoxia, whereas diabetic fibroblast production of VEGF was not upregulated in hypoxic conditions (Lerman et al, 2003). Unlike the acute inflammatory phase in normal healing, diabetic patients have a chronic moderate inflammation that reduces the number and hampers the function of activated macrophages, and also leads to reduced secretion of VEGF, resulting in the impairment of lymphatic vasculature repair and EPC dysfunction (Lerman et al, 2003). Consistently, reduced VEGF production decreases the number of platelets at the wound, reducing the formation of granulation tissue, which, in turn, further decreases VEGF secretion in areas of wound healing (Asai et al, 2006; Verheul & Pinedo, 2007).

While anti-VEGF therapies appear very effective as a means to reduce microvascular complications in the advanced stages of DR, pro-VEGF therapies appear to be equally promising to increase collateral vascular formation and reduce macrovascular complications associated with myocardial infarction and peripheral limb ischemia (Duh & Aiello, 1999). Thus, systemic treatment of one complication may theoretically exacerbate another one.

The VEGF paradox that occurs in diabetes is most likely a consequence of a diametrically opposed response to hypoxia in the several diabetic tissues. Capillary nonperfusion and loss of retinal capillaries that occur in DR can lead to retinal ischemia. Apparently, acute hypoxia rapidly activates retinal cells to release angiogenic growth factors, such as VEGF, leading to the formation of new blood vessels, a main feature of advanced stages of DR. Indeed, increased levels of VEGF in the vitreous and retina of diabetic patients are likely to be hypoxia-induced, since elevated levels of VEGF protein and mRNA are present in the ischemic retina adjacent to the areas of neovascularization. Moreover, *in vitro* hypoxia also induces expression of VEGF mRNA in retinal cells and is reported to induce expression of VEGF receptors in endothelial cells, indicating that sensitivity to VEGF is enhanced in the ischemic retina (Cai & Boulton, 2002).

However, it has also been shown that hyperglycaemia is a critical event implicated in the loss of cell response to hypoxia and in destabilization of HIF-1 (Catrina et al, 2004; Fadini et al,

2006; Gao et al, 2007), a key protein involved in the regulation of cell response to hypoxia. HIF-1 is an oxygen-dependent transcription factor that activates the expression of several genes, which helps cells and tissues to cope with hypoxia. Although VEGF is produced in response to a variety of stimuli, one of the best known involves activation of HIF. Consistently, downregulation of HIF-1 in response to hyperglycaemia is likely to account for decreased arteriogenic response triggered by myocardial ischemia in diabetic patients (Abaci et al, 1999; Larger et al, 2004) and high glucose was shown to reduce hypoxia- and HIF-induced VEGF expression in primary skin fibroblasts (Ceradini et al, 2008). Moreover, blood glucose levels were shown to be in linear relation with fatal outcome after an acute hypoxic challenge, suggesting a deleterious influence of hyperglycaemia on the ability of tissues to adapt to low oxygen tensions (Malmberg et al, 1999). Additionally, HIF-1α protein levels and VEGF mRNA levels are dramatically downregulated in skin wounds of diabetic patients and animal models of diabetes, as compared to skin wounds that share the same hypoxic environment but are not exposed to hyperglycaemia (Catrina et al, 2004; Sarkar et al, 2009; Thangarajah et al, 2009). Consistently, adenovirus-mediated transfer of stable HIF constructs to skin wounds demonstrated that stabilization of HIF-1α is necessary and sufficient for promoting wound healing in a diabetic environment (Botusan et al, 2008; Sarkar et al, 2009).

A variety of evidence suggests that the cell and tissue dysfunctions associated with diabetes are related, at least in part, with a differential cell response to hypoxia between the several diabetic tissues, which may account for the angiogenic and VEGF paradoxes that occur in diabetes.

1.2 The Hypoxia-Inducible Factor System

In response to low oxygen levels, animals increase the glycolysis flux to compensate the energy defective production due to decreased oxidative phosphorylation by the mitochondrial electron-chain. Moreover, erythropoiesis and angiogenesis are upregulated to achieve more efficient oxygen utilization. This adaptive response relies on a mechanism that uses oxygen deficit as a signal to activate transcription of a plethora of genes important for these processes. This mechanism comprises the regulation of the hypoxia-inducible factor system that plays an essential role in the maintenance of oxygen homeostasis and allows cells to survive under oxygen deprivation. Indeed, the HIF proteins upregulate the transcription of a variety of genes that helps cells to cope with hypoxia. HIF is regulated by fine-tuning mechanisms that are dependent on oxygen, both at the level of protein stability and transcriptional activity, which makes the protein inactive under normoxia, but inducible under hypoxia conditions.

Investigation on erythropoietin (EPO) induction, one of the most prominent responses to hypoxia, conducted to the first identification of HIF in 1992 (Semenza & Wang, 1992). In this study, it was identified a nuclear factor that binds to the *EPO* gene enhancer, only under hypoxia. It soon became obvious that the HIF system is a key regulator of a broad range of responses to hypoxia and it has been extensively studied during the last two decades.

1.2.1 The HIF family of proteins

HIF is transcriptional active only as a heterodimer and is composed of an oxygen-regulated α subunit and a constitutively expressed β subunit. Both subunits are members of the basic helix-loop-helix/Per-Arnt-Sim homology (bHLH/PAS) family of transcription factors (Wang et al, 1995), since both of the proteins contain these two characteristic domains. These domains are known to be involved in DNA binding and α/β heterodimer formation, respectively.

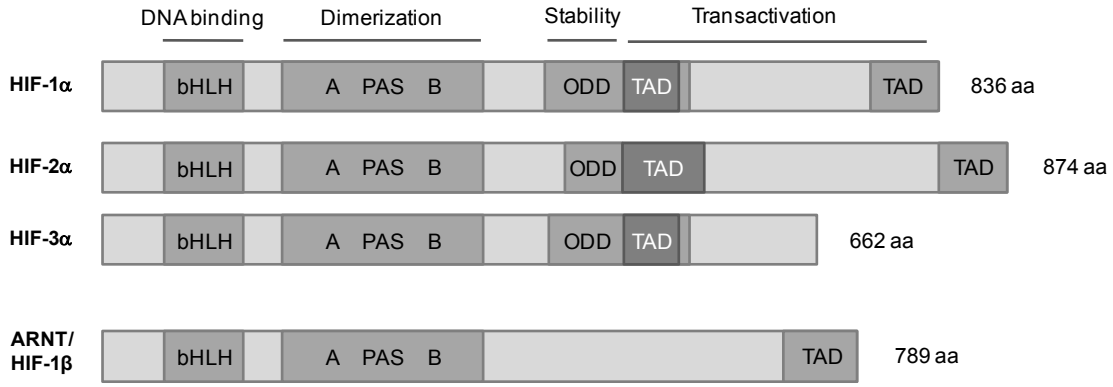

Figure 4. Schematic representation of HIF family member protein domains. Adapted from (Rankin & Giaccia, 2008).

There are three paralogues of the α subunit: HIF-1α, HIF-2α and HIF-3α (Figure 4). All are encoded by distinct gene loci and further diversity is generated by alternative mRNA splicing. HIF-1α and HIF-2α share similar domain structure and are regulated in a similar manner; however, the tissue expression of HIF-2α seems to be more limited. Moreover, both paralogues are able to heterodimerize with HIF-1β to form a functional HIF transcription factor (Chun et al, 2002; Gothie et al, 2000; Maynard et al, 2003; Mazure et al, 2004; Weidemann & Johnson, 2008). HIF-3α is less closely related and its role is not yet fully understood; however, HIF-3α is postulated to behave as a negative regulator of HIF-mediated transcription and human HIF-3α has multiple spliced variants (HIF-3α 1-6). HIF-3α gene lacks the C-terminal transactivation domain (C-TAD). A splicing variant form of HIF-3α, known as inhibitory PAS domain protein (IPAS), was shown to prevent the interaction between HIF-1α and HIF-1β, since IPAS dimerizes with HIF-1β and sequestrates HIF-1β from HIF-1α, which inhibits the transcription of the target genes (Makino et al, 2001; Makino et al, 2002). IPAS is induced by hypoxia and is likely to act as a negative feedback mechanism for the regulation of HIF-1α.

The human HIF-1α is an 826-aminoacid (120 kDa) protein. In the N-terminal it contains the bHLH domain (residues 17-71) and the PAS domain (residues 85-298), with PAS-A (residues 85-158) and PAS-B (residues 228-298) repeats (Wang et al, 1995; Zagorska & Dulak, 2004). Two transactivation domains, N-terminal and C-terminal TADs (also termed NAD and CAD), are both localized in the C-terminal half of HIF-1α (residues 531-575 and 786-826, respectively). Moreover,

the C-terminal part contains a domain responsible for degradation of HIF-1α under normoxic conditions (Zagorska & Dulak, 2004). This oxygen-dependent degradation domain (ODD at 401-603 residues) contains two PEST-like motifs: sequences rich in proline (P), glutamic acid (E), serine (S), and threonine (T) (residues 499-518 and 581-600), common between proteins with a short half-life (less than 2 hours). Additionally, HIF-1α contains two nuclear localization signals: N-NLS (residues 17-74) and C-NLS (residues 718-721). The C-terminal NLS is crucial in the nuclear import of HIF-1α, whereas the N-terminal one seems to be less important (Zagorska & Dulak, 2004) (Figure 4).

The human HIF-1β/ARNT protein has two isoforms (774 and 789 residues corresponding to 92 or 94 kDa, respectively) that differ by the presence of a 15 amino acid sequence encoded by a 45-bp alternative exon (Wang et al, 1995; Zagorska & Dulak, 2004).

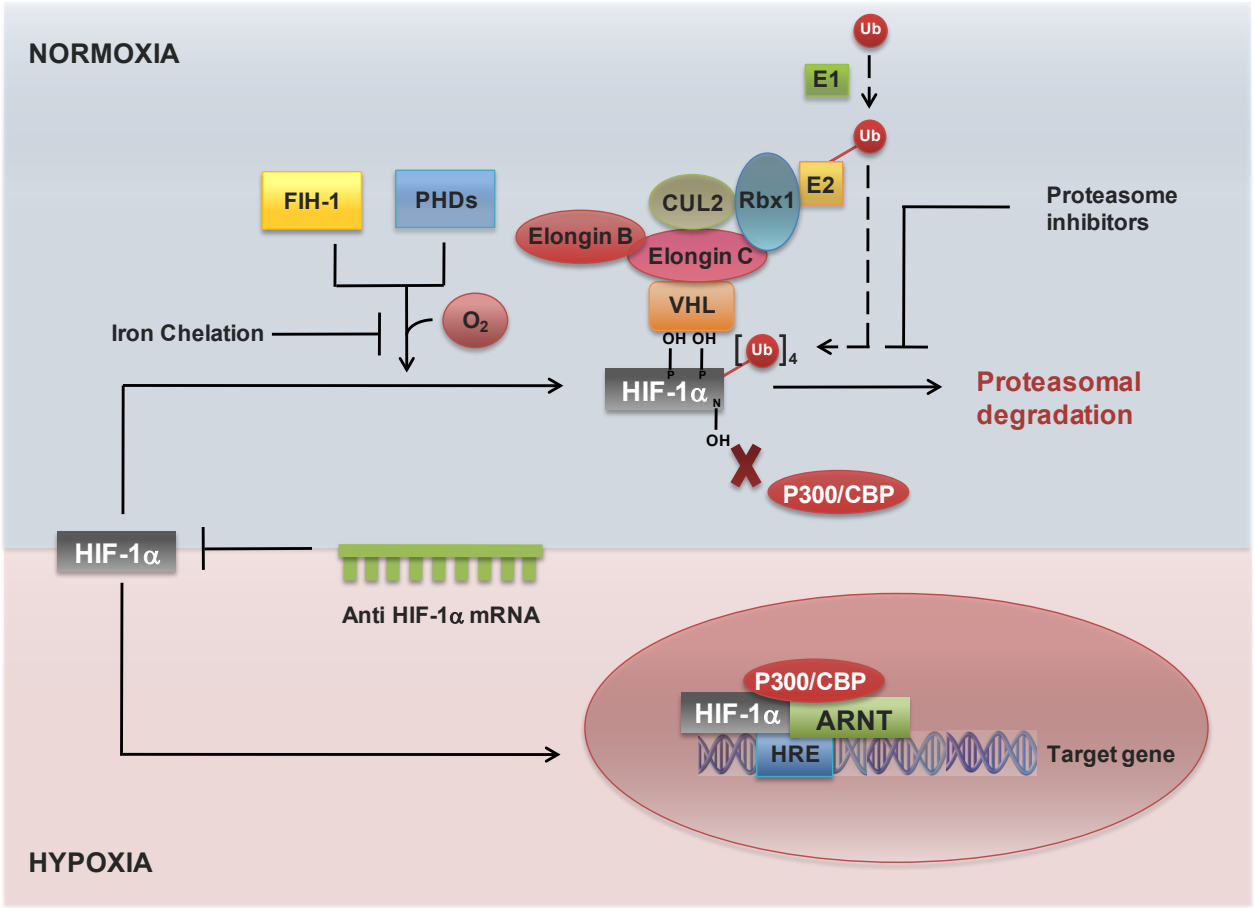

Figure 5. Schematic representation of the canonical HIF-1α degradation pathway. Adapted from (Harris, 2002).

1.2.2 Regulation of HIF-1α subunit by hydroxylation

Under normoxic conditions, HIF-1α subunit has a very short half-life, of less than 5 minutes (Huang et al, 1996; Lisy & Peet, 2008; Yu et al, 1998). Cells continuously synthesize and degrade the HIF-1α protein. However, under low levels of oxygen, the degradation of HIF-1α is inhibited

(Jiang et al, 1996). The interface between oxygen and the HIF-1α protein is provided by hydroxylation of two proline residues (Pro402 and Pro564 in human HIF-1α) in the ODD domain (Huang et al, 1998; Ivan et al, 2001; Jaakkola et al, 2001). This oxygen-dependent hydroxylation regulates the interaction with the von Hippel-Lindau tumour suppressor protein (pVHL) and is achieved by specific prolyl hydroxylase domain (PHD) enzymes. VHL is the recognition component of an ubiquitin ligase complex that targets HIF-1α for proteolysis by the ubiquitin-proteasome pathway under normoxia conditions (Maxwell et al, 1999; Ohh et al, 2000). Under hypoxic conditions, prolyl hydroxylation is inhibited, which blocks HIF-1α degradation by the proteasome. Thus, HIF-1α accumulates in the cell and is translocated into the nucleus, where it dimerizes with HIF-1β. The HIF-1α/HIF-1β heterodimeric complex then binds to a core pentanucleotide sequence (5'-RCGTG-3') in the hypoxia-responsive elements (HREs) of the promoter or enhancer sequences of the target genes (Chapman-Smith & Whitelaw, 2006; Kimura et al, 2001; Semenza & Wang, 1992) (Figure 5).

The transcriptional activity of HIF-1α is also regulated by another oxygen-dependent mechanism and involves the hydroxylation of a C-terminal asparagine residue (Asn803 in human HIF-1α). This hydroxylation is carried out by an asparagynil hydroxylase termed as factor-inhibiting HIF (FIH) and this modification inhibits the interaction of HIF-1α with the co-activators p300/CREB binding protein (CBP), preventing the transactivation activity of HIF-1 (Hewitson et al, 2002; Lando et al, 2002a; Lando et al, 2002b). Thus, in contrast to the prolyl hydroxylation that enables protein-protein interaction, the asparaginyl hydroxylation prevents protein recruitment (Figure 5).

1.2.3 The HIF partners

1.2.3.1 PHDs. HIF-prolyl hydroxylases, also known as prolyl hydroxylase domain proteins, form an evolutionary conserved subfamily of dioxygenases that require oxygen and 2-oxoglutarate (2-OG), as co-substrates, and iron and ascorbate as co-factors (Bruick & McKnight, 2001; Epstein et al, 2001; Schofield & Ratcliffe, 2005). The use of iron by PHDs explains the observed hypoxia-mimetic effects of iron chelators and iron antagonists, such as desferrioxamine and cobalt chloride, respectively (Salnikow et al, 2004; Wang & Semenza, 1993; Yuan et al, 2003).

Mammals are known to have four PHD members (PHD1, PHD2, PHD3 and a recently characterized protein named as P4H-TM). Both full-length PHD1 and PHD2 have about 400 amino acid residues (407 and 426 in humans, respectively) and share a well-conserved hydroxylase domain at the C-terminal. The N-terminal of PHD1 and PHD2 are more divergent and has poorly characterized functions. Human PHD3, the shorter member with 239 amino acids, contains the hydroxylase domain but only a short stretch of the N-terminal sequence (Epstein et al, 2001; Fong & Takeda, 2008).

At the mRNA level, all three PHDs are widely distributed among different organs, although PHD3 is the highest in the heart, whereas PHD1 is the highest in testes (Willam et al, 2006).

However, at the protein level, PHD2 is the most abundant isoform in all mouse organs and in different examined cell lines (Appelhoff et al, 2004; Berra et al, 2003). Studies using monoclonal antibodies indicate that PHDs are mostly located in the cytoplasm (Soilleux et al, 2005).

Two proline residues in human HIF-1α (P402 and P564), located in the ODD domain (Huang et al, 1998), have been shown to be hydroxylated and are part of a conserved consensus sequence LXXLAP (Masson et al, 2001). Patches of hydrophobic amino acid residues within the ODD domain are likely the most important elements in the recognition of the substrate. All PHDs are more active on the LXXLAP core containing the P564 and, in particular, PHD3 is virtually inactive on P402 LXXLAP core (Hirsila et al, 2003). In cultured cells, all three PHDs contribute to the regulation of both HIF-1α and HIF-2α, but preferences do exist. PHD1 and PHD3 are more active on HIF-2α than HIF-1α, whereas PHD2 preferentially hydroxylates HIF-1α (Appelhoff et al, 2004).

Oxygen is a key substrate for hydroxylation. All three PHDs have Km values for oxygen within the range 230-250 μM, slightly above the oxygen concentration in aqueous solutions saturated be ambient room air (Appelhoff et al, 2004). Since intracellular oxygen concentrations are typically below these values (4-40 μM), high Km values ensure the dependence of hydroxylase activity on oxygen when all other substrates and cofactors are present at adequate levels (Figure 6).

Although the major function of PHDs is to regulate the stability of HIF-1α, themselves are also regulatory targets. For instance, PHD1 and PHD3 are targeted for polyubiquitination and proteasome-dependent degradation by Siah1a/2 (Nakayama et al, 2004). Interestingly, Siah2 itself is strongly induced by hypoxia, which contributes to accelerated PHD degradation. Moreover, PHD2 and PHD3 genes contain HREs and are induced by HIF-1α under hypoxia. Furthermore, reactive oxygen species and nitric oxide, which levels increase during reduced availability of oxygen, inhibit the PHDs activity by chelating and oxidizing PHD bound-Fe (II) and Fe (III) (Metzen et al, 2003b; Pan et al, 2007). Additionally, TCA cycle intermediates may activate or inhibit PHDs activity. Indeed, 2-OG is an essential co-substrate for PHDs due to its role in Fe (II) coordination in the catalytic centre (Epstein et al, 2001). However, succinate and fumarate compete against 2-OG for binding to the active site (Selak et al, 2005).

1.2.3.2 VHL. The human *vhl* gene is translated into two VHL proteins: pVHL19 and pVHL30. VHL30 is a 213-aminoacid protein of about 24-30 kDa, while VHL19 is an 18-19 kDa isoform of 160 amino acids. VHL30 and VHL19 do not have redundant functions. Furthermore, both proteins were shown to have different subcellular localizations. While pVHL30 is found in the nucleus, cytosol and endoplasmic reticulum membrane, pVHL19 is only found in the nuclear and cytosolic fractions (Blankenship et al, 1999; Schoenfeld et al, 1998; Sufan et al, 2004).

During the last few years, it has been shown that pVHL is a multitasking protein. However, the best characterized function of pVHL is associated with HIF-1α regulation. VHL protein is the

recognition subunit of an ubiquitin ligase complex that targets HIF-α for oxygen-dependent degradation by the proteasome (Huang et al, 1998; Ivan et al, 2001; Jaakkola et al, 2001; Maxwell et al, 1999; Ohh et al, 2000). pVHL is in a complex with elongin B, elongin C, cullin 2 (Cul2), Rbx1 and NEDD8, forming an ubiquitin ligase complex called VBC (VHL-Elongin B-Elongin C) complex (Sufan et al, 2004). Elongin C bridges pVHL to Cul2 (Stebbins et al, 1999). Cul2 associates with elongin C, NEDD8 and Rbx1 (Pause et al, 1997). The RING (Really Interesting New Gene) finger protein Rbx1 (also known as ROCK1) is thought to recognize a cognate E2, which is required for the E3 ligase function of VBC complex (Ohta et al, 1999) (Figure 5). The crystal structure of the VBC complex reveals that VHL has two structural domains, an N-terminal β-domain rich in β-sheets structures and a C-terminal α-domain adopting a three-helix cluster structure (Stebbins et al, 1999). The α- and β-domains are connected by two linkers and an extensive interface of hydrogen bonds, indicating that are both rigidly connected. The VBC-HIF1α structure showed that the HIF-1α peptide binds the β-domain of VHL. The hydroxyproline inserts into a gap in the VHL hydrophobic core, precisely at the protein-binding site predicted by tumour-derived mutations. The 4-hydroxyl group of the hydroxyproline is recognized by a pair of buried serine and histidine residues on VHL (Hon et al, 2002; Min et al, 2002).

1.2.3.3 ARD-1. Arrest-defective-1 protein, a member of a large family of acetyltransferases, is known to induce acetylation of lysine 532 in the ODD domain of HIF-1α, close to proline 564. This post-translational modification appears to favour the recruitment of pVHL and degradation of HIF-1α by the proteasome (Jeong et al, 2002). Thus, ARD1 acts as a negative regulator of HIF-1α by making it less stable, like PHDs. Since N-acetyltransferases activity is not known to be dependent on oxygen, it could be expected that this modification occurs under both normoxia and hypoxia. However, the ARD-1 mRNA levels were found to slightly decrease under hypoxic conditions, suggesting that the level of HIF-1α acetylation may decrease under low oxygen (Mazure et al, 2004).

1.2.3.4 FIH-1. Factor-inhibiting HIF-1 is an asparaginyl hydroxylase that hydroxylates the asparagine 803 of HIF-1α, preventing the binding of the transcriptional co-activators p300/CBP to the HIF-1α C-terminal transactivation domain (Hewitson et al, 2002; Lando et al, 2002a; Lando et al, 2002b; Mahon et al, 2001). In opposition to PHDs, a consensus sequence for asparagine hydroxylation has not been identified, but the sequence around asparagine 803 is highly conserved between species. Indeed, the adjacent residue valine 802 seems to have a crucial role in this mechanism (Linke et al, 2004). This Val-Asn motif seems to be essential in the maintenance of the interaction between p300/CBP and the HIF-1α C-TAD. FIH-1 does not influence the stability of HIF-1α but, like the PHDs, FIH-1 requires 2-OG, Fe (II), ascorbate and dioxygen for catalysis of hydroxylation (Linke et al, 2004; Safran & Kaelin, 2003). However, unlike PHDs, FIH-1 is not inhibited by TCA metabolites (Hewitson et al, 2007).

FIH-1 protein expression has been detected at similar levels in all examined cell lines (Bracken et al, 2006). Immunocytochemical analyses have shown predominant FIH-1 cytosolic staining (Soilleux et al, 2005). Moreover, changes in the oxygen content do not appear to induce changes in FIH-1 subcellular distribution (Metzen et al, 2003a).

FIH-1 has an absolute requirement for oxygen to maintain enzymatic activity. The estimated Km value of FIH-1 for oxygen is approximately 90 μM (Koivunen et al, 2004). Given that physiological oxygen concentrations are around 4-40 μM and below the estimated Km, it seems that FIH-1 responds to relevant changes in the intracellular oxygen concentrations. Decreases in oxygen tension are likely to induce a direct decrease in the catalytic activity of FIH-1, as well as of PHDs (Lisy & Peet, 2008) (Figure 6).

FIH-1 has been shown to interact *in vitro* with pVHL; however the purpose of this interaction is physiologically unclear (Mahon et al, 2001). Moreover, it has been shown that FIH-1 interacts with another ubiquitin ligase, Siah-1 (Fukuba et al, 2007). Siah-1 induces polyubiquitination of FIH-1, as well as of PHDs, but its functional relevance is poorly understood.

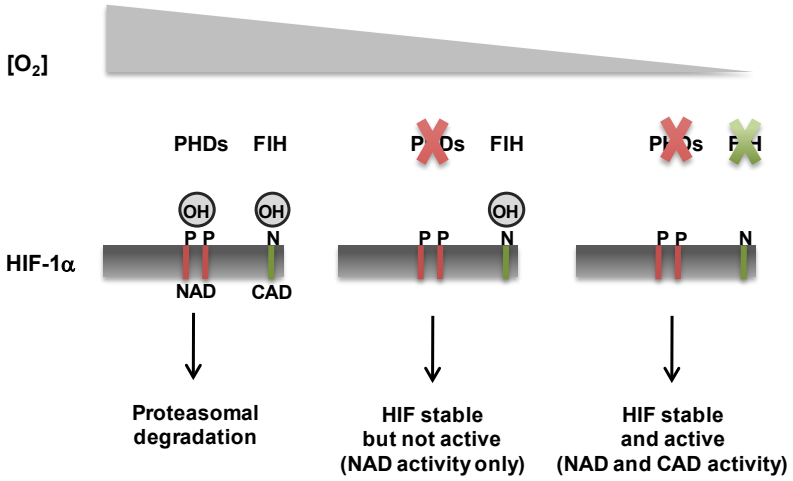

Figure 6. Hypothesized sequential activation of the NAD and CAD in gradients of hypoxia, predicted from *in vitro* derived Km values of PHDs and FIH for oxygen. Adapted from (Lisy & Peet, 2008).

1.2.3.5 P300/CBP. Nuclear p300 and CBP are homologous and ubiquitously expressed proteins which possess histone acetyltransferase activity (Yuan & Giordano, 2002). They act as transcriptional co-activators and are involved in the regulation of several transcription factors (Chan & La Thangue, 2001). p300 binds to the C-TAD of HIF-1α through its cysteine-histidine rich domain and increases transactivation of HIF-1, probably by increasing histone acetylation, which results in local remodelling of chromatin structure and greater access of the transcription factor to DNA (Carrozza et al, 2003). Inhibition of the interaction between p300/CBP and HIF-1α strongly abrogates hypoxia-induced gene expression (Kung et al, 2000). Interestingly, it has been shown that S-nitrosation on cysteine 800 of HIF-1α increases the interaction between p300 and HIF-1α, increasing its transcriptional activity (Yasinska & Sumbayev, 2003).

1.2.3.6 Other HIF-1 partners. The post-translational modifications of HIF-1α are rapidly and precisely modulated by the cellular oxygen concentration through complexes of proteins. The protein amplified osteosarcoma 9 (OS9) is another piece of the complex HIF-regulatory mechanisms since it is an essential component of a multiprotein complex that regulates HIF-1α levels in an O_2-dependent manner. OS-9 is known to interact with HIF-1α and PHD2 and is required for efficient hydroxylation and subsequent degradation of HIF-1α (Baek et al, 2005; Flashman et al, 2005). Recently, spermidine/spermine-N1-acetyltransferase-2 or SSAT2 was also shown to be an additional and essential component of the ubiquitin ligase complex VBC that binds to HIF-1α, VHL and elongin C and plays a crucial role in the rapid HIF-1α ubiquitination by the complex (Baek et al, 2007).

Deubiquitination, by reversing ubiquitination, has been recognized as an important regulatory step in ubiquitination-related processes. It has been shown that pVHL-interacting deubiquitinating enzyme 2 (VDU2 or Usp20), but not VDU1 (or Usp33), interacts with HIF-1α. Both proteins belong to the ubiquitin specific protease (USP) subclass of deubiquitinating enzymes and the enzymatic function is consistent with the presence of conserved Cys and His boxes in their molecular structures. Mutagenesis studies have demonstrated that these two conserved domains play important roles in the ubiquitin cleavage activity of both enzymes (Li et al, 2002a; Li et al, 2002b). In opposition to VDU1, VDU2 can specifically deubiquitinate and stabilize HIF-1α and increases expression of HIF-1 target genes (Li et al, 2005). These findings suggest that ubiquitination of HIF-1α is a dynamic process and that ubiquitinated HIF-1α might be rescued from degradation by VDU2 through deubiquitination.

The half-life of HIF-1α is also regulated in an O_2-independent manner by the competitive binding of either heat shock protein 90 (Hsp90), which stabilizes HIF-1α, or the anchoring receptor of the activated protein kinase C (RACK1), which interacts with elongin C, thereby promoting HIF-1α ubiquitination and proteasomal degradation, independently of PHD2 and VHL (Liu et al, 2007). Moreover, it has also been shown that histone deacetylase proteins (HDACs 4, 6 and 7) interact with HIF-1α, increasing the protein stability and transcriptional activity. Apparently, histone deacetylase inhibitors (HDACI) induce VHL and ubiquitin-independent proteasomal degradation of HIF-1α. Some authors have been shown that newly synthesized HIF-1α molecules interact with the molecular chaperones Hsp70 and Hsp90 to complete maturation. However, HDACI treatment apparently induces HDACs inhibition, resulting in hyperacetylation of Hsp90, accumulation of immature HIF-1α/Hsp70 complex and degradation by the proteasome (Kong et al, 2006). Nevertheless, the role of direct acetylation in the regulation of HIF-1α is controversial and poorly understood.

Other reports have also been showing that p53 is able to destabilize HIF-1α by a pVHL-independent mechanism. The regulation of HIF-1α by p53 is complex and still poorly understood. Mechanistically, the interaction between HIF-1α and p53 is proposed to be either direct or to be mediated by the p53 ubiquitin ligase murine double minute 2 (Mdm2). Consistently, there are

reports indicating that p53 is able to target HIF-1α for Mdm2-mediated ubiquitination and proteasomal degradation (Chen et al, 2003; Hansson et al, 2002; Ravi et al, 2000). However, the biological significance of such process is still unclear.

HIF-1α is also regulated by phosphorylation signalling cascades in an oxygen-independent manner. Both phosphoinositol 3-kinase (PI3K) and mitogen-activated protein kinase (MAPK) pathways can regulate HIF-1α protein levels, as well as its transactivation. Increased expression of HIF-1α via the PI3K signalling cascade may occur by gain-of-function mutations in upstream positive regulators, such as receptor tyrosine kinases and Ras, or loss-of-function mutations in tumour suppressors, such as phosphatase and tensin homolog (PTEN). The PI3K pathway can also increase the translation of HIF-1α mRNA by both mammalian target of rapamycin (mTOR)-dependent or -independent mechanisms (Maynard & Ohh, 2007). It is also known that phosphorylation of HIF-1α by MAPK improves the recruitment of p300/CBP to the C-TAD of HIF-1α, potentiating the transactivation of target genes (Sang et al, 2003). Phosphorylation of HIF-1α may also protect this subunit for exportin-dependent nuclear export (Mylonis et al, 2006).

Another important protein involved in HIF-1 regulation is the small ubiquitin-related modifier (SUMO), a member of the ubiquitin-like protein family. It has been shown that hypoxia induces SUMOylation of the ODD domain of HIF-1α by the SUMO-conjugating enzyme Ubc9 (Rizos et al, 2005). Interestingly, Chen *et al.* (2007) reported that VHL also recognizes and ubiquitinates SUMOylated HIF-1α. However, in the presence of the SUMO-specific isopeptidase SENP1, HIF-1α is deSUMOylated, escapes degradation and activates transcription of target genes (Cheng et al, 2007). Nevertheless, these findings are opposed to previous studies implicating SUMO in the activation of transcription, through HIF-1α stabilization. Indeed, recently was described a new hypoxia-induced protein, the RWD-containing SUMOylation Enhancer (RSUME), which overexpression enhances SUMO conjugation and has a stabilizing effect on HIF-1α (Carbia-Nagashima et al, 2007). Another study also reported that hypoxia-induced SUMOylation of HIF-1α reduces its transcriptional activity without affecting its half-life (Berta et al, 2007). Therefore, many important questions regarding the function of SUMOylation and deSUMOylation of HIF-1α remain unanswered.

1.2.4 HIF-1 target genes and biological functions

Many of the genes regulated by HIF-1, which are responsible for adaptation to low oxygen, also promote tumourigenic phenotypes and immortality of cancers. HIF-1 upregulates more than 70 genes that are involved in a plethora of adaptation and survival mechanisms, such as angiogenesis, anaerobic glucose metabolism, metastasis, cell motility, iron metabolism, growth, survival, apoptosis, telomere maintenance and drug-export mechanisms.

The most notable and well-known target protein induced by HIF-1 is VEGF (Carmeliet et al, 1998; Forsythe et al, 1996), a potent endothelial cell mitogen crucial for the angiogenic process.

HIF has also been shown to upregulate the expression of many other growth and survival factors for proliferation of new blood vessels, including TGF-α, TGF-β3, leptin, endoglin, survivin, cyclooxygenase-2, platelet-derived growth factor-β, insulin-like growth factor and insulin-like growth factor binding proteins 1-3 (Caniggia et al, 2000; Feldser et al, 1999; Grosfeld et al, 2002; Kaidi et al, 2006; Sanchez-Elsner et al, 2002; Tazuke et al, 1998; Zhang et al, 2003). In addition, HIF-1 induces the expression of nitric oxide synthase 2, heme-oxygenase-1 and endothelin-1 (Hu et al, 1998; Lee et al, 1997; Palmer et al, 1998), which increase the permeability and dilation of the vasculature. HIF further transactivates VEGFR-1 and -2 and the endothelial receptor tyrosine kinase Tie-2 (Elvert et al, 2003; Weidemann & Johnson, 2008).

The formation of new blood vessels further requires activation of genes that regulate matrix metabolism and remodelling, which increases the invasion potential of cells and changes the extracellular environment to promote migration. Indeed, hypoxia and HIF-1 activation regulate key players in this mechanism, such as autocrine motility factor, urokinase-type plasminogen activator receptor, collagen prolyl-4-hydroxylases, matrix metalloproteinases, E-cadherin (negatively), lysyl oxidase, tissue inhibitors of matrix metalloproteinases and the chemokine-receptor CXCR4 (Erler et al, 2006; Esteban et al, 2006; Gunaratnam et al, 2003; Maynard & Ohh, 2007; Weidemann & Johnson, 2008; Zagzag et al, 2005). The CXCR4-ligand stromal cell-derived factor-1 (SDF-1) is also induced by hypoxia and regulates adhesion, migration and homing of CXCR4-expressing EPCs. Increased expression and deposition of vimentin, an extracellular matrix component, is also regulated by HIF-1 and is known to induce dedifferentiation of extracellular matrix, promoting increased motility of cells (Maynard & Ohh, 2007).

To adapt to reduced oxygen availability and, subsequent, decreased oxidative phosphorylation, HIF-1 regulates multiple enzymes responsible for shifting the metabolism toward anaerobic glycolysis. Indeed, HIF-1 upregulates key glycolytic enzymes, such as phosphoglycerate kinase-1, lactate dehydrogenase A and pyruvate dehydrogenase kinase (PDK). PDK inhibits the enzyme pyruvate dehydrogenase by phosphorylation, which abrogates the conversion of pyruvate into acetyl-CoA, preventing pyruvate entry into the TCA cycle. Consequently, the oxygen consumption in the mitochondria decreases and the generation of reactive oxygen species under hypoxia is attenuated. Interestingly, the glucose metabolites pyruvate and oxaloacetate appear to regulate HIF-1α expression in cancer cell lines by inhibiting PHD-mediated hydroxylation of HIF-1α, contributing for a positive feedback control. HIF-1 also upregulates a more efficient isoform of cytochrome oxidase and the isoform predominant in normoxia is degraded by the HIF-1-regulated Lon protease. Moreover, the HIF-1 transcription factor increases the expression of the glucose transporters 1 and 3 and gluconeogenesis enzymes (Maynard & Ohh, 2007; Weidemann & Johnson, 2008).

Considering that glycolysis increases intracellular lactic acid concentration, HIF-1 also regulates intracellular pH. Indeed, HIF-1 has been demonstrated to regulate, at least, one member of the H^+/lactate co-transporter family, the monocarboxylate transporter that excretes lactic acid

from the cytoplasm. In addition, H^+ ions are transported out through the HIF-1-reguted Na^+/H^+ exchanger NHE1. Furthermore, HIF-1 also activates the expression of carbonic anhydrases IX and XII that convert the metabolic generated CO_2 into carbonic acid, which further contributes to intracellular alkalinization (Weidemann & Johnson, 2008).

Thus, HIF-1 mediates a wide range of developmental, physiological and cellular mechanisms that promote oxygen delivery to cells and allow cells to survive under oxygen deprivation.

1.3 The Ubiquitin-Proteasome Pathway

Before the discovery of the ubiquitin-proteasome system (UPS), proteolysis in cells was thought to rely primarily on lysosomes, which are membrane-bound organelles with an acidic lumen containing proteolytic enzymes that are able to degrade and/or recycle exogenous proteins, as well as aged and damaged organelles. Between the 1960s and 1980s, protein degradation was a neglected issue, considered to be a non-specific and dead-end process. Although it was known that proteins turn over, apparently by high specific processes, and that distinct proteins have half-lives that range from few minutes to several days, it was not widely appreciated. However, the discovery of the complex ubiquitin pathway revolutionized the field. Work on ATP-dependent protein degradation in reticulocytes, which lack lysosomes, suggested the presence of another intracellular degradation mechanism (Ciehanover et al, 1978). Subsequent work on post-translational modifications led to the identification of an unanticipated covalent modification of the histone 2A protein by a branched bond between a histone lysine residue and the C-terminal glycine residue of a protein called ubiquitin, which had no known function (Goldknopf & Busch, 1977). It was then found that a previously-identified protein associated with proteolytic degradation, known as ATP-dependent proteolysis factor 1 or APF-1, was the same protein as ubiquitin.

Much of the early work leading to the discovery of UPS occurred in the 1970s and early 1980s at the Technion (Israel Institute of Technology) in the laboratory of Avram Hershko, where Aaron Ciechanover worked as a graduate student. Hershko had spent a sabbatical year at the laboratory of Irwin Rose at the Fox Chase Cancer Centre, which provided key insights to the discovery. The three researchers shared the 2004 Nobel Prize in Chemistry for their work in discovering the UPP.

It is clear now that degradation of cellular proteins is a highly complex and regulated process that plays major roles in a variety of basic pathways, such as: 1) rapid removal of proteins; 2) regulation of gene transcription; 3) regulation of cell cycle; 4) protein quality control, through elimination of abnormally folded or damaged proteins; 5) function of the immune system, by involvement in the antigen presentation on MHC class I molecules; 6) source of amino acids; 7) inflammatory response, by NF-κB regulation; 8) cancer and cell survival, by p53 and HIF-1α regulation (Lecker et al, 2006). Therefore, with the innumerable UPS substrates and the myriad of

processes that UPS is involved, it is not surprising that abnormalities in the pathway are implicated in the pathogenesis of many diseases (Glickman & Ciechanover, 2002).

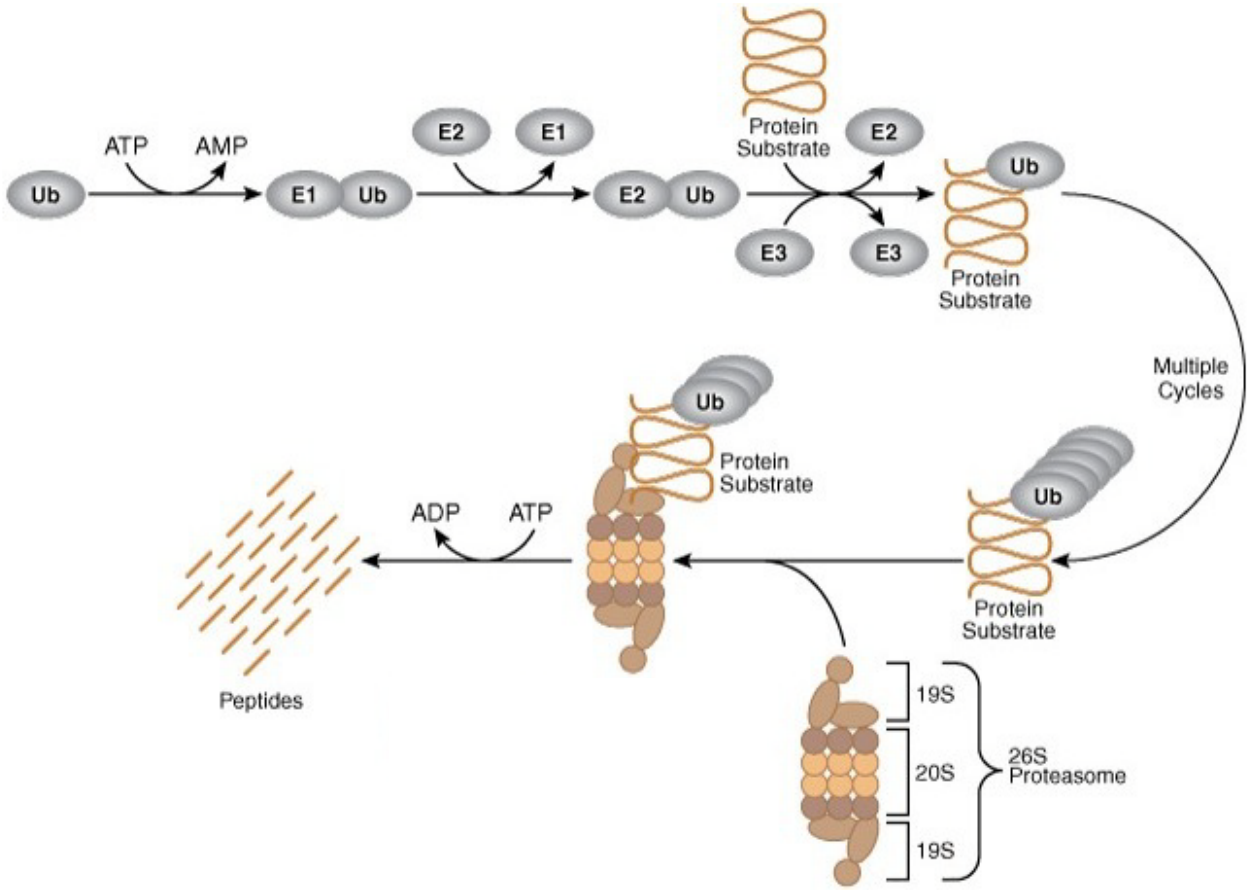

Figure 7. Schematic representation of the ubiquitin-proteasome pathway. Adapted from the *Cell SIgnaling Technology* website (www.cellsignal.com).

Degradation of a protein by UPS involves two distinct and successive steps: (i) covalent attachment of multiple ubiquitin molecules to the target protein; and (ii) degradation of the tagged protein by the 26S proteasome (Ciechanover, 1998; Glickman & Ciechanover, 2002; Myung et al, 2001). Conjugation of ubiquitin to the substrate occurs through a three step-mechanism. Initially, ubiquitin is activated in its C-terminal glycine (Gly 76) by the ubiquitin-activating enzyme, E1. This reaction involves hydrolysis of ATP to PPi (pyrophosphate) and generates a high-energy thiol ester intermediate. Following activation, ubiquitin is transferred by a transacylation reaction to the thiol group of the active site (a specific Cys residue) of an E2 enzyme (ubiquitin-carrier proteins or ubiquitin-conjugating enzymes, UBCs). Finally, E2 shuttles ubiquitin to a substrate either by itself or in cooperation with an ubiquitin-protein ligase (E3). The E3 enzyme catalyzes the last step in the conjugation process and it can occur either directly or indirectly. Some E3 enzymes directly mediate the covalent attachment of ubiquitin to the substrate, while other E3 enzymes function as a recognition/adaptor protein between the E2 enzyme and the substrate. In both situations, ubiquitin

is transferred to an ε-NH_2 group of a Lys residue of the substrate to generate an isopeptide bond. In successive reactions, a polyubiquitin chain is synthesized by transfer of additional ubiquitin moieties to Lys48 (K48) of the previously conjugated molecule. The chain serves as a recognition signal for the proteasome degradation (Ciechanover, 1998; Glickman & Ciechanover, 2002; Myung et al, 2001; Vernace et al, 2007) (Figure 7).

Together with K48, there are seven lysine residues in ubiquitin that can be used to form polyubiquitin chains: K6, K11, K27, K29, K33, K48 and K63. The least common of the 'linkage' sites are K27 and K29. K63 chain has an important role in several pathways, apparently independent on the degradation by the proteasome, including cell signalling, ribosomal function, DNA repair, activation of the NF-κB signalling complex and mitochondrial morphogenesis (Figure 8). K29 has similar characteristics as K48, while K6 chains seem to counteract proteasomal degradation (Shang et al, 2005; Vernace et al, 2007).

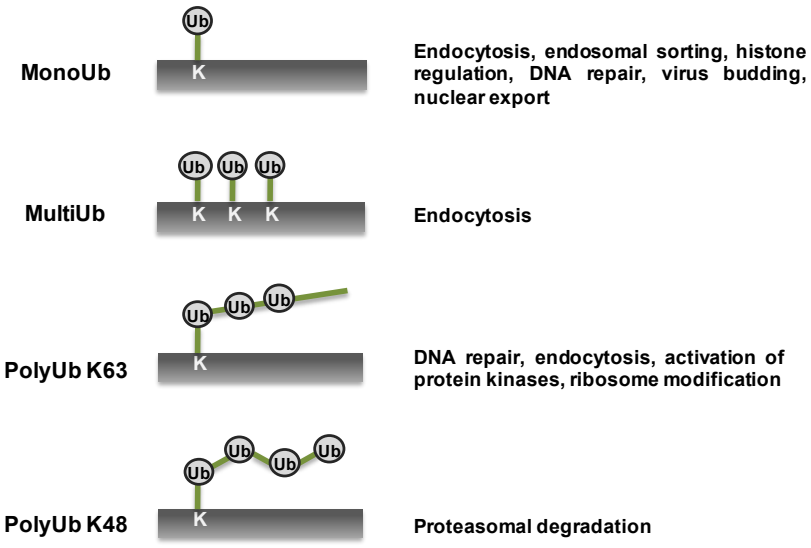

Figure 8. Schematic representation of the main ubiquitin chain formations.

Ubiquitination may also be regulated by deubiquitinating enzymes (DUBs), which cleave ubiquitin isopeptide linkages, remove ubiquitin molecules from ubiquitin-tagged proteins, recycle free ubiquitin in the cell and participate in the processing of ubiquitin precursors. DUBs can be grouped into, at least, five subfamilies based on their sequence similarities and mechanisms of action. Four of the subfamilies are cysteine proteases, while the fifth group is a zinc-dependent metalloprotease. The largest group of the cysteine proteases is the ubiquitin-specific protease (USPs) subfamily, which contains two well-conserved motifs, named Cys and His boxes, at the active site pocket. This subfamily can process ubiquitin precursors, remove ubiquitin from protein conjugates and disassemble ubiquitin chains. The second cysteine DUB subfamily is made up of the ubiquitin carboxy-terminal hydrolases (UCHs), which catalyze the removal of peptides or small molecules from the C-terminus of ubiquitin. Most UCHs cannot generate monomeric ubiquitin from

polyubiquitin chains. The remaining two cysteine protease subfamilies were discovered recently and include the ovarian tumour-related proteases (OTU) and the Machado-Josephin domain (MJD) group (Amerik & Hochstrasser, 2004).

The structure of the ubiquitination cascade appears to be hierarchical: apparently, a single E1 activates ubiquitin required for all conjugation reactions and transfers it to all known E2s. Each E2 acts with one or several E3s, and usually, most of E3s are found to interact with several different protein substrates via similar recognition motifs (Ciechanover, 1998; Glickman & Ciechanover, 2002; Hershko & Ciechanover, 1998) (Figure 9). However, this hierarchy is more complex and cannot be seen simply as a pyramid structure, but rather as a complex network of overlapping interactions between multiple components. For instance, specific E3s can often interact with more than one E2 and some substrates can be targeted by more than one E3. Moreover, each ubiquitinated substrate may also be targeted by several DUB enzymes.

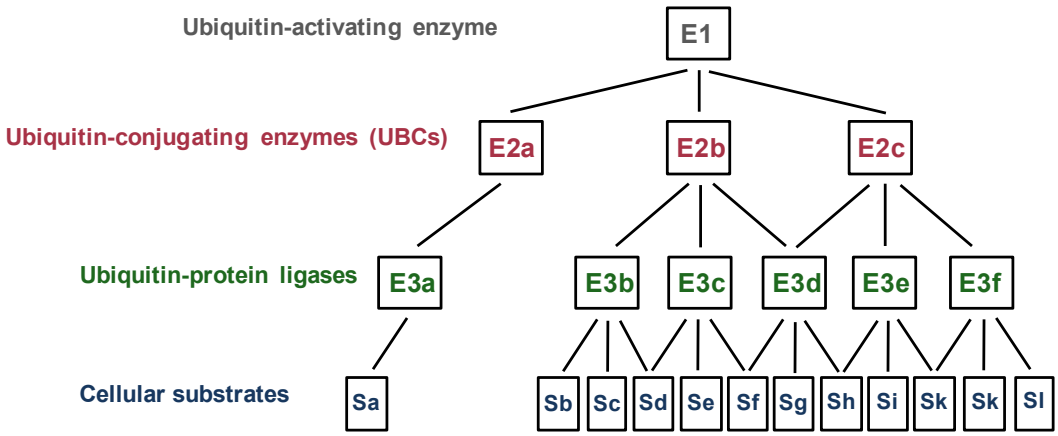

Figure 9. Schematic representation of the hierarchical structure of the ubiquitin system. Adapted from (Ciechanover, 1998).

1.3.1 The ubiquitin-conjugating machinery: E1, E2 and E3

1.3.1.1 E1 (ubiquitin-activating enzyme, UBA). E1 activates ubiquitin, via a two step intramolecular and ATP-dependent reaction, to generate a high-energy E1-thiolester~ubiquitin intermediate. The activated ubiquitin is then transferred to E2 (Hershko et al, 1983). Virtually, a single E1 appears to be responsible for the activation of ubiquitin required for all known ubiquitination processes. The yeast genome encodes for only one ubiquitin-activating enzyme, *UBA1*. Its deletion is lethal in yeast (McGrath et al, 1991) and mutation of the putative active-site Cys residue abolishes its ubiquitin-activation activity (Hatfield & Vierstra, 1992).

1.3.1.2 E2 (ubiquitin-conjugating enzymes, UBCs). The activated ubiquitin is transferred from E1 to a Cys residue of an E2 enzyme, generating another thiolester intermediate. Subsequently,

E2s catalyze covalent attachment of ubiquitin to target proteins or the transfer of the activated ubiquitin moiety to high-energy E3~ubiquitin intermediates when acting along with HECT [E6-associated protein (E6-AP) carboxyl terminus] homologous E3 proteins. They all share an ubiquitin-binding Cys residue active-site and are distinguished by the presence of a ~130 amino acid sequence (UBC domain) required for binding of distinct E3s. Mutation of the active-site Cys residue abolishes the UBC activity. Many E2s have been identified; at least, 13 in yeast (UBC 1-13) and many more in higher organisms (Glickman & Ciechanover, 2002; Hochstrasser, 1996; Myung et al, 2001).

1.3.1.3 E3 (ubiquitin-protein ligases). The E3 enzyme is a protein or a complex of proteins that interact both with the substrate and the E2 enzyme. The binding to the target substrate can occur either directly or indirectly, via ancillary proteins. In most cases, E3 acts like a scaffold that brings together the E2 and the substrate, facilitating the transfer of the activated ubiquitin-moiety from E2 to the substrate. In other cases, the activated ubiquitin is transferred from E2 to an internal Cys residue on E3 before conjugation of ubiquitin to an amine group in the target. Since the target proteins bind to the ubiquitin ligases prior to conjugation, E3s are key players in determining the high specificity of the UPP system (Ciechanover, 1994; Glickman & Ciechanover, 2002; Hershko & Ciechanover, 1998; Myung et al, 2001).

Although it has become clear that E3s are heterogeneous, they can be classified into three major groups: HECT domain family, RING finger family and U box-containing proteins (Figure 10).

In the HECT-domain E3s, the activated ubiquitin is transferred from E2 to a Cys residue on E3 before conjugation of ubiquitin to an ε-NH2 group of the target protein (Glickman & Ciechanover, 2002) (Figure 10). These E3 enzymes contain a 350-amino acid residue sequence homologous to the C-terminal sequence of E6-AP (Huibregtse et al, 1995). E6-AP is an associating protein of the E6 oncoprotein produced by human papillomavirus and was found to ubiquitinate the "genome guardian", p53. This sequence contains a conserved Cys residue to which the activated ubiquitin is transferred from E2.

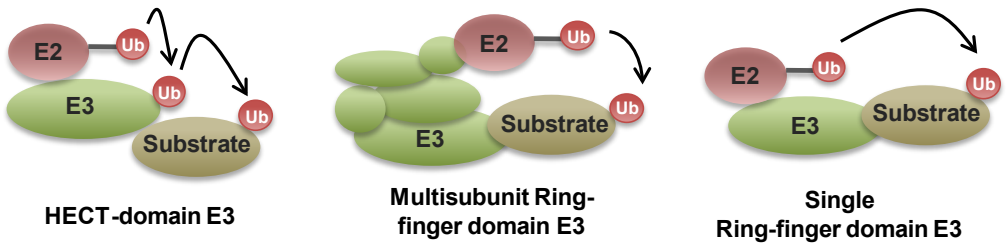

Figure 10. Schematic representation of the HECT-domain and Ring-finger domain E3 enzymes.

The RING finger domain E3s serve as a scaffold that brings together the E2 and the substrate and allows efficient transfer of the activated ubiquitin from E2 to the substrate (Jackson et

al, 2000; Joazeiro & Weissman, 2000). RING finger have been defined by a pattern of conserved Cys and His residues that form a cross-brace structure that binds two Zn^{2+} ions (Glickman & Ciechanover, 2002). The RING finger E3 family is composed of two distinct groups, single and multisubunit proteins (Figure 10). Certain members, such as Mdm2 (Geyer et al, 2000) and Parkin (Shimura et al, 2000), are monomers or homodimers and contain both the RING finger domain and the substrate-binding/recognition site in the same molecule. Many others are part of multisubunit complexes. Among them are the anaphase-promoting complex or APC (Page & Hieter, 1999) involved in degradation of cell cycle regulators, the pVHL-elonginB-elonginC-Cul2-Rbx1 complex (Iwai et al, 1999) involved in the degradation of HIF-1α and the Skp1-Cullin/Cdc53-F-box protein (SCF) complex involved in degradation of phosphorylated proteins involved in cell signalling and cell cycle (Deshaies, 1999). In the case of VBC, the RING finger domain component, Rbx1/Hrt1/ Roc1, is involved in E2 recruitment and assembly of other components of the complex, but not in substrate recognition (Glickman & Ciechanover, 2002). A different subunit, the pVHL subunit, carries out the substrate recognition function. The VBC appears to exhibit ubiquitin ligase activity only with E2s of the UbcH5 family (Glickman & Ciechanover, 2002).

The third family of E3 enzymes, the U box-containing proteins, are a modified version of the RING finger proteins, which lack the metal-chelating residues of the RING finger motif (Aravind & Koonin, 2000). Most of the conserved Cys residues of the RING finger are not conserved in the U-box. The structure is likely to be stabilized by hydrogen bonds and salt bridges (Glickman & Ciechanover, 2002). The molecular mechanisms by which U box-enzymes carry out ubiquitination and ubiquitin-chain elongation remain elusive. It is also unclear how behaves the E2-E3-substrate complex and the mechanism of ubiquitin transfer from E2 to the substrate. An interesting member of the family is CHIP (carboxy terminus of Hsc70-interacting protein) or STUB-1 (STIP1 homology and U-Box containing Protein-1), which binds abnormal or misfolded proteins that are recognized by molecular chaperones, leading to their degradation by the proteasome (Hoppe, 2005; Murata et al, 2003).

1.3.2 The structure of the proteasome

The proteasome holoenzyme (also known as the 26S proteasome) is a ~ 2.5MDa complex and recognizes specifically ubiquitin-tagged proteins. The overall structure can be divided into two major subcomplexes: the 20S core particle (CP) that contains the protease subunits and the 19S regulatory particle (RP) that regulates the function of the 20S CP (Glickman et al, 1998a; Groll et al, 1997). The size of the proteasome is about 150 angstroms (Å) by 115 Å and is relatively conserved between species. The interior chamber is about 53 Å wide and the entrance can be as narrow as 13 Å, suggesting that substrate proteins must be, at least partially, unfolded to enter inside the CP (Nandi et al, 2006) (Figure 11).

1.3.2.1 The 20S CP. The resolution of the crystal structure of the yeast 20S proteasome was an important advance in the studies of the 26S proteasome (Groll et al, 1997). The structure of the 20S is well conserved in virtually all organisms ranging from archaebacteria to humans (Myung et al, 2001): a hollow and barrel shape consisting of four stacked heptameric rings, forming a central chamber between both tips. Each ring is composed of seven subunits, which may be classified into two groups: the α-subunits (the outer two rings) and the β-subunits (the inner two rings). Thus, the general structure of the complex is $\alpha_{1\text{-}7}\beta_{1\text{-}7}\beta_{1\text{-}7}\alpha_{1\text{-}7}$ (Ciechanover, 1998; Glickman & Ciechanover, 2002; Myung et al, 2001). The two β-inner rings contain the proteolytic active sites (chymotrypsin-, trypsin- and caspase- or post-glutamyl peptidyl hydrolytic-like sites) facing inward into the proteolytic chamber (Orlowski & Wilk, 2000). The catalytic inactive α-chains play an essential role in stabilizing the two-ring structures of the β-chains and also play a role in the binding of the 19S cap regulatory complexes. The NH_2 termini of the α-subunits obstruct the access to the proteolytic chamber, suggesting that the proteasome channel is gated. The entry of substrates into the CP and the exit of the proteolytic products are blocked by the NH_2-terminal residues, which must be dislocated and rearranged in order to allow entrance and discharge of proteins/peptides (Ciechanover, 1998; Glickman & Ciechanover, 2002; Myung et al, 2001).

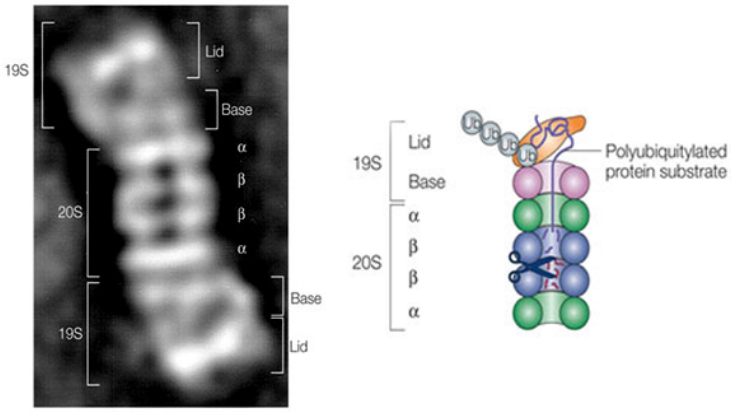

Figure 11. Electron-microscopy image of a 26S proteasome from *S. cerevisiae* and schematic representation of the 26S proteasome structure. Adapted from (Ciechanover, 2005).

1.3.2.2 The 19S RP. The 19S (also known as P700) serves multiple roles in regulating proteasomal activity: selecting substrates, preparing them for degradation, opening the 20S CP gated channel and translocating the unfolded substrates into the CP. In contrast to the ancestral proteasome found in archaebacteria, the eukaryotic proteasome contains an additional 19S regulatory complex, consisting of a lid and a base that binds to the 20S particle to form the 26S proteasome. The lid is known to recognize ubiquitinated substrates with high fidelity, whereas the base unfolds protein substrates and translocates them into the catalytic chamber of the 20S particle, in an ATP-dependent manner (Ciechanover, 1998; Glickman & Ciechanover, 2002; Myung et al, 2001). The base contains six ATPase subunits and caps the end of the 20S CP.

1.3.3 The mechanism of proteasome action

1.3.3.1 Ubiquitin recognition. After a protein has been ubiquitinated, it is recognized by the 19S RP in an ATP-dependent binding step. Chains containing at least four molecules of G76-K48 isopeptide-linked ubiquitin are necessary for efficient binding to the proteasome (Thrower et al, 2000). The relationship between binding to the proteasome and chain length is not proportionally cumulative, since chains of four ubiquitin molecules bind 100 times better than chains of two ubiquitins, whereas there is only 10-fold increase when eight more ubiquitin molecules are added to the chain (Glickman et al, 1998b; Rubin et al, 1998). Apparently, it is the surface provided by the four-subunit structure of a polyubiquitin chain that is recognized by the proteasome. The quaternary structure of ubiquitin polymers and the exact spatial relationship between each ubiquitin molecule is also critical for their ability to target substrates for degradation by the proteasome. Modification of proteins by polyubiquitin chains linked via Lys63 does not target proteins for proteasomal degradation, while polyubiquitin chains linked via Lys6, Lys11 and Lys48 all bind to the proteasomal subunit Rpn10 with similar affinities (Glickman & Ciechanover, 2002; Pickart, 2000; Thrower et al, 2000).

1.3.3.2 Substrate binding. It is plausible that all eight components of the base may engage in direct interactions with the substrates. The substrate must be properly positioned to be unfolded by the base and translocated into the CP; the distal positioning of the lid ensures that the ubiquitin chain on the substrate does not occlude access of the target protein to the channel.

Proteolysis of proteins by the proteasome is strictly ATP-dependent. It is likely that hydrolysis of ATP, cycles the RP between high- and low-affinity states, alternatively binding and releasing substrate (DeMartino et al, 1994; Glickman & Ciechanover, 2002; Hershko et al, 1984).

1.3.3.3 Unfolding, gating and translocation. The conformational changes associated with the ATPase cycle can be used in three processes: (i) gating the channel defined by the NH_2 termini of the α-ring subunits of the CP; (ii) unfolding the substrate; (iii) translocating the unfolded substrate through the channel into the lumen of the CP (Glickman & Ciechanover, 2002; Glickman et al, 1998b). Apparently, unfolding of protein substrates is required, since the estimated inner diameter of the CP channel is too narrow for proteins to enter in their naive state (Groll et al, 2000). Moreover, the passage of the unfolded substrate into the core requires prior deubiquitination of the substrate. The extent to which substrates must be unfolded before translocation is not known, but tertiary structure and some interactions, such disulfide bonds, are sufficient to inhibit degradation.

1.3.3.4 Deubiquitination. The polyubiquitin chain must be removed from the substrate by the RP before the substrate can be translocated via the narrow channel into the proteolytic chamber of the CP. Moreover, ubiquitin is also a product of the proteasomal degradation mechanism; ubiquitin is

released from the proteasome and recycled back into the ubiquitin pathway. The RP has been shown to contain an ubiquitin hydrolase that can act as deubiquitinating enzyme, removing ubiquitin from the substrates (Eytan et al, 1993; Holzl et al, 2000; Lam et al, 1997a; Lam et al, 1997b).

1.3.3.5 Proteolysis. In most cases, proteasomes cleave protein substrates into small peptides, varying between 3 and 23 amino acids in length, (Kisselev et al, 1999) and the proteins are hydrolyzed to the final products before the next substrate enters into the lumen. The peptide products of the proteasome are short lived and do not accumulate in the cell. Most of these peptides are rapidly hydrolyzed by downstream proteases and aminopeptidases (Glickman & Ciechanover, 2002).

The three β-subunits of the 20S CP, with proteolytic activities, preferentially cleave after different amino acids: β1 subunit (caspase-activity) cleaves after acidic or small hydrophobic amino acids, β2 (trypsin-activity) cuts after basic or small hydrophobic amino acids, while β5 (chymotrypsin-activity) hydrolyzes the peptide bond after hydrophobic residues containing aromatic rings (Dick et al, 1998). The mechanism of proteolysis by the β subunits of the 20S CP occurs through a threonine-dependent nucleophilic attack. This mechanism depends on a water molecule for deprotonation of the reactive threonine hydroxyl group.

1.3.4 Proteasome inhibitors

Most of the currently available inhibitors of the ubiquitin-proteasome pathway directly target and inhibit the 20S proteasome, the core of the proteolysis machinery, rather than the upstream ubiquitination and/or recognition of ubiquitinated protein substrates. These proteasome inhibitors are broadly categorized into two groups: synthetic analogs and natural products (Myung et al, 2001; Nalepa et al, 2006). Synthetic inhibitors are peptide-based compounds with diverse pharmacophores. These include peptide benzamides, peptide α-ketoamides, peptide aldehydes (ex. MG132, PSI), peptide α-ketoaldehydes, peptide vinyl sulfones (ex. NLVS, YLVS) and peptide boronic acids (ex. MG262, PS341). In contrast, natural proteasome inhibitors display a variety of core structures, as well as of pharmacophores. Known natural proteasome inhibitors include linear peptide epoxyketones (ex. epoxomicin), peptide macrocycles, γ-lactam thiol esters (ex. lactacystin) and the epipolythiodioxopiperazine toxin.

Peptide aldehydes have been widely used as inhibitors for both serine and cysteine proteases. Given that the aldehyde functional group is readily subjected to a nucleophilic attack by hydroxyl or thiol groups and that the proteasome uses the hydroxyl group of the amino terminal threonine as a nucleophile, it is not surprising that the commercially available peptide aldehydes were the first proteasome inhibitors to be identified. MG132, MG115 and PSI are all cell permeable and potent aldehyde inhibitors of the chymotrypsin-like activity, being widely used in studying the role of the proteasome in several cellular processes (Myung et al, 2001). Lactacystin and

epoxomicin are also frequently used in laboratory research and are the best known natural product inhibitors of the 20S proteasome (Dick et al, 1996; Meng et al, 1999). In opposition to MG132 and lactacystin, which show non-target specificity, epoxomicin is highly specific for the 20S proteasome.

Proteasome inhibitors have effective anti-tumour activity in cell culture, inducing apoptosis by disrupting the regulated degradation of pro-growth cell cycle proteins. This approach of selective induction of apoptosis in tumour cells has been shown to be highly effective in animal models and human trials. Bortezomib, a molecule developed by Millennium Pharmaceuticals and commercialized as Velcade, is the first proteasome inhibitor to reach clinical use as a chemotherapy agent. Bortezomib is used with high efficiency in the treatment of multiple myeloma (Hideshima et al, 2001).

1.4 CHIP-Dependent Protein Quality Control

Appropriate protein folding is crucial for optimum protein performance and normal cellular function. The protein quality control is a posttranslational mechanism whereby the molecular chaperones fold newly synthesized proteins and either refolds or degrades polypeptides that fail to reach or maintain a native structure, avoiding cellular impairment. This quality control system is essential because it prevents the accumulation of misfolded polypeptides with exposed hydrophobic surfaces that cause toxic-protein aggregation events. The inability to degrade obsolete proteins is frequently associated with some neurodegenerative disorders, such as Alzheimer's and Parkinson's disease (Cyr et al, 2002; McDonough & Patterson, 2003). The central players in the protein quality control are the molecular chaperones and the proteases. Indeed, chaperones bind exposed hydrophobic patches on proteins and facilitate the folding of nascent polypeptide chains, prevent protein aggregation and refold stress-damaged proteins. However, when an obsolete protein is not properly folded, it is somehow recognized as misfolded and degraded by the ubiquitin-proteasome pathway. It has been shown that the U-box containing protein CHIP is a crucial player in this quality control mechanism.

The heat-shock proteins 70 and 90 are major components of the cytosolic quality control machinery and assist both protein folding and degradation (Frydman, 2001; Hohfeld et al, 2001). To correctly fold proteins, both chaperones function together with other folding factors, termed as co-chaperones. Co-chaperones are known to regulate ATP hydrolysis, recognize non-native proteins and allow their interaction with the polypeptide-binding domains of Hsp70 and Hsp90. The most common co-chaperones that assist Hsp70 in protein folding include the Hsp40 proteins (Hdj1/Hdj2), Hip and Hop (Frydman, 2001; Hohfeld et al, 2001). On the other hand, Hsp90 is regulated by co-chaperones that include Hop, cyclophilins and p23 (Caplan, 1999; Young et al, 2001). In some cases, Hsp70 and Hsp90 function, sequentially, to fold the same substrate and Hop acts as a link between both chaperones. Conversely, to degrade proteins, Hsp70 and Hsp90 appear to interact with a set of co-chaperones that have degradation functions, such as Bag-1 and CHIP (Hohfeld et

al, 2001). However, Hsp40 is also a crucial component of the degrading machinery. Apparently, domains within these co-chaperones enable them to interact both with chaperones and with components of the ubiquitin-proteasome system (Figure 12). For instance, the choice between folding and degradation has become to be known as “molecular triage” (McDonough & Patterson, 2003), which relies both in different and common molecular players.

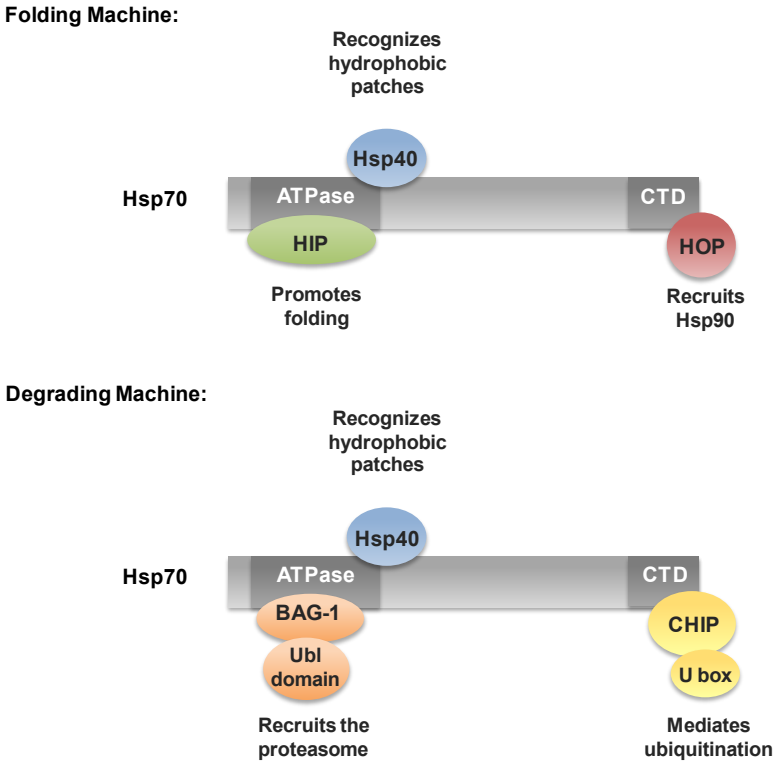

Figure 12. Schematic representation of the Hsp70 chaperone machines. Binding of distinct co-chaperones to Hsp70 may give rise to distinct chaperone machines involved in protein folding or protein degradation. Adapted from (Hohfeld et al, 2001).

The correct folding of nascent proteins involves the sequential action of multiple molecular chaperones and this process can take many minutes or even longer, and may often be unsuccessful (Frydman, 2001; Goldberg, 2003; Hartl & Hayer-Hartl, 2002). A large fraction of newly synthesized proteins is rapidly degraded. Over 30% of nascent proteins in eukaryotes are not properly folded and undergo rapid degradation (Goldberg, 2003; Schubert et al, 2000). Even when proteins are normally folded into the tertiary structure, the high density of protein molecules in the cytosol increases the spontaneous denaturation, which increases the probability of off-pathway reactions, such as aggregation. In addition, environmental stresses, such as heat, oxidation, glycation, high salt concentrations and ultraviolet, can result in the production of damaged proteins (Murata et al, 2001). However, these proteins with non-native or incorrect structures are rapidly removed inside the cell by the proteolytic systems (Goldberg, 2003; Murata et al, 2001; Wickner et al, 1999), which often rely on CHIP-mediated degradation mechanisms.

1.4.1 Characterization of CHIP

The CHIP cDNA encodes a 34.5 kDa protein containing three 34 amino-acid TPR (tetratricopeptide) domains at the N-terminal (Ballinger et al, 1999) and a U-box domain at the C-terminal (Murata et al, 2001) (Figure 13). The TPR domains bind molecular chaperones, such as Hsp70 and Hsp90 (Ballinger et al, 1999; Connell et al, 2001; Cyr et al, 2002; Scheufler et al, 2000), while the U-box domain plays a role in targeting proteins for ubiquitination and subsequent proteasome-dependent degradation. Between the TPR and U-box domains exists a central domain containing a high content of charged residues and two putative nuclear localizing signals (McDonough & Patterson, 2003).

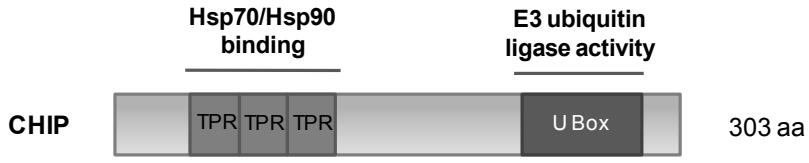

Figure 13. Schematic representation of the CHIP protein domains. Adapted from (Hohfeld et al, 2001).

CHIP homology studies across species indicate that human CHIP shares 98% amino acid similarity with mouse and 60% similarity with *Drosophila*. Significantly, the most highly conserved region is present at the U-box domain, having 87% homology among these species (Ballinger et al, 1999; McDonough & Patterson, 2003).

The tissue distribution of CHIP mRNA reveals that CHIP is ubiquitous expressed, being detected in the pancreas, lung, liver, placenta, kidney, skeletal muscle, heart and brain (McDonough & Patterson, 2003). However, CHIP is most highly expressed in tissues with high metabolic activity and protein turnover, such as heart, brain and skeletal muscle. CHIP can also be detected in most cell lines and primary cell cultures (Ballinger et al, 1999). CHIP is mainly localized at the cytosol, but it is also present in the nucleus (Meacham et al, 2001). Apparently, CHIP may undergo intracellular trafficking in response to cellular stress.

Through a yeast two-hybrid screening and *in vitro* binding assays, CHIP was shown to be a bona fide interaction partner with the major cytoplasmic chaperones, Hsc70 (constitutive isoform) and Hsp70 (inducible isoform) (Ballinger et al, 1999; McDonough & Patterson, 2003). The TPR domain and an adjacent charged region of CHIP (1-197 amino acids) are necessary for interaction with both proteins. CHIP interacts with the C-terminal domain of Hsc70 (540-650 amino acids region), which is known to contain a TPR-acceptor site that also interacts with the co-chaperone Hop through a TPR domain (Demand et al, 1998). However, is the N-terminal ATP-binding domain of Hsc70/Hsp70 that regulates substrate binding in a nucleotide-dependent manner. The molecular co-chaperone Hip promotes substrate binding by stabilizing the ADP-bound conformation (Hohfeld et al, 1995; Minami et al, 1996), whereas Bag-1 promotes substrate release by exchanging ATP for

ADP (Hohfeld & Jentsch, 1997). In contrast, CHIP inhibits the hydrolysis of ATP, which attenuates the substrate binding and refolding, leading to inhibition of the folding-refolding pathway dependent on Hsp70-Hcs70. This activity may provide a way to slow down the Hsp70 reaction cycle, under stressful conditions, or it may assist in targeting misfolded proteins to the UPP (McDonough & Patterson, 2003).

CHIP is also known to interact with Hsp90 and this interaction has approximately equivalent affinity as the interaction between CHIP and Hsp70 (Connell et al, 2001). However, in this case, CHIP seems to inhibit the function of proteins that require Hsp90 for conformational activation. For example, CHIP inhibits GR (glucocorticoid receptor) binding to Hsp90 and steroid-dependent transactivation ability. This effect of CHIP is accompanied by decreased steady-state levels of GR due to increased polyubiquitination and proteasome-dependent degradation of GR. This effect is both dependent on the U-box and TPR domains, suggesting that CHIP directly interacts with Hsp90 and directly induces ubiquitination of GR and its delivery to the proteasome (McDonough & Patterson, 2003). These interactions are not limited to GR; ErbB-2, another Hsp90 client protein, is also degraded by CHIP in a proteasome-dependent manner (Xu et al, 2002). However, these interactions are not limited to Hsp90 client proteins; cystic fibrosis transmembrane conductance regulator (CFTR), an Hsp70 client protein, undergoes CHIP-dependent degradation (Meacham et al, 2001) and luciferase undergoes CHIP-dependent ubiquitination *in vitro*, when it is misfolded and interacts with Hsp70 (Murata et al, 2001). In all the cases, the effects of CHIP are dependent on both the TPR and the U-box domains (McDonough & Patterson, 2003). However, the means by which ubiquitination occurs is not clear. In the case of ErbB-2, ubiquitination depends on the transfer of the client protein from Hsp90 to Hsp70 (Xu et al, 2002), indicating that the final ubiquitination complex consists of CHIP, Hsp70 and ErbB-2.

Despite slightly differences between the several CHIP-triggered mechanisms, all of them are consistent with a role for CHIP as a key component of the protein quality control mechanism dependent on molecular chaperones, which targets modified, misfolded and/or damaged proteins to the proteasome (McDonough & Patterson, 2003). Indeed, several lines of evidence suggest that CHIP participates in substrate “delivery” to the proteasome. For example, CHIP interacts with the S5a proteasome subunit, in yeast two-hybrid and GST pull-down assays, and the HC8 particle of the proteasome is detected in CHIP immunoprecipitates. Moreover, CHIP was shown to co-localize with the proteasome in cells treated with proteasome inhibitors. Thus, these and other evidences provide further support for the model that CHIP may participate in the delivery of misfolded and ubiquitinated proteins to the proteasome for degradation (McDonough & Patterson, 2003; Meacham et al, 2001; Murata et al, 2001).

Canonically, it is accepted that the ubiquitin ligase activity of CHIP depends on interactions with a specific family of E2 enzymes, the UBC4/UBC5 family, which in humans comprises the E2s UbcH5a, UbcH5b and UbcH5c (Jiang et al, 2001; Murata et al, 2001). Interestingly, the UBC4/UBC5 family members are “stress-activated” ubiquitin-conjugating enzymes (Seufert &

Jentsch, 1990). However, CHIP was also found to interact with the E2 UbcH13/Uev2a complex (Zhang et al, 2005). Moreover, it has been shown that the type of ubiquitin chain generated by CHIP mostly depends on the E2 associated. For example, purified CHIP with UbcH5 can form polyubiquitin chains containing all the seven (Lys^{6}, Lys^{11}, Lys^{27}, Lys^{29}, Lys^{33}, Lys^{48} and Lys^{63}) isopeptide linkages (Kim et al, 2007); however, K48 and K63 chains are the most abundant linkages formed by the CHIP/UbcH5 complex. In the case of the CHIP/UbcH13/Uev2a complex, it only has the ability to form Lys^{63} linkages (Kim et al, 2007; Zhang et al, 2005). However, the finding that CHIP can form polyubiquitin chains that contain all possible linkages and bifurcations raises a question about the biological significance of these novel chains.

CHAPTER 2

Chapter 2. Objectives

An increasing body of literature indicates that increased production of methylglyoxal (MGO) has an important role in the onset and development of many diabetic complications. For example, MGO is known to induce vascular dysfunction and increased cell death of pericytes and endothelial cells on diabetes. Moreover, increased levels of MGO have deleterious effects in proteins involved in a number of essential signalling pathways, such as the epidermal growth factor receptor (EGFR), the insulin-like growth factor 1-receptor (IGF1-R) and the protein serine/threonine kinase Raf-1 pathways. Therefore, the main goal of this study was to elucidate critical molecular mechanisms that underlie MGO-induced cell dysfunction on diabetes.

A main feature of diabetic complications is the impairment of the cell response to hypoxia, which is associated with vascular dysfunction and cell death. The cell response to low oxygen is primarily regulated by the transcription factor HIF-1 (hypoxia-inducible factor-1), which is responsible for the activation of protective and adaptive mechanisms that help cells to cope with hypoxia. Therefore, any mechanism that destabilizes HIF-1 is likely to have a negative impact on cell adaptation to hypoxia. Recently, it has been shown that hyperglycaemia leads to downregulation of HIF-1 and that the blood glucose levels are in linear relation with fatal outcome after an acute hypoxic challenge, suggesting a deleterious influence of hyperglycaemia on the ability of tissues to adapt to low oxygen. However, the molecular mechanisms involved in destabilization of HIF-1 by high glucose remain elusive. In this work, we hypothesize that increased production of MGO is the link between hyperglycaemia and destabilization of HIF-1 in diabetes. Therefore, one of the main purposes of this work was to investigate the molecular mechanisms implicated in destabilization of HIF-1 by high glucose or increased levels of MGO.

Considering that, as an indirect effect of downregulation of HIF-1, MGO may decrease the levels of VEGF (vascular endothelial growth factor) secreted by cells and that MGO increases the expression of Ang-2 (angiopoietin-2), through inactivation of the Ang-2 gene co-repressor mSin3A (mammalian Sin3 homolog A), we further aimed to study the effect of the crosstalk between these two events in endothelial cell function. Ang-2 is known to be a key destabilizing signal for vessels, leading to their regression in the absence of pro-angiogenic factors, such as VEGF. Therefore, we hypothesize that a MGO-induced imbalance between these two growth factors may lead to endothelial cell death and vascular regression, which are main features of diabetes.

Finally, this study also aimed to address the role of MGO in the function of protein quality control system, since diabetes is characterized by the accumulation of modified and toxic proteins and impairment of critical components of this system.

Altogether, this study aimed at understanding the central role of MGO in critical features of many diabetic complications, such as the loss of cell response to hypoxia and the accumulation of obsolete and toxic proteins, both contributing to cell damage and endothelial dysfunction. By

understanding these molecular mechanisms, it might be possible to envision new therapeutic approaches to diabetes and to generate new animal models that may help to elucidate critical aspects of the disease.

CHAPTER 3

Chapter 3. Material and methods

3.1 Cell culture and treatments

The retinal pigment epithelium cell line ARPE-19 (LGC Promochem, Teddington, UK) was cultured in Dulbecco's modified Eagle's medium/Ham's F12 (DMEM:F12) (1:1) supplemented with 10% fetal bovine serum (FBS), antibiotics (100 U/ml penicillin, 100 μg/ml streptomycin and 250 ng/ml amphotericin B) and GlutaMax (1x). The renal cell carcinoma cell line RCC4 VHL $^{-/-}$ (kindly provided by Dr. C. Buys from the University Medical Centre of Groningen) was grown in RPMI (Roswell Park Memorial Institute) 1640 medium also supplemented with 10% FBS, antibiotics and glutamine. The conditionally immortalized rat retinal endothelial cell line TR-iBRB (Hosoya et al, 2001) was maintained at 33ºC under 5% CO_2 in Dulbecco's modified eagle medium (DMEM) with low glucose (5.5 mM), supplemented with 10% FBS, 100 U/ml penicillin and 100 μg/ml streptomycin. All media, GlutaMax and antibiotics were purchased from Invitrogen (Carlsbad, CA, USA). When appropriated, cells were treated with the following agents: 10 μM epoxomicin (Boston Biochem, Cambridge, MA, USA), 20 μM MG132 or Z-LLL-CHO (Calbiochem, San Diego, CA, USA), 10 μM MG262 or Z-Leu-Leu-Leu-B$(OH)_2$ (Boston Biochem, Cambridge, MA, USA), 250 μM cobalt chloride ($CoCl_2$; Sigma-Aldrich, St. Louis, MO, USA), 1 - 3 mM methylglyoxal (MGO; Sigma-Aldrich, St. Louis, MO, USA), recombinant $VEGF_{165}$ (R&D Systems, Minneapolis, MN, USA) and recombinant Ang-2 (R&D Systems, Minneapolis, MN, USA). An incubator Nuaire N4950E (Nuaire, Plymouth, MN, USA) was used to perform the hypoxic treatments (2% O_2, 5% CO_2, 37ºC). For the treatments of TR-iBRB cells with the pre-conditioned media of ARPE-19 cells, Centricon centrifugal filter devices (Millipore-Chemicon, Billerica, MA, USA) with a 10 NMWL membrane were used to eliminate MGO that might remain in the media following the treatments of ARPE-19 cells. The components of the pre-conditioned media (3 ml of total volume) were concentrated to a volume of 100 μl and subsequently resuspended to a final volume of 3 ml with fresh medium. Levels of MGO in the media were assessed by HPLC through MGO derivatization with 1,2-diamino-4,5-dimethoxybenzene reagent (DDB; Invitrogen, Carlsbad, CA, USA), as mentioned below. Levels of MGO that remained in the culture medium after centrifugation and resuspension were virtually undetectable (at least, lower than the detection limit of the HPLC system).

3.2 Animal models

Male diabetic Goto-Kakizaki (GK) and control Wistar rats (6 months old) were obtained from local breeding colonies maintained at the animal facility of the Faculty of Medicine – University of Coimbra by the group of Dr. Raquel M. Seiça (Physiology Group). The animals were subjected to a constant daily cycle of 12 hours of light and 12 hours dark with constant temperature (22 - 24ºC)

and humidity (50 - 60ºC). Rats were given free access to water and to standard commercial pellet chow diet (AO4; Panlab, Barcelona, Spain). After anesthetization and sacrifice, eyes were enucleated and retinas isolated. Retinas were frozen in liquid nitrogen or in OCT tissue embedding matrix (Thermo Scientific, Waltham, MA, USA) at -45ºC for subsequent cryosectioning. All procedures involving animals were performed in accordance with the Association for Research in Vision and Ophthalmology (ARVO) Statement for the Use of Animals in Ophthalmic and Vision Research. Retinas used for Western Blot (WB) or HPLC were homogenized with a Potter Elvehjem homogenizer in 300 µl of lysis buffer [50 mM Tris-HCl pH 7.4, 250 mM NaCl, 1% NP-40 and 1x protease inhibitor cocktail (Roche Applied Science, Indianapolis, IN, USA)], incubated for 1 hour on ice and briefly sonicated. Cell lysates were centrifuged at 16,000 g for 10 minutes at 4ºC, the supernatants were transferred to new tubes and used to determine protein concentration through the BCA method (Pierce-Thermo Scientific, Waltham, MA, USA). In the case of lysates used for HPLC, 100 µl of sample (at 1 µg/µl) were mixed with 100 µl 0.2 M HCl and all other procedures were performed as explained below. In the case of samples used for WB, they were denaturated with 2x Laemmli buffer and boiled at 100ºC for 5 minutes. Samples were then separated by SDS-PAGE, transferred onto polyvinylidene fluoride (PVDF) membranes and immunoblotted for several proteins, as mentioned on the WB method (below).

3.3 Measurement of the blood glucose and glycated haemoglobin levels

Rat blood samples were collected after overnight fasting from the tail vein. Fasting glycaemia and glycaemia at 2 hours after intraperitoneal glucose administration (1.8 g/kg) were determined through the glucose oxidase method using an Elite Glucometer (Bayer, Berlin, Germany). The percentage of glycated hemoglobin in the plasma was determined using a DCA 2000+ Analyzer (Bayer, Berlin, Germany).

3.4 *In-vivo* Evans blue staining of retinal vessels

Animals were anesthetized [ketamine chloride (75 mg/kg, im, Parke-Davis, Ann Arbor, MI, USA) and chlorpromazine chloride (2.65 mg/kg, im, LabVitoria, Amadora, Portugal)] and injected through the jugular vein with an Evans blue (Sigma- Aldrich, St. Louis, MO, USA)-PBS solution (100 mg/Kg of body weight). Evans blue is a dye that combines with plasma albumin, allowing for detection of vessel leakage sites. Thirty minutes later, the animals were killed by cervical dislocation and the eyes were enucleated. Retinal whole flat mounts were prepared. Briefly, the retina was dissected after vitreous removal and spread on clean glass slides and mounted in medium under coverslips. Retinal flat mounts were analyzed by a Leica DFC350 FX fluorescence microscopy (Leica-Microsystems, Bannockburn, IL, USA) to evaluate the capillary leakage sites.

3.5 Western blot analysis

After appropriate treatments, cells were washed twice in phosphate-buffered saline (PBS) solution, denatured with 2x Laemmli buffer, boiled at 100ºC for 5 minutes and sonicated. Whole cell extracts were resolved by SDS-PAGE and electrophoretically transferred onto polyvinylidene fluoride (PVDF) membranes. The membranes were blocked with 5% nonfat milk in TBS-T (20 mM Tris, 150 mM NaCl,0.2% Tween 20, pH 7.6) and probed for several proteins, using specific primary and horseradish peroxidise (HRP)-conjugated secondary antibodies. The antibodies used for this work are listed in Table 1. Immunoreactive bands were visualized with an ECL (enhanced chemioluminescence) system (GE Healthcare Bio-Sciences, Uppsala, Sweden).

3.6 Nuclear extract preparation

Cells were washed twice in PBS and lysed with 4 packed cell volumes of Buffer A (10 mM HEPES, 10 mM KCl, 0.1 mM EDTA, 0.4% NP-40, 1 mM DTT, 2 mM PMSF and 1x protease inhibitor cocktail) and incubated on ice for 30 minutes. Cell lysates were centrifuged at 16,000 g at 4ºC for 5 minutes. Nuclear pellets were resuspended in 3.5 packed cell volumes of Buffer B (20 mM HEPES, 0.4 M NaCl, 1 mM EDTA, 10% Glycerol, 1 mM DTT, 2 mM PMSF and 1x protease inhibitor cocktail), incubated for 1 hour on ice and briefly sonicated. After centrifugation at 16,000 g for 5 minutes at 4ºC, supernatants containing the nuclear proteins were used to perform immunoblot against HIF-1α and Lamin-B. Protein concentration was determined using the BCA method (Pierce-Thermo Scientific, Waltham, MA, USA).

3.7 Pulse-chase assays

ARPE-19 cells cultured in 60 x 15 mm plates were incubated in methionine- and cysteine-free DMEM for 40 minutes and subsequently washed twice with ice-cold PBS. L-[^{35}S] methionine/ cysteine (PerkinElmer, Waltham, MA, USA) were then added to a final concentration of 100 μCi/ml and cells were incubated for 4 hours under hypoxic conditions. After metabolic labelling, the radioactive medium was removed and cells were washed twice with PBS. Cells were then recultured in complete medium containing ten fold excess of methionine/cysteine and treated as mentioned in the respective figures. Cells were harvested at different time points in 100 μl of 0.5% NP-40 lysis buffer (50 mM Tris-HCl pH 7.4, 150 mM NaCl, 10 mM IOD, 2 mM PMSF, 20 mM Na_3MoO_4 and 1x protease inhibitor cocktail). Samples were pre-cleared with 25 μl of Protein G Sepharose (GE Healthcare Bio-Sciences, Uppsala, Sweden) for 30 minutes and then HIF-1α was immunoprecipitated as described below. Proteins were resolved by SDS-PAGE, the gels were dried and radiolabelled HIF-1α protein was assessed by autoradiography.

Table 1. List of primary and secondary antibodies used for Western Blot.

Antibody	Host	Clone/Cat.#	~ M.W. (kDa)	Dilution	Company/Supplier
Anti-HIF-1α	Mouse	H1alpha67	120	1:500	Abcam, Cambridge, UK
Anti-Actin	Mouse	C4	43	1:1,000	Millipore-Chemicon, Billerica, MA, USA
Anti-V5 tag	Mouse	2F11F7	PMW + 2.8	1:2,000	Invitrogen, Carlsbad, CA, USA
Anti-Ubiquitin	Mouse	FK1	*	1:1,000	Biomol, Farmingdale, NY, USA
Anti-Ubiquitin	Mouse	P4D1	**	1:1,000	Covance, Princeton, NJ, USA
Anti-c-myc tag	Mouse	9E10	PMW + 1.2	1:500	Zymed- Invitrogen, Carlsbad, CA, USA
Anti-Hsp70	Mouse	C92F3A-5	70	1:300	Stressgen, Farmingdale, NY, USA
Anti-CML	Mouse	CMS-10	-	1:500	TransGenic INC., Kumamoto, Japan
Anti-Argpyrimidine	Mouse	-	-	1:500	Dr. K. Uchida, Nagoya University
Anti-Bcl-2	Mouse	C-2	28	1:300	Santa Cruz Biotechnology, Santa Cruz, CA, USA
Anti-Lamin B	Mouse	101-B7	68	1:500	Calbiochem, San Diego, CA, USA
Anti-Nrf2	Mouse	383727	70	1:1,000	R&D Systems, Minneapolis, MN, USA
Anti-MG-H1	Mouse	-	-	1:500	Dr. M. Brownlee, A.Einstein C.Medicine, NY, USA
Anti-Hsf-1	Rat	10H8	85	1:1,000	Stressgen, Farmingdale, NY, USA
Anti-Hsp90	Rat	16F1	90	1:1,000	Stressgen, Farmingdale, NY, USA
Anti-Hsc70	Rat	1B5	73	1:2,000	Stressgen, Farmingdale, NY, USA
Anti-VEGFA (Ab4)	Rabbit	PC315 #	34-50	1:400	Calbiochem, San Diego, CA, USA
Anti-Ang-2	Rabbit	Ab65835 #	75	1:300	Abcam, Cambridge, UK
Anti-BAX (Δ21)	Rabbit	sc-6236 #	23	1:300	Santa Cruz Biotechnology, Santa Cruz, CA, USA
Anti-Ki67	Rabbit	SP6	359	1:300	Abcam, Cambridge, UK
Anti-HA tag (SG77)	Rabbit	715500 #	PMW + 2.2	1:200	Zymed-Invitrogen, Carlsbad, CA, USA
Anti-Hsp40	Rabbit	SPA-400 #	40	1:2,000	Stressgen, Farmingdale, NY, USA
Anti-STUB1/CHIP	Goat	ab2482 #	35	1:500	Abcam, Cambridge, UK
Anti-Mouse-HRP	Goat	626520 #	-	1:7,500	Bio-Rad, Hercules, CA, USA
Anti-Rat-HRP	Goat	-	-	1:7,500	Bio-Rad, Hercules, CA, USA
Anti-Rabbit-HRP	Goat	656120 #	-	1:7,500	Bio-Rad, Hercules, CA, USA
Anti-Goat-HRP	Rabbit	611620 #	-	1:7,500	Bio-Rad, Hercules, CA, USA

PMW – Protein molecular weight

* FK1 antibody – only recognizes polyubiquitinated proteins; does not recognize monoubiquitination or free ubiquitin.

** P4D1 antibody – recognizes free ubiquitin (8 kDa), polyubiquitin and ubiquitin-conjugated proteins.

Clone/Cat. # – Clone designation or catalog number of the antibodies.

Note: Antibodies with no specified MW correspond to antibodies that may immunoblot several modified proteins across the membrane.

3.8 Immunoprecipitation

ARPE-19 cells cultured in 60 x 15 mm plates were washed twice with PBS, scraped off the dishes and collected in ice-cold PBS. Pellets were resuspended in 100 μl of lysis buffer (50 mM Tris-HCl pH 7.4, 150 mM NaCl, 10 mM IOD, 2 mM PMSF, 20 mM Na_3MoO_4, 0.5% NP-40 and protease inhibitor cocktail), incubated for 30 minutes on ice and briefly sonicated. Following centrifugation at 16,000 g for 10 minutes, 20 μl of the supernatants were denaturated with 2x Laemmli buffer (input). The remaining supernatants (80 μl) were transferred to new tubes and 2.5 μg of anti-HIF-1α or anti-c-myc antibodies were added. Subsequently, 300 μl of lysis buffer, with no NP-40, were added to the mixture and the samples were incubated overnight at 4ºC with gentle agitation. Thereafter, 50 μl of protein G-Sepharose (GE Healthcare Bio-Sciences, Uppsala, Sweden) were added to the samples and incubations proceeded at 4ºC for 2 hours. Beads were washed 3 times with lysis buffer and the immunoprecipitated proteins were eluted with 2x Laemmli buffer and boiled at 100ºC. Eluted samples were loaded on SDS-PAGE and western blot analyses were performed using anti-ubiquitin, anti-HIF-1α, anti-Hsp70, anti-Hsp40, anti-V5 or anti-c-myc antibodies.

3.9 Derivatization of carbonyl-containing proteins

After the treatments, ARPE-19 cells cultured in 60 x 15 mm plates were washed twice with ice-cold PBS and lysed in 100 μl of lysis buffer (50 mM Tris-HCl pH 7.6 supplemented with 1% NP-40 and protease inhibitor cocktail). For derivatization of carbonyl-containing proteins, equal amounts of protein were mixed with equal volume of 10 mM 2,4-dinitrophenylhydrazine (DNPH; Invitrogen, Carlsbad, CA, USA) in 10% trifluoroacetic acid and incubated at room temperature for 15 minutes. The reaction was stopped by precipitation of proteins with 20% trichloroacetic acid. The pellet was washed with ethylacetate:ethanol (1:1) to remove free DNPH. Subsequently, the pellet was solubilized with Laemmli buffer. Samples were resolved by SDS-PAGE and transferred to PVDF membranes. Membranes were probed with an antibody against dinitrophenylhydrazone derivatives (Dako, Glostrup, Denmark).

3.10 High performance liquid chromatography (HPLC)

ARPE-19 cells (7 x 10^5 cells) cultured and treated in 60 x 15mm plates were washed with ice-cold PBS, scraped in 100 μl acetic acid (0.1 M) and homogenized by sonication. The intracellular concentration of MGO was determined according to a modification of a previously reported method (Schalkwijk et al, 1999). Briefly, 50 μl of sample were mixed with 200 μl of 0.1 M potassium phosphate buffer pH 7.0, 200 μl of ethanol and 50 μl of freshly prepared 20 mM DDB

(dissolved in 10 mM HCl). The mixture was incubated at room temperature for at least four hours and then centrifuged during 10 minutes at 16,000 g. Subsequently, MGO was determined through reverse-phase HPLC. The HPLC system consisted of a L-6200A Intelligent Pump, a F-1080 Fluorescence Detector (Hitachi, Tokyo, Japan) and a Waters μBondapak^{TM} C18 column (10 μM, 3.9 x 300 mm) (Waters, Milford, MA, USA). Mobile phase A was a mixture of 10mM potassium phosphate buffer (pH 3.0) and acetonitrile (90/10, v/v). Mobile phase B consisted of a mixture of acetonitrile and water (70/30, v/v). Samples (20 μl) were injected and separation was performed with a linear gradient from 0-100% mobile phase B over 28 minutes. The flow rate was set at 1.0 ml/min and fluorescence detection was performed with excitation and emission wavelengths of 352 nm and 385 nm, respectively. MGO was determined by integration of peak areas (Figure 14) using appropriate external standards.

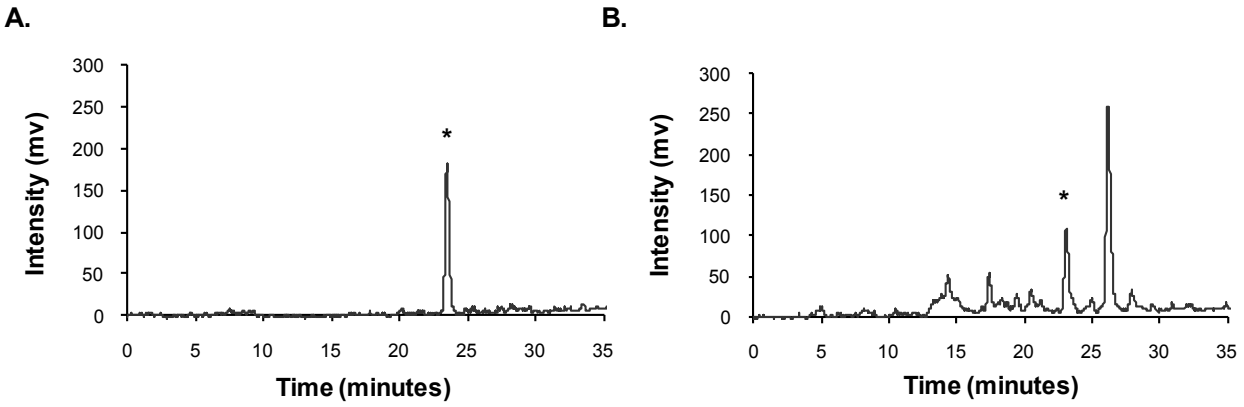

Figure 14. Examples of HPLC profiles used for quantification of intracellular MGO levels. (A) Profile of a pure MGO external standard at 166.5 nM. (B) Profile of a cell or tissue extract. The peaks signed with an asterisk (*) correspond to the MGO elution and detection.

3.11 Immunocytochemistry

Cells grown on coverslips were fixed with 4% paraformaldehyde (PFA) for 10 minutes, while retina frozen sections (5 - 7 μm thickness) were fixed with ice cold-acetone for 10 minutes. The fixed samples were permeabilized with 1% Triton X-100 (v/v) for 10 minutes and blocked with goat serum (1:10) for 20 minutes prior the incubation with primary antibodies (Table 2) for 1 hour at room temperature (cells) or overnight at 4ºC (retina). The samples were then rinsed three times with 0.02% Bovine Serum Albumin (BSA) in PBS and incubated with 1:5,000 DAPI (Invitrogen, Carlsbad, CA, USA) and 1:100 FITC/Texas Red-conjugated goat anti-mouse or anti-rabbit (Invitrogen, Carlsbad, CA, USA) for 1 hour at room temperature. The coverslips were then washed with 0.02% BSA and mounted with Glycergel (Dako, Glostrup, Denmark). The samples were imaged by confocal microscopy and/or fluorescence microscopy using a confocal image system

MRC600 Bio-Rad, Hercules, CA, USA) and a Leica DFC350 FX fluorescence microscope (Leica-Microsystems, Bannockburn, IL, USA), respectively.

Table 2. List of primary and secondary antibodies used for immunocytochemistry.

Antibody	Host	Clone/Cat.#	Dilution	Company/Supplier
Anti-HIF-1α	Mouse	H1alpha67	1:100	Abcam, Cambridge, UK
Anti-Ubiquitin	Mouse	FK1	1:200	Biomol, Farmingdale, NY, USA
Anti-Bcl-2	Mouse	C-2	1:50	Santa Cruz Biotechnology, Sta. Cruz, CA, USA
Anti-VEGFA (Ab4)	Rabbit	PC315 #	1:50	Calbiochem, San Diego, CA, USA
Anti-Ang-2	Rabbit	ab65835 #	1:50	Abcam, Cambridge, UK
Anti-BAX (Δ21)	Rabbit	sc-6236 #	1:50	Santa Cruz Biotechnology, Sta. Cruz, CA, USA
Anti-HA tag (SG77)	Rabbit	715500 #	1:100	Zymed-Invitrogen, Carlsbad, CA, USA
Anti-VWF	Rabbit	IS527 #	1:100	Dako, Heverlee, Belgium
Anti-Mouse-Texas Red	Goat	T862 #	1:100	Zymed-Invitrogen, Carlsbad, CA, USA
Anti-Rabbit-FITC	Goat	656111 #	1:100	Zymed-Invitrogen, Carlsbad, CA, USA

3.12 Measurement of the 20S proteasome activities

Cells cultured in 60 x 15 mm were washed twice with PBS, lysed with 100 µl of 50 mM Tris pH 7.6, 1 mM DTT and briefly sonicated. After centrifugation (16,000 g for 10 minutes at 4ºC), the protein concentration was determined using the Coomassie method (Pierce-Thermo Scientific, Waltham, MA, USA) and 40 µg of protein were incubated with the following fluorogenic substrates in a 96-well plate: 100 µM Suc-LLVY-MCA/ for the chymotrypsin-like activity (Biomol-Enzo Life Sciences, Farmingdale, NY, USA); 25 µM Boc-LRR-MCA for the trypsin-like activity (Biomol-Enzo Life Sciences, Farmingdale, NY, USA); 150 µM Z-LLE-MCA for the caspase-like activity (Calbiochem, San Diego, CA, USA). The proteasome activities were monitored during 1 hour at 37ºC, in periods of 5 minutes (excitation wavelength at 380 nm; emission wavelength at 460 nm). Absorbance was measured on a Biotek Synergy HT spectrophotometer (Biotek, Winooski, VT, USA), using the Gen 5 software to monitor the results (Biotek, Winooski, VT, USA).

3.13 Quantitative real-time PCR

Following the treatments, total RNA from ARPE-19 cells cultured in 60 x 15 mm plates was purified according to the manufacturer's specifications of Qiagen RNeasy mini kit (Qiagen, Valencia, CA, USA) and quantified at 260 nm according to the following formula [RNA] = 44 µg/ml x A_{260} x dilution factor. Total RNA samples were then treated with RNase-free DNase I (GE

Healthcare Bio-Sciences, Uppsala, Sweden), to avoid genomic DNA contamination. SuperScript II Reverse Transcriptase (Invitrogen, Carlsbad, CA, USA) and random hexadeoxynucleotide primers were used to synthesize the first cDNA strand.

Pre-developed and inventoried TaqMan assays (Applied Biosystems, Foster City, CA, USA) for human HIF-1α (Assay ID Hs00936368_m1 FAM/MGB probe) and eukaryotic 18S rRNA endogenous control (Assay ID 4310893E VIC/TAMRA probe) were used to perform multiplex Real-Time Quantitative PCR for HIF-1α. Briefly, 10 µl of 2xTaqMan Universal PCR Master Mix (Applied Biosystems, Foster City, CA, USA) were mixed with 7 µl of Rnase-free water, 1 µl of human HIF-1α assay, 1 µl of eukaryotic 18S rRNA and 1 µl of cDNA at 200 ng/µl (for each multiplex reaction).

Table 3. Pairs of primers used for RT-PCR.

Gene/ Accession N.º	Primer	Sequence	[ ] (nM)
hVEGFA	Sense	5′-CAGAATCATCACGAAGTG-3’	300
NM_001025366.1	Antisense	5′-TCTGCATGGTGATGTTGGAC-3’	300
hHspB1	Sense	5’-GCTGACGGTCAAGACCAAGG-3’	300
NM_001540.3	Antisense	5’-GGGGGCAG CGTGTATTTCC-3’	300
hHspB2	Sense	5’-CGAGTACGAATTTGCCAACC-3’	300
NM_001541.3	Antisense	5’-AGTAGCCATGGTAGAGTGTG-3’	300
hHsc70	Sense	5’-ATACCTCCTGCACCCCGAG-3’	300
NM_006597.3	Antisense	5’-TTGCTCAAACGGCCCTTGTC-3’	300
hHsp70	Sense	5’-GTGCAGTTGCCTACAGGATTAAC-3’	300
NM_002154.3	Antisense	5’-TCGGCTGTCTCCTTCAGTTTG-3’	300
hHsp90	Sense	5’-TTCCACGTCTCTGCATTCC-3’	500
NM_001017963.2	Antisense	5’-CTTGGGTCTGGGTTTCCTC-3’	500
18S rRNA	Sense	5’-GTCTGCCCTATCAACTTTC-3’	100
NR_003286.2	Antisense	5’-TTCCTTGGATGTGGTAGC-3’	100

For human VEGF, HspB1, HspB2, Hsc70, Hsp70 and Hsp90 mRNA quantification, the SYBR Green PCR master mix reagent (Bio-Rad, Hercules, CA, USA) was used and cDNA amplification was performed according to the manufacturer’s protocols. 18S rRNA was used as endogenous control and the set of primers represented in Table 3 were used for single amplification reactions. Briefly, 12.5 µl of 2x SYBR Green PCR reagent were mixed with the sense and antisense primers (to the final concentrations indicated in Table 3), cDNA (200 ng for VEGF RTPCR or 100 ng for HSPs RTPCR) and RNase-free water in a final reaction volume of 25 µl (*per* each single reaction). Control reactions, in which no reverse transcription took place (RT minus), were used to exclude DNA contamination occurrence.

All the Real-Time PCR analyses were conducted on a ABI Prism 7000 quantitative PCR system (Applied Biosystems, Foster City, CA, USA). cDNA amplification was performed according to the standard program of the ABI Prism system - Step 1: 50ºC for 2 minutes; Step 2: 95ºC for 10 minutes; Step 3 (40 cycles) each cycle: ramp 1 – 95ºC for 15 seconds (denaturation); ramp 2 – 60ºC for 1 minute (annealing and extension). Relative quantification was performed based on the $\Delta\Delta C_T$ method, which relies on direct comparison of C_T values, which represent the cycle number at which the amplification plot crosses the threshold and there is a significant detectable increase in fluorescence. The normalized target gene expression level in samples was calculated by using the formula: $2^{-\Delta\Delta CT}$, where $\Delta\Delta C_T = \Delta C_T$ (sample) - ΔC_T (calibrator) and ΔC_T is calculated as $\Delta C_T = C_T$ target gene (i.e. HIF-1α; VEGF) - C_T reference gene (i.e. 18S rRNA).

3.14 Human CHIP short-hairpin RNA (shRNA) production

Five different sets of complementary oligonucleotides (encoding shRNA target sequences) were designed using the BLOCK-iT ™ RNAi Designer (Invitrogen, Carlsbad, CA, USA), against the open-reading frame (ORF) region of human STUB-1 gene (NM_005861.2). The RNA interference target sequence, represented in Table 4, is underlined and the loop of the short-hairpin is bolded.

Table 4. Pairs of oligonucleotides used for the production of shRNAs against human CHIP.

shRNA	Strand	Sequence
A	Top	5'-CACCGGCCTTGTGCTACCTGAAGAT**CGAA**ATCTTCAGGTAGCACAAGGCC-3'
	Bottom	5'-AAAAGGCCTTGTGCTACCTGAAGAT**TTCG**ATCTTCAGGTAGCACAAGGCC-3'
B	Top	5'-CACCGGAGATGGAGAGCTATGATGA**CGAA**TCATCATAGCTCTCCATCTCC-3'
	Bottom	5'-AAAAGGAGATGGAGAGCTATGATGA**TTCG**TCATCATAGCTCTCCATCTCC-3'
C	Top	5'-CACCGAAGCGCTGGAACAGCATTGA**CGAA**TCAATGCTGTTCCAGCGCTTC-3'
	Bottom	5'-AAAAGAAGCGCTGGAACAGCATTGA**TTCG**TCAATGCTGTTCCAGCGCTTC-3'
D	Top	5'-CACCGGCTATGAAGGAGGTTATTGA**CGAA**TCAATAACCTCCTTCATAGCC-3'
	Bottom	5'-AAAAGGCTATGAAGGAGGTTATTGA**TTCG**TCAATAACCTCCTTCATAGCC-3'
E	Top	5'-CACCGCATTCATCTCTGAGAATGGC**CGAA**GCCATTCTCAGAGATGAATGC-3'
	Bottom	5'-AAAAGCATTCATCTCTGAGAATGGC**TTCG**GCCATTCTCAGAGATGAATGC-3'

The oligonucleotides of each pair were annealed according the BLOCK-IT™ pENTR/U6 entry vector kit protocol (Invitrogen, Carlsbad, CA, USA). Annealed primers were separated by 3% agarose electrophoresis, visualized by staining with ethidium bromide (EB) and purified using the QIAquick PCR purification kit (Qiagen, Valencia, CA, USA). Subsequently, the purified annealing products (double stranded oligonucleotide) were cloned into linearized pENTR/U6 vector through a

ligation reaction using a T4 DNA ligase (1 U/µl). The ligation products were used to transform One Shot® TOP10 competent *E.coli* cells (Invitrogen, Carlsbad, CA, USA), which were spread on LB agar plates containing 50 µg/ml kanamycin and incubated overnight at 37ºC. Eight kanamycin-resistant colonies were analyzed per each ligation reaction to confirm the cloning efficiency. The screening was done by PCR using the U6 forward (5'-GGACTATCATATGCTTACCG-3') and M13 reverse (5'-CAGGAAACAGCTATGAC-3') primers.

Once identified the positive entry-clones, were chosen 3 positive-clones per each set of double stranded oligonucleotide pair. The selected clones were inoculated into 5 ml of LB containing 50 µg/ml kanamycin and grown overnight at 37ºC and 180 RPM. Plasmid DNA from each clone was purified using the QIAprep Spin Miniprep Kit (Qiagen, Valencia, CA, USA) and spectrophotometric quantified at 260 nm. Purified DNA was used to transfect 293-FT cells and the knockdown efficiency was determined by western blot against CHIP/STUB-1. The most efficient clones were selected and DNA was used to continue the protocol.

Subsequently, a LR recombination reaction, between pAD/BLOCK-iT^{TM} DEST (containing *att*R sites) and the selected pENTR ^{TM}/U6 entry vectors (containing *att*L sites), was performed using the LR Clonase II enzyme (Invitrogen, Carlsbad, CA, USA), to generate expression clones. TOP10 competent *E.coli* cells were transformed with 3 µl of the LR recombination reaction and positive-clones were screened as mentioned before, using the PCR primers pAd forward (5'-GACTTTGACC GTTTACGTGGAGAC-3') and pAD reverse (5'-CCTTAAGCCACGCCCACACATTTC-3').

Two positive-colonies from shRNA B and shRNA D were used to proceed. All plasmids were verified by DNA sequencing. Produced and purified pAd/BLOCK-iT-DEST expression vectors were digested with *Pac* I enzyme (New England Biolabs, Ipswich, MA, USA), according the manufacturer's instructions, which allows exposure of the left and right viral inverted terminal repeats (ITRs) and removal of the bacterial sequences (i.e. pUC origin). Digested plasmid DNA was purified using phenol/chloroform extraction followed by ethanol precipitation. Purified DNA was subsequently resuspended in TE buffer pH 8.0.

Pac I-digested pAd/BLOCK-iT-DEST plasmids were use to transfect 293A cells that allows adenovirus production from the E1-deleted pAd/BLOCK-iT-DEST vector. This cell line supplies the E1 proteins *in trans* that are required for expression of adenoviral late genes, and thus viral replication. Cells were trypsinized 48 hours post-transfection and transferred to a sterile 10 cm tissue culture plate containing complete culture medium. The culture medium was replaced by fresh medium every 2 - 3 days, until visible regions of cytophathic effect (CPE) were observed (typically 7 - 10 days post-transfection). Infections proceeded until approximately 80% CPE was observed (typically 10 - 13 days post-transfection). The adenovirus-containing cells were squirted off the plate and were harvested, together with the media, in a sterile capped tube. After the harvesting process, adenovirus-containing cells and media were frozen and thawed several times (repeated freeze/thaw cycles), followed by centrifugation. The freeze/thaw cycles allow cell lysis and release of intracellular viral particles. The supernatant obtained from centrifugation was stocked at -80ºC in

cryovials. Before proceeding with transduction of mammalian cells to express the shRNAs, the adenoviral stocks were tittered and optimal multiplicity of infection (MOI - defined as the optimal number of virus particles per cell) was determined according to the manufacturer's protocol.

3.15 Polymerase chain reaction (PCR)

For DNA amplification, all the reagents were combined in PCR-tubes in a final reaction volume of 25 µl [10x DNA polymerase buffer (1x), 2.5 µl of 2 mM dNTPs (200 µM), 1 µl of 25 mM $MgCl_2$ (1 mM), 1 µl of 100 µM forward primer (250 nM), 1 µl of 100 µM reverse primer (250 nM), 16-17 µl of sterile ddH_2O, 0.1 µl of 5 U/µl *Taq* Polymerase (Takara Bio, Shiga, Japan), template DNA (1 µl of plasmid DNA at 0.1-1 ng/µl or pick a colony from a Luria Broth (LB) agar plate and dip it into the PCR mixture)]. DNA amplification in a thermal cycler was performed according to the following program – Cycle 1: 95ºC for 2 minutes; Cycles 2 - 32 (each cycle): ramp 1- 95ºC for 1 minute; ramp 2- annealing temperature appropriate for each primers pair for 30 seconds; ramp 3- 72ºC for the necessary time to occur complete DNA sequence extension (*Taq* Polymerase - 35/100 nucleotides per second); Final Cycle: 72ºC for 10 minutes. The PCR products were separated by 1-3% agarose electrophoresis and visualized by staining with EB.

3.16 Plasmids

Human CHIP/STUB1 (GeneBank accession number NM_005861) was amplified by PCR from a human leukocyte cDNA library using the following flanking primers containing *Eco*RI and *Sal*I restriction sites: forward primer 5'-GCGCGAATTCATGAAGGGCAAGGAGGAGAAGGAGGG-3'; reverse primer 5'-GCAGGTCGACTCAGTAGTCCTCCACCCAGCCATTCTC-3'. Human GLO I (GeneBank accession number NM_006708) was PCR-amplified from the pCMS-EGFP hGLOI vector (Miller et al, 2006) using the following flanking primers containing *Eco*RI and *Sal*I restriction sites: forward primer 5'-CAGCGAATTCATGGCAGAACCGCAGCCCCCGTC-3'; reverse primer 5'-TCTCGTCGACCTACATTAAGGTTGCCATTTTGTT-3'. Both amplified sequences were cloned into pENTRV5-C2 (Hume et al, 2006; Lopes et al, 2007) to generate pENTR/V5-hCHIP and pENTR/V5-hGLOI. In order to produce hCHIP and hGLOI adenovirus, these vectors were recombined with the pAd/BLOCKiT-DEST adenoviral vector from Invitrogen (Carlsbad, CA, USA) using Gateway technology according to manufacturers' instructions. For this work, we have also used the following plasmids: pcDNA3 hHIF-1α wt-V5 and pcDNA3 hHIF-1α (P402A and P564A)-V5 (provided by Dr. T. Hagen - University of Nottingham) (Hagen et al, 2003); pcDNA6 hHdj1/Hsp40 wt-V5 (provided by Dr. B. Y. Ahn - Korea University) (Sohn et al, 2006); pcDNA3 HA-hHIF1α wt (provided by Dr. F. Bunn - Brigham and Women's Hospital - Harvard) (Huang et al, 1998); pcDNA3.1 c-myc-hCHIP wt, pcDNA3.1 c-myc-hCHIP K30A, pcDNA3.1 c-myc-hCHIP H260Q (originally provided by Dr. C. Patterson - North Carolina University) (Xu et al, 2002); pT81 HRE-

luciferase (provided by Dr. S. Catrina - Karolinska Institute) (Catrina et al, 2004); pGL4.23 HSE wt (x4)-Luciferase, pGL4.23 HSE mut (x4)-Luciferase (provided by Dr. Ueli Schibler - University of Geneva) (Reinke et al, 2008).

3.17 Transient transfection

One day before transfection, cells were seeded in 60 x 15mm plates so that the cells were 90% confluent at the time of transfection. For each transfection sample, 4 µg of plasmid DNA were diluted in 100 µl of Opti-MEM I Reduced Serum Medium (Invitrogen, Carlsbad, CA, USA). Subsequently, 10 µl of Lipofectamine 2000 (Invitrogen, Carlsbad, CA, USA) transfection reagent were diluted in 100 µl of Opti-MEM I Medium and incubated for 5 minutes at room temperature. After 5 minutes of incubation, diluted DNA and diluted Lipofectamine were combined and incubated together for 20 minutes at room temperature. Meanwhile, the culture medium of each well was removed, cells were washed twice with PBS and cultured in 2 ml of Opti-MEM I Medium. After the incubation, the DNA/Lipofectamine complexes (total volume 200 µl) were added to each well. The wells were mixed gently and cells were incubated at 37ºC in a CO_2 incubator for 24-30 hours prior to test for transgene expression. Opti-MEM I Medium was replaced by full DMEM:F12 medium (with FBS) after 6 hours of DNA/Lipofectamine incubation.

3.18 Reporter-luciferase gene assay

ARPE-19 cells were plated in 24-well plates at subconfluent density and transfected with pT81 HRE-luciferase, pGL4.23 HSE wt (x4)-Luciferase or pGL4.23 HSE mut (x4)-Luciferase, using Lipofectamine 2000 (Invitrogen, Carlsbad, CA, USA). The plasmid pT81/HRE-luciferase contains three tandem copies of the erythropoietin hypoxia response element (HRE) in front of the herpes simplex thymidine kinase promoter (Catrina et al, 2004). The plasmids pGL4.23 HSE-Luciferase contain four copies of the wild-type or mutated form of a heat shock element (HSE) and a minimal promoter upstream of a firefly luciferase reporter gene (Reinke et al, 2008). The mutant form does not bind the transcription factor Hsf-1 or heat shock factor-1. Twenty-four hours after transfection cells were treated as mentioned and then assayed for luciferase activity. Briefly, the culture medium was removed and cells were washed twice with PBS. Cells were then lysed with 100 µl of lysis buffer (8 mM $MgCl_2$, 1 mM DTT, 1 mM EDTA, 15% Glycerol, 1% Triton X-100 (v/v), 25 mM Tris-phosphate pH 7.6). The cell lysates were incubated for 30 minutes on ice and then centrifuged at 16,000 g for 10 minutes. The protein concentration of the samples was determined through the BCA method and all the samples were normalized for the same protein concentration. For evaluation of the luciferase activity, an ATP buffer (8 mM $MgCl_2$, 1 mM DTT, 1 mM EDTA, 15% Glycerol, 2 mM ATP, 25 mM Tris-phosphate pH 7.6) and a 167 µM D-luciferin (Sigma-Aldrich, St. Louis, MO, USA) solution were used, both automatically injected by the luminometer injector

system into an opaque 96-well plate, containing 30 µg of protein lysates. Measurements were performed using a LMax II 384 ROM v1.04 reader and SoftMax Pro 5 software (Molecular Devices, Sunnyvale, CA, USA), as described by the manufacturer's protocol.

3.19 Determination of VEGF and Ang-2 levels in supernatants

The concentrations of diffusible Ang-2 and $VEGF_{121, 165}$ in the cell culture supernatants were measured by Quantikine enzyme-linked immunosorbent (ELISA) assay kits using monoclonal antibodies directed against human Ang-2 or human VEGF, according the manufacturer's protocol (R&D Systems, Minneapolis, MN, USA). Briefly, cell culture supernatant samples or standards were added to a 96-well plate, previously coated with a mouse monoclonal antibody against VEGF or Ang-2, and incubated for 2 hours at room temperature. Subsequently, samples were aspirated and wells washed three times. In the last wash step, plate was inverted and blotted it against clean paper towel to efficiently dry the wells. Wells were then incubated with a horseradish-peroxidase (HRP)-conjugated polyclonal antibody against VEGF or Ang-2 for 2 hours at room temperature. After incubation, wells were aspirated and washed three times, as mentioned before. Subsequently, wells were incubated with the substrate solution, which is a 1:1 mixture of a hydrogen peroxide solution and a tetramethylbenzidine (TMB) chromogen solution, for 20 minutes at room temperature and protected from light. The reaction was stopped by adding 2 N H_2SO_4. Absorbance was measured at 450 nm, with wavelength correction at 570 nm, on a Biotek Synergy HT spectrophotometer (Biotek, Winooski, VT, USA), using the Gen 5 software to monitor the results (Biotek, Winooski, VT, USA).

3.20 BrdU incorporation colorimetric assay

Cells seeded onto a 96-well plate were incubated with 5-bromo-2'-deoxyuridine (BrdU; Roche Applied Science, Indianapolis, IN, USA) labelling solution to a final concentration of 10 µM for 6 hours at 37ºC. Subsequently, labelling solution was removed by taping-off the plate and 200 µl of FixDenat was added to the cells for 30 minutes at room temperature. FixDenat induces cell fixation and DNA denaturation, making BrdU accessible for binding to an anti-BrdU antibody. Thirty minutes later, FixDenat was removed and 100 µl of peroxidase-conjugated anti-BrdU antibody (1:100 dilution) was added per well. Antibody was incubated for 90 minutes at room temperature. Subsequently, cells were washed three times and the substrate solution tetramethyl-benzidine (TMB) was added. Cells were incubated at room temperature until colour development was sufficient for photometric detection (5 - 30 minutes). The entire procedure was performed as described by the manufacturer's protocol (Roche Applied Science, Indianapolis, IN, USA) and absorbance was measured at 370 nm (reference wavelength at 492 nm) on a Biotek Synergy HT spectrophotometer (Biotek, Winooski, VT, USA).

3.21 MTT cell viability assay

After the treatments, ARPE-19 cells seeded onto 24-well plates were washed twice with PBS and incubated with 0.5 mg/ml MTT [3-(4,5-dimethylthiazol-2-yl)-2,5-diphenyltetrazolium bromide; Invitrogen, Carlsbad, CA, USA] in Krebs buffer (130 mM NaCl, 4 mM KCl, 1.5 mM $MgCl_2$, 1 mM $CaCl_2$, 6 mM glucose, 10 mM HEPES, pH 7.4) for 2 hours at 37°C in a cell culture incubator. Subsequently, supernatants were removed and the precipitated dye was dissolved in 300 µl 0.04 M HCl (in isopropanol) and quantified at a wavelength of 570 nm, with wavelength correction at 620 nm, using a Biotek Synergy HT spectrophotometer (Biotek, Winooski, VT, USA).

3.22 Caspase-3 cleavage activity colorimetric assay

TR-iBRB cells cultured in 100 x 20 mm were lysed according to the manufacturer's protocol (R&D Systems, Minneapolis, MN, USA) and protein concentration was determined and normalized using the BCA method (Pierce-Thermo Scientific, Waltham, MA, USA). To 50 µl of protein lysate (2-4 mg/ml) was added 50 µl of 2x Reaction Buffer/DTT and 5 µl of a specific caspase-3 substrate that is conjugated to the colour reporter molecule p-nitroanaline (DEVD-pNA; R&D Systems, Minneapolis, MN, USA), in a 96-well plate. The reaction was incubated for 2 hours at 37ºC. The assay was performed as described by the manufacturer's protocol (R&D Systems, Minneapolis, MN, USA) and the cleavage of the DEVD-pNA peptide was spectrophotometric quantified at a wavelength of 405 nm using a Biotek Synergy HT spectrophotometer (Biotek, Winooski, VT, USA).

3.23 Fibrin gel *in-vitro* angiogenesis assay

This angiogenesis assay is based on the use of fibrin gels formed in culture dishes by mixing fibrinogen and thrombin. To obtain these fibrin gel matrix, 30 µl of fibrinogen solution was added per well of a 96-well plate. Subsequently, 20 µl of thrombin was added and the plate was immediately and gently shacked. The plate was placed at 37ºC for 15 - 60 minutes to allow polymerization. In the meanwhile, TR-iBRB cells, resuspended in positive control media or test media, were embedded within the fibrinogen/thrombin polymerized gels at a final density of 5 x 10^4 cells/ml, as described by the manufacture's protocol (Millipore-Chemicon, Billerica, MA, USA). Cells were incubated overnight at 37ºC in a cell culture incubator. On the next day, the culture medium was removed, as much as possible without disturbing the gel (i.e. inverting the plate onto sterile gauze), and was added a new layer of fibrinogen (30 µl) and thrombin (20 µl), as mentioned before, in order to cover the cells. After 5 minutes of gel polymerization at 37ºC, the test media or the positive control media were added and cells were incubated during 24, 48 and 72 hours at 37ºC in a cell culture incubator. Phase-contrast images were taken using an inverted light microscope at 100 and 200 X of magnification.

3.24 Statistical analysis

Data are reported as the mean ± standard deviation (SD) or standard error of the mean (SEM) of at least three independent experiments. Comparisons between multiple groups were performed by one-way analysis of variance test (ANOVA) with the Dunnet's or Tukey's multiple comparison tests, while comparisons between two groups were performed using *t* test analysis [GraphPad Prism 5.0 software (GraphPad Software, La Jolla, CA, USA)]. In all cases, $p < 0.05$ was considered significant.

CHAPTER 4

Chapter 4. The chaperone-dependent ubiquitin ligase CHIP targets HIF-1α for degradation in the presence of methylglyoxal

4.1 Abstract

The hypoxia-inducible factor-1 (HIF-1) plays a key role in cell adaptation to low oxygen and stabilization of HIF-1 is vital to ensure cell survival under hypoxia. In this work, it is identified a new molecular mechanism whereby methylglyoxal (MGO), which accumulates in diabetes, leads to a rapid proteasome-dependent degradation of HIF-1α. Significantly, MGO-induced degradation of HIF-1α does not require the recruitment of the canonical ubiquitin ligase von Hippel Lindau (pVHL) nor does it require hydroxylation of the proline residues P402/P564 on HIF-1α. Moreover, we identified CHIP (carboxy terminus of Hsp70-interacting protein) as the E3 ligase that ubiquitinates HIF-1α in the presence of MGO. Consistently, silencing of endogenous CHIP or overexpression of glyoxalase I (GLO I) both stabilize HIF-1α under hypoxia in the presence of MGO. Data shows that increased association of Hsp40/70 with HIF-1α leads to recruitment of CHIP, which promotes polyubiquitination and degradation of HIF-1α. Moreover, MGO-induced destabilization of HIF-1α leads to a dramatic decrease in HIF-1 transcriptional activity, as well as to decreased expression of the vascular endothelial growth factor (VEGF).

Altogether, data is consistent with a new pathway for degradation of HIF-1α in response to intracellular accumulation of MGO. Moreover, it is suggested that MGO accumulation is the link between high glucose and the loss of cell response to hypoxia in diabetes.

4.2 Introduction

Cell response to ischemia is primarily regulated by the transcription factor HIF-1 (Semenza & Wang, 1992) that triggers protective and adaptive mechanisms, promoting cell survival under hypoxia. Therefore, any mechanism that destabilizes HIF-1 has a negative impact on the cellular adaptation to low oxygen.

HIF-1 is a heterodimer composed of two subunits: a labile HIF-1α subunit and a stable HIF-1β subunit. Under normoxia, HIF-1α is hydroxylated in prolines 402 and 564 in the oxygen dependent degradation domain by specific prolyl hydroxylases. Once hydroxylated, HIF-1α binds to the VHL protein, which is part of an ubiquitin ligase complex, resulting in HIF-1α polyubiquitination and subsequent degradation by the proteasome (Huang et al, 1998; Ivan et al, 2001; Jaakkola et al, 2001). In addition, the asparagine 803 is also hydroxylated inhibiting the interaction of HIF-1α with the co-activator p300, which induces repression of HIF-1 transcriptional activity (Kallio et al, 1998). When oxygen becomes limiting, the proline residues are not hydroxylated and HIF-1α escapes degradation, accumulating in the cell. Then, it is imported into the nucleus, where it

dimerizes with HIF-1β and binds to hypoxia responsive elements (HREs), enabling transcriptional activation of more than 70 genes that help cells to cope and survive under hypoxia, such as VEGF (Kimura et al, 2001; Semenza & Wang, 1992).

Recently, it was shown that diabetes and hyperglycaemia leads to downregulation of HIF-1 and to an impairment of the cell response to hypoxia (Catrina et al, 2004; Liu et al, 2008; Semenza, 2009). For example, downregulation of HIF-1 in response to hyperglycaemia is likely to account for the decreased arteriogenic response triggered by myocardial ischemia in diabetic patients (Abaci et al, 1999; Larger et al, 2004). Consistently, blood glucose levels were shown to be in linear relation with fatal outcome after an acute hypoxic challenge, suggesting a deleterious influence of hyperglycaemia on the ability of tissues to adapt to low oxygen (Malmberg et al, 1999). In addition, levels of HIF-1 are dramatically downregulated in skin wounds and ulcers of diabetic patients and animal models of diabetes as compared to venous ulcers that share the same hypoxic environment but are not exposed to hyperglycaemia (Catrina et al, 2004; Liu et al, 2008; Sarkar et al, 2009). These and other evidences strongly suggest that cell and tissue dysfunction associated with diabetes is related, at least in part, with a loss of cell response to hypoxia. However, the molecular mechanisms underlying this dysfunction remain to be elucidated.

In this work, it is hypothesized that increased production of MGO is the link between high glucose and destabilization of HIF-1 in diabetes. MGO is a highly reactive α-oxoaldehyde formed as a by-product of glycolysis (Kalapos, 1999; Ramasamy et al, 2006). Indeed, high glucose leads to intracellular accumulation of MGO in several tissues and increased concentration of MGO in cells and tissues has been implicated in the pathophysiology of a variety of diseases, including several diabetic complications (Kalapos, 1999; Ramasamy et al, 2006). MGO is known to react with free amino groups of lysine and arginine residues of proteins, leading to the formation of advanced glycation end products (AGEs) (Kalapos, 1999), and increased levels of MGO have deleterious effects in a number of essential signalling pathways (Du et al, 2006; Portero-Otin et al, 2002). Of significance, AGEs were shown to impair the angiogenic process in a model of ischemia-induced retinopathy (Stitt et al, 2005) .

Herein, it is shown that MGO-induced modification of HIF-1α recruits Hsp40/70, which in turn recruit CHIP, leading to increased polyubiquitination of HIF-1α and its proteasome-dependent degradation, accounting for impairment of the cell response to hypoxia.

4.3 Results

4.3.1 High glucose induces intracellular accumulation of MGO, leading to decreased half-life of HIF-1α

Hyperglycaemia was shown to be involved in the loss of cell response to hypoxia in diabetes, through a mechanism that is likely to involve downregulation of HIF-1α. Indeed, data

show that levels of HIF-1α are downregulated under hypoxia in cells treated with high glucose over a period of 10 days, as compared to cells maintained in basal glucose concentration (Figure 15A).

In this study, a retinal pigment epithelium cell line (ARPE-19) was used to investigate the role of high glucose in regulation of HIF-1. RPE cells are a good model to evaluate cell response to hypoxia and regulation of HIF-1 since these cells are extremely sensitive to variations in oxygen (Yu & Cringle, 2005) and glucose concentrations (Coffe et al, 2006) and are a major source of VEGF in the retina, a gene well known to be upregulated by hypoxia and HIF-1 (Kimura et al, 2001; Slomiany & Rosenzweig, 2004).

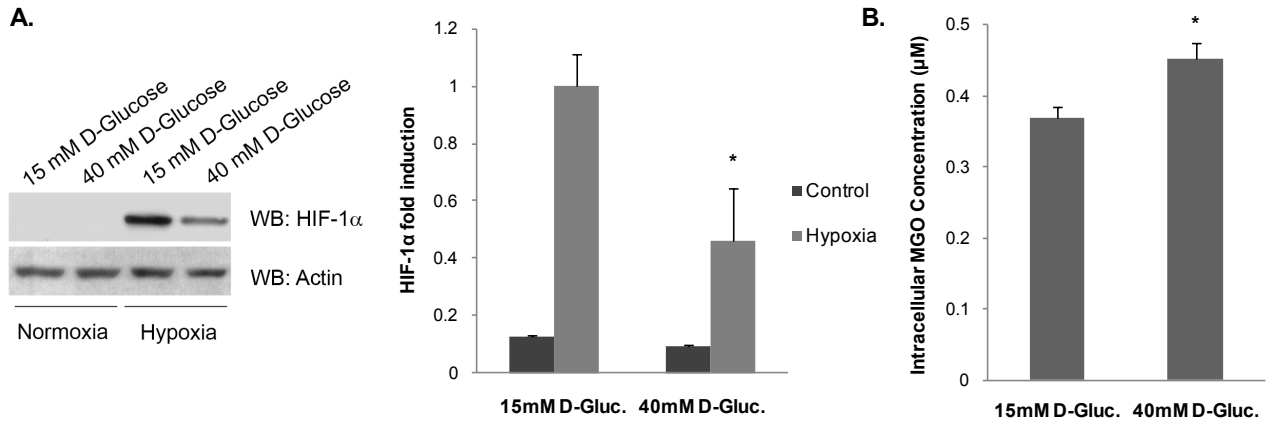

Figure 15. High glucose destabilizes the HIF-1α protein under hypoxia and leads to intracellular accumulation of MGO. (A) ARPE-19 cells were grown in 15 mM (basal DMEM: F12 medium) or 40 mM of D-glucose during 10 days. During the last 6 hours of incubation, cells were exposed to hypoxia (2% O_2). After the treatments, proteins were separated by SDS-PAGE, transferred to PVDF membranes and probed against HIF-1α and actin. The results represent the mean ± SD of at least three independent experiments. * $p < 0.05$, significantly different from control (one-way ANOVA). (B) ARPE-19 cells were grown in DMEM: F12 medium containing 15 mM or 40 mM of D-glucose during 10 days. Cells were then lysed in 0.1 M acetic acid and the intracellular levels of MGO were determined by HPLC after derivatization with DDB. The results represent the mean ± SD of at least three independent experiments. * $p < 0.05$, significantly different from control (t test).

To further emphasize the relevance of high glucose-induced downregulation of HIF-1α, the intracellular levels of MGO following exposure of ARPE-19 cells to high glucose were assessed. Data show that after 10 days of incubation with high glucose (40 mM), the intracellular levels of MGO increased about 23%, reaching the concentration of 0.45 ± 0.024 μM (Figure 15B). Consistently, Figures 16A and 16B show that treatment of cells with MGO induces destabilization of HIF-1α that has previously accumulated under hypoxia, in a dose and time-dependent manner. After 30 minutes of incubation with 3 mM MGO there is a decrease of about 50% in the levels of HIF-1α, whereas after 3 hours of incubation HIF-1α is virtually undetectable (Figure 16B). Consistently, immunofluorescence data shows that hypoxia leads to a remarkable accumulation of HIF-1α in the nucleus, while MGO induces a marked decrease in the levels of HIF-1α present in the nuclear region (Figure 16C). As a control, it is shown that the effect of MGO cannot be generalized

to all transcription factors. Indeed, MGO does not downregulate other transcription factors, such as NF-E2 related factor 2 (Nrf-2) (Figure 16D). Moreover, incubation of RPE cells with 3 mM MGO for 30 minutes or for 3 hours resulted in an intracellular accumulation of MGO of 1.54 ± 0.246 μM or 0.96 ± 0.247 μM, respectively (Figure 16E). The decrease of MGO after 3 hours of incubation probably reflects the scavenging by glyoxalases (Ceradini et al, 2008; Miller et al, 2006), as well as irreversible binding of MGO to proteins and other cell components (Ramasamy et al, 2006). These concentrations are within the physiological range reported in pathological conditions, such as diabetes (Beisswenger et al, 1999; Han et al, 2007).

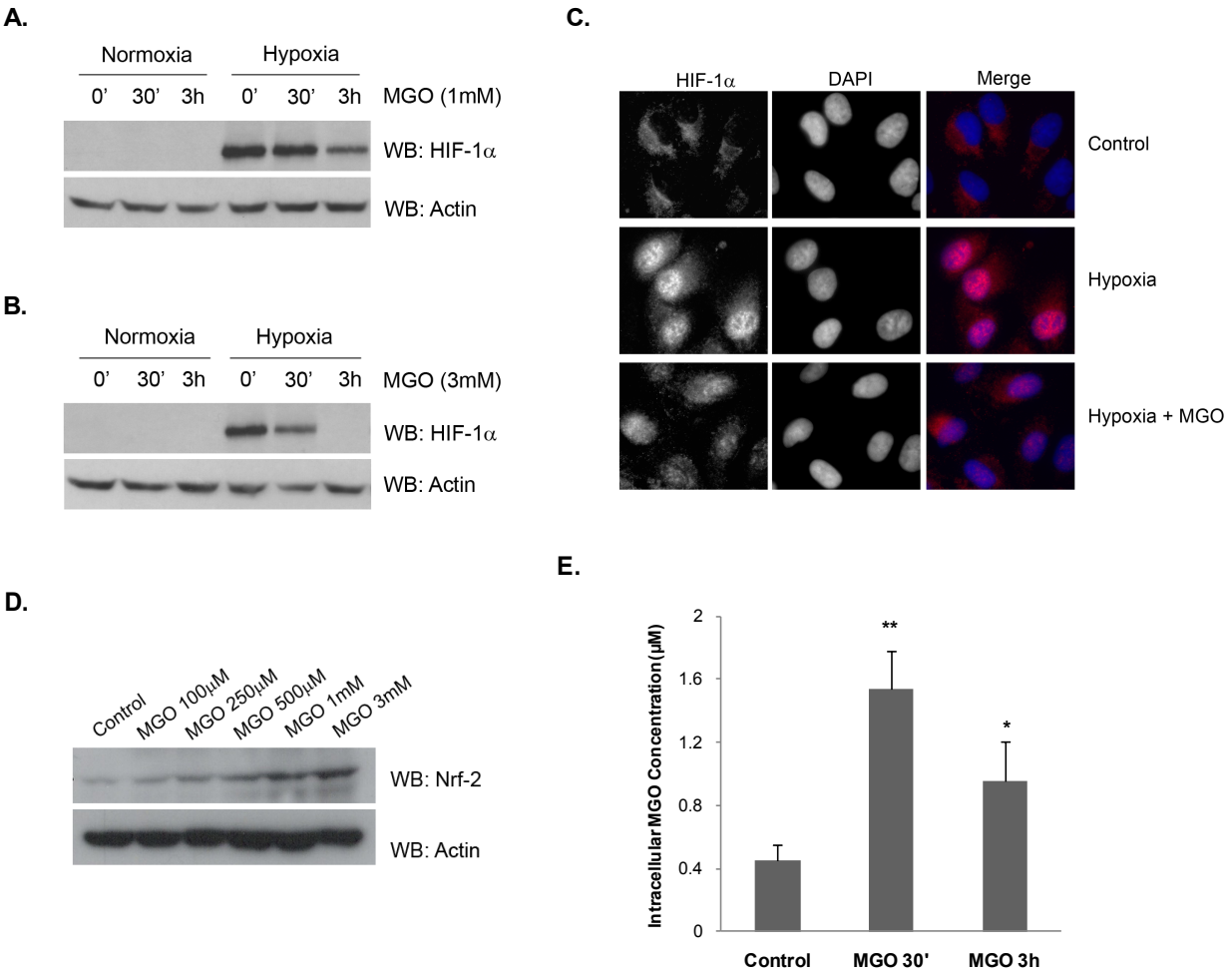

Figure 16. MGO destabilizes the HIF-1α protein under hypoxia. (A and B) ARPE-19 cells were exposed to hypoxia (2% O_2) for 6 hours and MGO (1 mM or 3 mM) was added for 30 minutes or 3 hours. The cell lysates were analyzed by WB using antibodies against HIF-1α and actin. (C) ARPE-19 cells were subjected to hypoxia (2% O_2) for 6 hours either in the absence or presence of MGO (3 mM for 90 minutes). The subcellular distribution of HIF-1α was assessed by immunofluorescence (400 x of magnification). (D) ARPE-19 cells were treated with different MGO concentrations (100 μM to 3 mM) for 2 hours. The cell lysates were analyzed by WB using antibodies against Nrf-2 and actin. (E) ARPE-19 cells were treated with 3 mM of MGO for 30 minutes or 3 hours. Cells were then lysed in acetic acid (0.1 M) and the intracellular levels of MGO were determined by HPLC after derivatization with DDB. The results represent the mean ± SD of at least three independent experiments. * $p < 0.05$ and ** $p < 0.01$, significantly different from control (one-way ANOVA with the Dunnet's comparison test).

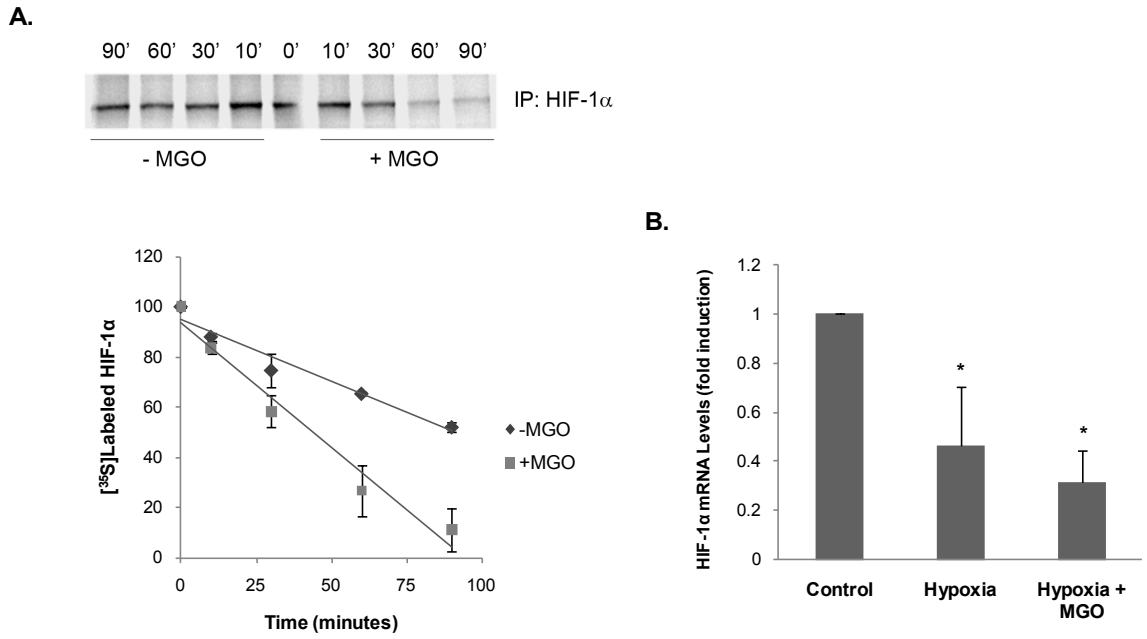

Figure 17. MGO leads to decreased half-life of HIF-1α protein under hypoxia. (A) After metabolic labelling with L-[^{35}S] methionine/cysteine under hypoxia, ARPE-19 cells were maintained under hypoxia, either in the absence or the presence of 3 mM MGO. Cells were harvested at 0, 10, 30, 60 and 90 minutes in 0.5% NP-40 lysis buffer. HIF-1α was immunoprecipitated and radiolabelled HIF-1α protein was assessed by SDS-PAGE and autoradiography. (B) ARPE-19 cells were subjected to hypoxia (2% O_2) for 6 hours in absence or presence of 3 mM MGO for 1 hour. HIF-1α mRNA and 18S rRNA levels were quantified through RT-PCR. The results represent the mean ± SD of at least three independent experiments. * $p < 0.05$, significantly different from control (one-way ANOVA, Dunnet's comparison test).

Pulse-chase experiments clearly show that MGO decreases the half-life of HIF-1α by about two fold, from 98 minutes to 47 minutes (Figure 17A). This indicates that MGO indeed downregulates HIF-1α by promoting increased degradation of the transcription factor. Levels of mRNA for HIF-1α decrease under hypoxia, as well as in the presence of MGO (Figure 17B). The difference on the levels of HIF-1α mRNA between hypoxia and hypoxia plus MGO is not statistically significant ($p > 0.05$). It should be noted that the decrease in mRNA for HIF-1α does not necessarily translate into a decrease in the abundance of the protein. In fact, hypoxia leads to a 2.5 fold decrease in mRNA levels of HIF-1α (Figure 17B), whereas the levels of protein dramatically increase (Figure 16A). The decrease in mRNA for HIF-1α under hypoxia has been widely reported and reflects the complex regulatory process of cell response to low oxygen, which includes induction of a natural antisense RNA of HIF-1 (aHIF) (Thrash-Bingham & Tartof, 1999; Uchida et al, 2004). Based on this and other reports, as well as on our observation that MGO induces a decrease in the half-life of HIF-1α, it is clear that reduction on the levels of HIF-1α can be predominantly ascribed to an increase in protein degradation.

Of significance, overexpression of GLO I prevents intracellular accumulation of MGO (Figure 18A) and promotes stabilization of HIF-1α under hypoxia following treatment either with high glucose (Figure 18B) or with MGO (Figure 18C).

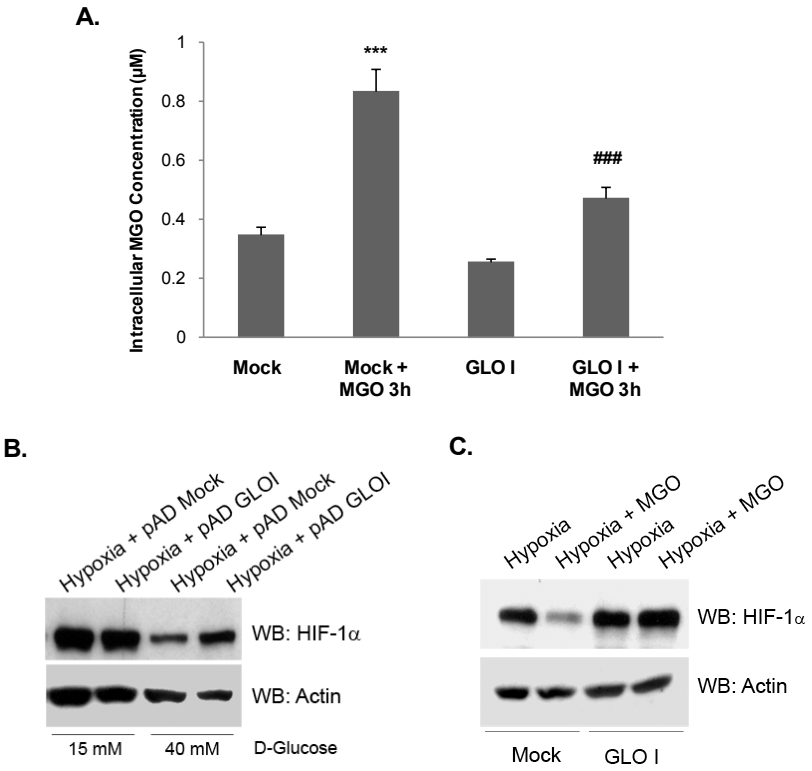

Figure 18. GLO I overexpression stabilizes HIF-1α under high glucose or MGO treatment. (A) ARPE-19 cells were infected with pAD hGLOI adenovirus for 48 hours. By the end of the infection, cells were treated with 3 mM of MGO for 3 hours. The intracellular levels of MGO were determined by HPLC. The results represent the mean ± SD of at least three independent experiments. *** $p < 0.001$, significantly different from Mock; ### $p < 0.001$, significantly different from Mock + MGO3h (one-way ANOVA with the Tukey's multiple comparison test). (B) ARPE-19 cells were grown in 15 mM (basal DMEM: F12 medium) or 40 mM of D-glucose during 10 days. After 8 days of incubation, cells were infected with pAD hGLOI adenovirus for 48 hours. During the last 6 hours of incubation, cells were subjected to hypoxia and subsequently lysed. Whole cell lysates were analyzed by WB against HIF-1α and actin. (C) ARPE-19 cells were infected with pAD hGLOI adenovirus for 48 hours. During the last 6 hours of incubation, cells were subjected to hypoxia in the presence or absence of MGO (3 mM for 3 hours). Subsequently, cells were lysed and the proteins were separated by SDS-PAGE, transferred to PVDF membranes and probed against HIF-1α and actin.

4.3.2 MGO decreases the transcriptional activity of HIF-1α

The downregulation of HIF-1α following exposure to MGO consistently leads to a decrease in HIF-1 transcriptional activity. HIF-1 binds to HREs of target genes and initiates transcription of a number of genes, including VEGF. Data represented in Figure 19A shows that hypoxia leads to a significant increase in HIF-1α transcriptional activity as evaluated by an HRE-luciferase associated reporter gene assay. Incubation with MGO dramatically decreases the activity of luciferase, suggesting a strong decrease of the HIF-1 transcriptional activity. Consistent with this decrease in the transcriptional activity, the levels of VEGF mRNA also decrease in the presence of MGO as compared to hypoxic cells in the absence of MGO (Figure 19B). The levels of VEGF secreted into the culture medium also decrease as compared to cells subjected only to hypoxia (Figure 19C).

Downregulation of HIF-1 transcriptional activity can also be detected under normoxia following treatment with MGO, which can be ascribed to low, but detectable, levels of HIF-1α in controls (as revealed by longer exposure of WB films).

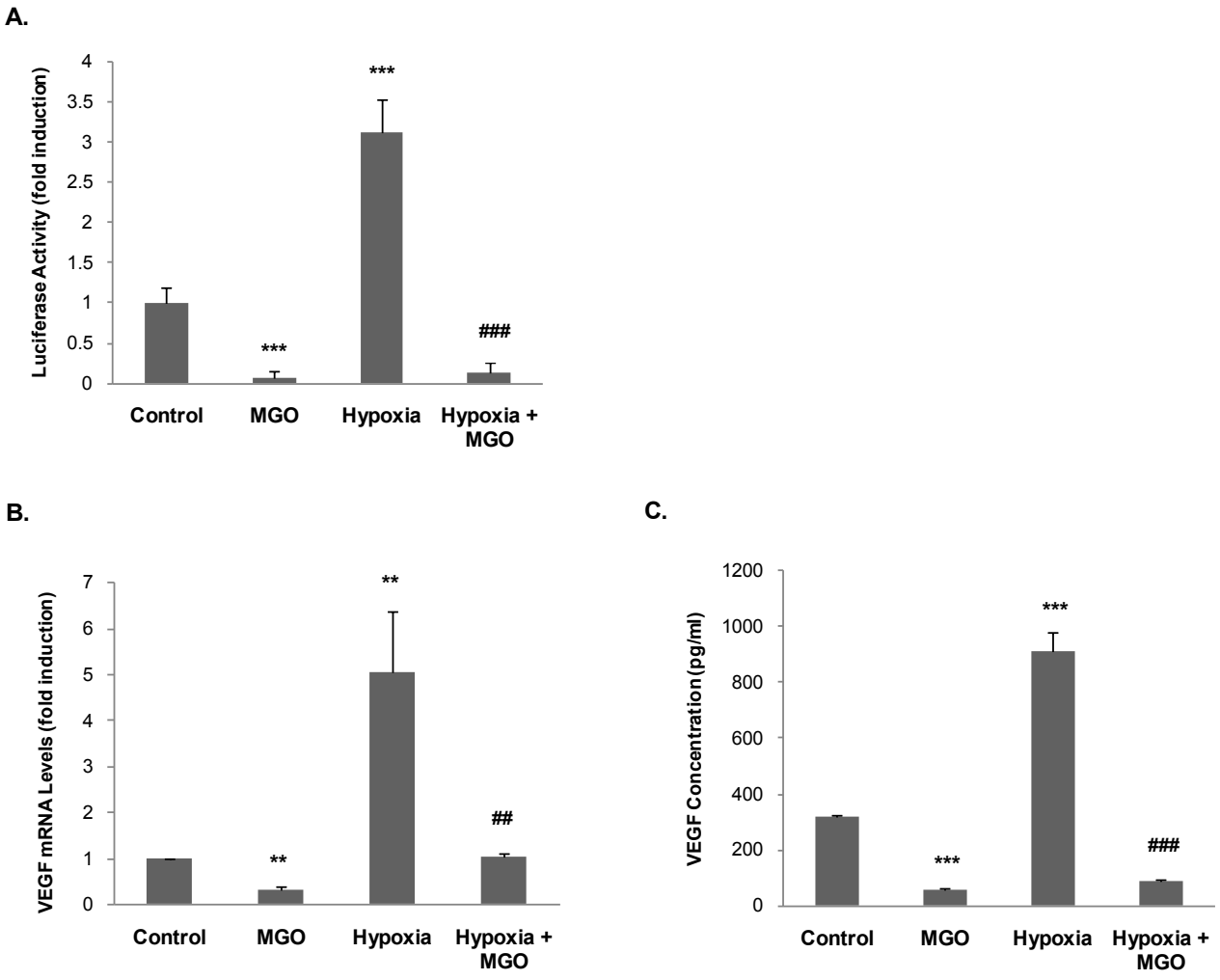

Figure 19. MGO decreases the transcriptional activity of HIF-1 and the release of $VEGF_{121/165}$ into the culture medium. (A) ARPE-19 cells were transiently transfected with the pT81 HRE-luciferase vector and were subjected to hypoxia (2% O_2) for 6 hours in the absence or presence of MGO (1 mM for 4 hours). Subsequently, the luciferase activity was determined and the values were expressed as fold induction over control. The results represent the mean ± SD of at least three independent experiments. *** $p < 0.001$, significantly different from control; ### $p < 0.001$, significantly different from hypoxia (one-way ANOVA, Tukey's multiple comparison test). (B) ARPE-19 cells were subjected to hypoxia (2% O_2) for 6 hours either in the absence or the presence of MGO (1 mM for 4 hours). Total RNA was used to synthesize cDNA, which, in turn, was used as template to quantify VEGF mRNA and 18S rRNA through RT-PCR. The results represent the mean ± SD of at least three independent experiments. ** $p < 0.01$, significantly different from control; ## $p < 0.01$, significantly different from hypoxia (one-way ANOVA, Tukey's multiple comparison test). (C) ARPE-19 cells were subjected to hypoxia (2% O_2) for 6 hours either in the absence or in the presence of MGO (1 mM for 4 hours). The concentration of the diffusible $VEGF_{121}$ and $VEGF_{165}$ isoforms were determined by ELISA using a monoclonal antibody against human $VEGF_{121/165}$. The results represent the mean ± SD of at least three independent experiments. *** $p < 0.001$, significantly different from control; ### $p < 0.001$, significantly different from hypoxia (one-way ANOVA, Tukey's multiple comparison test).

4.3.3 MGO induces ubiquitination and proteasome-dependent degradation of HIF-1α

Methylglyoxal has recently been shown to modify HIF-1α in arginine residues (Ceradini et al, 2008), probably leading to changes in protein conformation. Indeed, immunoprecipitation experiments show that MGO modifies lysine and arginine residues of HIF-1α, increasing its immunoreactivity against Nε-carboxymethyl-lysine (CML) and Nα-acetyl-Nδ-(5-hydro-5-methyl)-4-imidazolone (MG-H1) antibodies, respectively (Figure 20). Thus, we hypothesized that modification by MGO might stimulate proteasome-dependent degradation of HIF-1α, as a result of post-translational modifications.

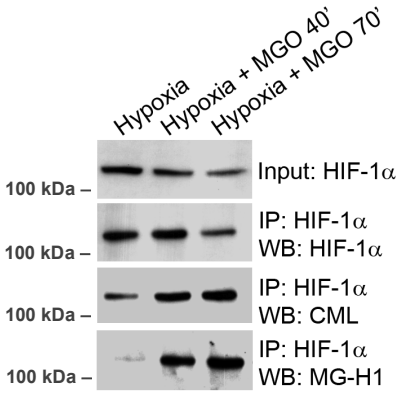

Figure 20. MGO modifies HIF-1α leading to the formation of MG-H1 and CML-adducts. ARPE-19 cells were subjected to hypoxia (2% O_2) for 6 hours and, subsequently, incubated with MGO (3 mM) for 40 and 70 minutes. HIF-1α was immunoprecipitated and the immunoprecipitates were probed against CML and MG-H1.

Treatment of cells with proteasome inhibitors, following incubation with MGO, results in the accumulation of high molecular weight bands that immunoreact with anti-HIF-1α antibodies (Figure 21A). It should be noted that the effect of MGO under hypoxia is quite different from the effect under proteasome inhibition (compare lane 2 with lane 4 on Figure 21B). Indeed, under hypoxia and MGO, HIF-1α is readily degraded, whereas in the presence of MG132 there is an apparent loss of HIF-1α (120 kDa), but accumulation of high molecular weight forms of the protein that correspond to ubiquitinated forms of HIF-1α, as confirmed by immunoprecipitation experiments (Figure 21C). This suggests that proteasome inhibition prevents degradation whereas ubiquitination of HIF-1α is still maintained and that MGO-induced degradation of HIF-1α is proteasome-dependent and involves ubiquitination of the protein. Immunofluorescence data further confirm these results. Data show that proteasome inhibition *per se* decreases the levels of polyubiquitin conjugates in the nucleus, consistent with previous reports (Mailand et al, 2007; Takeshita et al, 2009). However, addition of MGO changes the distribution of ubiquitin in the cell, strongly increasing the nuclear co-localization between ubiquitin conjugates and HIF-1α (Figure 21D). It is further shown that proteasome inhibitor MG132 (or epoxomicin) prevents MGO-induced

degradation of HIF-1α and extends the half-life of the protein by about 1.7 fold (Figure 21E). Taken together, these observations indicate that HIF-1α is modified by MGO and that such modification results in ubiquitin-dependent degradation of the protein.

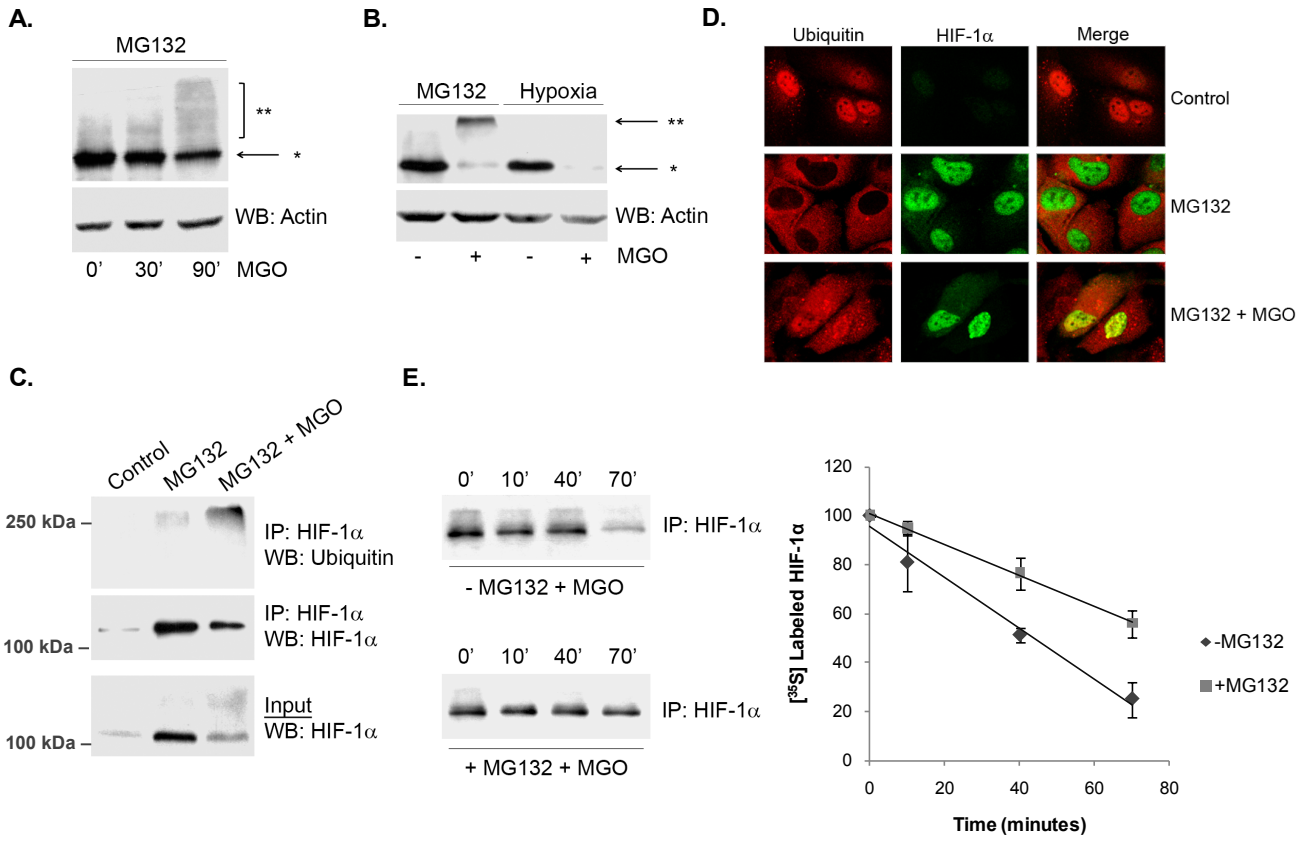

Figure 21. MGO induces polyubiquitination and degradation of HIF-1α. (A and B) ARPE-19 cells were treated with MG132 (20 μM) for 4 hours or subjected to hypoxia (2% O_2) for 6 hours and then incubated with MGO (3 mM) for 30 minutes and 90 minutes (A) or 3 hours (B). The cell lysates were analyzed by WB against HIF-1α and the PVDF membranes were overexposed to reveal higher molecular weight bands; * HIF-1α of 120 kDa; ** posttranslational modified HIF-1α (with higher molecular weights). (C) ARPE-19 cells were treated with MG132 (20 μM) for 4 hours either in the presence or absence of 3 mM MGO (for the last 90 minutes of incubation). HIF-1α was immunoprecipitated and immunoprecipitates were probed against HIF-1α and ubiquitin (P4D1). (D) ARPE-19 cells cultured in coverslips were transfected with HA tagged HIF-1α. Subsequently, cells were treated with MG132 (20 μM) for 4 hours in the absence or presence of 3 mM MGO for 90 minutes. Cells were fixed with 4% PFA for 10 minutes and used for immunocytochemistry using specific antibodies directed against HA and ubiquitin (FK1) (630 x of magnification). (E) ARPE-19 cells were incubated with L-[^{35}S] methionine/cysteine under hypoxia. After metabolic labelling, cells were maintained under hypoxia, in the presence of 3 mM of MGO and either in the absence or presence of MG132 (20 μM). Cells were harvested at 0, 10, 40 and 70 minutes in 0.5% NP-40 lysis buffer. HIF-1α was immunoprecipitated and radiolabelled HIF-1α protein was assessed by SDS-PAGE and autoradiography.

However, because proteasome inhibitors do not fully prevent HIF-1α degradation, it seems reasonable to suggest that other degradation pathways are likely to be involved in HIF-1α degradation induced by MGO. An alternative explanation is that, even in the presence of inhibitors

such as MG132, a residual proteasomal activity is maintained (Figure 22), which might be sufficient to sustain some level of degradation of HIF-1α in the presence of MGO.

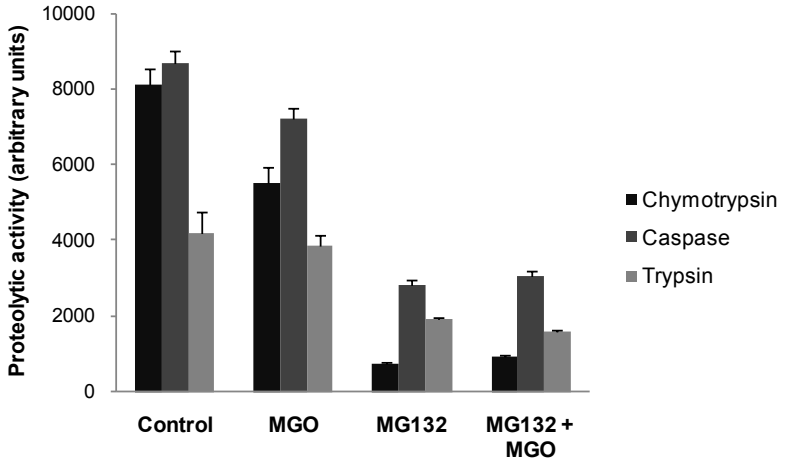

Figure 22. MGO does not increase the 20S proteasome activity and MG132 does not completely inhibit the proteolytic activity of the proteasome. Cells were treated with the proteasome inhibitor MG132 (20 μM) for 4 hours, either in the absence or presence of MGO (3 mM for 3 hours). The 20S proteasome activities were determined by *in vitro* fluorogenic assays, using specific substrates for each activity: Suc-LLVY-MCA (chymotrypsin-like activity), Z-LLE-MCA (caspase-like activity) and Boc-LRR-MCA (trypsin-like activity). The values reported in the graph correspond to measurements after 30 minutes of activity.

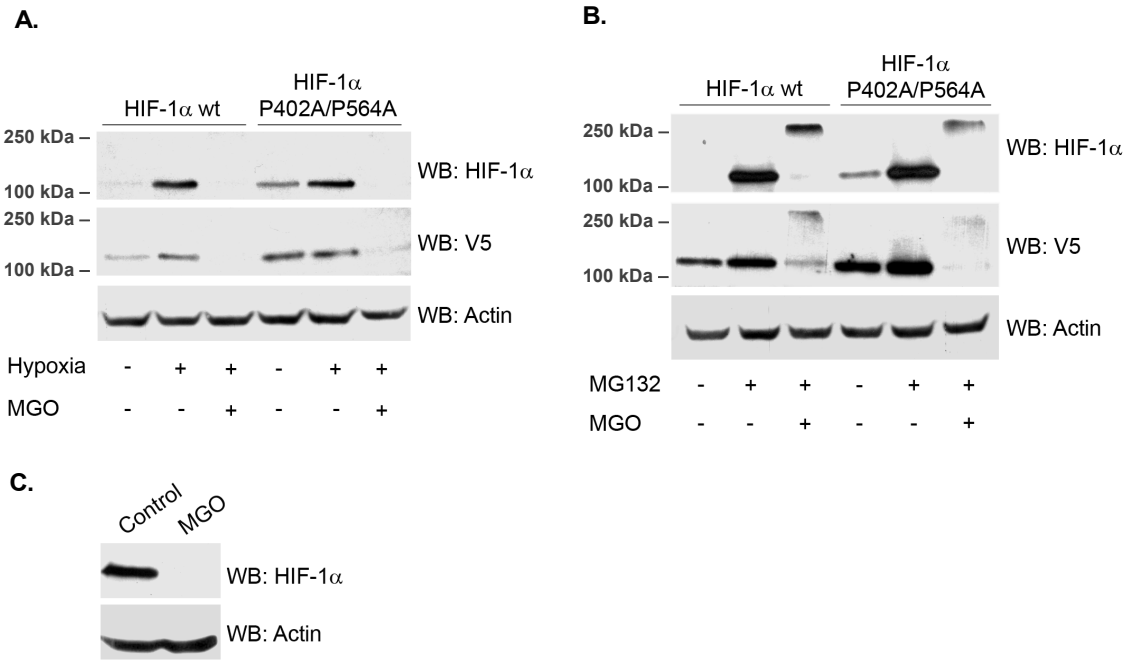

Figure 23. Destabilization of HIF-1α induced by MGO is independent on VHL. (A and B) ARPE-19 cells were transiently transfected with HIF-1α wt-V5 or HIF-1α (P402A/P564A)-V5 plasmids. Cells were subsequently subjected to hypoxia (2% O_2) for 6 hours (A) or treated with MG132 (20 μM) for 4 hours (B), in the absence or presence of MGO (3 mM for 3 hours). The cell lysates were immunoblotted against HIF-1α and V5. (C) RCC4 $VHL^{-/-}$ cells were treated with MGO (3 mM for 3 hours) and cell lysates were analyzed by WB for HIF-1α and actin.

4.3.4 Destabilization of HIF-1α induced by MGO is independent on pVHL and HIF-1α proline hydroxylation

The canonical pathway for HIF-1α degradation requires recruitment of the ubiquitin ligase pVHL and prior hydroxylation of prolines 402 and 564 on HIF-1α. ARPE-19 cells were transfected with a mutant HIF-1α where the proline residues 402 and 564 were mutated to alanine (P402A/P564A). Results presented in Figure 23A show that mutant HIF-1α is readily degraded in the presence of MGO indicating that prolines 402 and 564 are not required for MGO-induced degradation of HIF-1α. Moreover, both wild-type and mutated HIF-1α accumulate as high molecular weight bands in the presence of proteasome inhibitors, indicating that the mechanism whereby mutant HIF-1α is degraded in the presence of MGO does not require proline hydroxylation but is still dependent on the proteasome (Figure 23B). To further confirm that this new pathway is independent on pVHL, a VHL deficient cell line (RCC4 $VHL^{-/-}$) was treated with MGO. Results in Figure 23C show that in untreated cells, HIF-1α is inherently stable, whereas treatment with MGO results in destabilization and rapid degradation of the protein.

4.3.5 CHIP is the ligase that ubiquitinates HIF-1α in the presence of MGO

MGO is likely to destabilize HIF-1α by inducing post-translational modification of the transcription factor, thus we suggest that ligases that target post-translational modified proteins are likely candidates to promote HIF-1α ubiquitination. Because CHIP is a chaperone-binding ubiquitin ligase that bridges between the ubiquitin-proteasome pathway and molecular chaperones (Connell et al, 2001; Marques et al, 2006; Murata et al, 2001), we investigated whether CHIP is the ligase responsible for HIF-1α ubiquitination in the presence of MGO. ARPE-19 cells were transfected with c-myc CHIP and subsequently treated with the proteasome inhibitor MG132 (or epoxomicin) in the presence or in the absence of MGO. Data in Figure 24A show that treatment with MGO increases the association between CHIP and HIF-1α. In the absence of MGO there is also evidence for limited interaction between both proteins, suggesting a potential role for CHIP in degradation of HIF-1α under normoxia. To further investigate this possibility, ARPE-19 cells overexpressing a stable HIF-1α mutant (P402A/P564A) were co-transfected with increasing amounts of CHIP. Data consistently show a significant decrease in the levels of HIF-1α (Figure 24B). However, under physiological conditions and normoxia, the majority of HIF-1α in cells is presumably degraded via VHL and the physiological function of CHIP-mediated degradation of HIF-1α, in these conditions, is not clear.

Following treatment with MGO and proteasome inhibitors, HIF-1α that co-precipitates with CHIP migrates at higher molecular weights (Figure 24C), consistent with ubiquitinated forms of the transcription factor. Significantly, overexpression of CHIP in the presence of MGO reveals an accumulation of polyubiquitinated forms of HIF-1α (Figure 25A). Moreover, CHIP mutants that

either do not bind chaperones (K30A) or do not present ubiquitin ligase activity (H260Q) decrease the ubiquitination of HIF-1α (Figure 25B) and partially stabilize the protein (Figure 25C), above the levels observed in control. Moreover, data consistently show that CHIP K30A does not co-immunoprecipitate with HIF-1α, while both wild type CHIP and the mutant CHIP H260Q bind to and co-precipitate with HIF-1α (Figure 25B).

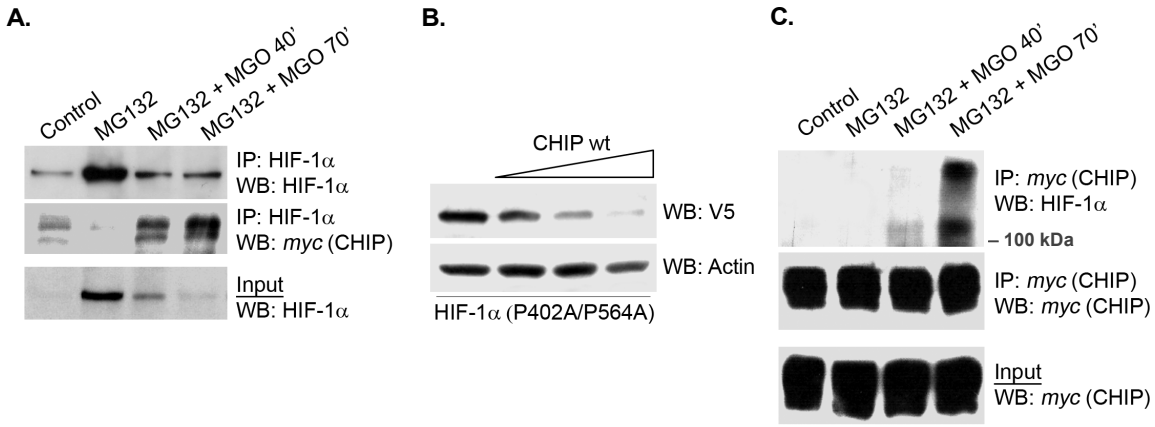

Figure 24. MGO increases the interaction between HIF-1α and CHIP. (A) ARPE-19 cells were transiently transfected with CHIP wt c-myc plasmid and treated with MG132 (20 μM) for 4 hours in the absence or presence of MGO (3 mM for 40 or 70 minutes). HIF-1α was immunoprecipitated and the immunoprecipitates were probed against *c*-myc and HIF-1α. (B) ARPE-19 cells were transfected with the HIF-1α (P402A/P564A)-V5 plasmid simultaneously with increasing amounts (1, 2 and 4 μg DNA) of CHIP wt c-myc. Proteins were separated by SDS-PAGE, transferred to PVDF membranes and probed with monoclonal antibodies against V5 and actin. (C) ARPE-19 cells were transiently transfected with c-myc tagged CHIP wt plasmid and treated with MG132 (20 μM) for 4 hours in the absence or presence of MGO (3 mM for 40 or 70 minutes). C-myc was immunoprecipitated and the immunoprecipitates were probed against HIF-1α and c-myc.

Simultaneous overexpression of the two mutants is more effective in stabilizing HIF-1α, than individual overexpression (Figure 25C). In consistence with our model, this is likely to reflect the need for both ubiquitin ligase activity and binding of chaperones to trigger CHIP-mediated degradation of HIF-1α in the presence of MGO. One may speculate that the synergistic effect of the two mutants is related to their specific mechanisms of action and competition with endogenous CHIP. For example, in the presence of both mutants, CHIP H260Q may block access of endogenous CHIP to its binding site on HIF-1α, thus contributing to stabilize the transcription factor. On the other hand, CHIP K30A may sequester the E2 or other cofactors required for the activity of endogenous CHIP. In addition, overexpression of mutant CHIP is likely to account for the formation of non-functional CHIP dimmers with endogenous CHIP (Nikolay et al, 2004). These hypotheses may justify the greater stabilization of HIF-1α in the presence of both mutants.

The observation that the mutant K30A CHIP is unable to bind and ubiquitinate HIF-1α suggests that binding to chaperones is essential for CHIP-dependent targeting and ubiquitination of HIF-1α. Indeed, results in Figure 26A show that treatment with MGO increases the association

between Hsp40/70 and HIF-1α. We further observed that simultaneous overexpression of Hsp40 and Hsp70 increases the levels of CHIP associated with HIF-1α in the presence of MGO, suggesting that CHIP/HIF-1α association is mediated by Hsp40/Hsp70 (Figure 26B). Interestingly, binding of Hsp40 appears to be dependent on prior association of Hsp70 to HIF-1α (Figure 26B).

It should be noted that MGO-induced degradation of HIF-1α under hypoxia is extremely rapid (Figure 17A) and HIF-1α protein-protein interactions are virtually undetectable in these conditions. Considering that data clearly shows that MGO-induced degradation of HIF-1α is independent on VHL and that proteasome is still involved in CHIP-dependent degradation of HIF-1α in the presence of MGO, we have performed a number of experiments using proteasome inhibitors, since this increases the half-life of HIF-1α (Figure 21E), allowing for detection of HIF-1α interactions with its binding partners, such as CHIP, Hsp40 and Hsp70 (Figures 24, 25 and 26).

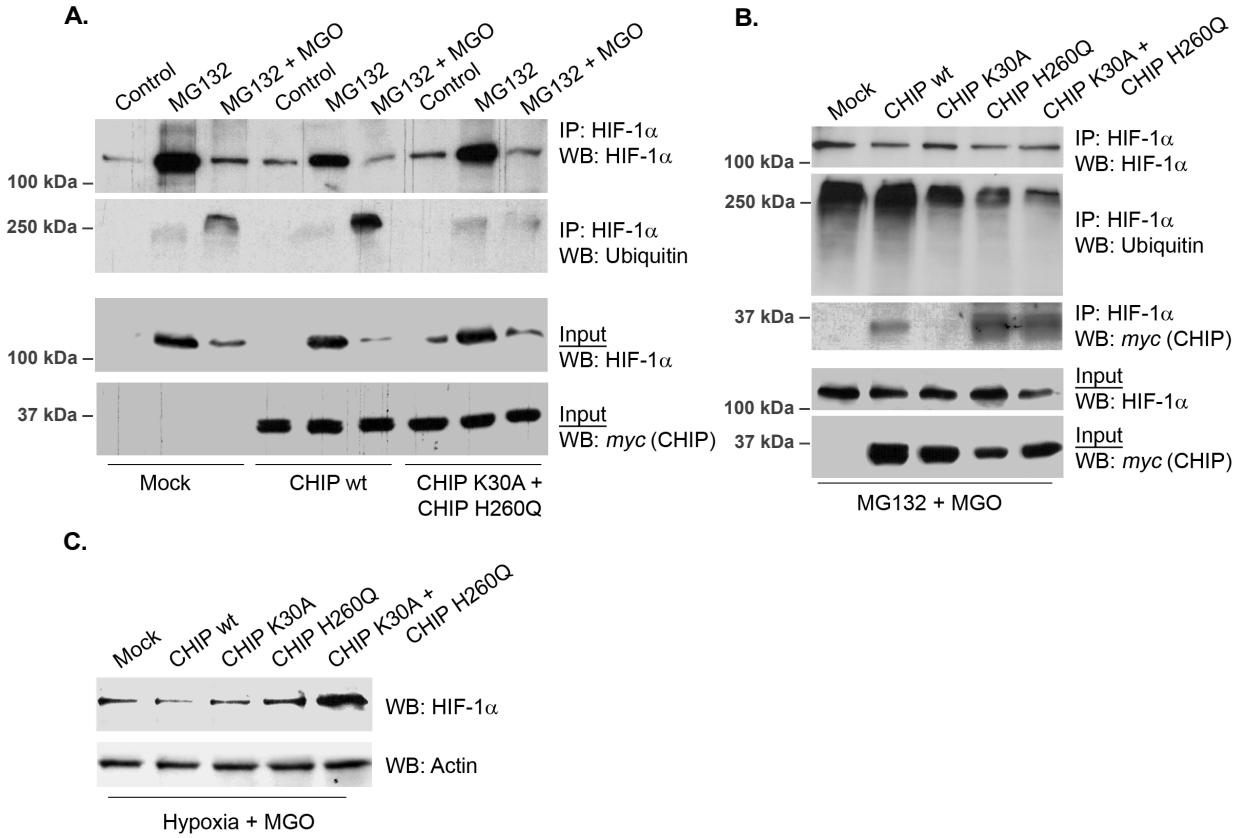

Figure 25. CHIP polyubiquitinates HIF-1α in the presence of MGO. (A) ARPE-19 cells were transfected with CHIP wt c-myc or with a combination of the mutants CHIP K30A c-myc and CHIP H260Q c-myc and treated with MG132 (20 μM) for 4 hours in the absence or presence of MGO (3 mM for 70 minutes). HIF-1α immunoprecipitates were immunoblotted against HIF-1α and ubiquitin (P4D1). (B) ARPE-19 cells were transfected with CHIP wt c-myc or with the dominant negatives CHIP K30A c-myc and CHIP H260Q c-myc, simultaneously or separately, and treated with MG132 (20 μM) for 4 hours in the absence or presence of MGO (3 mM for 70 minutes). HIF-1α was then immunoprecipitated and the immunoprecipitates were blotted against HIF-1α, c-myc and ubiquitin (P4D1). (C) ARPE-19 cells were transfected with CHIP wt c-myc, CHIP K30A c-myc or/and CHIP H260Q c-myc dominant negatives, either simultaneously or individually, and subjected to hypoxia for 6 hours in the absence or presence of MGO (3 mM for 70 minutes). Proteins were separated by SDS-PAGE, transferred to PVDF membranes and probed against HIF-1α and actin.

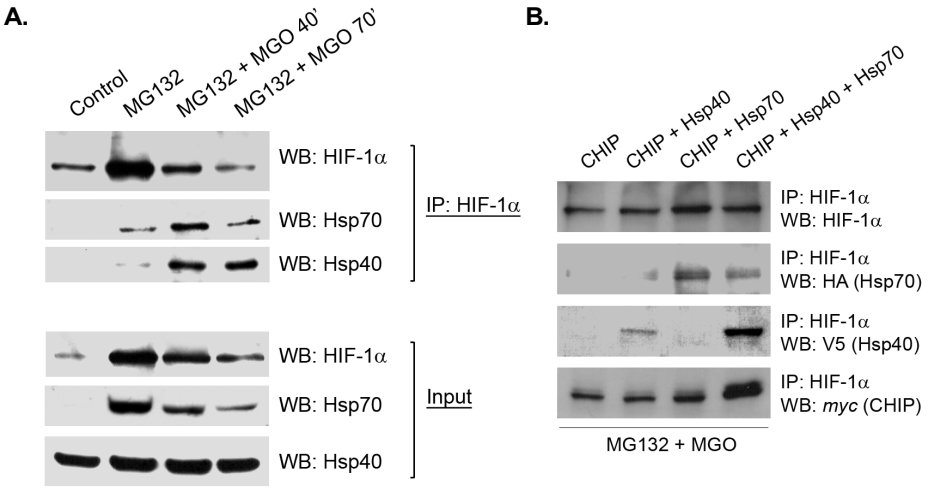

Figure 26. MGO induces interaction between HIF-1α and the molecular chaperones Hsp40 and Hsp70. (A) ARPE-19 cells were treated with MG132 (20 μM for 4 hours) either in the presence or in the absence of MGO (3 mM for 40 or 70 minutes). HIF-1α was immunoprecipitated and the immunoprecipitates were probed using antibodies against HIF-1α, Hsp70 and Hsp40. (B) ARPE-19 cells were transfected with CHIP-c-myc simultaneously with V5-tagged Hsp40 and/or HA-tagged Hsp70. Cells were subsequently treated with MG132 (20 μM) for 4 hours and MGO (3 mM) for the last 70 minutes of incubation. HIF-1α was immunoprecipitated and the immunoprecipitates were blotted against HA, V5 and c-myc.

Loss of function studies, by silencing CHIP with shRNAs (Figures 27A and 27B), clearly show a biological function for this new degradation pathway. Indeed, depletion of endogenous CHIP by shRNAs leads to decreased accumulation of high molecular weight bands that cross-react with anti-HIF-1α antibodies (Figure 27C). In addition, silencing of CHIP results in decreased ubiquitination of HIF-1α and stabilization of the protein under hypoxia in the presence of MGO (Figure 27D). Significantly, silencing of CHIP prevents degradation of HIF-1α under high glucose and hypoxia (Figure 27E), emphasizing the physiological relevance of CHIP-mediated degradation of HIF-1α induced by MGO and high glucose.

Altogether, data is consistent with a model in which MGO-induced modification of HIF-1α recruits Hsp40/70, which in turn recruit CHIP, leading to increased polyubiquitination of HIF-1α and its proteasome-dependent degradation (Figure 28). Moreover, we show that MGO-induced degradation of HIF-1α is independent on VHL, proline hydroxylation and oxygen availability. However, this alternative mechanism is likely to contribute to the pathophysiology of diseases, in which stabilization of HIF-1α is vital to ensure cell survival under hypoxia, such as several diabetic complications.

4.4 Discussion

In this study, it is elucidated a new pathway for degradation of the α subunit of the transcription factor HIF-1. Data here presented is consistent with a molecular mechanism in which

HIF-1α modification by MGO leads to increased association with the molecular chaperones Hsp40/70 which, in turn, recruit CHIP, leading to polyubiquitination and proteasome-dependent degradation of HIF-1α. It is further shown that this mechanism is independent on the recruitment of pVHL and does not require HIF-1α proline hydroxylation.

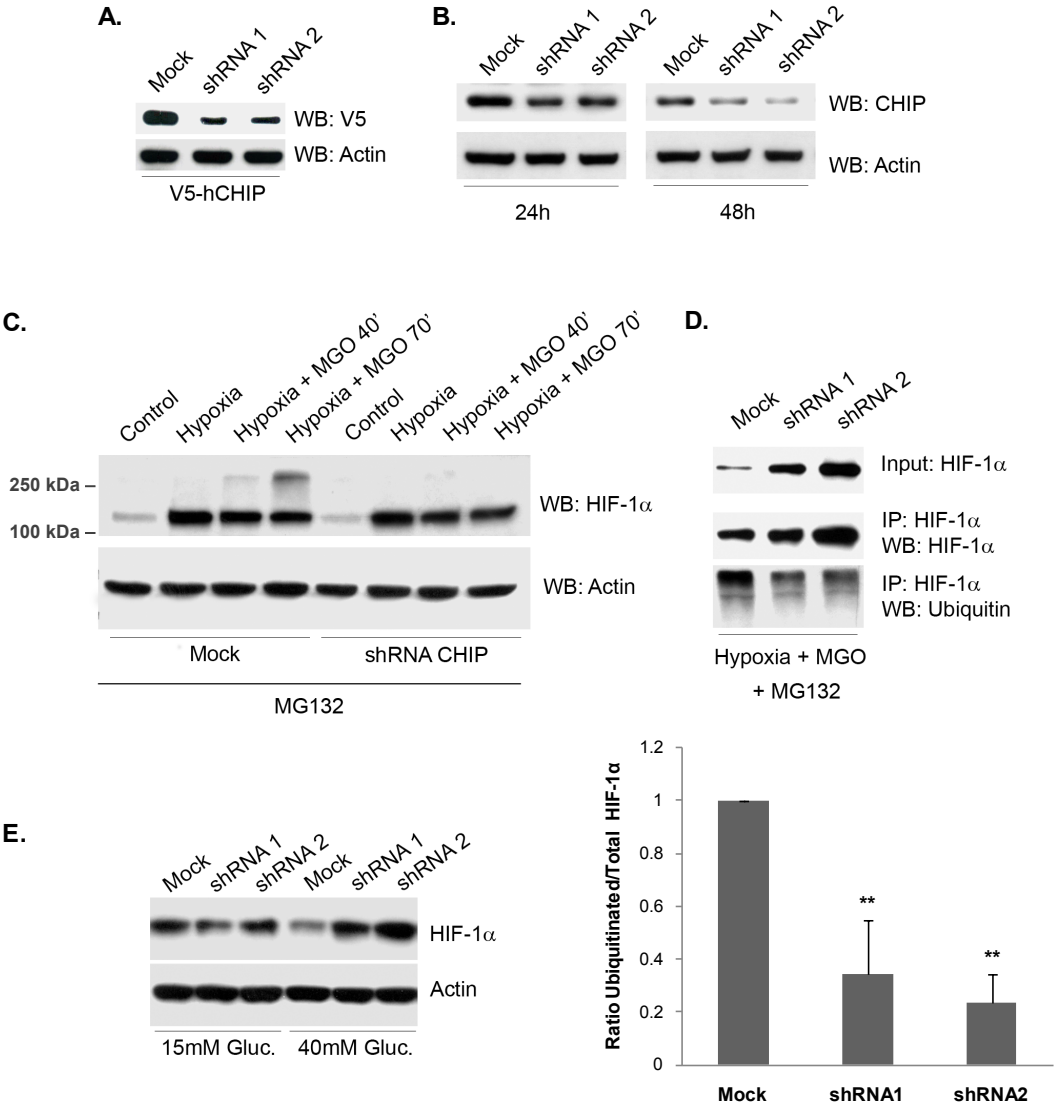

Figure 27. CHIP-silencing stabilizes HIF-1α in the presence of MGO. (A) ARPE-19 cells were co-infected with pAd V5-hCHIP and pAd shRNA-hCHIP for 24 hours. The cell lysates were analyzed by western blot using anti-V5 and anti-actin antibodies. (B) ARPE-19 cells were infected with pAd shRNA-hCHIP for 24 and 48 hours. Cells were subsequently lysed and protein extracts were immunoblotted against endogenous CHIP and actin. (C and D) ARPE-19 cells were infected with pAd shRNA-hCHIP for 24/48 hours and during the last 6 hours of incubation, cells were subjected to hypoxia in the presence of MG132 (20 μM for 4 hours) and MGO (3 mM for the last 40 or 70 minutes). Cell lysates were immunoblotted against HIF-1α and actin (C) or used to immunoprecipitate HIF-1α and probe the immunoprecipitates against HIF-1α and ubiquitin (P4D1) (D). The graph data represent the mean ± SD of at least three independent experiments. ** $p < 0.01$, significantly different from control (one-way ANOVA with the Dunnet's comparison test) (D). (E) ARPE-19 cells were grown in 15 mM (basal DMEM: F12 medium) or 40 mM of D-glucose during 10 days. After 8 days of incubation, cells were infected with pAd shRNA-hCHIP for 48 hours. During the last 6 hours of incubation, cells were subjected to hypoxia and subsequently lysed. Proteins were blotted against HIF-1α and actin.

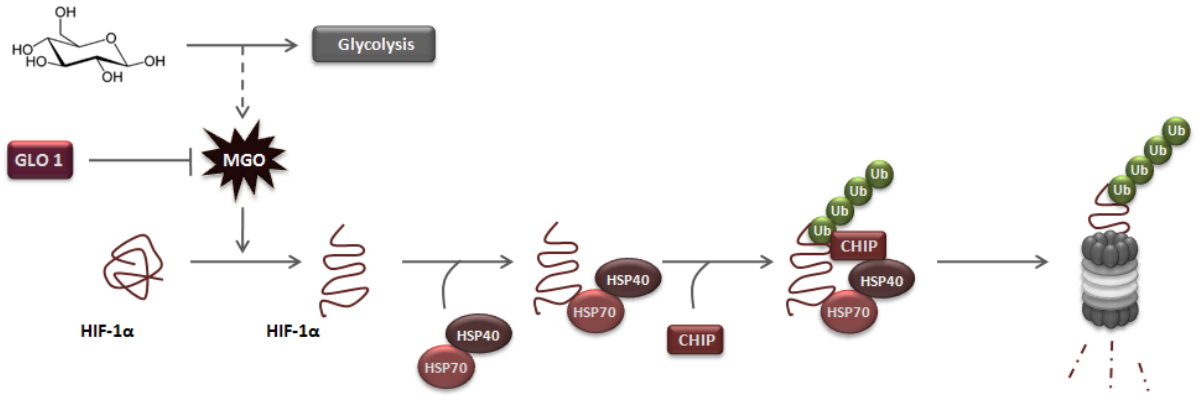

Figure 28. Proposed model for HIF-1α degradation induced by MGO. MGO induces modifications on HIF-1α protein (formation of MG-H1 and CML-adducts) and promotes increased association of Hsp40/70 to HIF-1α. This association leads to recruitment of CHIP, which promotes polyubiquitination and proteasomal degradation of HIF-1α. MGO-induced degradation of HIF-1α is activated under high glucose and is inhibited by overexpression of GLO I.

The new mechanism here reported is triggered by accumulation of MGO and is likely to have a significant physiological impact in conditions of high availability of glucose, such as diabetes. Indeed, we show that exposure of cells to high glucose leads to a sustained increase in the intracellular levels of MGO, which are sufficient to activate degradation of HIF-1α. Moreover, scavenging of intracellular MGO by overexpressing glyoxalase I prevents degradation of HIF-1α under high glucose. Consistently, MGO-induced degradation of HIF-1α leads to decreased transcriptional activity of HIF-1 and decreased expression of VEGF under hypoxia. The reduction on VEGF expression under high glucose and in response to hypoxia was also described before (Ceradini et al, 2008; Thangarajah et al, 2009). The authors suggest that increased levels of MGO under hyperglycaemia induce HIF-1α (Ceradini et al, 2008) and p300 modifications (Thangarajah et al, 2009), which are sufficient to disrupt the interaction between HIF-1α/HIF-1β and HIF-1α/p300, leading to loss of HIF-1 transcriptional activity and poor response to hypoxia. Although this and other modifications induced by MGO cannot be excluded and are likely to account for the plethora of noxious effects of MGO in cells, this study provides robust data that elucidates a new molecular mechanism for degradation of HIF-1α in the presence of MGO. Moreover, MGO-induced degradation of HIF-1α is likely to account for the loss of cell response to hypoxia under high glucose.

In the canonical mechanism for activation of HIF-1, HIF-1α is believed to be inherently stable under hypoxia and pVHL is thought to be virtually the only ubiquitin ligase targeting HIF-1α for proteasomal degradation under normoxia. Over the last five years, a number of reports have suggested that HIF-1α might be destabilized under hypoxia and that interaction of HIF-1α with specific ancillary proteins might promote its degradation. In many instances the mechanism and molecular events that underlie HIF-1α targeting for pVHL/oxygen-independent degradation are not well understood. Nevertheless, a few proteins were shown to interact with HIF-1α promoting its

proteasome-dependent degradation and some proteins were recently identified as putative components of ubiquitin ligase complexes that are able to ubiquitinate HIF-1α, promoting its proteasomal degradation. These include SMURF2, p53/Mdm2 complex, RACK1 and HAF (Hansson et al, 2002; Koh et al, 2008; Liu et al, 2007; Ravi et al, 2000; Tang & Lasky, 2003). Of significance for the results discussed here, is the report that p53 is not involved in destabilization of HIF-1α under high glucose, since destabilization of HIF-1α is still observed in cells deficient in p53 when exposed to hyperglycaemia (Catrina et al, 2004). More recently, it was also shown that HIF-1α can be destabilized by a mechanism that is independent on both pVHL and p53 (Kong et al, 2006). This pathway is activated in response to histone deacetylase inhibitors (HDACIs) and appears to involve destabilization of the Hsp70/90 chaperone axis, resulting in proteasomal degradation of HIF-1α (Kong et al, 2006).

To the best of our knowledge, there are very few studies elucidating unequivocal ubiquitin ligases that target HIF-1α to degradation in a VHL-independent manner. However herein, we do elucidate an entirely novel mechanism for ubiquitination and degradation of HIF-1α in a VHL-independent manner. Significantly, this alternative pathway is activated in response to intracellular accumulation of MGO and involves recruitment of Hsp70/40 and ubiquitination of the transcription factor by the E3 ligase CHIP. However, we do not exclude the possibility that this pathway might be activated by other forms of stress nor do we exclude a function for CHIP-dependent degradation of HIF-1α under normal physiological conditions.

CHIP has a critical role in protein quality control by ubiquitinating misfolded or otherwise damaged proteins through interaction with molecular chaperones (Ballinger et al, 1999; Murata et al, 2003). The observation that CHIP is also able to ubiquitinate HIF-1α reveals a new function for CHIP and an unanticipated association between, high glucose, ubiquitin-proteasome pathway and cell response to hypoxia.

It is conceivable that the mechanism reported in this manuscript is involved in MGO-induced downregulation of other cellular proteins. However, based on the present data and on the current state of art it seems prudent neither to generalize the mechanism nor to restrict it to HIF-1α. For example, MGO was shown to downregulate the phosphorylation of STAT3 and decrease its transcription activity (Lee et al, 2009). Moreover, MGO was also shown to modify the co-repressor mSin3A, which results in increased recruitment of O-GlcNAc-transferase, with consequent increased modification of the transcription factor Sp3 by O-linked N-acetylglucosamine (Yao et al, 2007). MGO is also known to suppress TNF-α-induced NF-κB activation by inhibiting NF-κB/DNA binding (Laga et al, 2007). To the best of our knowledge, the effect of MGO on these and other transcription factors does not result in increased protein degradation. Consistently, we observed that the transcription factor Nrf-2 is not downregulated by MGO. However, it is still possible that some transcription factors or other proteins may be downregulated in response to MGO. Indeed, there are few examples where treatment with MGO was shown to lead to proteasome-dependent degradation of selected substrates. For example, it was shown that Raf-1 protein-serine/threonine

kinase is degraded by an ubiquitin-proteasome-dependent mechanism in response to MGO (Du et al, 2006). Moreover, CML-modified proteins in glyoxal-treated cells were shown to be substrates for ubiquitin conjugation and eventually for degradation by the 26S proteasome (Bulteau et al, 2001). These observations raise the possibility that the ubiquitin-proteasome pathway might be implicated in degradation of proteins modified by MGO and presumably by other glycation products, which typically accumulate in diabetes.

The results reported in this chapter are consistent with a number of sparse results and provide a rational for observations such as that hyperglycaemia inhibits hypoxia-induced stabilization of HIF-1α. Moreover, it is identified CHIP as the ubiquitin ligase that promotes proteasomal degradation of HIF-1α in the presence of MGO. Significantly, loss of function studies, have clearly shown that endogenous CHIP is required to target HIF-1α for proteasomal degradation in the presence of MGO. This observation highlights the importance of this pathway under physiological conditions, as well as on pathologies associated with high glucose and/or disruption of cell response to hypoxia, such as diabetes.

CHAPTER 5

Chapter 5. Methylglyoxal induces endothelial dysfunction by disrupting the balance between VEGF and Ang-2

5.1 Abstract

Deregulation of angiogenesis, vasodegeneration and endothelial dysfunction are all cardinal features of various diabetic complications, accounting, for example, for reduced heart collateral vessel development, impaired wound healing, retinal damage and renal failure. Methylglyoxal (MGO) has been implicated in the molecular events that lead to endothelial dysfunction in diabetes. In this study, we hypothesize that increased levels of MGO, both in cell cultures and animal models of diabetes, disrupts the balance between VEGF (vascular endothelial growth factor) and Ang-2 (angiopoietin-2) secreted by retinal epithelial cells. We further suggest that this imbalance is a key-destabilizing signal leading to apoptosis and decreased proliferation of endothelial cells.

Indeed, we show that MGO increases the levels of Ang-2 and decreases the levels of VEGF secreted by retinal pigment epithelium (RPE) cells in response to hypoxia. VEGF downregulation is likely to be related both to decreased HIF-1α protein levels and decreased HIF-1 transcriptional activity. Data further shows that MGO-induced imbalance in the ratio VEGF/Ang-2 significantly changes the levels of BAX and Bcl-2 in endothelial cells exposed to pre-conditioned medium obtained from RPE cells. Moreover, this imbalance is accompanied by an increase of caspase-3 activity and decreased proliferation of endothelial cells. The data obtained in cell culture systems was shown to be consistent with observations in the retinas of an animal model of diabetes (GK rat), where increased levels of MGO is associated with changes in cellular distribution and protein levels of HIF-1α, VEGF, Ang-2, BAX and Bcl-2, as well as with increased vascular permeability.

In conclusion, MGO-induced imbalance in the ratio between VEGF and Ang-2 secreted by epithelial cells activates the apoptotic cascade and decreases proliferation of endothelial cells, possibly contributing to endothelial and vascular dysfunction in diabetes.

5.2 Introduction

Vascular dysfunction is a main feature of diabetes and involves both micro and macroangiopathy (Cooper et al, 1997). Progressive and long-term vascular complications of diabetes include cardiovascular disease, chronic renal failure, retinal damage, neuropathy and poor wound healing. The majority of these vascular complications are associated, in a more or less obvious way, with impaired angiogenic response (Shoji et al, 2006). For example, although late stages of diabetic retinopathy (DR) are associated with choroidal neovascularization, endothelial cell damage, extensive capillary regression and widespread inner retinal ischemia are at the origin of the disease (Cai & Boulton, 2002; Engerman, 1989; Hammes et al, 2002). Indeed, studies in

retinal capillaries revealed that the loss of pericytes and formation of acellular capillaries are early morphologic changes in a diabetic retina (Cai & Boulton, 2002; Engerman, 1989; Hammes et al, 2002). However, the molecular mechanisms that underlie endothelial dysfunction in diabetes are still unclear.

Among the plethora of hyperglycaemia-mediated mechanisms proposed to induce vascular dysfunction in diabetes, there is increasing evidence that accumulation of MGO and formation of advanced glycation end products (AGEs) may contribute for impaired angiogenic response (Stitt et al, 2005). MGO is a highly reactive α-oxoaldehyde formed as a by-product of glycolysis and its production is enhanced by high levels of glucose (Kalapos, 1999; Ramasamy et al, 2006). MGO is associated with the formation of acellular capillaries and pericytes dropout in diabetic rats (Hammes, 2003; Hammes et al, 2003). Moreover, it has been shown that AGEs attenuate the angiogenic response *in vitro* (Teixeira & Andrade, 1999), while *in vivo* inhibition of AGEs formation, in diabetic mice, can restore ischemia-induced angiogenesis in peripheral limbs (Tamarat et al, 2003). Interestingly, MGO increases the expression of Ang-2 (Hammes et al, 2004; Yao et al, 2007) in diabetic retinas, which in the absence of pro-angiogenic factors induce vessel destabilization and regression (Holash et al, 1999; Maisonpierre et al, 1997; Yancopoulos et al, 2000). Indeed, the function of Ang-2 appears to be highly dependent on the presence of VEGF (Feng et al, 2008; Holash et al, 1999; Maisonpierre et al, 1997; Oshima et al, 2004). For example, in models of solid tumours, increased levels of Ang-2 in the presence of low concentrations of VEGF were shown to result in endothelial cell death and vessel regression, whereas in the presence of high levels of VEGF there is increased endothelial proliferation and angiogenesis is stimulated.

In this study, we show that treatment of RPE cells with MGO results in decreased secretion of VEGF. Conversely, data shows that MGO leads to an increase in the levels of Ang-2 secreted by these cells. The net result is a dramatic decrease in the ratio between VEGF and Ang-2 secreted into the culture medium. This, in turn, leads to a significant decrease in proliferation, as well as to increased activity of caspase-3 in endothelial cells incubated with pre-conditioned media of RPE cells or incubated with different ratios of recombinant VEGF/Ang-2.

5.3 Results

5.3.1 MGO increases the levels of Ang-2 and decreases the levels of VEGF secreted by retinal pigment epithelial cells

It was recently shown that MGO increases the expression of Ang-2 by a mechanism dependent on the modification of the corepressor mammalian Sin3 homolog A (mSin3A) (Yao et al, 2007). Moreover, considering prior data, it is anticipated that MGO further decreases the levels of VEGF secreted by cells under hypoxia, since VEGF is a target gene of HIF-1. Indeed, through immunoblot we observed that MGO increases the levels of Ang-2 and decreases the levels of

VEGF (Figure 29A), thus leading to a dramatic change in the balance VEGF/Ang-2. Consistently, MGO increases the levels of Ang-2 and strongly decreases the levels of VEGF secreted by RPE cells to the culture medium in response to hypoxia (Figure 29B).

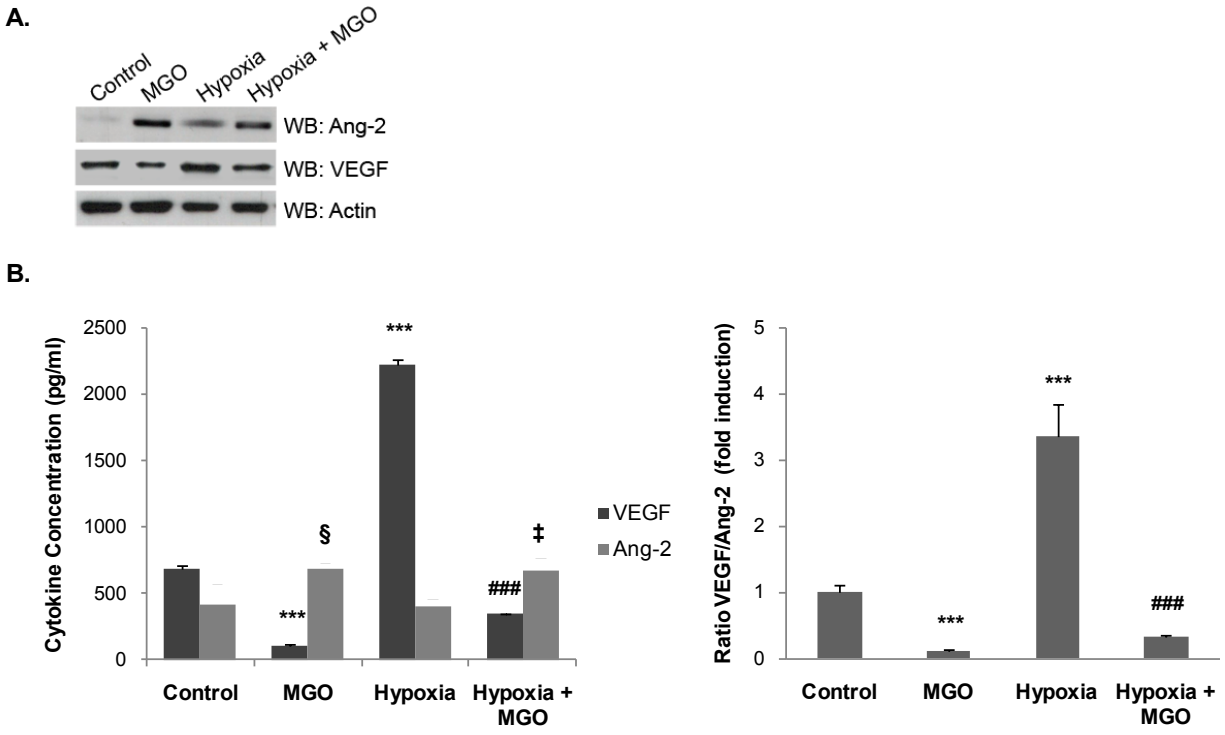

Figure 29. MGO disrupts the balance between VEGF and Ang-2 produced and secreted by retinal epithelial cells. (A) ARPE-19 cells were exposed to hypoxia (2% O_2) for 6 hours and treated with 3 mM MGO for 90 minutes. The cell lysates were analyzed by western blot using anti-VEGF, anti-Ang-2 and anti-actin antibodies. (B) ARPE-19 cells were subjected to hypoxia (2% O_2) for 12 hours either in the absence or in the presence of 1 mM MGO. The concentration of diffusible Ang-2 and $VEGF_{121/165}$ isoforms secreted into the culture medium was determined by ELISA using specific monoclonal antibodies against human VEGF and Ang-2. The results represent the mean $\pm$ SD of at least three independent experiments. § < 0.05 and *** p < 0.001, significantly different from control; ‡ p < 0.05 and $^{###}$ p < 0.001, significantly different from hypoxia (one-way ANOVA with the Tukey's multiple comparison test).

5.3.2 Pre-conditioned medium from retinal epithelial cells, treated with MGO, activates apoptosis and decreases proliferation of retinal endothelial cells

VEGF/Ang-2 imbalance is likely to induce endothelial dysfunction. Here, it is hypothesized that this imbalance induced by MGO in RPE cells leads to activation of apoptosis and decreases proliferation of endothelial cells. To evaluate this hypothesis, retinal endothelial cells (TR-iBRB) were treated with pre-conditioned media obtained from ARPE-19 cells subjected to hypoxia in the presence or in the absence of MGO.

Considering that ARPE-19 cells are derived from human (*Homo sapiens*) and TR-iBRB cells are derived from rat (*Rattus norvegicus*), the homology of VEGFA and Ang-2 between both species was analyzed before proceeding.

A.

```
                  1                                                  50
hVEGFA      (1)   MTDRQTDTAPSPSYHLLPGRRRTVDAAASRGQGPEPAPGGGVEGVGARGV
rVEGFA      (1)   MTDRQTDTAPSPSAHLLAGGQPTVDAAASREQEPKPAPGGGVEGVGARGI
                  51                                                 100
hVEGFA     (51)   ALKLFVQLLGCSRFGGAVVRAGEAEPSGAARSASSGREEPQPEEGEEEEE
rVEGFA     (51)   ARKLFVQLLGSSLSGVAVVCAAGGKPIGAGRSASSGLEKPGPEK-RGEKE
                  101                                                150
hVEGFA    (101)   KEEERGPQWRLGARKPGSWTGEAAVCADSAPAARAPQALARASGRGGRVA
rVEGFA    (100)   KEEERGPQWALGSREPGSWTGEAAVCADSAPAARAPQAPARASVPEGRGA
                  151                                                200
hVEGFA    (151)   RRGAEESGPPHSPSRRGSASRAGPGRASETMNFLLSWVHWSLALLLYLHH
rVEGFA    (150)   RQGAQESGLPRSPSRRGSASRAGPGRASETMNFLLSWVHWTLALLLYLHH
                  201                                                250
hVEGFA    (201)   AKWSQAAPMAEGGGQNHHEVVKFMDVYQRSYCHPIETLVDIFQEYPDEIE
rVEGFA    (200)   AKWSQAAPTTEGE-QKAHEVVKFMDVYQRSYCRPIETLVDIFQEYPDEIE
                  251                                                300
hVEGFA    (251)   YIFKPSCVPLMRCGGCCNDEGLECVPTEESNITMQIMRIKPHQGQHIGEM
rVEGFA    (249)   YIFKPSCVPLMRCAGCCNDEALECVPTSESNVTMQIMRIKPHQSQHIGEM
                  301                                                350
hVEGFA    (301)   SFLQHNKCECRPKKDRARQEKKSVRGKGKGQKRKRKKSRYKSWSVYVGAR
rVEGFA    (299)   SFLQHSRCECRPKKDRTKPEKKSVRGKGKGQKRKRKKSRFKSWSVH----
                  351                                                400
hVEGFA    (351)   CCLMPWSLPGPHPCGPCSERRKHLFVQDPQTCKCSCKNTDSRCKARQLEL
rVEGFA    (345)   ------------CEPCSERRKHLFVQDPQTCKCSCKNTDSRCKARQLEL
                  401      412
hVEGFA    (401)   NERTCRCDKPRR
rVEGFA    (382)   NERTCRCDKPRR
```

B.

```
                  1                                                  50
hAng-2      (1)   MWQIVFFTLSCDLVLAAAYNNFRKSMDSIGKKQYQVQHGSCSYTFLLPEM
rAng-2      (1)   MWQIVFLTFGCDLVLASAYNNFRKSVDSTGRRQYQVQNGPCSYTFLLPET
                  51                                                 100
hAng-2     (51)   DNCRSSSSPYVSNAVQRDAPLEYDDSVQRLQVLENIMENNTQWLMKLENY
rAng-2     (51)   DSCRSSSSPYMSNAVQRDAPLDYDDSVQRLQVLENILENNTQWLMKLENY
                  101                                                150
hAng-2    (101)   IQDNMKKEMVEIQQNAVQNQTAVMIEIGTNLLNQTAEQTRKLTDVEAQVL
rAng-2    (101)   IQDNMKKEMVEIQQNVVQNQTAVMIEIGTSLLNQTAAQTRKLTDVEAQVL
                  151                                                200
hAng-2    (151)   NQTTRLELQLLEHSLSTNKLEKQILDQTSEINKLQDKNSFLEKKVLAMED
rAng-2    (151)   NQTTRLELQLLQHSISTNKLEKQILDQTSEINKLQDKNSFLEKKVLDMED
                  201                                                250
hAng-2    (201)   KHIIQLQSIKEEKDQLQVLVSKQNSIIEELEKKIVTATVNNSVLQKQQHD
rAng-2    (201)   KHSVQLQSMKEQKDQLQVLVSKQSSVIDELEKKLVTATVNNSVLQKQQHD
                  251                                                300
hAng-2    (251)   LMETVNNLLTMMSTSNSAKDPTVAKEEQISFRDCAEVFKSGHTTNGIYTL
rAng-2    (251)   LMETVNSLLTMMSSPDYKSSVAVPKEEKTTFRDCAEIFKSGLTTSGIYTL
                  301                                                350
hAng-2    (301)   TFPNSTEEIKAYCDMEAGGGGWTIIQRREDGSVDFQRTWKEYKVGFGNPS
rAng-2    (301)   TFPNSTEEVKAYCDMDMGGGGWTVIQHREDGSVDFQRTWKEYKEGFGSPL
                  351                                                400
hAng-2    (351)   GEYWLGNEFVSQLTNQQRYVLKIHLKDWEGNEAYSLYEHFYLSSEELNYR
rAng-2    (351)   GEYWLGNEFVSQLTSGHRYVLKIQLKDWEGSEAHSLYEHFYLSGEESNYR
                  401                                                450
hAng-2    (401)   IHLKGLTGTAGKISSISQPGNDFSTKDGDNDKCICKCSQMLTGGWWFDAC
rAng-2    (401)   IHLTGLTGTAGKISSISQPGSDFSTKDSDNDKCICKCSQMLTGGWWFDAC
                  451                                              496
hAng-2    (451)   GPSNLNGMYYPQRQNTNKFNGIKWYYWKGSGYSLKATTMMIRPADF
rAng-2    (451)   GPSNLNGQYYPQKQNTNKFNGIKWYYWKGSGYSLKATTMMIRPADF
```

Figure 30. VEGF (A) and Ang-2 (B) sequence alignments between *Homo sapiens* and *Rattus norvegicus* species. **F** – non-similar; **M** – Identical; **A** – Block of similar; **KF** – Receptor-binding interface. Sequences were obtained from the US National Center for Biotechnology Information (NCBI) databases. Alignments and homology studies were performed using the Vector NTI 10 software (Invitrogen, Carlsbad, CA, USA) and the NCBI alignment tools available in the website *www.ncbi.nlm.nih.gov/*.

As observed in Figure 30, the sequences of both VEGFA and Ang-2 are highly conserved between both species; human VEGFA (NP_001020537.2) shares 84% of consensus positions with rat VEGFA (NP_114024.2), while human Ang-2 (NP_001138.1) shares 90.7% of consensus positions with the rat Ang-2 protein (NP_604449.1). Moreover, data published in NCBI databases mention that the VEGFA binding interface comprises the 230-233, 267, 269-272, 287-290 residues, while the F468A/Y474A/Y475A and K467E/K472E Ang-2 mutants do not bind Tie2 (Barton et al, 2005) (Barton, Structure 2005). VEGF and Ang-2 sequence alignments show that the previously mentioned residues (underlined in Figure 30) are fully conserved between both species. Thus, this homology study excludes incompatibility between human VEGFA and Ang-2 with rat VEGFR and Tie-2 receptors, respectively.

After the homology studies and the validation of our pre-conditioned cell culture system, the levels of BAX and Bcl-2 in endothelial cells were determined by immunoblot. It is well established that BAX/Bcl-2 ratio determines the response to a death signal (Oltvai et al, 1993), being a marker of activation of apoptosis. Moreover, induction of BAX expression is known to initiate death in the absence of any additional signal (Xiang et al, 1996), resulting in a downstream program of mitochondrial dysfunction, as well as activation of caspases. In this study, we observed that the pre-conditioned medium of ARPE-19 cells subjected to hypoxia strongly increases the Bcl-2 levels in endothelial cells (Figure 31). Conversely, the pre-conditioned medium of ARPE-19 cells simultaneously subjected to hypoxia and MGO decreases the Bcl-2/BAX ratio (Figure 31) in TR-iBRB cells, suggesting activation of apoptosis. We further observed that incubation of endothelial cells with this pre-conditioned medium decreases the levels of the proliferation marker Ki67 (Figure 32A and 32B) and decreases the incorporation of BrdU, a synthetic thymidine-analogue, in DNA (Figure 32C), indicating decreased proliferation of endothelial cells.

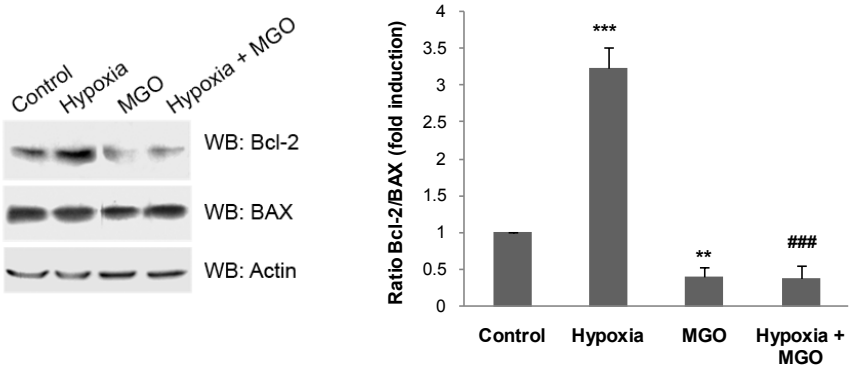

Figure 31. Pre-conditioned medium from retinal epithelial cells treated with MGO activates apoptosis in retinal endothelial cells. ARPE-19 cells were exposed to hypoxia (2% O_2) for 12 hours either in the absence or in the presence of 1 mM MGO. The pre-conditioned media was used to incubate TR-iBRB cells for 24 hours. The cell lysates were analyzed by western blotting using specific antibodies against BAX, Bcl-2 and actin. The results represent the mean ± SD of at least three independent experiments. ** $p < 0.01$ and *** $p < 0.001$, significantly different from control; ### $p < 0.001$, significantly different from hypoxia (one-way ANOVA with the Tukey's multiple comparison test).

5.3.3 Ang-2, in the presence of low levels of VEGF, decreases proliferation and activates apoptosis of retinal endothelial cells

Hypoxia and MGO are likely to change the levels of several growth factors and cytokines released by RPE cells, possibly leading to changes in the BAX/Bcl-2 ratio and compromising survival of endothelial cells. To specifically assess the role of VEGF and Ang-2 in the proliferation and survival of endothelial cells, we treated TR-iBRB cells with recombinant VEGF and Ang-2 within the same ratios of VEGF/Ang-2 as those that were released by ARPE-19 cells following treatment with MGO and/or hypoxia. We observed that Ang-2, in the presence of high levels of VEGF (a condition that "mimics" hypoxia), strongly decreases the levels of BAX (Figure 33A) in endothelial cells. On the other hand, we found that Ang-2, in the presence of low levels of VEGF (a condition that "mimics" hypoxia and MGO treatment), induces a strong decrease in the Bcl-2 levels (Figure 33A), dramatically altering the BAX/Bcl-2 ratio and presumably leading to apoptosis. To further confirm this hypothesis, we determined the proteolytic activity of caspase-3, a key executioner of apoptosis (Cohen, 1997; Porter & Janicke, 1999; Smulson et al, 1998), by using a specific caspase-3 substrate. Indeed, data shows that in the presence of low levels of VEGF, Ang-2 significantly increases caspase-3 activity (Figure 33B).

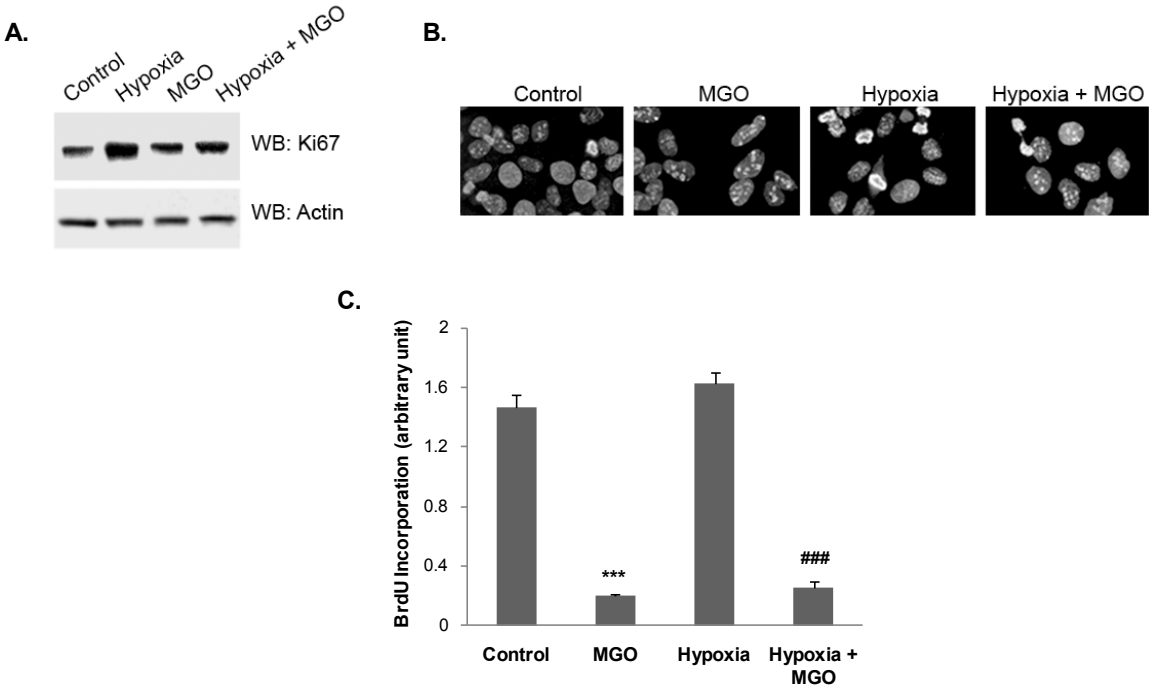

Figure 32. Pre-conditioned medium from RPE cells treated with MGO decreases proliferation of retinal endothelial cells. (A and B) TR-iBRB cells, incubated on pre-conditioned media of ARPE-19 cells, were used to assess the protein levels (A) and the cellular distribution (B) of the proliferation marker Ki67, by WB and immunofluorescence, respectively. (C) TR-iBRB cells, incubated on pre-conditioned media of ARPE-19 cells, were incubated with BrdU and detection of BrdU incorporated into DNA was assessed according to the manufacturers' instructions. The results represent the mean ± SD of at least three independent experiments. *** $p < 0.001$, significantly different from control; ### $p < 0.001$, significantly different from hypoxia (one-way ANOVA with the Tukey's multiple comparison test).

Consistently, we also observed that this condition decreases the incorporation of BrdU in DNA (Figure 34A), indicating decreased cell proliferation. In order to further assess the role of the VEGF/Ang-2 ratio in proliferation of retinal endothelial cells, it was performed a fibrin gel *in-vitro* angiogenic assay to assess the ability of cultured cells to form tube-like structures. When cultured within a fibrin gel and subjected to angiogenic signals, endothelial cells rapidly align and form interconnecting networks. By using different ratios of VEGF/Ang-2, we observed that Ang-2 in the presence of high levels of VEGF induce accentuated cell proliferation (Figure 34B). Moreover, endothelial cells align, forming closed polygons and a network of proto-tubes. However, Ang-2 in the presence of low levels of VEGF does not favour the formation of proto-tubes or closed polygons, but rather induces isolated-growing cells and few emergent tubes with low complexity (Figure 34B).

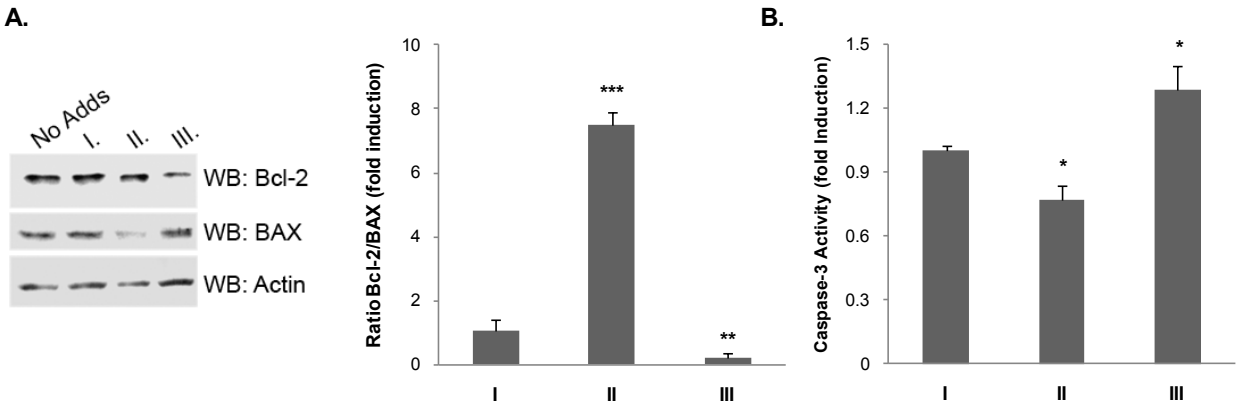

Figure 33. In the presence of low levels of VEGF, Ang-2 activates apoptosis in retinal endothelial cells. (A) TR-iBRB cells, cultured in DMEM without serum, were incubated with the following concentrations of recombinant $VEGF_{165}$ and Ang-2 for 24 hours: I – 6 ng/ml VEGF + 4 ng/ml Ang-2; II – 20 ng/ml VEGF + 4 ng/ml Ang-2; III – 0.5 ng/ml VEGF + 7 ng/ml Ang-2. Subsequently, the cell lysates were analyzed by western blot against BAX, Bcl-2 and actin. The results represent the mean $\pm$ SD of at least three independent experiments. ** $p < 0.01$ and *** $p < 0.001$, significantly different from condition I (one-way ANOVA with the Dunnet's multiple comparison test). (B) TR-iBRB cells, incubated as previously described, were used to determine the caspase-3 cleavage activity by spectrophotometry. The results represent the mean $\pm$ SD of at least three independent experiments. * $p < 0.05$, significantly different from condition I (one-way ANOVA with the Tukey's comparison test).

5.3.4 The retinas of diabetic rats present increased levels of MGO and changes in the expression and distribution of HIF-1α, VEGF and Ang-2

In this study, we found that MGO destabilizes HIF-1α under hypoxia and imbalances the ratio VEGF/Ang-2 secreted by RPE cells, activating apoptosis and decreasing proliferation of endothelial cells in culture. In order to assess the relevance of these data in a more physiological context, we investigated whether some of the cardinal MGO-induced modifications in cell culture systems would also be present in retinas of an animal model of diabetes. For this purpose, it was used the Goto-Kakizaki (GK) animal model of diabetes (Goto et al, 1976). GK rats are

characterized by increased fasting glycaemia, glycaemia after 2 hours of glucose administration and glycated hemoglobin (Table 5), all of them being cardinal features of diabetes.

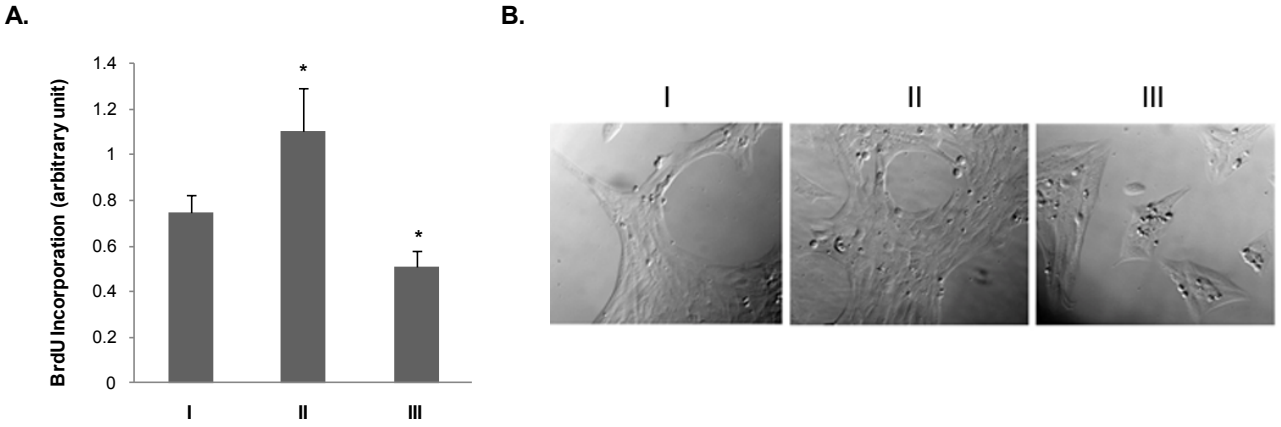

Figure 34. In the presence of low levels of VEGF, Ang-2 decreases proliferation of retinal endothelial cells. (A) TR-iBRB cells, cultured in DMEM without serum, were incubated with the following concentrations of recombinant $VEGF_{165}$ and Ang-2 for 24 hours: I – 6 ng/ml VEGF + 4 ng/ml Ang-2; II – 20 ng/ml VEGF + 4 ng/ml Ang-2; III – 0.5 ng/ml VEGF + 7 ng/ml Ang-2. Subsequently, cells were used to determine the proliferation activity through BrdU incorporation in DNA. The results represent the mean $\pm$ SD of at least three independent experiments. * $p < 0.05$, significantly different from condition I (one-way ANOVA with the Tukey's comparison test). (B) TR-iBRB cells were embedded within fibrinogen/ thrombin polymerized gels and incubated with recombinant $VEGF_{165}$ and Ang-2 proteins, as mentioned before. Phase-contrast images were taken using an inverted light microscope 48 hours following embedding.

Table 5. GK rats present a biochemical diabetic phenotype. Body weight, overnight fasting glycaemia, glycaemia after 2 hours of glucose administration and plasma glycated hemoglobin levels of 6-month aged GK and Wistar rats. The results represent the mean ± SEM and are representative of each group, composed of at least ten animals. * $p < 0.05$, *** $p < 0.001$, significantly different from control (unpaired t test) (data kindly provided by Dr. Raquel Seiça, Physiology Group – IBILI, Faculty of Medicine, University of Coimbra, Portugal).

Parameter	Wistar	GK
Body Weight (g)	400 ± 22.1	357 ± 8.4 *
Fasting Glycaemia (mg/dL)	66 ± 2.3	99 ± 3.3 *
Glycaemia at 2 hours (mg/dL)	83 ± 3.1	303 ± 9.2 ***
Glycated Hemoglobin (%)	3.5 ± 0.12	5.2 ± 0.08 *

Data shows that the retinas of GK rats have increased levels of MGO as compared to age-matched control Wistar retinas (Figure 35). It was further observed important changes in the expression and distribution of some of the key proteins studied in the cell culture systems. For example, it was observed by immunoblot that diabetic retinas present decreased levels of HIF-1α and VEGF and increased levels of Ang-2 as compared to non-diabetic retinas (Figure 36A). By immunohistochemistry, we further observed that HIF-1α protein is less abundant in the retina of diabetic rats and is mostly expressed at the retinal pigment epithelium (RPE) and outer plexiform

(OPL) layers of non-diabetic animals (Figure 36B). Consistent with our model, data also shows that VEGF expression is lower in diabetic retinas as compared to non-diabetic retinas. Indeed, VEGF is highly expressed at the retinal pigment epithelium (RPE) and ganglion cell (GCL) layers of Wistar animals (Figure 36C). Moreover, data shows that Ang-2 is more abundant in the retina of GK rats (Figure 36D). Taken together, these changes are likely to contribute to a general imbalance between VEGF and Ang-2 across the retina of diabetic animals.

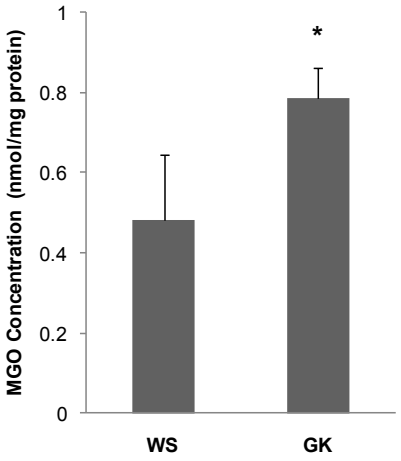

Figure 35. GK retinas have increased levels of MGO as compared to Wistar retinas. GK and Wistar retinas were lysed and used to determine the levels of MGO by HPLC after derivatization with DDB. The results represent the mean ± SD and are representative of each group, composed of at least three animals. * $p < 0.05$, significantly different from control (unpaired t test).

Immunohistochemistry data further shows changes in the expression and distribution of BAX and Bcl-2 between retinas of diabetic and non-diabetic animals (Figure 37A and 37B). For example, GK rats appear to have low levels of Bcl-2 and higher levels of BAX, which may result in an increased amount of apoptotic endothelial cells and, consequently, vessel regression, which would translate in less staining for vWF, a specific marker of endothelial cells (Figure 37C).

Interestingly, data also shows increased vessel permeability in the retina of GK rats as compared to Wistar retinas, as observed by *in-vivo* staining of the retina vasculature with Evans blue (Figure 38). Evans blue dye is known to combine with plasma albumin and is a well characterized tool to monitor vessel leakage. This increased vascular permeability is a main feature of diabetes and is a consequence of increased capillary fenestration and formation of gaps between endothelial cells, by disruption of tight junctions (Harhaj & Antonetti, 2004). Indeed, in the early stages of DR, increased capillary leakage is involved in the blood-retinal barrier breakdown.

Altogether, data obtained in animals are consistent with *in vitro* cell culture data and supports a model in which increased levels of MGO decreases the ratio between VEGF and Ang-2 released by active secretory cells, such as RPE cells, leading to apoptosis and decreased proliferation of neighbouring endothelial cells.

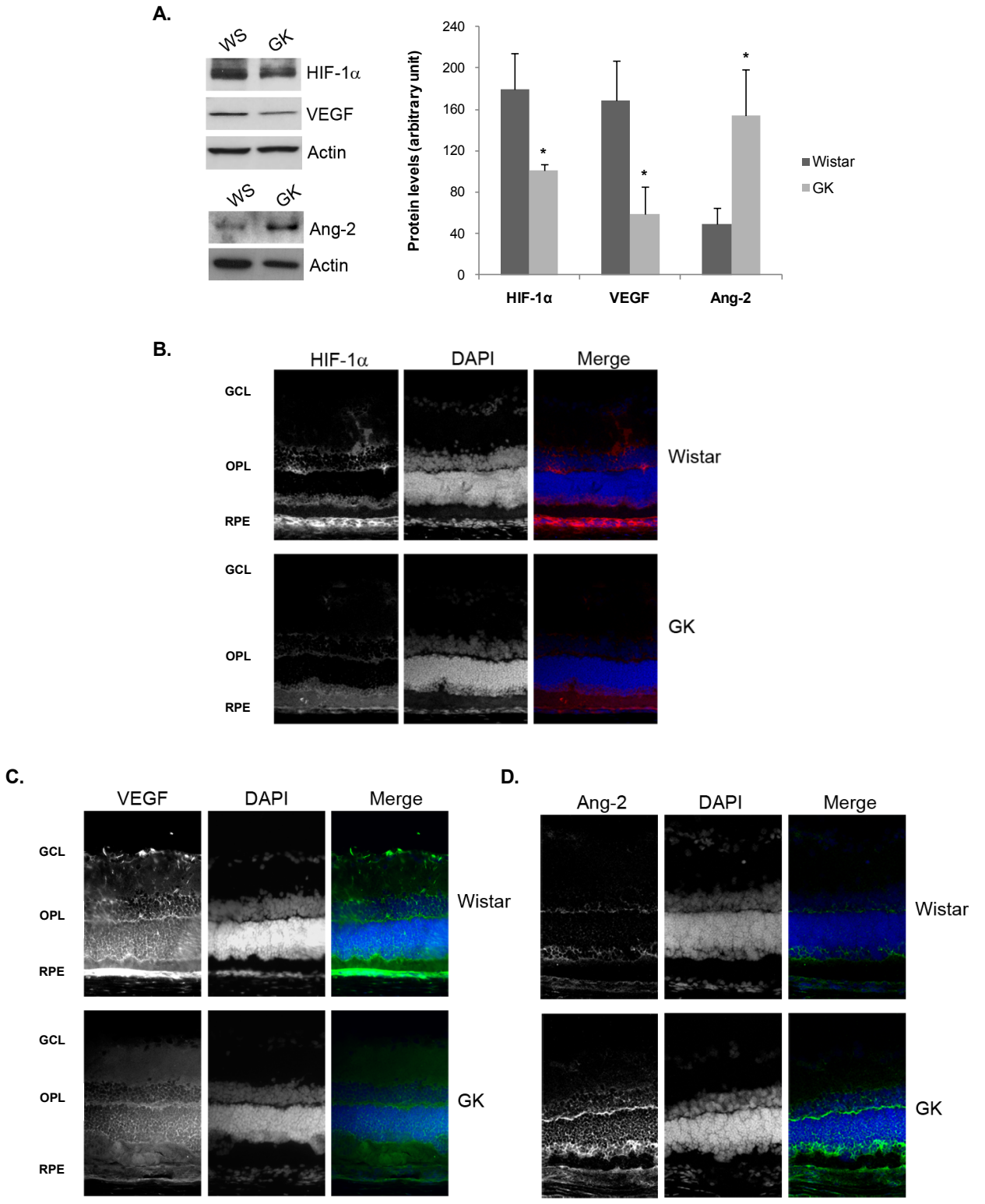

Figure 36. GK retinas have changes in the expression and distribution of HIF-1α, VEGF and Ang-2 as compared to Wistar retinas. (A) Wistar and GK retina extracts were immunoblotted against HIF-1α, VEGF, Ang-2 and actin. Western blots are representative of each group, composed of at least three animals. The results represent the mean ± SD; * $p < 0.05$, significantly different from Wistar (unpaired t test). (B, C and D) Cryosectioned GK and Wistar retinas were fixed and used to perform immunohistochemistry using antibodies against HIF-1α (A), VEGF (B) and Ang-2 (C). Retinas were imaged by fluorescence microscopy and images are representative of each group of animals (100 x of magnification). GCL - ganglion cell layer; OPL - outer plexiform layer; RPE - retinal pigment epithelium.

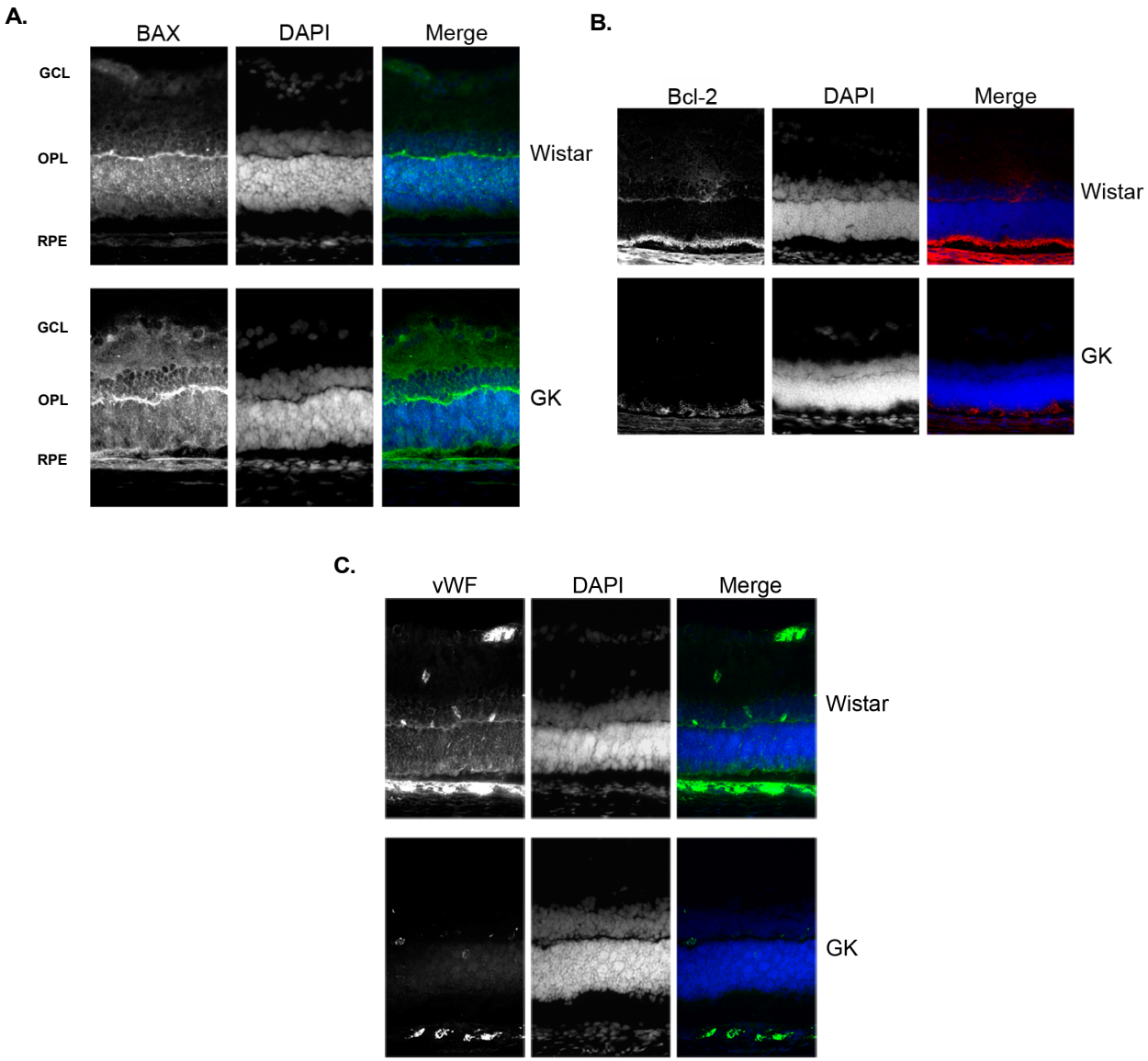

Figure 37. GK retinas present changes in the distribution of BAX, Bcl-2 and vWF as compared to Wistar retinas. (A, B, C) GK and Wistar retinas were frozen in OCT tissue embedding matrix and subsequently cryosectioned. Retina slices with 5-7 µm thickness were fixed with ice cold-acetone and used to perform immunohistochemistry using specific antibodies against BAX (A), Bcl-2 (B) and vWF (C). Retinas were imaged by fluorescence microscopy and images are representative of each group of animals (100 x of magnification). GCL - ganglion cell layer; OPL - outer plexiform layer; RPE - retinal pigment epithelium.

5.4 Discussion

Hyperglycaemia appears to be a critical factor in the aetiology of diabetes and initiates a number of downstream events, such as pericyte dropout, vascular obstruction and capillary non-perfusion (Waltenberger, 2001), which culminate in tissue ischemia. Cell response to hypoxia is a fairly complex process that involves activation of HIF-1, a critical step to help cells and tissues to survive and adapt to low oxygen. However, hyperglycaemia was shown to disrupt, at least in part,

the ability of tissues to respond and adapt to hypoxia (Abaci et al, 1999; Catrina et al, 2004; Kido et al, 2005; Malmberg et al, 1999) and destabilization of HIF-1α by high-glucose appears to be at the origin of the loss of cell response to hypoxia in diabetes (Catrina et al, 2004). Indeed, in chapter 4 it is shown that high-glucose induces degradation of HIF-1α by a mechanism dependent on increased production and intracellular accumulation of MGO, establishing a new molecular link between hyperglycaemia and destabilization of HIF-1α. Data also suggests that impairment of the cell and tissue response to hypoxia, in situations of increased availability of MGO, is related, at least in part, with downregulation of VEGF, a crucial pro-survival and pro-angiogenic factor.

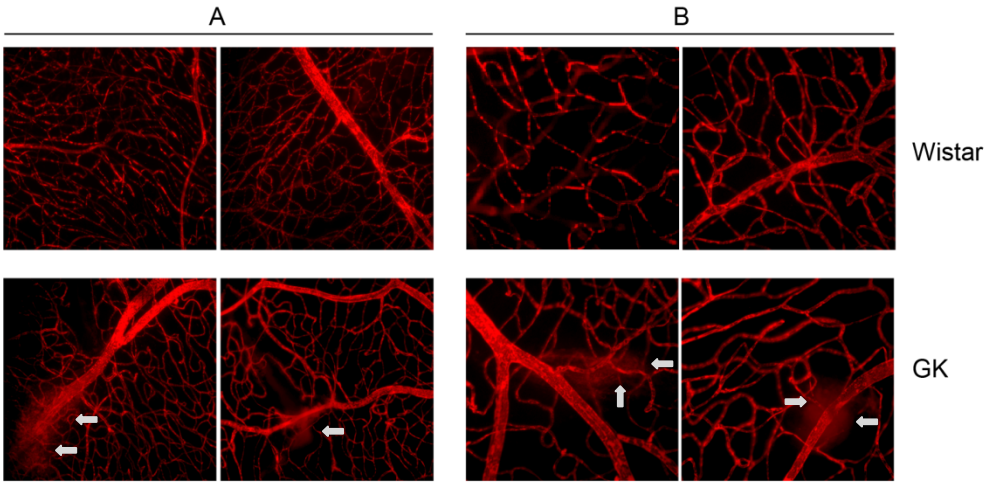

Figure 38. GK retinas present increased vascular permeability as compared to Wistar retinas. GK and Wistar rats were injected with an Evans blue solution through the jugular vein 30 minutes before animal kill. Flat-mounted retinas were imaged by fluorescence microscopy and images are representative of each group of animals (A – 100 x of magnification; B – 200 x of magnification); arrows - leakage sites.

Several lines of evidence suggest that an imbalance between the levels of a variety of growth factors might be associated with the development of diverse vascular complications and impairment of the angiogenic response in diabetes. Vascularization is regulated by complex context-dependent interactions between, among others, Ang-2 and VEGF. Changes in the regulation of either factor are likely to be involved in alterations of the angiogenic remodelling program. Diabetes induces a significant increase in retinal expression of Ang-2 in rats (Hammes et al, 2004), while diabetic Ang-$2^{+/-}$ mice present both decreased pericyte loss and reduced acellular capillary formation, as compared to diabetic wild-type strain Ang-$2^{+/+}$ (Hammes et al, 2002). Moreover, experimental evidence suggests that decreased levels of VEGF might be associated with wound-healing disorders in diabetic patients (Altavilla et al, 2001) and simvastatin-induced VEGF expression or topical VEGF application ameliorates impaired wound-healing (Bitto et al, 2008; Galiano et al, 2004; Singh et al, 2007). Consistently, following an ischemic insult, VEGF levels in diabetic hearts remain significantly lower than those in nondiabetics (Marfella et al, 2002; Marfella et al, 2004). Of significance, myocardial ischemia-induced VEGF expression is significantly

impaired in diabetic patients (Tuo et al, 2008) and some of these changes can be reversed by decreasing the levels of Ang-2. These and other observations highlight the critical role for the VEGF/Ang-2 balance in the regulation of angiogenesis, myocardial injury (Tuo et al, 2008) and in other pathophysiological complications associated with diabetes.

Accumulation of MGO has been implicated in the development of many vascular complications of diabetes (Kalapos, 1999). Significantly, increased retinal levels of MGO in diabetic rats are associated with the formation of acellular capillaries, pericytes dropout (Hammes, 2003; Hammes et al, 2003) and deregulation of angiogenesis (Berlanga et al, 2005), which are major structural lesions of DR. For example, MGO was shown to increase the expression of Ang-2, a key destabilizing factor involved in the initiation of the angiogenic remodelling program (Yao et al, 2007). Consistently, in this work we show that MGO increases the levels of Ang-2 produced and secreted by RPE cells and decreases the levels of VEGF secreted by these cells. The resulting imbalance in the ratio VEGF/Ang-2 leads to increased endothelial cell death and decreased proliferation, which are likely to account for vascular regression and deregulation of the angiogenic response in diabetes.

Diabetes has been characterized by an “angiogenic paradox”, since both pro- and anti-angiogenic conditions coexist in chronic diabetes. Some microvascular tissues are associated with increased expression of growth factors resulting in neovascularization. This response has a significant role in advanced stages of DR, which seems to be ameliorated upon angiogenesis inhibition. Conversely, decreased expression of pro-angiogenic factors is associated with impairment of new blood vessels formation leading to poor wound healing, coronary artery and peripheral limb disease, which is ameliorated by induction of growth factors release. Thus, two apparently diametric angiogenic responses occur in diabetes and generate an intriguing paradox (Duh & Aiello, 1999).

Several reports suggest that VEGF plays a central role in mediating these diabetic vascular complications and is likely to be at the basis of the angiogenic paradox on diabetes. In the specific case of DR, it is clearly known that VEGF is a major mediator of intraocular neovascularization, serving a pivotal role in the aetiology of advanced stages of DR. Indeed, VEFG concentrations are markedly elevated in both vitreous and ocular aqueous fluids of patients with active proliferative DR compared with samples from patients without diabetes, with nonproliferative DR or with quiescent proliferative DR (Aiello et al, 1994; Duh & Aiello, 1999). However, early stages of DR are characterized by opposite phenotypes, mainly associated with formation of acellular capillaries, pericytes dropout, impairment of the angiogenic response and increased vessel permeability, accounting for blood-retinal barrier breakdown.

Despite all the advances in the understanding of DR, the nature and time course of molecular changes in the diabetic retina are poorly characterized and studies on VEGF mRNA have produced conflicting results. For example, retinal VEGF mRNA levels have been reported by independent studies to be unchanged at 3 months, increased at 6 months and decreased at

6 months duration of streptozotocin (STZ)-induced diabetic rats (Brucklacher et al, 2008). Moreover, a recent study, based on a gene expression profile, shows a consistent decrease in VEGF mRNA expression at the retina of 1 and 3 month-aged STZ-induced diabetic rats (Brucklacher et al, 2008). This work also shows that the decrease of the VEGF mRNA levels is accompanied by increased vascular permeability and caspase-3 activity, two main features of the early stages of DR, which are classically associated with high expression of VEGF, a fact that was not corroborated by the study. Indeed, in the work here reported it is shown that increased vessel permeability and apoptosis susceptibility are accompanied by decreased levels of VEGF in a 6-month aged GK diabetic rat. Thus, it seems that there are multiple phases in the regulation of *vegf* gene expression in DR and it is not prudent to generalize its upregulation for all the stages of this diabetic complication.

In conclusion, the results reported in this study are consistent with a number of diverse observations that implicate the VEGF/Ang-2 crosstalk in the vascular complications observed on diabetes. In this study, we suggest that high glucose, by increasing the intracellular levels of MGO, is likely to disrupt the balance between VEGF and Ang-2, resulting in the development of cardinal features of the early stages of diabetic vascular complications, such as endothelial cell death and vascular regression.

CHAPTER 6

Chapter 6. Methylglyoxal impairs critical components of the protein quality control

6.1 Abstract

Increased production and accumulation of methylglyoxal (MGO), as well as increased modification of proteins by glycoxidation are hallmarks of normal aging and diabetes. MGO was shown to modify proteins and to contribute to the accumulation of obsolete proteins that can be toxic to cells. However, the effect of MGO on the cell systems responsible for repairing or degrading damaged proteins is still unclear. In this study, the effect of MGO on the function of the ubiquitin-proteasome system (UPS) and on molecular chaperones – two cooperative mechanisms associated with protein quality control, was investigated. Here, it is shown that treatment of cells with MGO leads to accumulation of ubiquitin conjugates and depletion of free ubiquitin. Moreover, MGO significantly decreases the proteolytic activity of the 20S proteasome. Data further show that MGO decreases the levels of the molecular chaperones Hsc70 and Hsp90 and induces the formation of CHIP-, Hsp40- and ubiquitin-containing aggregates. The formation of large aggregates containing CHIP is a consequence of its binding to misfolded proteins and to molecular chaperones. Moreover, dysfunction of the chaperones/CHIP/UPS axis is associated with accumulation of oxidized and argpyrimidine-modified proteins, which is likely to be associated with decreased cell viability and proliferation. Interestingly, data further show that the cellular stress induced by MGO is counteracted, at least in part, by the activation of heat shock factor-1 (Hsf-1), the main transcription factor involved in the regulation of the expression of heat shock proteins (HSPs) and response to cellular stress. Indeed, in this work it is shown that MGO induces oligomerization of Hsf-1 and increases its transcriptional activity.

Altogether, data indicates that MGO induces cellular stress and disrupts the protein quality control system by impairing the activity of the UPS, by disrupting the levels of several molecular chaperones and by inducing the accumulation of modified proteins in the cell. However, these MGO-induced changes seem to be sensed by the Hsf-1 system, which is crucial to help cells to cope with cellular stress.

6.2 Introduction

MGO is a highly reactive α-oxoaldehyde that is formed in cells primarily from the triose phosphate intermediates of glycolysis, dyhydroxyacetone phosphate and glyceraldehyde 3-phosphate (Ramasamy et al, 2006). This by-product of glycolysis induces rapid and non-enzymatic modification of free amino groups of lysine and arginine residues of proteins, leading to the generation of advanced glycation end products (AGEs) (Shinohara et al, 1998). The posttranslational modification of proteins by MGO is known to contribute to normal aging, as well as to a number of diseases, including cancer, diabetes and other disorders (Ramasamy et al, 2006).

Indeed, hyperglycaemia triggers enhanced production of MGO on diabetes (Brownlee, 2005; Ramasamy et al, 2006), leading to vascular dysfunction (Hammes, 2003), while AGEs exacerbate and accelerate a number of characteristics of many age-related diseases (Brownlee, 1995; Tian et al, 2005).

MGO is known to induce aggregation and structural modifications in proteins through cross-linking and formation of chemical adducts (Biswas et al, 2008; Monnier et al, 1996). In eukaryotic cells, the proteasome contributes to prevent the accumulation of non-functional, potentially toxic proteins. This proteolytic system is of particular importance in protecting cells against harsh conditions, such as heat shock, glycation or oxidative stress (Goldberg, 2003), and is an important player in the protein quality control system in eukaryotic cells. However, when the generation of obsolete proteins exceeds the capacity of the cell to degrade them, there is a progressive accumulation of damaged proteins, which often become insoluble over time and are potentially toxic to cells (Goldberg, 2003). Accumulation of damaged proteins, ultimately, occurs when the proteolytic systems and molecular chaperones, which normally prevent aggregation (for example, Hsc70 and Hsp90) (Frydman, 2001; Hartl & Hayer-Hartl, 2002), cannot keep up with the rate of production of misfolded or otherwise damaged proteins.

The carboxy terminus of the Hsc70-interacting protein (CHIP) is a key player in protein quality control since it is a molecular link between chaperones and the UPS. Indeed, CHIP has both a tetratricopeptide repeat (TPR) motif and a U-box domain (Ballinger et al, 1999). The TPR motif associates with chaperones, such as Hsp40, Hsc70 and Hsp90, while the U-box domain has ubiquitin ligase activity. Thus, CHIP has a critical role in protein quality control by ubiquitinating misfolded or post-translationally modified proteins through interaction with molecular chaperones (Murata et al, 2003).

It has been suggested that the activity of the proteasome can be compromised upon aging (Vernace et al, 2007) and diabetes (Portero-Otin et al, 1999). For example, the levels of the proteasome activator PA28 are decreased in muscle extracts of diabetic rats (Merforth et al, 2003), which might result in accumulation of glycated and toxic proteins, typically observed in diabetic tissues. Furthermore, formation of amyloid-aggregates in β-cells, on type 2 diabetes, is highly enhanced by MGO (Chen et al, 2006) and this is known to impair the UPS, leading to apoptosis (Casas et al, 2007). On the other hand, it has been suggested that UPS activity decreases with aging, which may further account for the accumulation of modified and toxic proteins in cells, contributing to cell injury and death (Vernace et al, 2007). There is also increasing evidence showing that molecular chaperones, such as α-crystallin and Hsp27 (Satish Kumar et al, 2004; Schalkwijk et al, 2006), are themselves major targets of MGO-induced modification and aggregation. These and other evidences indicate that age- and diabetes-dependent accumulation of MGO is likely to account for impairment of the protein-quality control mechanism. However, the effect of MGO in the function of UPS and on molecular chaperones is still not clear.

Herein, it is shown that increased levels of MGO lead to accumulation of ubiquitin conjugates and depletion of free ubiquitin in the cell. The accumulation of ubiquitin conjugates is presumably due to both MGO-induced impairment of UPS and MGO-induced disruption of chaperones. Data presented, in this chapter, further shows that MGO downregulates Hsc70 and Hsp90 and promotes the formation of large aggregates containing Hsp40, CHIP and ubiquitin. Consistently, the effects of MGO lead to accumulation of modified proteins in the cell and to decreased cell viability. Moreover, increased activation of Hsf-1 is also observed, which is likely to be a counteracting mechanism to the MGO-induced cellular stress.

6.3 Results

6.3.1 MGO impairs the 20S proteasome activity and leads to accumulation of ubiquitin conjugates

Increased production and accumulation of MGO has been associated with cell and tissue dysfunction in diabetes and aging (Ramasamy et al, 2006), both characterized by decreased proteasome activity (Merforth et al, 2003; Vernace et al, 2007). However, the putative effect of MGO on proteasome activity and on the accumulation of obsolete proteins remains to be clarified.

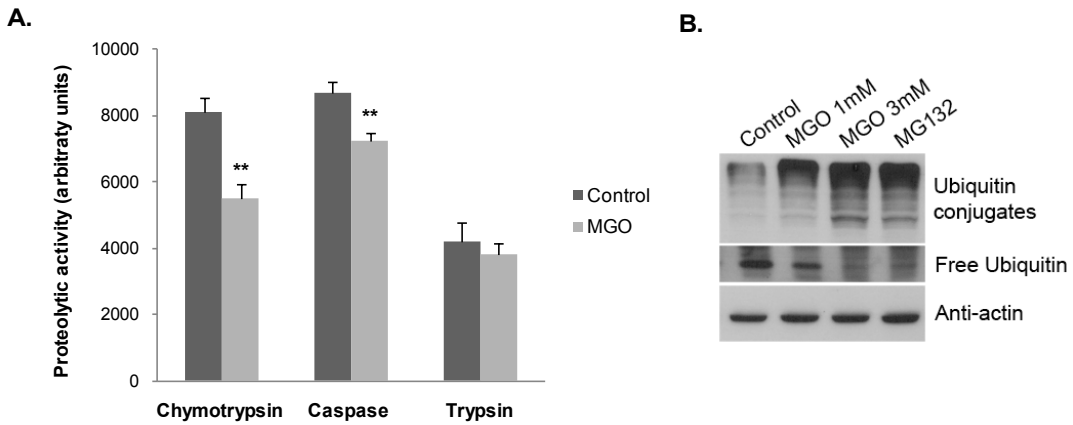

Figure 39. MGO decreases the 20S proteasome activity, depletes free ubiquitin and leads to accumulation of ubiquitin conjugates. (A) ARPE-19 cells were treated with 3 mM MGO for 3 hours and the cell extracts were used to measure the proteolytic activities of the 20S proteasome (chymotrypsin-like, caspase-like and trypsin-like activities) using specific fluorogenic substrates. The results correspond to the measurement at 30 minutes of activity and represent the mean $\pm$ SD of at least three independent experiments. ** $p < 0.01$, significantly different from control; t test. (B) ARPE-19 cells were treated with 1mM MGO, 3mM MGO or 20 µM MG132 for 3 hours and the proteins were separated by SDS-PAGE, transferred to PVDF membranes and probed with monoclonal antibodies against ubiquitin and actin.

To evaluate the effect of MGO on the proteasome activity, we used a human retinal pigment epithelium cell line (ARPE-19). This cell type represents an appropriate model for this study, since it has a very active and functional UPS (Obin et al, 1994; Shang et al, 2005). Moreover, the retinal

pigment epithelium has a high rate of glucose consumption and its ubiquitin-proteasome system has been shown to be affected during aging and diabetes (Brownlee, 1995; Coffe et al, 2006; Tian et al, 2005). Indeed, accumulation of MGO during aging is associated with accumulation of lipofuscin aggregates and drusen's formation (Tian et al, 2005).

To assess 20S proteasome activity, ARPE-19 cells were treated with MGO and the cell extracts were used to measure the three peptidase activities of the 20S proteasome using fluorogenic substrates. Figure 39A shows that MGO significantly decreases the chymotrypsin-like ($p < 0.01$) and caspase-like ($p < 0.01$) activities of the 20S proteasome. Western blot analysis of ARPE-19 cell extracts treated with MGO revealed that MGO increases the accumulation of ubiquitin conjugates and decreases the levels of free ubiquitin (Figure 39B). This result is comparable to data obtained in the presence of a proteasome inhibitor (such as MG132) and suggests that MGO does induce proteasome inhibition.

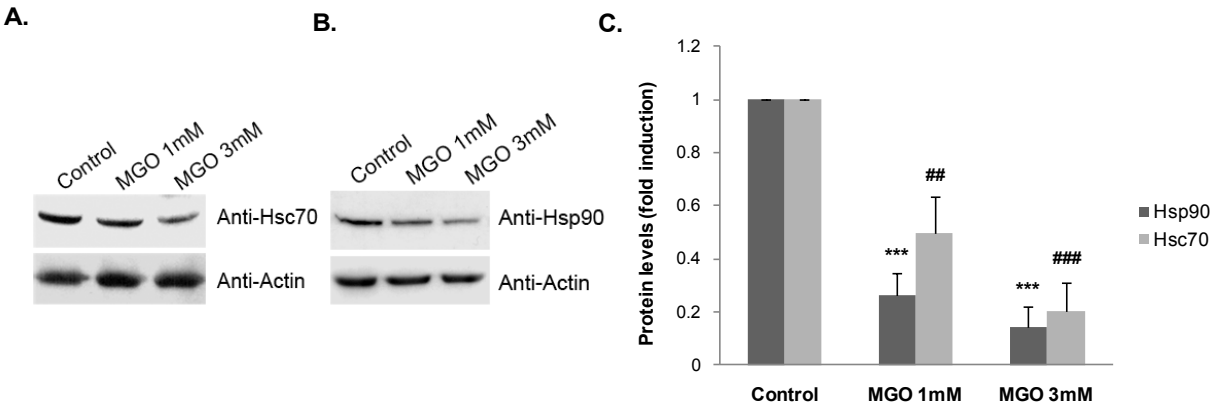

Figure 40. MGO decreases the levels of Hsc70 and Hsp90. (A, B, C) ARPE-19 cells were treated with 1 mM MGO or 3 mM MGO for 3 hours and the cell lysates were analyzed by western blotting using anti-Hsc70 (A), Hsp90 (B) and anti-actin antibodies. The quantified results represent the mean ± SD of at least three independent experiments. *** $p < 0.001$, ## $p < 0.01$, ### $p < 0.001$, significantly different from control; one-way ANOVA (Dunnet's *post hoc* test) (C).

6.3.2 MGO decreases the levels of Hsc70 and Hsp90

MGO is known to induce modification of proteins by glycoxidation (Kang, 2006; Lee et al, 1998; Rondeau et al, 2008; Shinohara et al, 1998; Thornalley, 2008). Accumulation of damaged proteins can be toxic and interfere with normal cell function. Therefore, repair or elimination of MGO- or otherwise-damaged proteins is critical to ensure proper cell function and survival. This function is supported by a complex quality control mechanism that relies on molecular chaperones and UPS, which can either refold damaged proteins or direct them to proteasomal degradation. The molecular chaperones Hsc70 and Hsp90 bind to unfolded proteins and both contribute to regulate protein quality control (Connell et al, 2001; Goldberg, 2003; Murata et al, 2001; Park et al, 2007). Therefore, it is likely that destabilization of these chaperones may compromise protein quality

control. Data obtained in this study show that in addition to inhibiting the proteasome, MGO induces a decrease in the levels of Hsc70 and Hsp90 proteins (Figure 40A and 40B).

6.3.3 MGO induces the formation of CHIP- and Hsp40-containing aggregates

Hsp40 and CHIP are crucial regulators of the protein quality control (Connell et al, 2001; Marques et al, 2006; Murata et al, 2001). Damaged proteins are often recognized and bound to Hsp40, which in turn recruits Hsc70. Hsp40 functions in cooperation with the co-chaperone CHIP, which has ubiquitin ligase activity and, therefore, is able to ubiquitinate damaged proteins, promoting their UPS-dependent degradation (Goldberg, 2003). Data represented in Figures 41A, 40B and 40C shows that MGO strongly increases, in a time- and dose-dependent manner, the accumulation of bands with high molecular weights that present immunoreactivity for CHIP/STUB-1 and Hsp40 antibodies.

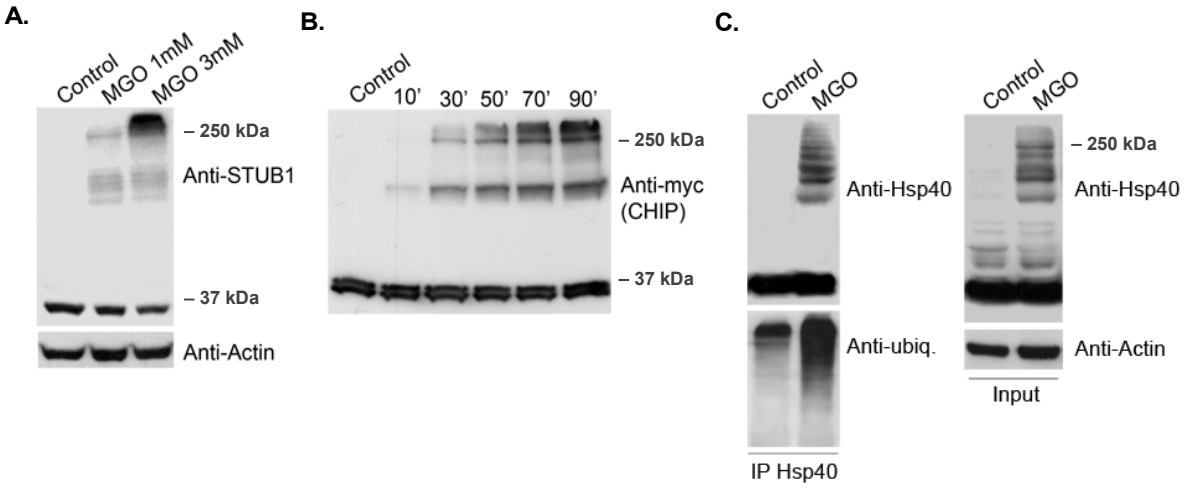

Figure 41. MGO induces formation of large aggregates containing ubiquitin, CHIP and Hsp40. (A) ARPE-19 cells were treated with 1 mM MGO or 3 mM MGO for 3 hours and the cell lysates were analyzed by western blotting using specific antibodies against STUB-1/CHIP and actin. (B) ARPE-19 cells were transfected with c-myc-CHIP wt and treated with 3 mM MGO for 15, 30, 50, 79 and 90 minutes. Proteins were separated by SDS-PAGE, transferred to PVDF membranes and probed against c-myc and actin. (C) ARPE-19 cells were treated with 1 mM MGO or 3 mM MGO for 3 hours. The cell lysates were used to immunoprecipitate Hsp40 and immunoblot the immunoprecipitates against ubiquitin.

Moreover, we observed that MGO increases the ubiquitination of Hsp40- and CHIP- positive aggregates (Figure 41C and 42A). However, ubiquitination on its own does not fully explains the posttranslational modification of CHIP-containing aggregates, since MG132 strongly increases ubiquitination of the protein and does not induce accumulation of bands with high molecular weights, consistent with CHIP-containing aggregates. We suggest that these high molecular weight bands correspond to ubiquitinated substrates that undergo MGO-induced post-translational modifications, ending up in large aggregates containing ubiquitinated proteins, chaperone and co-

chaperone complexes, including Hsp40 and CHIP. This could be a result of the cooperative action of chaperones and UPS in rescuing or degrading misfolded and/or post-translational modified substrates. It is conceivable that some of these aggregates will become insoluble, accounting for age- and diabetes-related cell damage. To further pursue this issue, ARPE-19 cells were transfected with a mutant CHIP that cannot bind chaperones (CHIP K30A) or with a mutant CHIP with no ubiquitin ligase activity (CHIP H260Q). Data shows that the accumulation of bands with high molecular weight, with reactivity for CHIP, decreases when CHIP does not contain chaperone-binding affinity (Figure 42B). Conversely, accumulation of high molecular weight complexes is potentiated by overexpression of CHIP with no ubiquitin ligase activity (Figure 42B). This suggests that the accumulation of CHIP-containing high molecular weight complexes is dependent on both activities of CHIP and is likely to be a consequence of CHIP being trapped in ubiquitinated complexes containing molecular chaperones and obsolete/misfolded proteins.

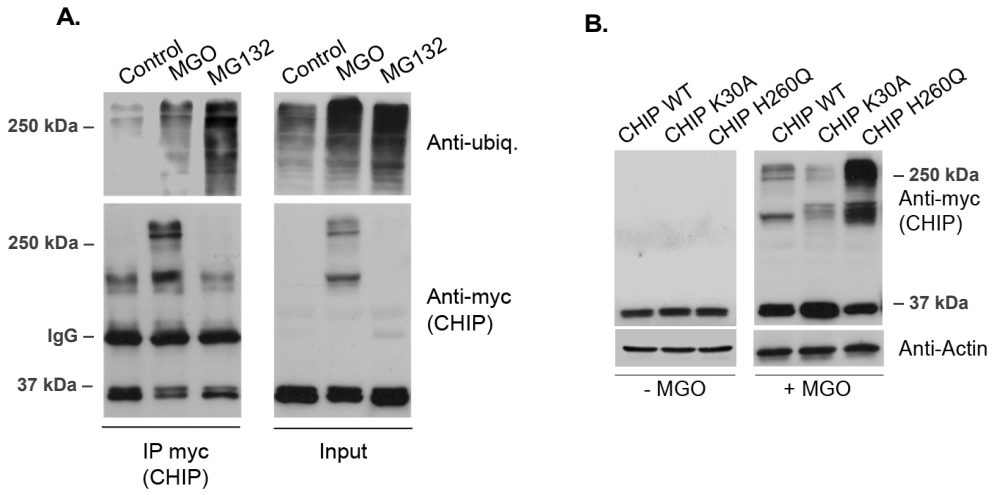

Figure 42. Accumulation of CHIP-containing high molecular weight complexes is dependent on both activities of CHIP. (A) ARPE-19 cells were transfected with c-myc-CHIP wt and treated with 3 mM MGO for 3 hours. C-myc (CHIP) was immunoprecipitated and the immunoprecipitates were probed using a monoclonal antibody against ubiquitin. (B) ARPE-19 cells were transfected with c-myc CHIP wt, c-myc CHIP K30A or c-myc CHIP H260Q. Cells were subsequently treated with 3 mM MGO for 3 hours and the cell lysates were immunoblotted against c-myc and actin.

6.3.4 MGO leads to the accumulation of modified proteins and decreases cell viability

Considering that MGO impairs the UPS and disrupts the chaperones axis, we suggest that MGO is likely to disrupt the protein quality control system in the cell, leading to a potentially toxic accumulation of damaged proteins. Indeed, we observed that MGO strongly increases the levels of modified and oxidized proteins (Figure 43A). Moreover, we further observed increased accumulation of AGEs in the presence of MGO, as revealed by increased immunoreactivity of whole protein extracts against an anti-argpyrimidine antibody (Figure 43B). This indicates that MGO may exert its noxious effects at different levels: by direct modification of cell proteins (glycoxidation)

or by disrupting the protein quality control systems in the cell, including UPS and molecular chaperones. In addition, the impairment of protein quality control and protein modifications induced by MGO are likely to lead to the accumulation of obsolete and toxic proteins, which is accompanied by a significant decrease in cell viability (Figure 43C) and decreased proliferation (Figure 43D).

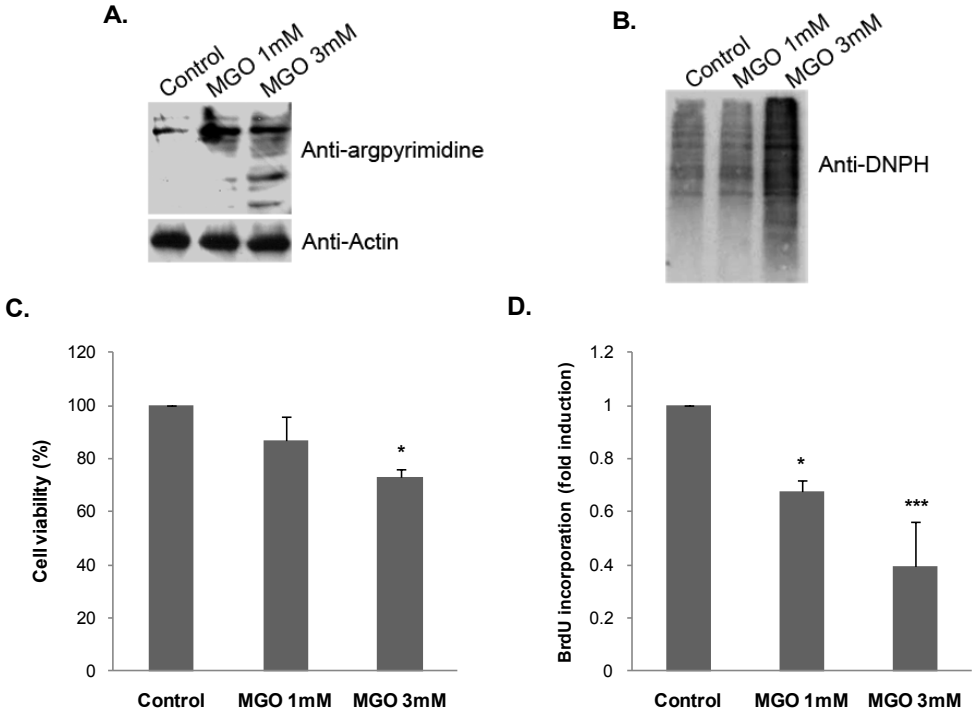

Figure 43. MGO induces accumulation of oxidized and argpyrimidine-modified proteins and decreases cell proliferation and viability. (A) ARPE-19 cells were treated with 1 mM MGO or 3 mM MGO for 3 hours and the cell lysates were used to derivatize proteins with DNPH. Derivatized proteins were separated by SDS-PAGE, transferred to PVDF membranes and probed with an antibody against dinitrophenylhydrazone derivatives. (B) ARPE-19 cells were treated with 1mM or 3 mM MGO for 3 hours and the cell lysates were immunoblotted against argpyrimidine and actin. (C) ARPE-19 cells were treated with 1 mM MGO or 3 mM MGO for 3 hours and used to assess cell viability through the MTT colorimetric assay. The results represent the mean $\pm$ SD of at least three independent experiments. * $p < 0.05$, significantly different from control; one-way ANOVA (Dunnet's *post hoc* test). (D) ARPE-19 cells cultured in a 96-well plate were incubated with BrdU and simultaneously treated with 1 mM MGO or 3 mM MGO for 3 hours. BrdU incorporated in DNA was measured using a specific antibody against BrdU conjugated with peroxidase. The quantified results represent the mean $\pm$ SD of at least three independent experiments. * $p < 0.05$, *** $p < 0.001$, significantly different from control; one-way ANOVA (Dunnet's *post hoc* test).

6.3.5 Activation of Hsf-1 counteracts the MGO-induced decrease in molecular chaperone levels

Stimuli that induce cellular stress and protein damage normally activate sensing mechanisms and stress responses, which often include a dramatic change in the pattern of gene expression and increased synthesis of molecular chaperones. Increased expression of heat-shock proteins generally result in repair of obsolete proteins and survival of the cell (Pirkkala et al, 2001).

The inducible expression of HSPs is mainly regulated by Hsf-1, which acquires DNA binding activity and induces transcription of the heat shock genes.

As previously shown, MGO constitutes a potent stressor by impairing UPS activity and leading to the accumulation of damaged and modified proteins in the cell. Considering that Hsf-1 is crucial for cell response against damage and stress, the involvement of Hsf-1 in the cellular response to the noxious effects induced by MGO was tested.

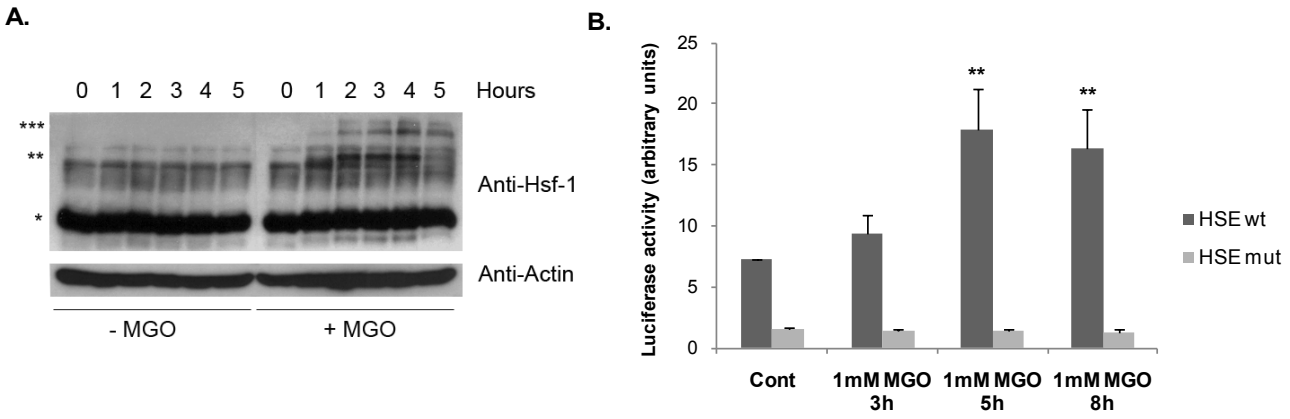

Figure 44. MGO-induced stress activates Hsf-1 through increased oligomerization and DNA-binding activity. (A) ARPE-19 cells were treated with 1 mM MGO for 3, 5 or 8 hours and the cell lysates were analyzed by western blot using specific antibodies against Hsf-1 and actin. * Monomeric Hsf-1 (~ 80 kDa); ** Dimeric Hsf-1 (~ 160 kDa); *** Trimeric Hsf-1 (~ 230 kDa). (B) ARPE-19 cells were transiently transfected with the HSE wt (x4)-luciferase or HSE mut (x4)-luciferase vectors and were treated with 1 mM MGO for 3, 5 or 8 hours. Subsequently, the luciferase activity was determined by luminescence. The quantified results represent the mean ± SD of at least three independent experiments. ** $p < 0.01$, significantly different from control; one-way ANOVA (Dunnet's *post hoc* test).

Oligomerization of Hsf-1 and gain of DNA binding activity are well characterized indicators of activation of the Hsf-1-dependent stress response. Indeed, in this study it is shown that Hsf-1 is mostly present in the monomeric/inactive form under normal conditions. However, MGO induces the formation of Hsf-1 homodimers, followed by the formation of Hsf-1 homotrimers (Figure 44A), which suggests Hsf-1 activation. To further evaluate the activation of Hsf-1 by MGO-induced stress, we examined the ability of Hsf-1 to bind heat-shock elements (HSE) on DNA and activate transcription of the genes under the control of this conserved sequence. Indeed, through an HSE-luciferase reporter gene assay, we observed that MGO specifically increases the transcriptional activity of Hsf-1 (Figure 44B). Moreover, mRNA and protein levels of several molecular chaperones (HspB1, HspB2, Hsp70, Hsp90, Hsc70), which are regulated by Hsf-1, further emphasize the activation of Hsf-1 by MGO and the existence of a heat-shock response against MGO-induced stress (Figure 45). In an initial phase (after 3 hours of incubation with 1 mM MGO), MGO decreases the mRNA and protein levels of these proteins, compromising the ability of cells to cope with stress. However, this response is reverted for longer periods of incubation with MGO (8 hours), suggesting a cellular response against stress, which is likely to be triggered by Hsf-1. Of great significance, we

observed that activation of Hsf-1 and increased expression of molecular chaperones is accompanied by an increase in cellular viability, which becomes statistically significant after 10 hours of incubation with 1 mM MGO (as compared to shorter periods of incubation; $p < 0.05$, one-way ANOVA), which suggests adaptation against the noxious effects induced by MGO (*data not shown*).

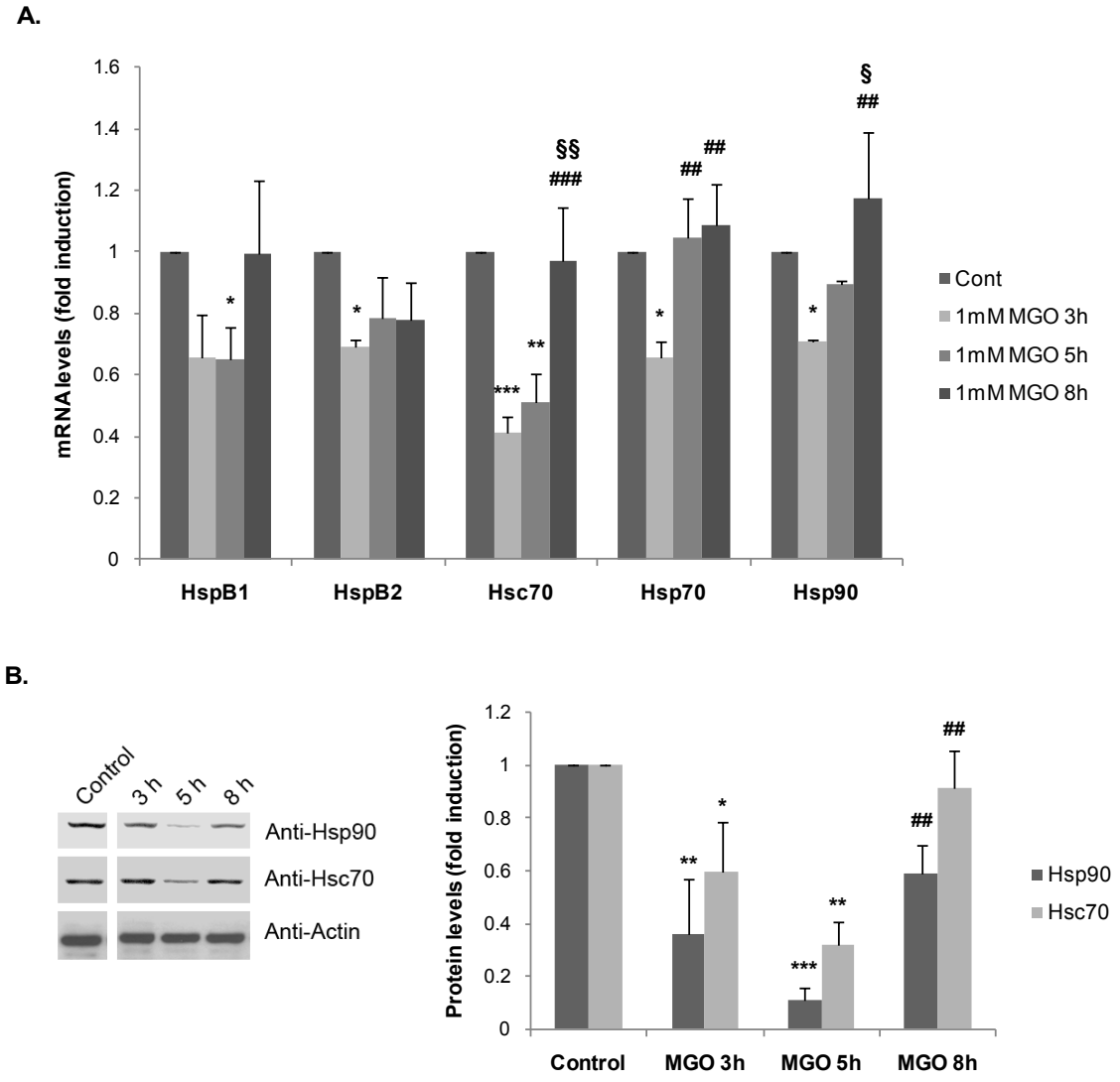

Figure 45. The mRNA and protein levels of several molecular chaperones increase for longer periods of MGO incubation. (A) ARPE-19 cells were treated with 1 mM MGO for 3, 5 or 8 hours. Total RNA was used to synthesize cDNA, which, in turn, was used as template to quantify HspB1, HspB2, Hsc70, Hsp70 and Hsp90 mRNA and 18S rRNA through RT-PCR. The quantified results represent the mean ± SD of at least three independent experiments.* $p < 0.05$, ** $p < 0.01$, *** $p < 0.001$, significantly different from the respective control; ## $p < 0.01$ and ### $p < 0.001$, significantly different from the corresponding "MGO 3h" condition; § $p < 0.05$, §§ $p < 0.01$, significantly different from the corresponding "MGO 5h" condition; one-way ANOVA (Tukey's *post hoc* test). (B) ARPE-19 cells were treated with 1 mM MGO for 3, 5 or 8 hours and the cell lysates were analyzed by western blot using anti-Hsc70, Hsp90 and anti-actin antibodies. The quantified results represent the mean ± SD of at least three independent experiments. * $p < 0.05$, ** $p < 0.01$ and *** $p < 0.001$, significantly different from the respective control; one-way ANOVA (Tukey's *post hoc* test); ## $p < 0.01$, significantly different from the corresponding "MGO 5h" condition; one-way ANOVA (Tukey's test).

6.4 Discussion

Increased production of methylglyoxal, increased modification of proteins by glycoxidation and accumulation of damaged proteins are all hallmarks of normal aging and of a number of diseases, such as diabetes and cancer (Brownlee, 1995; Ramasamy et al, 2006). MGO is known to be toxic and to interfere with a plethora of critical mechanisms in the cell. For example, MGO impairs the mitochondria-respiratory chain and increases the production of reactive oxygen species, particularly the anion superoxide, contributing to increased oxidation of proteins (Ray et al, 1994; Rosca et al, 2002; Rosca et al, 2005). On the other hand, MGO reacts with free ε-NH_2 groups of basic amino acid residues, through glycation, altering the structure and function of proteins (Bulteau et al, 2001). These and other posttranslational modifications induce exposure of hydrophobic patches of the proteins and loss of secondary and tertiary structure (Bulteau et al, 2001; Friguet et al, 1994). These changes were proposed to act as a recognition signal for degradation by the proteasome (Ferrington et al, 2001; Grune et al, 1997; Lasch et al, 2001). Canonically, the recognition of the exposed hydrophobic domains of modified proteins is mediated by molecular chaperones, such as Hsc70 and Hsp90. Binding of chaperones is often suggested to recruit the ubiquitin ligase CHIP, which ubiquitinates the modified proteins and targets them for proteasomal degradation (Goldberg, 2003). However, the function of the proteasome has also been reported to be impaired upon aging, which may account for inefficient removal of damaged proteins (Bulteau et al, 2001; Friguet et al, 2000; Petropoulos et al, 2000). For example, oxidative inactivation of the proteasome was reported in many types of cells and proteasome activity was shown to decrease in glyoxal-treated cells as compared to controls (Bulteau et al, 2001). Consistently, in this study we show that MGO impairs the ubiquitin-proteasome pathway and destabilizes several molecular chaperones that are crucial for protein quality control. These impairments are likely to contribute for the accumulation of modified proteins and decreased cell proliferation and viability.

In fact, a number of independent studies have shown that MGO modifies and destabilizes several molecular chaperones, such as Hsp27 and α-crystallin (Kumar et al, 2007; Nagaraj et al, 2003; Oya-Ito et al, 2006; Sakamoto et al, 2002; Satish Kumar et al, 2004; Schalkwijk et al, 2006). Despite some controversial studies, it is becoming increasingly clear that molecular chaperones and co-chaperones constitute a group of proteins that can be critically affected by MGO. Indeed, in this work, it is observed that Hsp40, Hsc70, Hsp90 and CHIP are all destabilized by MGO. The protein levels of Hsc70 and Hsp90 decrease in the presence of MGO. On the other hand, CHIP and Hsp40 become aggregated following treatment with MGO. These findings lead us to hypothesize that, in addition to other established toxic effects, MGO acts by disrupting the protein quality control system. Indeed, we show that treatment of cells with MGO leads to formation of Hsp40- and CHIP-containing ubiquitinated aggregates and that the overexpression of a ligase-dead CHIP increased the levels of CHIP-positive aggregates. Moreover, the overexpression of a mutant CHIP, which

does not bind chaperones, suggests that formation of these aggregates is mediated by ancillary chaperones that bind to CHIP. These findings lead us to suggest that CHIP is being trapped in aggregates of modified proteins, which are recognized by the chaperone-binding site of CHIP and are, at least, partially targeted for degradation by the ubiquitin ligase activity of this protein. These data also emphasize the dual role of CHIP in the recognition of damaged proteins and in the targeting of these proteins for degradation. However, data also shows that CHIP overexpression is not sufficient to entirely compensate for the accumulation of modified proteins, thus accounting for increased cell toxicity. Indeed, we show that impairment of UPS and destabilization of molecular chaperones is accompanied by decreased proliferation and decreased cell viability. Consistently, high levels of MGO and accumulation of aggregates induced by MGO have been extensively correlated with the loss of cell viability and cell death (Denis et al, 2002; Jan et al, 2005; Miller et al, 2006).

This works emphasizes the critical role of MGO in the damage of proteins, which accounts for cell injury and cell death. Hsf-1 has been identified as a key player in the response to cellular stress, mediating stress-induced heat shock gene expression on the basis of its ability to display inducible DNA binding activity, oligomerization and nuclear localization in response to environmental stressors (Pirkkala et al, 2001; Voellmy, 2004). Indeed, this study shows that Hsf-1 is activated in the presence of increased levels of MGO, as observed by increased trimerization and increased transcriptional activity. Ultimately, the stress induced by MGO appears to be, at least, partially compensated by the activation of Hsf-1, which increases the expression of several inducible heat shock proteins, known to improve refolding of damaged proteins, protein quality control and cell survival. This response shows that cells have finely tuned sensing mechanisms that counteract, at least in part, abnormal changes induced by stress-inducers. However, these mechanisms are virtually fallible and can be compromised under acute and highly severe stresses or chronic mild stresses. This may explain the inefficiency of cells to properly respond to stress in some pathological states or diseases, such as some neurodegenerative disorders and diabetes, both characterized by severe impairment of cellular viability and accumulation of damaged and, even, aggregated proteins.

Altogether, data lead us to suggest that MGO-induced post-translational modifications in proteins lead to recruitment of molecular chaperones, in an attempt to repair the misfolded proteins. CHIP is subsequently recruited and acts as a switch, directing substrates from protein refolding to protein degradation. However, our observations suggest that formation of CHIP- and chaperones-containing large ubiquitinated aggregates may become difficult to process by either pathway (refolding or degradation), particularly if the proteasome is also inhibited, leading to the sequestering of CHIP and molecular chaperones in these protein aggregates.

The data gathered suggest that accumulation of MGO, which occurs in a variety of situations, such as diabetes and aging, impairs both the ubiquitin-proteasome system and the protein quality control dependent on CHIP and molecular chaperones, leading to accumulation of

toxic aggregates and increased cell death. However, these MGO-induced changes also appear to elicit a response from the Hsf-1 system, which is crucial to help cells to cope with cellular stress and to re-establish homeostasis.

CHAPTER 7

Chapter 7. General conclusions

The major complications of diabetes are associated with micro and macroangiopathies and high levels of glucose appear to be a driving force in the development of such vascular complications. Multiple biochemical pathways have been proposed to account for the pathogenesis of diabetes (Brownlee, 2005). Increased production and intracellular accumulation of methylglyoxal (MGO) is one of the central pathways that is likely to be a molecular link between hyperglycaemia and a number of pathological changes associated with diabetes, including endothelial dysfunction.

Endothelial dysfunction in diabetes is, to a large extent, associated with deregulation of the cell and tissue response to ischemia. Despite being an area of very active research, the link between hyperglycaemia and endothelial dysfunction, including the loss of cell response to hypoxia and destabilization of the hypoxia inducible factor-1 (HIF-1), has remained elusive. The data presented in this thesis show that increased production of MGO might be a link between both events and highlights a new model for the loss of cell response to hypoxia and endothelial dysfunction in diabetes.

The canonical pathway for degradation of HIF-1α under normoxia involves the targeting of the protein by the Von Hippel Lindau ubiquitin ligase (pVHL). To the best of our knowledge, there are only a very few recent studies to propose that HIF-1α may be targeted for degradation by pathways that do not require pVHL. However, the vast majority of such studies do not elucidate the molecular mechanisms involved nor do they identify the E3 ligases that target HIF-1α for degradation. This work shows an entirely new mechanism for degradation of HIF-1α that is activated in response to hyperglycaemia-induced accumulation of MGO. This finding is a novel and important contribution since it provides insight into a new molecular mechanism that promotes destabilization of an important transcription factor, which is likely to have a strong impact across a number of diseases, such as diabetes.

Data presented in chapter 4 shows that MGO modifies the HIF-1α protein, leading to the formation of Nε-carboxymethyl-lysine (CML) and Nα-acetyl-Nδ-(5-hydro-5-methyl)-4-imidazolone (MG-H1) adducts, which induces a rapid proteasome-dependent degradation of HIF-1α (Figure 46). The degradation of HIF-1α requires its prior ubiquitination through a mechanism independent on the ubiquitin ligase VHL and on proline hydroxylation. Significantly, data shows that the carboxy terminus of Hsp70-interacting protein (CHIP) is the E3 ligase that ubiquitinates HIF-1α in the presence of MGO. Consistently, silencing of endogenous CHIP and overexpression of glyoxalase I stabilize HIF-1α under hypoxia in the presence of MGO. Data further shows that increased association of the heat shock proteins Hsp40/70 with HIF-1α leads to recruitment of CHIP, which promotes polyubiquitination and proteasomal degradation of HIF-1α (Figure 28). Moreover, MGO-induced destabilization of HIF-1α leads to a dramatic decrease in HIF-1 transcriptional activity and expression of the vascular endothelial growth factor (VEGF) (Figure 46), which may explain the

loss of cell response to hypoxia and endothelial dysfunction in situations of increased availability of MGO, such as diabetes.

Independent data indicates that MGO modifies the co-repressor mammalian Sin3 homolog A (mSin3A), leading to increased expression of angiopoietin-2 (Ang-2) (Yao et al, 2007), which is known to be a key destabilizing signal for vessels, leading to regression in the absence of pro-angiogenic factors, such as VEGF. For example, diabetes induces a significant increase in retinal expression of Ang-2 (Hammes et al, 2004), while diabetic Ang-$2^{+/-}$ mice present both decreased pericytes loss and reduced acellular capillary formation, as compared to the diabetic wild-type strain Ang-$2^{+/+}$ (Hammes et al, 2002). Moreover, decreased levels of VEGF are associated with some angiogenesis and arteriogenesis disorders in diabetic patients, which are attenuated by decreasing the levels of Ang-2 (Altavilla et al, 2001; Tuo et al, 2008). Based on these and other evidences, we suggest that MGO destabilizes the levels of Ang-2 and VEGF, leading to cell death and decreased proliferation of endothelial cells, which are likely to account for vascular dysfunction (Figure 46). Consistently, data presented in this thesis shows that MGO imbalances the ratio between VEGF and Ang-2 secreted by epithelial cell. This imbalance was shown to induce apoptosis and decreased proliferation of endothelial cells (chapter 5), which characterize a number of microvascular complications on diabetes.

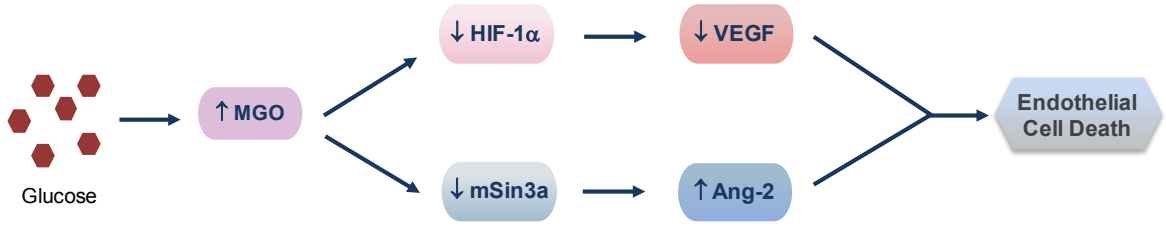

Figure 46. Working model for the endothelial dysfunction in diabetes. High glucose in diabetes leads to increased production and intracellular accumulation of MGO. MGO destabilizes HIF-1α under hypoxia, leading to decreased expression of VEGF and impairment of the angiogenic response. In addition, MGO is known to modify the co-repressor mSin3A, which culminates in increased expression of Ang-2. The imbalance in the ratio between VEGF and Ang-2 induces apoptosis and decreased proliferation of endothelial cells, which may account for the formation of acellular capillaries and endothelial dysfunction associated with diabetes.

Data presented in this thesis further shows that MGO may also compromise cell function and viability by impairing the ubiquitin-proteasome system and molecular chaperones involved in the protein quality control, leading to accumulation of modified, obsolete and potentially toxic proteins. Indeed, data presented in chapter 6 shows that MGO induces accumulation of ubiquitin conjugates, depletion of free ubiquitin and decreases the proteolytic activity of the 20S proteasome. Moreover, MGO decreases the levels of molecular chaperones (HSPs), induces the formation of CHIP-, Hsp40- and ubiquitin-containing aggregates and leads to accumulation of modified proteins, accounting for decreased cellular viability. Interestingly, data further shows that the cellular stress

induced by MGO is counteracted, at least in part, by the activation of heat shock factor-1 (Hsf-1), the main transcription factor involved in the regulation of the expression of heat shock proteins and response to cellular stress (Figure 47).

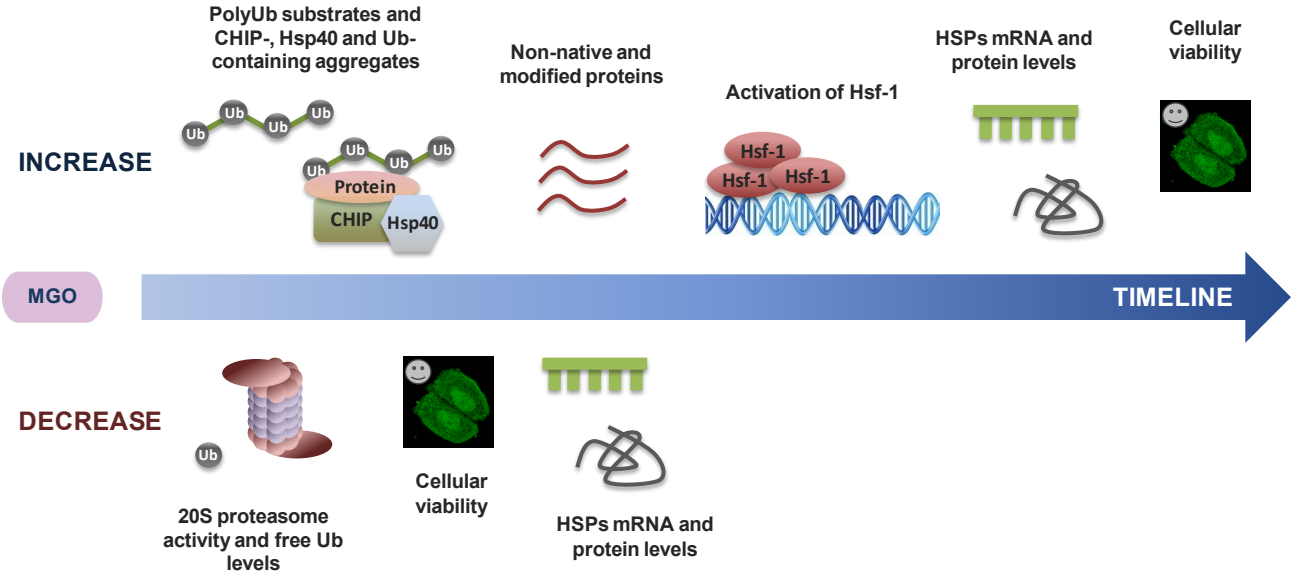

Figure 47. Working model for the MGO-induced events involving critical components of the protein quality control system. MGO leads to accumulation of ubiquitin conjugates, depletion of free ubiquitin and decreases the 20S proteasome activity. In parallel, MGO decreases the levels of molecular chaperones and increases the accumulation of CHIP-, Hsp40- and ubiquitin-containing aggregates, as well as of modified proteins, which is accompanied by decreased cellular viability. Interestingly, these MGO-induced changes appear to elicit a response from the Hsf-1 system, which is crucial to help cells to cope with cellular stress. Indeed, Hsf-1 is likely to be involved in the upregulation of mRNA and protein levels of several molecular chaperones that will re-establish the protein quality control system and cellular viability.

Altogether, this work elucidates two novel molecular mechanisms that may hopefully shed the foundation for a better understanding of two main features of diabetes: the loss of cell response to hypoxia and the accumulation of obsolete and toxic proteins in affected cells. In this respect, this work may also constitute an important and solid foundation for future approaches to further clarify the molecular mechanisms of cell dysfunction in diabetes. Moreover, this work may help to envision new strategies for prevention and therapy of cell dysfunction in diabetes.

REFERENCES

References

Abaci A, Oguzhan A, Kahraman S, Eryol NK, Unal S, Arinc H, Ergin A (1999) Effect of diabetes mellitus on formation of coronary collateral vessels. *Circulation* **99**(17)**:** 2239-2242

Aiello LP, Avery RL, Arrigg PG, Keyt BA, Jampel HD, Shah ST, Pasquale LR, Thieme H, Iwamoto MA, Park JE, et al. (1994) Vascular endothelial growth factor in ocular fluid of patients with diabetic retinopathy and other retinal disorders. *N Engl J Med* **331**(22)**:** 1480-1487

Aiello LP, Northrup JM, Keyt BA, Takagi H, Iwamoto MA (1995) Hypoxic regulation of vascular endothelial growth factor in retinal cells. *Arch Ophthalmol* **113**(12)**:** 1538-1544

Altavilla D, Saitta A, Cucinotta D, Galeano M, Deodato B, Colonna M, Torre V, Russo G, Sardella A, Urna G, Campo GM, Cavallari V, Squadrito G, Squadrito F (2001) Inhibition of lipid peroxidation restores impaired vascular endothelial growth factor expression and stimulates wound healing and angiogenesis in the genetically diabetic mouse. *Diabetes* **50**(3)**:** 667-674

Amerik AY, Hochstrasser M (2004) Mechanism and function of deubiquitinating enzymes. *Biochim Biophys Acta* **1695**(1-3)**:** 189-207

Appelhoff RJ, Tian YM, Raval RR, Turley H, Harris AL, Pugh CW, Ratcliffe PJ, Gleadle JM (2004) Differential function of the prolyl hydroxylases PHD1, PHD2, and PHD3 in the regulation of hypoxia-inducible factor. *J Biol Chem* **279**(37)**:** 38458-38465

Aravind L, Koonin EV (2000) The U box is a modified RING finger - a common domain in ubiquitination. *Curr Biol* **10**(4)**:** R132-134

Asai J, Takenaka H, Katoh N, Kishimoto S (2006) Dibutyryl cAMP influences endothelial progenitor cell recruitment during wound neovascularization. *J Invest Dermatol* **126**(5)**:** 1159-1167

Baek JH, Liu YV, McDonald KR, Wesley JB, Hubbi ME, Byun H, Semenza GL (2007) Spermidine/spermine-N1-acetyltransferase 2 is an essential component of the ubiquitin ligase complex that regulates hypoxia-inducible factor 1alpha. *J Biol Chem* **282**(32)**:** 23572-23580

Baek JH, Mahon PC, Oh J, Kelly B, Krishnamachary B, Pearson M, Chan DA, Giaccia AJ, Semenza GL (2005) OS-9 interacts with hypoxia-inducible factor 1alpha and prolyl hydroxylases to promote oxygen-dependent degradation of HIF-1alpha. *Mol Cell* **17**(4)**:** 503-512

Baelde HJ, Eikmans M, Lappin DW, Doran PP, Hohenadel D, Brinkkoetter PT, van der Woude FJ, Waldherr R, Rabelink TJ, de Heer E, Bruijn JA (2007) Reduction of VEGF-A and CTGF expression in diabetic nephropathy is associated with podocyte loss. *Kidney Int* **71**(7)**:** 637-645

Ballinger CA, Connell P, Wu Y, Hu Z, Thompson LJ, Yin LY, Patterson C (1999) Identification of CHIP, a novel tetratricopeptide repeat-containing protein that interacts with heat shock proteins and negatively regulates chaperone functions. *Mol Cell Biol* **19**(6)**:** 4535-4545

Barton WA, Tzvetkova D, Nikolov DB (2005) Structure of the angiopoietin-2 receptor binding domain and identification of surfaces involved in Tie2 recognition. *Structure* **13**(5)**:** 825-832

Beisswenger PJ, Howell SK, Touchette AD, Lal S, Szwergold BS (1999) Metformin reduces systemic methylglyoxal levels in type 2 diabetes. *Diabetes* **48**(1)**:** 198-202

Berlanga J, Cibrian D, Guillen I, Freyre F, Alba JS, Lopez-Saura P, Merino N, Aldama A, Quintela AM, Triana ME, Montequin JF, Ajamieh H, Urquiza D, Ahmed N, Thornalley PJ (2005)

Methylglyoxal administration induces diabetes-like microvascular changes and perturbs the healing process of cutaneous wounds. *Clin Sci (Lond)* **109**(1)**:** 83-95

Berra E, Benizri E, Ginouves A, Volmat V, Roux D, Pouyssegur J (2003) HIF prolyl-hydroxylase 2 is the key oxygen sensor setting low steady-state levels of HIF-1alpha in normoxia. *EMBO J* **22**(16)**:** 4082-4090

Berta MA, Mazure N, Hattab M, Pouyssegur J, Brahimi-Horn MC (2007) SUMOylation of hypoxia-inducible factor-1alpha reduces its transcriptional activity. *Biochem Biophys Res Commun* **360**(3)**:** 646-652

Biswas A, Wang B, Miyagi M, Nagaraj RH (2008) Effect of methylglyoxal modification on stress-induced aggregation of client proteins and their chaperoning by human alphaA-crystallin. *Biochem J* **409**(3)**:** 771-777

Biswas S, Ray M, Misra S, Dutta DP, Ray S (1997) Selective inhibition of mitochondrial respiration and glycolysis in human leukaemic leucocytes by methylglyoxal. *Biochem J* **323 (Pt 2):** 343-348

Bitto A, Minutoli L, Altavilla D, Polito F, Fiumara T, Marini H, Galeano M, Calo M, Lo Cascio P, Bonaiuto M, Migliorato A, Caputi AP, Squadrito F (2008) Simvastatin enhances VEGF production and ameliorates impaired wound healing in experimental diabetes. *Pharmacol Res* **57**(2)**:** 159-169

Blankenship C, Naglich JG, Whaley JM, Seizinger B, Kley N (1999) Alternate choice of initiation codon produces a biologically active product of the von Hippel Lindau gene with tumor suppressor activity. *Oncogene* **18**(8)**:** 1529-1535

Botusan IR, Sunkari VG, Savu O, Catrina AI, Grunler J, Lindberg S, Pereira T, Yla-Herttuala S, Poellinger L, Brismar K, Catrina SB (2008) Stabilization of HIF-1alpha is critical to improve wound healing in diabetic mice. *Proc Natl Acad Sci U S A* **105**(49)**:** 19426-19431

Bracken CP, Fedele AO, Linke S, Balrak W, Lisy K, Whitelaw ML, Peet DJ (2006) Cell-specific regulation of hypoxia-inducible factor (HIF)-1alpha and HIF-2alpha stabilization and transactivation in a graded oxygen environment. *J Biol Chem* **281**(32)**:** 22575-22585

Brownlee M (1995) Advanced protein glycosylation in diabetes and aging. *Annu Rev Med* **46:** 223-234

Brownlee M (2001) Biochemistry and molecular cell biology of diabetic complications. *Nature* **414**(6865)**:** 813-820

Brownlee M (2005) The pathobiology of diabetic complications: a unifying mechanism. *Diabetes* **54**(6)**:** 1615-1625

Brownlee M, Vlassara H, Cerami A (1984) Nonenzymatic glycosylation and the pathogenesis of diabetic complications. *Ann Intern Med* **101**(4)**:** 527-537

Brucklacher RM, Patel KM, VanGuilder HD, Bixler GV, Barber AJ, Antonetti DA, Lin CM, LaNoue KF, Gardner TW, Bronson SK, Freeman WM (2008) Whole genome assessment of the retinal response to diabetes reveals a progressive neurovascular inflammatory response. *BMC Med Genomics* **1:** 26

Bruick RK, McKnight SL (2001) A conserved family of prolyl-4-hydroxylases that modify HIF. *Science* **294**(5545)**:** 1337-1340

Bulteau AL, Verbeke P, Petropoulos I, Chaffotte AF, Friguet B (2001) Proteasome inhibition in glyoxal-treated fibroblasts and resistance of glycated glucose-6-phosphate dehydrogenase to 20 S proteasome degradation in vitro. *J Biol Chem* **276**(49)**:** 45662-45668

Cai J, Boulton M (2002) The pathogenesis of diabetic retinopathy: old concepts and new questions. *Eye* **16**(3)**:** 242-260

Caniggia I, Mostachfi H, Winter J, Gassmann M, Lye SJ, Kuliszewski M, Post M (2000) Hypoxia-inducible factor-1 mediates the biological effects of oxygen on human trophoblast differentiation through TGFbeta(3). *J Clin Invest* **105**(5)**:** 577-587

Caplan AJ (1999) Hsp90's secrets unfold: new insights from structural and functional studies. *Trends Cell Biol* **9**(7)**:** 262-268

Carbia-Nagashima A, Gerez J, Perez-Castro C, Paez-Pereda M, Silberstein S, Stalla GK, Holsboer F, Arzt E (2007) RSUME, a small RWD-containing protein, enhances SUMO conjugation and stabilizes HIF-1alpha during hypoxia. *Cell* **131**(2)**:** 309-323

Carmeliet P, Dor Y, Herbert JM, Fukumura D, Brusselmans K, Dewerchin M, Neeman M, Bono F, Abramovitch R, Maxwell P, Koch CJ, Ratcliffe P, Moons L, Jain RK, Collen D, Keshert E (1998) Role of HIF-1alpha in hypoxia-mediated apoptosis, cell proliferation and tumour angiogenesis. *Nature* **394**(6692)**:** 485-490

Carmeliet P, Storkebaum E (2002) Vascular and neuronal effects of VEGF in the nervous system: implications for neurological disorders. *Semin Cell Dev Biol* **13**(1)**:** 39-53

Carrozza MJ, Utley RT, Workman JL, Cote J (2003) The diverse functions of histone acetyltransferase complexes. *Trends Genet* **19**(6)**:** 321-329

Casas S, Gomis R, Gribble FM, Altirriba J, Knuutila S, Novials A (2007) Impairment of the ubiquitin-proteasome pathway is a downstream endoplasmic reticulum stress response induced by extracellular human islet amyloid polypeptide and contributes to pancreatic beta-cell apoptosis. *Diabetes* **56**(9)**:** 2284-2294

Catrina SB, Okamoto K, Pereira T, Brismar K, Poellinger L (2004) Hyperglycemia regulates hypoxia-inducible factor-1alpha protein stability and function. *Diabetes* **53**(12)**:** 3226-3232

Ceradini DJ, Yao D, Grogan RH, Callaghan MJ, Edelstein D, Brownlee M, Gurtner GC (2008) Decreasing intracellular superoxide corrects defective ischemia-induced new vessel formation in diabetic mice. *J Biol Chem* **283**(16)**:** 10930-10938

Chan HM, La Thangue NB (2001) p300/CBP proteins: HATs for transcriptional bridges and scaffolds. *J Cell Sci* **114**(Pt 13)**:** 2363-2373

Chapman-Smith A, Whitelaw ML (2006) Novel DNA binding by a basic helix-loop-helix protein. The role of the dioxin receptor PAS domain. *J Biol Chem* **281**(18)**:** 12535-12545

Chen D, Li M, Luo J, Gu W (2003) Direct interactions between HIF-1 alpha and Mdm2 modulate p53 function. *J Biol Chem* **278**(16)**:** 13595-13598

Chen K, Maley J, Yu PH (2006) Potential implications of endogenous aldehydes in beta-amyloid misfolding, oligomerization and fibrillogenesis. *J Neurochem* **99**(5)**:** 1413-1424

Cheng J, Kang X, Zhang S, Yeh ET (2007) SUMO-specific protease 1 is essential for stabilization of HIF1alpha during hypoxia. *Cell* **131**(3)**:** 584-595

Chou E, Suzuma I, Way KJ, Opland D, Clermont AC, Naruse K, Suzuma K, Bowling NL, Vlahos CJ, Aiello LP, King GL (2002) Decreased cardiac expression of vascular endothelial growth factor and its receptors in insulin-resistant and diabetic States: a possible explanation for impaired collateral formation in cardiac tissue. *Circulation* **105**(3)**:** 373-379

Chun YS, Choi E, Kim TY, Kim MS, Park JW (2002) A dominant-negative isoform lacking exons 11 and 12 of the human hypoxia-inducible factor-1alpha gene. *Biochem J* **362**(Pt 1)**:** 71-79

Ciechanover A (1994) The ubiquitin-proteasome proteolytic pathway. *Cell* **79**(1)**:** 13-21

Ciechanover A (1998) The ubiquitin-proteasome pathway: on protein death and cell life. *EMBO J* **17**(24)**:** 7151-7160

Ciechanover A (2005) Proteolysis: from the lysosome to ubiquitin and the proteasome. *Nat Rev Mol Cell Biol* **6**(1)**:** 79-87

Ciehanover A, Hod Y, Hershko A (1978) A heat-stable polypeptide component of an ATP-dependent proteolytic system from reticulocytes. *Biochem Biophys Res Commun* **81**(4)**:** 1100-1105

Coffe V, Carbajal RC, Salceda R (2006) Glucose metabolism in rat retinal pigment epithelium. *Neurochem Res* **31**(1)**:** 103-108

Cohen GM (1997) Caspases: the executioners of apoptosis. *Biochem J* **326 (Pt 1):** 1-16

Connell P, Ballinger CA, Jiang J, Wu Y, Thompson LJ, Hohfeld J, Patterson C (2001) The co-chaperone CHIP regulates protein triage decisions mediated by heat-shock proteins. *Nat Cell Biol* **3**(1)**:** 93-96

Cooper ME, Gilbert RE, Jerums G (1997) Diabetic vascular complications. *Clin Exp Pharmacol Physiol* **24**(9-10)**:** 770-775

Cyr DM, Hohfeld J, Patterson C (2002) Protein quality control: U-box-containing E3 ubiquitin ligases join the fold. *Trends Biochem Sci* **27**(7)**:** 368-375

Degenhardt TP, Thorpe SR, Baynes JW (1998) Chemical modification of proteins by methylglyoxal. *Cell Mol Biol (Noisy-le-grand)* **44**(7)**:** 1139-1145

Demand J, Luders J, Hohfeld J (1998) The carboxy-terminal domain of Hsc70 provides binding sites for a distinct set of chaperone cofactors. *Mol Cell Biol* **18**(4)**:** 2023-2028

DeMartino GN, Moomaw CR, Zagnitko OP, Proske RJ, Chu-Ping M, Afendis SJ, Swaffield JC, Slaughter CA (1994) PA700, an ATP-dependent activator of the 20 S proteasome, is an ATPase containing multiple members of a nucleotide-binding protein family. *J Biol Chem* **269**(33)**:** 20878-20884

Denis U, Lecomte M, Paget C, Ruggiero D, Wiernsperger N, Lagarde M (2002) Advanced glycation end-products induce apoptosis of bovine retinal pericytes in culture: involvement of diacylglycerol/ceramide production and oxidative stress induction. *Free Radic Biol Med* **33**(2)**:** 236-247

Deshaies RJ (1999) SCF and Cullin/Ring H2-based ubiquitin ligases. *Annu Rev Cell Dev Biol* **15:** 435-467

Dick LR, Cruikshank AA, Grenier L, Melandri FD, Nunes SL, Stein RL (1996) Mechanistic studies on the inactivation of the proteasome by lactacystin: a central role for clasto-lactacystin beta-lactone. *J Biol Chem* **271**(13)**:** 7273-7276

Dick TP, Nussbaum AK, Deeg M, Heinemeyer W, Groll M, Schirle M, Keilholz W, Stevanovic S, Wolf DH, Huber R, Rammensee HG, Schild H (1998) Contribution of proteasomal beta-subunits to the cleavage of peptide substrates analyzed with yeast mutants. *J Biol Chem* **273**(40)**:** 25637-25646

Donnelly R, Idris I, Forrester JV (2004) Protein kinase C inhibition and diabetic retinopathy: a shot in the dark at translational research. *Br J Ophthalmol* **88**(1)**:** 145-151

Du J, Zeng J, Ou X, Ren X, Cai S (2006) Methylglyoxal downregulates Raf-1 protein through a ubiquitination-mediated mechanism. *Int J Biochem Cell Biol* **38**(7)**:** 1084-1091

Du XL, Edelstein D, Dimmeler S, Ju Q, Sui C, Brownlee M (2001) Hyperglycemia inhibits endothelial nitric oxide synthase activity by posttranslational modification at the Akt site. *J Clin Invest* **108**(9)**:** 1341-1348

Du XL, Edelstein D, Rossetti L, Fantus IG, Goldberg H, Ziyadeh F, Wu J, Brownlee M (2000) Hyperglycemia-induced mitochondrial superoxide overproduction activates the hexosamine pathway and induces plasminogen activator inhibitor-1 expression by increasing Sp1 glycosylation. *Proc Natl Acad Sci U S A* **97**(22)**:** 12222-12226

Du Y, Smith MA, Miller CM, Kern TS (2002) Diabetes-induced nitrative stress in the retina, and correction by aminoguanidine. *J Neurochem* **80**(5)**:** 771-779

Duh E, Aiello LP (1999) Vascular endothelial growth factor and diabetes: the agonist versus antagonist paradox. *Diabetes* **48**(10)**:** 1899-1906

Elvert G, Kappel A, Heidenreich R, Englmeier U, Lanz S, Acker T, Rauter M, Plate K, Sieweke M, Breier G, Flamme I (2003) Cooperative interaction of hypoxia-inducible factor-2alpha (HIF-2alpha) and Ets-1 in the transcriptional activation of vascular endothelial growth factor receptor-2 (Flk-1). *J Biol Chem* **278**(9)**:** 7520-7530

Engerman RL (1989) Pathogenesis of diabetic retinopathy. *Diabetes* **38**(10)**:** 1203-1206

Epstein AC, Gleadle JM, McNeill LA, Hewitson KS, O'Rourke J, Mole DR, Mukherji M, Metzen E, Wilson MI, Dhanda A, Tian YM, Masson N, Hamilton DL, Jaakkola P, Barstead R, Hodgkin J, Maxwell PH, Pugh CW, Schofield CJ, Ratcliffe PJ (2001) C. elegans EGL-9 and mammalian homologs define a family of dioxygenases that regulate HIF by prolyl hydroxylation. *Cell* **107**(1)**:** 43-54

Erler JT, Bennewith KL, Nicolau M, Dornhofer N, Kong C, Le QT, Chi JT, Jeffrey SS, Giaccia AJ (2006) Lysyl oxidase is essential for hypoxia-induced metastasis. *Nature* **440**(7088)**:** 1222-1226

Esteban MA, Tran MG, Harten SK, Hill P, Castellanos MC, Chandra A, Raval R, O'Brien T S, Maxwell PH (2006) Regulation of E-cadherin expression by VHL and hypoxia-inducible factor. *Cancer Res* **66**(7)**:** 3567-3575

Eytan E, Armon T, Heller H, Beck S, Hershko A (1993) Ubiquitin C-terminal hydrolase activity associated with the 26 S protease complex. *J Biol Chem* **268**(7)**:** 4668-4674

Fadini GP, Sartore S, Schiavon M, Albiero M, Baesso I, Cabrelle A, Agostini C, Avogaro A (2006) Diabetes impairs progenitor cell mobilisation after hindlimb ischaemia-reperfusion injury in rats. *Diabetologia* **49**(12)**:** 3075-3084

Feldser D, Agani F, Iyer NV, Pak B, Ferreira G, Semenza GL (1999) Reciprocal positive regulation of hypoxia-inducible factor 1alpha and insulin-like growth factor 2. *Cancer Res* **59**(16)**:** 3915-3918

Feng Y, Pfister F, Schreiter K, Wang Y, Stock O, Vom Hagen F, Wolburg H, Hoffmann S, Deutsch U, Hammes HP (2008) Angiopoietin-2 deficiency decelerates age-dependent vascular changes in the mouse retina. *Cell Physiol Biochem* **21**(1-3)**:** 129-136

Ferrington DA, Sun H, Murray KK, Costa J, Williams TD, Bigelow DJ, Squier TC (2001) Selective degradation of oxidized calmodulin by the 20 S proteasome. *J Biol Chem* **276**(2)**:** 937-943

Flashman E, McDonough MA, Schofield CJ (2005) OS-9: another piece in the HIF complex story. *Mol Cell* **17**(4)**:** 472-473

Fong GH, Takeda K (2008) Role and regulation of prolyl hydroxylase domain proteins. *Cell Death Differ* **15**(4)**:** 635-641

Forsythe JA, Jiang BH, Iyer NV, Agani F, Leung SW, Koos RD, Semenza GL (1996) Activation of vascular endothelial growth factor gene transcription by hypoxia-inducible factor 1. *Mol Cell Biol* **16**(9)**:** 4604-4613

Friguet B, Bulteau AL, Chondrogianni N, Conconi M, Petropoulos I (2000) Protein degradation by the proteasome and its implications in aging. *Ann N Y Acad Sci* **908:** 143-154

Friguet B, Szweda LI, Stadtman ER (1994) Susceptibility of glucose-6-phosphate dehydrogenase modified by 4-hydroxy-2-nonenal and metal-catalyzed oxidation to proteolysis by the multicatalytic protease. *Arch Biochem Biophys* **311**(1)**:** 168-173

Frydman J (2001) Folding of newly translated proteins in vivo: the role of molecular chaperones. *Annu Rev Biochem* **70:** 603-647

Fukuba H, Yamashita H, Nagano Y, Jin HG, Hiji M, Ohtsuki T, Takahashi T, Kohriyama T, Matsumoto M (2007) Siah-1 facilitates ubiquitination and degradation of factor inhibiting HIF-1alpha (FIH). *Biochem Biophys Res Commun* **353**(2)**:** 324-329

Galiano RD, Tepper OM, Pelo CR, Bhatt KA, Callaghan M, Bastidas N, Bunting S, Steinmetz HG, Gurtner GC (2004) Topical vascular endothelial growth factor accelerates diabetic wound healing through increased angiogenesis and by mobilizing and recruiting bone marrow-derived cells. *Am J Pathol* **164**(6)**:** 1935-1947

Gao W, Ferguson G, Connell P, Walshe T, Murphy R, Birney YA, O'Brien C, Cahill PA (2007) High glucose concentrations alter hypoxia-induced control of vascular smooth muscle cell growth via a HIF-1alpha-dependent pathway. *J Mol Cell Cardiol* **42**(3)**:** 609-619

Geyer RK, Yu ZK, Maki CG (2000) The MDM2 RING-finger domain is required to promote p53 nuclear export. *Nat Cell Biol* **2**(9)**:** 569-573

Glickman MH, Ciechanover A (2002) The ubiquitin-proteasome proteolytic pathway: destruction for the sake of construction. *Physiol Rev* **82**(2)**:** 373-428

Glickman MH, Rubin DM, Coux O, Wefes I, Pfeifer G, Cjeka Z, Baumeister W, Fried VA, Finley D (1998a) A subcomplex of the proteasome regulatory particle required for ubiquitin-conjugate degradation and related to the COP9-signalosome and eIF3. *Cell* **94**(5)**:** 615-623

Glickman MH, Rubin DM, Fried VA, Finley D (1998b) The regulatory particle of the Saccharomyces cerevisiae proteasome. *Mol Cell Biol* **18**(6)**:** 3149-3162

Goldberg AL (2003) Protein degradation and protection against misfolded or damaged proteins. *Nature* **426**(6968)**:** 895-899

Goldknopf IL, Busch H (1977) Isopeptide linkage between nonhistone and histone 2A polypeptides of chromosomal conjugate-protein A24. *Proc Natl Acad Sci U S A* **74**(3)**:** 864-868

Gothie E, Richard DE, Berra E, Pages G, Pouyssegur J (2000) Identification of alternative spliced variants of human hypoxia-inducible factor-1alpha. *J Biol Chem* **275**(10)**:** 6922-6927

Goto Y, Kakizaki M, Masaki N (1976) Production of spontaneous diabetic rats by repetition of selective breeding. *Tohoku J Exp Med* **119**(1)**:** 85-90

Groll M, Bajorek M, Kohler A, Moroder L, Rubin DM, Huber R, Glickman MH, Finley D (2000) A gated channel into the proteasome core particle. *Nat Struct Biol* **7**(11)**:** 1062-1067

Groll M, Ditzel L, Lowe J, Stock D, Bochtler M, Bartunik HD, Huber R (1997) Structure of 20S proteasome from yeast at 2.4 A resolution. *Nature* **386**(6624)**:** 463-471

Grosfeld A, Andre J, Hauguel-De Mouzon S, Berra E, Pouyssegur J, Guerre-Millo M (2002) Hypoxia-inducible factor 1 transactivates the human leptin gene promoter. *J Biol Chem* **277**(45)**:** 42953-42957

Grune T, Reinheckel T, Davies KJ (1997) Degradation of oxidized proteins in mammalian cells. *FASEB J* **11**(7)**:** 526-534

Gunaratnam L, Morley M, Franovic A, de Paulsen N, Mekhail K, Parolin DA, Nakamura E, Lorimer IA, Lee S (2003) Hypoxia inducible factor activates the transforming growth factor-alpha/epidermal growth factor receptor growth stimulatory pathway in VHL(-/-) renal cell carcinoma cells. *J Biol Chem* **278**(45)**:** 44966-44974

Hagen T, Taylor CT, Lam F, Moncada S (2003) Redistribution of intracellular oxygen in hypoxia by nitric oxide: effect on HIF1alpha. *Science* **302**(5652)**:** 1975-1978

Halder J, Ray M, Ray S (1993) Inhibition of glycolysis and mitochondrial respiration of Ehrlich ascites carcinoma cells by methylglyoxal. *Int J Cancer* **54**(3)**:** 443-449

Hammes HP (2003) Pathophysiological mechanisms of diabetic angiopathy. *J Diabetes Complications* **17**(2 Suppl)**:** 16-19

Hammes HP, Du X, Edelstein D, Taguchi T, Matsumura T, Ju Q, Lin J, Bierhaus A, Nawroth P, Hannak D, Neumaier M, Bergfeld R, Giardino I, Brownlee M (2003) Benfotiamine blocks three major pathways of hyperglycemic damage and prevents experimental diabetic retinopathy. *Nat Med* **9**(3)**:** 294-299

Hammes HP, Lin J, Renner O, Shani M, Lundqvist A, Betsholtz C, Brownlee M, Deutsch U (2002) Pericytes and the pathogenesis of diabetic retinopathy. *Diabetes* **51**(10)**:** 3107-3112

Hammes HP, Lin J, Wagner P, Feng Y, Vom Hagen F, Krzizok T, Renner O, Breier G, Brownlee M, Deutsch U (2004) Angiopoietin-2 causes pericyte dropout in the normal retina: evidence for involvement in diabetic retinopathy. *Diabetes* **53**(4)**:** 1104-1110

Hammes HP, Martin S, Federlin K, Geisen K, Brownlee M (1991) Aminoguanidine treatment inhibits the development of experimental diabetic retinopathy. *Proc Natl Acad Sci U S A* **88**(24)**:** 11555-11558

Han Y, Randell E, Vasdev S, Gill V, Gadag V, Newhook LA, Grant M, Hagerty D (2007) Plasma methylglyoxal and glyoxal are elevated and related to early membrane alteration in young, complication-free patients with Type 1 diabetes. *Mol Cell Biochem* **305**(1-2)**:** 123-131

Hansson LO, Friedler A, Freund S, Rudiger S, Fersht AR (2002) Two sequence motifs from HIF-1alpha bind to the DNA-binding site of p53. *Proc Natl Acad Sci U S A* **99**(16)**:** 10305-10309

Harhaj NS, Antonetti DA (2004) Regulation of tight junctions and loss of barrier function in pathophysiology. *Int J Biochem Cell Biol* **36**(7)**:** 1206-1237

Harris AL (2002) Hypoxia--a key regulatory factor in tumour growth. *Nat Rev Cancer* **2**(1)**:** 38-47

Hartl FU, Hayer-Hartl M (2002) Molecular chaperones in the cytosol: from nascent chain to folded protein. *Science* **295**(5561)**:** 1852-1858

Hatfield PM, Vierstra RD (1992) Multiple forms of ubiquitin-activating enzyme E1 from wheat. Identification of an essential cysteine by in vitro mutagenesis. *J Biol Chem* **267**(21)**:** 14799-14803

Hershko A, Ciechanover A (1998) The ubiquitin system. *Annu Rev Biochem* **67:** 425-479

Hershko A, Heller H, Elias S, Ciechanover A (1983) Components of ubiquitin-protein ligase system. Resolution, affinity purification, and role in protein breakdown. *J Biol Chem* **258**(13)**:** 8206-8214

Hershko A, Leshinsky E, Ganoth D, Heller H (1984) ATP-dependent degradation of ubiquitin-protein conjugates. *Proc Natl Acad Sci U S A* **81**(6)**:** 1619-1623

Hewitson KS, Lienard BM, McDonough MA, Clifton IJ, Butler D, Soares AS, Oldham NJ, McNeill LA, Schofield CJ (2007) Structural and mechanistic studies on the inhibition of the hypoxia-inducible transcription factor hydroxylases by tricarboxylic acid cycle intermediates. *J Biol Chem* **282**(5)**:** 3293-3301

Hewitson KS, McNeill LA, Riordan MV, Tian YM, Bullock AN, Welford RW, Elkins JM, Oldham NJ, Bhattacharya S, Gleadle JM, Ratcliffe PJ, Pugh CW, Schofield CJ (2002) Hypoxia-inducible factor (HIF) asparagine hydroxylase is identical to factor inhibiting HIF (FIH) and is related to the cupin structural family. *J Biol Chem* **277**(29)**:** 26351-26355

Hideshima T, Richardson P, Chauhan D, Palombella VJ, Elliott PJ, Adams J, Anderson KC (2001) The proteasome inhibitor PS-341 inhibits growth, induces apoptosis, and overcomes drug resistance in human multiple myeloma cells. *Cancer Res* **61**(7)**:** 3071-3076

Hirsila M, Koivunen P, Gunzler V, Kivirikko KI, Myllyharju J (2003) Characterization of the human prolyl 4-hydroxylases that modify the hypoxia-inducible factor. *J Biol Chem* **278**(33)**:** 30772-30780

Hochstrasser M (1996) Ubiquitin-dependent protein degradation. *Annu Rev Genet* **30:** 405-439

Hohenstein B, Hausknecht B, Boehmer K, Riess R, Brekken RA, Hugo CP (2006) Local VEGF activity but not VEGF expression is tightly regulated during diabetic nephropathy in man. *Kidney Int* **69**(9)**:** 1654-1661

Hohfeld J, Cyr DM, Patterson C (2001) From the cradle to the grave: molecular chaperones that may choose between folding and degradation. *EMBO Rep* **2**(10)**:** 885-890

Hohfeld J, Jentsch S (1997) GrpE-like regulation of the hsc70 chaperone by the anti-apoptotic protein BAG-1. *EMBO J* **16**(20)**:** 6209-6216

Hohfeld J, Minami Y, Hartl FU (1995) Hip, a novel cochaperone involved in the eukaryotic Hsc70/Hsp40 reaction cycle. *Cell* **83**(4)**:** 589-598

Holash J, Maisonpierre PC, Compton D, Boland P, Alexander CR, Zagzag D, Yancopoulos GD, Wiegand SJ (1999) Vessel cooption, regression, and growth in tumors mediated by angiopoietins and VEGF. *Science* **284**(5422)**:** 1994-1998

Holzl H, Kapelari B, Kellermann J, Seemuller E, Sumegi M, Udvardy A, Medalia O, Sperling J, Muller SA, Engel A, Baumeister W (2000) The regulatory complex of Drosophila melanogaster 26S proteasomes. Subunit composition and localization of a deubiquitylating enzyme. *J Cell Biol* **150**(1)**:** 119-130

Hon WC, Wilson MI, Harlos K, Claridge TD, Schofield CJ, Pugh CW, Maxwell PH, Ratcliffe PJ, Stuart DI, Jones EY (2002) Structural basis for the recognition of hydroxyproline in HIF-1 alpha by pVHL. *Nature* **417**(6892)**:** 975-978

Hoppe T (2005) Multiubiquitylation by E4 enzymes: 'one size' doesn't fit all. *Trends Biochem Sci* **30**(4)**:** 183-187

Hosoya K, Tomi M, Ohtsuki S, Takanaga H, Ueda M, Yanai N, Obinata M, Terasaki T (2001) Conditionally immortalized retinal capillary endothelial cell lines (TR-iBRB) expressing differentiated endothelial cell functions derived from a transgenic rat. *Exp Eye Res* **72**(2)**:** 163-172

Hu J, Discher DJ, Bishopric NH, Webster KA (1998) Hypoxia regulates expression of the endothelin-1 gene through a proximal hypoxia-inducible factor-1 binding site on the antisense strand. *Biochem Biophys Res Commun* **245**(3)**:** 894-899

Huang LE, Arany Z, Livingston DM, Bunn HF (1996) Activation of hypoxia-inducible transcription factor depends primarily upon redox-sensitive stabilization of its alpha subunit. *J Biol Chem* **271**(50)**:** 32253-32259

Huang LE, Gu J, Schau M, Bunn HF (1998) Regulation of hypoxia-inducible factor 1alpha is mediated by an O2-dependent degradation domain via the ubiquitin-proteasome pathway. *Proc Natl Acad Sci U S A* **95**(14)**:** 7987-7992

Huang Q, Yuan Y (1997) Interaction of PKC and NOS in signal transduction of microvascular hyperpermeability. *Am J Physiol* **273**(5 Pt 2)**:** H2442-2451

Huibregtse JM, Scheffner M, Beaudenon S, Howley PM (1995) A family of proteins structurally and functionally related to the E6-AP ubiquitin-protein ligase. *Proc Natl Acad Sci U S A* **92**(11)**:** 5249

Hume AN, Tarafder AK, Ramalho JS, Sviderskaya EV, Seabra MC (2006) A coiled-coil domain of melanophilin is essential for Myosin Va recruitment and melanosome transport in melanocytes. *Mol Biol Cell* **17**(11)**:** 4720-4735

Ivan M, Kondo K, Yang H, Kim W, Valiando J, Ohh M, Salic A, Asara JM, Lane WS, Kaelin WG, Jr. (2001) HIFalpha targeted for VHL-mediated destruction by proline hydroxylation: implications for O2 sensing. *Science* **292**(5516)**:** 464-468

Iwai K, Yamanaka K, Kamura T, Minato N, Conaway RC, Conaway JW, Klausner RD, Pause A (1999) Identification of the von Hippel-lindau tumor-suppressor protein as part of an active E3 ubiquitin ligase complex. *Proc Natl Acad Sci U S A* **96**(22)**:** 12436-12441

Jaakkola P, Mole DR, Tian YM, Wilson MI, Gielbert J, Gaskell SJ, Kriegsheim A, Hebestreit HF, Mukherji M, Schofield CJ, Maxwell PH, Pugh CW, Ratcliffe PJ (2001) Targeting of HIF-alpha to the von Hippel-Lindau ubiquitylation complex by O2-regulated prolyl hydroxylation. *Science* **292**(5516)**:** 468-472

Jackson PK, Eldridge AG, Freed E, Furstenthal L, Hsu JY, Kaiser BK, Reimann JD (2000) The lore of the RINGs: substrate recognition and catalysis by ubiquitin ligases. *Trends Cell Biol* **10**(10)**:** 429-439

Jan CR, Chen CH, Wang SC, Kuo SY (2005) Effect of methylglyoxal on intracellular calcium levels and viability in renal tubular cells. *Cell Signal* **17**(7)**:** 847-855

Jeong JW, Bae MK, Ahn MY, Kim SH, Sohn TK, Bae MH, Yoo MA, Song EJ, Lee KJ, Kim KW (2002) Regulation and destabilization of HIF-1alpha by ARD1-mediated acetylation. *Cell* **111**(5)**:** 709-720

Jiang BH, Semenza GL, Bauer C, Marti HH (1996) Hypoxia-inducible factor 1 levels vary exponentially over a physiologically relevant range of O2 tension. *Am J Physiol* **271**(4 Pt 1)**:** C1172-1180

Jiang J, Ballinger CA, Wu Y, Dai Q, Cyr DM, Hohfeld J, Patterson C (2001) CHIP is a U-box-dependent E3 ubiquitin ligase: identification of Hsc70 as a target for ubiquitylation. *J Biol Chem* **276**(46)**:** 42938-42944

Joazeiro CA, Weissman AM (2000) RING finger proteins: mediators of ubiquitin ligase activity. *Cell* **102**(5)**:** 549-552

Kaidi A, Qualtrough D, Williams AC, Paraskeva C (2006) Direct transcriptional up-regulation of cyclooxygenase-2 by hypoxia-inducible factor (HIF)-1 promotes colorectal tumor cell survival and enhances HIF-1 transcriptional activity during hypoxia. *Cancer Res* **66**(13)**:** 6683-6691

Kalapos MP (1999) Methylglyoxal in living organisms: chemistry, biochemistry, toxicology and biological implications. *Toxicol Lett* **110**(3)**:** 145-175

Kallio PJ, Okamoto K, O'Brien S, Carrero P, Makino Y, Tanaka H, Poellinger L (1998) Signal transduction in hypoxic cells: inducible nuclear translocation and recruitment of the CBP/p300 coactivator by the hypoxia-inducible factor-1alpha. *Embo J* **17**(22)**:** 6573-6586

Kang JH (2006) Oxidative modification of human ceruloplasmin by methylglyoxal: an in vitro study. *J Biochem Mol Biol* **39**(3)**:** 335-338

Kido M, Du L, Sullivan CC, Li X, Deutsch R, Jamieson SW, Thistlethwaite PA (2005) Hypoxia-inducible factor 1-alpha reduces infarction and attenuates progression of cardiac dysfunction after myocardial infarction in the mouse. *J Am Coll Cardiol* **46**(11)**:** 2116-2124

Kim HT, Kim KP, Lledias F, Kisselev AF, Scaglione KM, Skowyra D, Gygi SP, Goldberg AL (2007) Certain pairs of ubiquitin-conjugating enzymes (E2s) and ubiquitin-protein ligases (E3s) synthesize nondegradable forked ubiquitin chains containing all possible isopeptide linkages. *J Biol Chem* **282**(24)**:** 17375-17386

Kimura H, Weisz A, Ogura T, Hitomi Y, Kurashima Y, Hashimoto K, D'Acquisto F, Makuuchi M, Esumi H (2001) Identification of hypoxia-inducible factor 1 ancillary sequence and its function in vascular endothelial growth factor gene induction by hypoxia and nitric oxide. *J Biol Chem* **276**(3)**:** 2292-2298

Kisselev AF, Akopian TN, Woo KM, Goldberg AL (1999) The sizes of peptides generated from protein by mammalian 26 and 20 S proteasomes. Implications for understanding the degradative mechanism and antigen presentation. *J Biol Chem* **274**(6)**:** 3363-3371

Koh MY, Darnay BG, Powis G (2008) Hypoxia-associated factor, a novel E3-ubiquitin ligase, binds and ubiquitinates hypoxia-inducible factor 1alpha, leading to its oxygen-independent degradation. *Mol Cell Biol* **28**(23)**:** 7081-7095

Koivunen P, Hirsila M, Gunzler V, Kivirikko KI, Myllyharju J (2004) Catalytic properties of the asparaginyl hydroxylase (FIH) in the oxygen sensing pathway are distinct from those of its prolyl 4-hydroxylases. *J Biol Chem* **279**(11)**:** 9899-9904

Kong X, Lin Z, Liang D, Fath D, Sang N, Caro J (2006) Histone deacetylase inhibitors induce VHL and ubiquitin-independent proteasomal degradation of hypoxia-inducible factor 1alpha. *Mol Cell Biol* **26**(6)**:** 2019-2028

Kumar PA, Kumar MS, Reddy GB (2007) Effect of glycation on alpha-crystallin structure and chaperone-like function. *Biochem J* **408**(2)**:** 251-258

Kung AL, Wang S, Klco JM, Kaelin WG, Livingston DM (2000) Suppression of tumor growth through disruption of hypoxia-inducible transcription. *Nat Med* **6**(12)**:** 1335-1340

Laga M, Cottyn A, Van Herreweghe F, Vanden Berghe W, Haegeman G, Van Oostveldt P, Vandekerckhove J, Vancompernolle K (2007) Methylglyoxal suppresses TNF-alpha-induced NF-kappaB activation by inhibiting NF-kappaB DNA-binding. *Biochem Pharmacol* **74**(4)**:** 579-589

Lam YA, DeMartino GN, Pickart CM, Cohen RE (1997a) Specificity of the ubiquitin isopeptidase in the PA700 regulatory complex of 26 S proteasomes. *J Biol Chem* **272**(45)**:** 28438-28446

Lam YA, Xu W, DeMartino GN, Cohen RE (1997b) Editing of ubiquitin conjugates by an isopeptidase in the 26S proteasome. *Nature* **385**(6618)**:** 737-740

Lando D, Peet DJ, Gorman JJ, Whelan DA, Whitelaw ML, Bruick RK (2002a) FIH-1 is an asparaginyl hydroxylase enzyme that regulates the transcriptional activity of hypoxia-inducible factor. *Genes Dev* **16**(12)**:** 1466-1471

Lando D, Peet DJ, Whelan DA, Gorman JJ, Whitelaw ML (2002b) Asparagine hydroxylation of the HIF transactivation domain a hypoxic switch. *Science* **295**(5556)**:** 858-861

Larger E, Marre M, Corvol P, Gasc JM (2004) Hyperglycemia-induced defects in angiogenesis in the chicken chorioallantoic membrane model. *Diabetes* **53**(3)**:** 752-761

Lasch P, Petras T, Ullrich O, Backmann J, Naumann D, Grune T (2001) Hydrogen peroxide-induced structural alterations of RNAse A. *J Biol Chem* **276**(12)**:** 9492-9502

Lecker SH, Goldberg AL, Mitch WE (2006) Protein degradation by the ubiquitin-proteasome pathway in normal and disease states. *J Am Soc Nephrol* **17**(7)**:** 1807-1819

Lee C, Yim MB, Chock PB, Yim HS, Kang SO (1998) Oxidation-reduction properties of methylglyoxal-modified protein in relation to free radical generation. *J Biol Chem* **273**(39)**:** 25272-25278

Lee EY, Chung CH, Kim JH, Joung HJ, Hong SY (2006) Antioxidants ameliorate the expression of vascular endothelial growth factor mediated by protein kinase C in diabetic podocytes. *Nephrol Dial Transplant* **21**(6)**:** 1496-1503

Lee HK, Seo IA, Suh DJ, Lee HJ, Park HT (2009) A novel mechanism of methylglyoxal cytotoxicity in neuroglial cells. *J Neurochem* **108**(1)**:** 273-284

Lee PJ, Jiang BH, Chin BY, Iyer NV, Alam J, Semenza GL, Choi AM (1997) Hypoxia-inducible factor-1 mediates transcriptional activation of the heme oxygenase-1 gene in response to hypoxia. *J Biol Chem* **272**(9)**:** 5375-5381

Lerman OZ, Galiano RD, Armour M, Levine JP, Gurtner GC (2003) Cellular dysfunction in the diabetic fibroblast: impairment in migration, vascular endothelial growth factor production, and response to hypoxia. *Am J Pathol* **162**(1)**:** 303-312

Li Z, Na X, Wang D, Schoen SR, Messing EM, Wu G (2002a) Ubiquitination of a novel deubiquitinating enzyme requires direct binding to von Hippel-Lindau tumor suppressor protein. *J Biol Chem* **277**(7)**:** 4656-4662

Li Z, Wang D, Messing EM, Wu G (2005) VHL protein-interacting deubiquitinating enzyme 2 deubiquitinates and stabilizes HIF-1alpha. *EMBO Rep* **6**(4)**:** 373-378

Li Z, Wang D, Na X, Schoen SR, Messing EM, Wu G (2002b) Identification of a deubiquitinating enzyme subfamily as substrates of the von Hippel-Lindau tumor suppressor. *Biochem Biophys Res Commun* **294**(3)**:** 700-709

Linke S, Stojkoski C, Kewley RJ, Booker GW, Whitelaw ML, Peet DJ (2004) Substrate requirements of the oxygen-sensing asparaginyl hydroxylase factor-inhibiting hypoxia-inducible factor. *J Biol Chem* **279**(14)**:** 14391-14397

Lisy K, Peet DJ (2008) Turn me on: regulating HIF transcriptional activity. *Cell Death Differ* **15**(4)**:** 642-649

Liu L, Marti GP, Wei X, Zhang X, Zhang H, Liu YV, Nastai M, Semenza GL, Harmon JW (2008) Age-dependent impairment of HIF-1alpha expression in diabetic mice: Correction with electroporation-facilitated gene therapy increases wound healing, angiogenesis, and circulating angiogenic cells. *J Cell Physiol* **217**(2)**:** 319-327

Liu YV, Baek JH, Zhang H, Diez R, Cole RN, Semenza GL (2007) RACK1 competes with HSP90 for binding to HIF-1alpha and is required for O(2)-independent and HSP90 inhibitor-induced degradation of HIF-1alpha. *Mol Cell* **25**(2)**:** 207-217

Lopes VS, Ramalho JS, Owen DM, Karl MO, Strauss O, Futter CE, Seabra MC (2007) The ternary Rab27a-Myrip-Myosin VIIa complex regulates melanosome motility in the retinal pigment epithelium. *Traffic* **8**(5)**:** 486-499

Mahon PC, Hirota K, Semenza GL (2001) FIH-1: a novel protein that interacts with HIF-1alpha and VHL to mediate repression of HIF-1 transcriptional activity. *Genes Dev* **15**(20)**:** 2675-2686

Mailand N, Bekker-Jensen S, Faustrup H, Melander F, Bartek J, Lukas C, Lukas J (2007) RNF8 ubiquitylates histones at DNA double-strand breaks and promotes assembly of repair proteins. *Cell* **131**(5)**:** 887-900

Maisonpierre PC, Suri C, Jones PF, Bartunkova S, Wiegand SJ, Radziejewski C, Compton D, McClain J, Aldrich TH, Papadopoulos N, Daly TJ, Davis S, Sato TN, Yancopoulos GD (1997) Angiopoietin-2, a natural antagonist for Tie2 that disrupts in vivo angiogenesis. *Science* **277**(5322)**:** 55-60

Makino Y, Cao R, Svensson K, Bertilsson G, Asman M, Tanaka H, Cao Y, Berkenstam A, Poellinger L (2001) Inhibitory PAS domain protein is a negative regulator of hypoxia-inducible gene expression. *Nature* **414**(6863)**:** 550-554

Makino Y, Kanopka A, Wilson WJ, Tanaka H, Poellinger L (2002) Inhibitory PAS domain protein (IPAS) is a hypoxia-inducible splicing variant of the hypoxia-inducible factor-3alpha locus. *J Biol Chem* **277**(36)**:** 32405-32408

Malmberg K, Norhammar A, Wedel H, Ryden L (1999) Glycometabolic state at admission: important risk marker of mortality in conventionally treated patients with diabetes mellitus and acute myocardial infarction: long-term results from the Diabetes and Insulin-Glucose Infusion in Acute Myocardial Infarction (DIGAMI) study. *Circulation* **99**(20)**:** 2626-2632

Marfella R, D'Amico M, Di Filippo C, Piegari E, Nappo F, Esposito K, Berrino L, Rossi F, Giugliano D (2002) Myocardial infarction in diabetic rats: role of hyperglycaemia on infarct size and early expression of hypoxia-inducible factor 1. *Diabetologia* **45**(8)**:** 1172-1181

Marfella R, Esposito K, Nappo F, Siniscalchi M, Sasso FC, Portoghese M, Di Marino MP, Baldi A, Cuzzocrea S, Di Filippo C, Barboso G, Baldi F, Rossi F, D'Amico M, Giugliano D (2004) Expression of angiogenic factors during acute coronary syndromes in human type 2 diabetes. *Diabetes* **53**(9)**:** 2383-2391

Marques C, Guo W, Pereira P, Taylor A, Patterson C, Evans PC, Shang F (2006) The triage of damaged proteins: degradation by the ubiquitin-proteasome pathway or repair by molecular chaperones. *FASEB J* **20**(6)**:** 741-743

Masson N, Willam C, Maxwell PH, Pugh CW, Ratcliffe PJ (2001) Independent function of two destruction domains in hypoxia-inducible factor-alpha chains activated by prolyl hydroxylation. *EMBO J* **20**(18)**:** 5197-5206

Maxwell PH, Wiesener MS, Chang GW, Clifford SC, Vaux EC, Cockman ME, Wykoff CC, Pugh CW, Maher ER, Ratcliffe PJ (1999) The tumour suppressor protein VHL targets hypoxia-inducible factors for oxygen-dependent proteolysis. *Nature* **399**(6733)**:** 271-275

Maynard MA, Ohh M (2007) The role of hypoxia-inducible factors in cancer. *Cell Mol Life Sci* **64**(16)**:** 2170-2180

Maynard MA, Qi H, Chung J, Lee EH, Kondo Y, Hara S, Conaway RC, Conaway JW, Ohh M (2003) Multiple splice variants of the human HIF-3 alpha locus are targets of the von Hippel-Lindau E3 ubiquitin ligase complex. *J Biol Chem* **278**(13)**:** 11032-11040

Mazure NM, Brahimi-Horn MC, Berta MA, Benizri E, Bilton RL, Dayan F, Ginouves A, Berra E, Pouyssegur J (2004) HIF-1: master and commander of the hypoxic world. A pharmacological approach to its regulation by siRNAs. *Biochem Pharmacol* **68**(6)**:** 971-980

McDonough H, Patterson C (2003) CHIP: a link between the chaperone and proteasome systems. *Cell Stress Chaperones* **8**(4)**:** 303-308

McGrath JP, Jentsch S, Varshavsky A (1991) UBA 1: an essential yeast gene encoding ubiquitin-activating enzyme. *EMBO J* **10**(1)**:** 227-236

McLellan AC, Thornalley PJ, Benn J, Sonksen PH (1994) Glyoxalase system in clinical diabetes mellitus and correlation with diabetic complications. *Clin Sci (Lond)* **87**(1)**:** 21-29

Meacham GC, Patterson C, Zhang W, Younger JM, Cyr DM (2001) The Hsc70 co-chaperone CHIP targets immature CFTR for proteasomal degradation. *Nat Cell Biol* **3**(1)**:** 100-105

Meng L, Mohan R, Kwok BH, Elofsson M, Sin N, Crews CM (1999) Epoxomicin, a potent and selective proteasome inhibitor, exhibits in vivo antiinflammatory activity. *Proc Natl Acad Sci U S A* **96**(18)**:** 10403-10408

Merforth S, Kuehn L, Osmers A, Dahlmann B (2003) Alteration of 20S proteasome-subtypes and proteasome activator PA28 in skeletal muscle of rat after induction of diabetes mellitus. *Int J Biochem Cell Biol* **35**(5)**:** 740-748

Metzen E, Berchner-Pfannschmidt U, Stengel P, Marxsen JH, Stolze I, Klinger M, Huang WQ, Wotzlaw C, Hellwig-Burgel T, Jelkmann W, Acker H, Fandrey J (2003a) Intracellular localisation of human HIF-1 alpha hydroxylases: implications for oxygen sensing. *J Cell Sci* **116**(Pt 7)**:** 1319-1326

Metzen E, Zhou J, Jelkmann W, Fandrey J, Brune B (2003b) Nitric oxide impairs normoxic degradation of HIF-1alpha by inhibition of prolyl hydroxylases. *Mol Biol Cell* **14**(8)**:** 3470-3481

Miller AG, Smith DG, Bhat M, Nagaraj RH (2006) Glyoxalase I is critical for human retinal capillary pericyte survival under hyperglycemic conditions. *J Biol Chem* **281**(17)**:** 11864-11871

Min JH, Yang H, Ivan M, Gertler F, Kaelin WG, Jr., Pavletich NP (2002) Structure of an HIF-1alpha -pVHL complex: hydroxyproline recognition in signaling. *Science* **296**(5574)**:** 1886-1889

Minami Y, Hohfeld J, Ohtsuka K, Hartl FU (1996) Regulation of the heat-shock protein 70 reaction cycle by the mammalian DnaJ homolog, Hsp40. *J Biol Chem* **271**(32)**:** 19617-19624

Monnier VM (1989) Towards a Maillard theory of ageing. In *The Maillard Reaction in Aging, Diabetes and Nutrition*, Baynes JWaM, V. M. (ed), pp 1-22. New York: Alan R. Liss Inc.

Monnier VM, Nagaraj RH, Portero-Otin M, Glomb M, Elgawish AH, Sell DR, Friedlander MA (1996) Structure of advanced Maillard reaction products and their pathological role. *Nephrol Dial Transplant* **11 Suppl 5:** 20-26

Murata S, Chiba T, Tanaka K (2003) CHIP: a quality-control E3 ligase collaborating with molecular chaperones. *Int J Biochem Cell Biol* **35**(5)**:** 572-578

Murata S, Minami Y, Minami M, Chiba T, Tanaka K (2001) CHIP is a chaperone-dependent E3 ligase that ubiquitylates unfolded protein. *EMBO Rep* **2**(12)**:** 1133-1138

Mylonis I, Chachami G, Samiotaki M, Panayotou G, Paraskeva E, Kalousi A, Georgatsou E, Bonanou S, Simos G (2006) Identification of MAPK phosphorylation sites and their role in the localization and activity of hypoxia-inducible factor-1alpha. *J Biol Chem* **281**(44)**:** 33095-33106

Myung J, Kim KB, Crews CM (2001) The ubiquitin-proteasome pathway and proteasome inhibitors. *Med Res Rev* **21**(4)**:** 245-273

Nagaraj RH, Oya-Ito T, Padayatti PS, Kumar R, Mehta S, West K, Levison B, Sun J, Crabb JW, Padival AK (2003) Enhancement of chaperone function of alpha-crystallin by methylglyoxal modification. *Biochemistry* **42**(36)**:** 10746-10755

Nakagawa T, Sato W, Sautin YY, Glushakova O, Croker B, Atkinson MA, Tisher CC, Johnson RJ (2006) Uncoupling of vascular endothelial growth factor with nitric oxide as a mechanism for diabetic vasculopathy. *J Am Soc Nephrol* **17**(3)**:** 736-745

Nakamura S, Makita Z, Ishikawa S, Yasumura K, Fujii W, Yanagisawa K, Kawata T, Koike T (1997) Progression of nephropathy in spontaneous diabetic rats is prevented by OPB-9195, a novel inhibitor of advanced glycation. *Diabetes* **46**(5)**:** 895-899

Nakayama K, Frew IJ, Hagensen M, Skals M, Habelhah H, Bhoumik A, Kadoya T, Erdjument-Bromage H, Tempst P, Frappell PB, Bowtell DD, Ronai Z (2004) Siah2 regulates stability of prolyl-hydroxylases, controls HIF1alpha abundance, and modulates physiological responses to hypoxia. *Cell* **117**(7)**:** 941-952

Nalepa G, Rolfe M, Harper JW (2006) Drug discovery in the ubiquitin-proteasome system. *Nat Rev Drug Discov* **5**(7)**:** 596-613

Nandi D, Tahiliani P, Kumar A, Chandu D (2006) The ubiquitin-proteasome system. *J Biosci* **31**(1)**:** 137-155

Nemet I, Varga-Defterdarovic L, Turk Z (2006) Methylglyoxal in food and living organisms. *Mol Nutr Food Res* **50**(12)**:** 1105-1117

Nikolay R, Wiederkehr T, Rist W, Kramer G, Mayer MP, Bukau B (2004) Dimerization of the human E3 ligase CHIP via a coiled-coil domain is essential for its activity. *J Biol Chem* **279**(4)**:** 2673-2678

Nishikawa T, Edelstein D, Du XL, Yamagishi S, Matsumura T, Kaneda Y, Yorek MA, Beebe D, Oates PJ, Hammes HP, Giardino I, Brownlee M (2000) Normalizing mitochondrial superoxide production blocks three pathways of hyperglycaemic damage. *Nature* **404**(6779)**:** 787-790

Obin M, Nowell T, Taylor A (1994) The photoreceptor G-protein transducin (Gt) is a substrate for ubiquitin-dependent proteolysis. *Biochem Biophys Res Commun* **200**(3)**:** 1169-1176

Ohh M, Park CW, Ivan M, Hoffman MA, Kim TY, Huang LE, Pavletich N, Chau V, Kaelin WG (2000) Ubiquitination of hypoxia-inducible factor requires direct binding to the beta-domain of the von Hippel-Lindau protein. *Nat Cell Biol* **2**(7)**:** 423-427

Ohta T, Michel JJ, Schottelius AJ, Xiong Y (1999) ROC1, a homolog of APC11, represents a family of cullin partners with an associated ubiquitin ligase activity. *Mol Cell* **3**(4)**:** 535-541

Oltvai ZN, Milliman CL, Korsmeyer SJ (1993) Bcl-2 heterodimerizes in vivo with a conserved homolog, Bax, that accelerates programmed cell death. *Cell* **74**(4)**:** 609-619

Orlowski M, Wilk S (2000) Catalytic activities of the 20 S proteasome, a multicatalytic proteinase complex. *Arch Biochem Biophys* **383**(1)**:** 1-16

Oshima Y, Deering T, Oshima S, Nambu H, Reddy PS, Kaleko M, Connelly S, Hackett SF, Campochiaro PA (2004) Angiopoietin-2 enhances retinal vessel sensitivity to vascular endothelial growth factor. *J Cell Physiol* **199**(3)**:** 412-417

Oya-Ito T, Liu BF, Nagaraj RH (2006) Effect of methylglyoxal modification and phosphorylation on the chaperone and anti-apoptotic properties of heat shock protein 27. *J Cell Biochem* **99**(1)**:** 279-291

Oya T, Hattori N, Mizuno Y, Miyata S, Maeda S, Osawa T, Uchida K (1999) Methylglyoxal modification of protein. Chemical and immunochemical characterization of methylglyoxal-arginine adducts. *J Biol Chem* **274**(26)**:** 18492-18502

Page AM, Hieter P (1999) The anaphase-promoting complex: new subunits and regulators. *Annu Rev Biochem* **68:** 583-609

Palmer LA, Semenza GL, Stoler MH, Johns RA (1998) Hypoxia induces type II NOS gene expression in pulmonary artery endothelial cells via HIF-1. *Am J Physiol* **274**(2 Pt 1)**:** L212-219

Pan Y, Mansfield KD, Bertozzi CC, Rudenko V, Chan DA, Giaccia AJ, Simon MC (2007) Multiple factors affecting cellular redox status and energy metabolism modulate hypoxia-inducible factor prolyl hydroxylase activity in vivo and in vitro. *Mol Cell Biol* **27**(3)**:** 912-925

Park JY, Takahara N, Gabriele A, Chou E, Naruse K, Suzuma K, Yamauchi T, Ha SW, Meier M, Rhodes CJ, King GL (2000) Induction of endothelin-1 expression by glucose: an effect of protein kinase C activation. *Diabetes* **49**(7)**:** 1239-1248

Park SH, Bolender N, Eisele F, Kostova Z, Takeuchi J, Coffino P, Wolf DH (2007) The cytoplasmic Hsp70 chaperone machinery subjects misfolded and endoplasmic reticulum import-incompetent proteins to degradation via the ubiquitin-proteasome system. *Mol Biol Cell* **18**(1)**:** 153-165

Pause A, Lee S, Worrell RA, Chen DY, Burgess WH, Linehan WM, Klausner RD (1997) The von Hippel-Lindau tumor-suppressor gene product forms a stable complex with human CUL-2, a member of the Cdc53 family of proteins. *Proc Natl Acad Sci U S A* **94**(6)**:** 2156-2161

Petropoulos I, Conconi M, Wang X, Hoenel B, Bregegere F, Milner Y, Friguet B (2000) Increase of oxidatively modified protein is associated with a decrease of proteasome activity and content in aging epidermal cells. *J Gerontol A Biol Sci Med Sci* **55**(5)**:** B220-227

Phillips SA, Mirrlees D, Thornalley PJ (1993) Modification of the glyoxalase system in streptozotocin-induced diabetic rats. Effect of the aldose reductase inhibitor Statil. *Biochem Pharmacol* **46**(5)**:** 805-811

Pickart CM (2000) Ubiquitin in chains. *Trends Biochem Sci* **25**(11)**:** 544-548

Pirkkala L, Nykanen P, Sistonen L (2001) Roles of the heat shock transcription factors in regulation of the heat shock response and beyond. *FASEB J* **15**(7)**:** 1118-1131

Porter AG, Janicke RU (1999) Emerging roles of caspase-3 in apoptosis. *Cell Death Differ* **6**(2)**:** 99-104

Portero-Otin M, Pamplona R, Bellmunt MJ, Ruiz MC, Prat J, Salvayre R, Negre-Salvayre A (2002) Advanced glycation end product precursors impair epidermal growth factor receptor signaling. *Diabetes* **51**(5)**:** 1535-1542

Portero-Otin M, Pamplona R, Ruiz MC, Cabiscol E, Prat J, Bellmunt MJ (1999) Diabetes induces an impairment in the proteolytic activity against oxidized proteins and a heterogeneous effect in nonenzymatic protein modifications in the cytosol of rat liver and kidney. *Diabetes* **48**(11)**:** 2215-2220

Ramasamy R, Yan SF, Schmidt AM (2006) Methylglyoxal comes of AGE. *Cell* **124**(2)**:** 258-260

Rankin EB, Giaccia AJ (2008) The role of hypoxia-inducible factors in tumorigenesis. *Cell Death Differ* **15**(4)**:** 678-685

Ravi R, Mookerjee B, Bhujwalla ZM, Sutter CH, Artemov D, Zeng Q, Dillehay LE, Madan A, Semenza GL, Bedi A (2000) Regulation of tumor angiogenesis by p53-induced degradation of hypoxia-inducible factor 1alpha. *Genes Dev* **14**(1)**:** 34-44

Ray S, Dutta S, Halder J, Ray M (1994) Inhibition of electron flow through complex I of the mitochondrial respiratory chain of Ehrlich ascites carcinoma cells by methylglyoxal. *Biochem J* **303 (Pt 1):** 69-72

Reinke H, Saini C, Fleury-Olela F, Dibner C, Benjamin IJ, Schibler U (2008) Differential display of DNA-binding proteins reveals heat-shock factor 1 as a circadian transcription factor. *Genes Dev* **22**(3)**:** 331-345

Rizos H, Woodruff S, Kefford RF (2005) p14ARF interacts with the SUMO-conjugating enzyme Ubc9 and promotes the sumoylation of its binding partners. *Cell Cycle* **4**(4)**:** 597-603

Rondeau P, Singh NR, Caillens H, Tallet F, Bourdon E (2008) Oxidative stresses induced by glycoxidized human or bovine serum albumin on human monocytes. *Free Radic Biol Med* **45**(6)**:** 799-812

Rosca MG, Monnier VM, Szweda LI, Weiss MF (2002) Alterations in renal mitochondrial respiration in response to the reactive oxoaldehyde methylglyoxal. *Am J Physiol Renal Physiol* **283**(1)**:** F52-59

Rosca MG, Mustata TG, Kinter MT, Ozdemir AM, Kern TS, Szweda LI, Brownlee M, Monnier VM, Weiss MF (2005) Glycation of mitochondrial proteins from diabetic rat kidney is associated with excess superoxide formation. *Am J Physiol Renal Physiol* **289**(2)**:** F420-430

Rother KI (2007) Diabetes treatment--bridging the divide. *N Engl J Med* **356**(15)**:** 1499-1501

Rubin DM, Glickman MH, Larsen CN, Dhruvakumar S, Finley D (1998) Active site mutants in the six regulatory particle ATPases reveal multiple roles for ATP in the proteasome. *EMBO J* **17**(17)**:** 4909-4919

Safran M, Kaelin WG, Jr. (2003) HIF hydroxylation and the mammalian oxygen-sensing pathway. *J Clin Invest* **111**(6)**:** 779-783

Sakamoto H, Mashima T, Yamamoto K, Tsuruo T (2002) Modulation of heat-shock protein 27 (Hsp27) anti-apoptotic activity by methylglyoxal modification. *J Biol Chem* **277**(48)**:** 45770-45775

Salnikow K, Donald SP, Bruick RK, Zhitkovich A, Phang JM, Kasprzak KS (2004) Depletion of intracellular ascorbate by the carcinogenic metals nickel and cobalt results in the induction of hypoxic stress. *J Biol Chem* **279**(39)**:** 40337-40344

Sanchez-Elsner T, Botella LM, Velasco B, Langa C, Bernabeu C (2002) Endoglin expression is regulated by transcriptional cooperation between the hypoxia and transforming growth factor-beta pathways. *J Biol Chem* **277**(46)**:** 43799-43808

Sang N, Stiehl DP, Bohensky J, Leshchinsky I, Srinivas V, Caro J (2003) MAPK signaling up-regulates the activity of hypoxia-inducible factors by its effects on p300. *J Biol Chem* **278**(16)**:** 14013-14019

Sarkar K, Fox-Talbot K, Steenbergen C, Bosch-Marce M, Semenza GL (2009) Adenoviral transfer of HIF-1alpha enhances vascular responses to critical limb ischemia in diabetic mice. *Proc Natl Acad Sci U S A* **106**(44)**:** 18769-18774

Satish Kumar M, Mrudula T, Mitra N, Bhanuprakash Reddy G (2004) Enhanced degradation and decreased stability of eye lens alpha-crystallin upon methylglyoxal modification. *Exp Eye Res* **79**(4)**:** 577-583

Schalkwijk CG, Posthuma N, ten Brink HJ, ter Wee PM, Teerlink T (1999) Induction of 1,2-dicarbonyl compounds, intermediates in the formation of advanced glycation end-products, during heat-sterilization of glucose-based peritoneal dialysis fluids. *Perit Dial Int* **19**(4)**:** 325-333

Schalkwijk CG, van Bezu J, van der Schors RC, Uchida K, Stehouwer CD, van Hinsbergh VW (2006) Heat-shock protein 27 is a major methylglyoxal-modified protein in endothelial cells. *FEBS Lett* **580**(6)**:** 1565-1570

Scheufler C, Brinker A, Bourenkov G, Pegoraro S, Moroder L, Bartunik H, Hartl FU, Moarefi I (2000) Structure of TPR domain-peptide complexes: critical elements in the assembly of the Hsp70-Hsp90 multichaperone machine. *Cell* **101**(2)**:** 199-210

Schoenfeld A, Davidowitz EJ, Burk RD (1998) A second major native von Hippel-Lindau gene product, initiated from an internal translation start site, functions as a tumor suppressor. *Proc Natl Acad Sci U S A* **95**(15)**:** 8817-8822

Schofield CJ, Ratcliffe PJ (2005) Signalling hypoxia by HIF hydroxylases. *Biochem Biophys Res Commun* **338**(1)**:** 617-626

Schubert U, Anton LC, Gibbs J, Norbury CC, Yewdell JW, Bennink JR (2000) Rapid degradation of a large fraction of newly synthesized proteins by proteasomes. *Nature* **404**(6779)**:** 770-774

Selak MA, Armour SM, MacKenzie ED, Boulahbel H, Watson DG, Mansfield KD, Pan Y, Simon MC, Thompson CB, Gottlieb E (2005) Succinate links TCA cycle dysfunction to oncogenesis by inhibiting HIF-alpha prolyl hydroxylase. *Cancer Cell* **7**(1)**:** 77-85

Semenza GL (2009) Regulation of oxygen homeostasis by hypoxia-inducible factor 1. *Physiology (Bethesda)* **24:** 97-106

Semenza GL, Wang GL (1992) A nuclear factor induced by hypoxia via de novo protein synthesis binds to the human erythropoietin gene enhancer at a site required for transcriptional activation. *Mol Cell Biol* **12**(12)**:** 5447-5454

Seufert W, Jentsch S (1990) Ubiquitin-conjugating enzymes UBC4 and UBC5 mediate selective degradation of short-lived and abnormal proteins. *EMBO J* **9**(2)**:** 543-550

Shang F, Deng G, Liu Q, Guo W, Haas AL, Crosas B, Finley D, Taylor A (2005) Lys6-modified ubiquitin inhibits ubiquitin-dependent protein degradation. *J Biol Chem* **280**(21)**:** 20365-20374

Shimura H, Hattori N, Kubo S, Mizuno Y, Asakawa S, Minoshima S, Shimizu N, Iwai K, Chiba T, Tanaka K, Suzuki T (2000) Familial Parkinson disease gene product, parkin, is a ubiquitin-protein ligase. *Nat Genet* **25**(3)**:** 302-305

Shinohara M, Thornalley PJ, Giardino I, Beisswenger P, Thorpe SR, Onorato J, Brownlee M (1998) Overexpression of glyoxalase-I in bovine endothelial cells inhibits intracellular advanced glycation endproduct formation and prevents hyperglycemia-induced increases in macromolecular endocytosis. *J Clin Invest* **101**(5)**:** 1142-1147

Shoji T, Koyama H, Morioka T, Tanaka S, Kizu A, Motoyama K, Mori K, Fukumoto S, Shioi A, Shimogaito N, Takeuchi M, Yamamoto Y, Yonekura H, Yamamoto H, Nishizawa Y (2006) Receptor for advanced glycation end products is involved in impaired angiogenic response in diabetes. *Diabetes* **55**(8)**:** 2245-2255

Singh AK, Gudehithlu KP, Patri S, Litbarg NO, Sethupathi P, Arruda JA, Dunea G (2007) Impaired integration of endothelial progenitor cells in capillaries of diabetic wounds is reversible with vascular endothelial growth factor infusion. *Transl Res* **149**(5)**:** 282-291

Slomiany MG, Rosenzweig SA (2004) Autocrine effects of IGF-I-induced VEGF and IGFBP-3 secretion in retinal pigment epithelial cell line ARPE-19. *Am J Physiol Cell Physiol* **287**(3)**:** C746-753

Smulson ME, Pang D, Jung M, Dimtchev A, Chasovskikh S, Spoonde A, Simbulan-Rosenthal C, Rosenthal D, Yakovlev A, Dritschilo A (1998) Irreversible binding of poly(ADP)ribose polymerase cleavage product to DNA ends revealed by atomic force microscopy: possible role in apoptosis. *Cancer Res* **58**(16)**:** 3495-3498

Sohn SY, Kim SB, Kim J, Ahn BY (2006) Negative regulation of hepatitis B virus replication by cellular Hsp40/DnaJ proteins through destabilization of viral core and X proteins. *J Gen Virol* **87**(Pt 7)**:** 1883-1891

Soilleux EJ, Turley H, Tian YM, Pugh CW, Gatter KC, Harris AL (2005) Use of novel monoclonal antibodies to determine the expression and distribution of the hypoxia regulatory factors PHD-1, PHD-2, PHD-3 and FIH in normal and neoplastic human tissues. *Histopathology* **47**(6)**:** 602-610

Stebbins CE, Kaelin WG, Jr., Pavletich NP (1999) Structure of the VHL-ElonginC-ElonginB complex: implications for VHL tumor suppressor function. *Science* **284**(5413)**:** 455-461

Stevens VJ, Rouzer CA, Monnier VM, Cerami A (1978) Diabetic cataract formation: potential role of glycosylation of lens crystallins. *Proc Natl Acad Sci U S A* **75**(6)**:** 2918-2922

Stitt A, Gardiner TA, Alderson NL, Canning P, Frizzell N, Duffy N, Boyle C, Januszewski AS, Chachich M, Baynes JW, Thorpe SR (2002) The AGE inhibitor pyridoxamine inhibits development of retinopathy in experimental diabetes. *Diabetes* **51**(9)**:** 2826-2832

Stitt AW, McGoldrick C, Rice-McCaldin A, McCance DR, Glenn JV, Hsu DK, Liu FT, Thorpe SR, Gardiner TA (2005) Impaired retinal angiogenesis in diabetes: role of advanced glycation end products and galectin-3. *Diabetes* **54**(3)**:** 785-794

Sufan RI, Jewett MA, Ohh M (2004) The role of von Hippel-Lindau tumor suppressor protein and hypoxia in renal clear cell carcinoma. *Am J Physiol Renal Physiol* **287**(1)**:** F1-6

Swamy MS, Abraham EC (1987) Lens protein composition, glycation and high molecular weight aggregation in aging rats. *Invest Ophthalmol Vis Sci* **28**(10)**:** 1693-1701

Takeshita T, Wu W, Koike A, Fukuda M, Ohta T (2009) Perturbation of DNA repair pathways by proteasome inhibitors corresponds to enhanced chemosensitivity of cells to DNA damage-inducing agents. *Cancer Chemother Pharmacol* **64**(5)**:** 1039-1046

Tamarat R, Silvestre JS, Huijberts M, Benessiano J, Ebrahimian TG, Duriez M, Wautier MP, Wautier JL, Levy BI (2003) Blockade of advanced glycation end-product formation restores ischemia-induced angiogenesis in diabetic mice. *Proc Natl Acad Sci U S A* **100**(14)**:** 8555-8560

Tang TT, Lasky LA (2003) The forkhead transcription factor FOXO4 induces the down-regulation of hypoxia-inducible factor 1 alpha by a von Hippel-Lindau protein-independent mechanism. *J Biol Chem* **278**(32)**:** 30125-30135

Tazuke SI, Mazure NM, Sugawara J, Carland G, Faessen GH, Suen LF, Irwin JC, Powell DR, Giaccia AJ, Giudice LC (1998) Hypoxia stimulates insulin-like growth factor binding protein 1 (IGFBP-1) gene expression in HepG2 cells: a possible model for IGFBP-1 expression in fetal hypoxia. *Proc Natl Acad Sci U S A* **95**(17)**:** 10188-10193

Teixeira AS, Andrade SP (1999) Glucose-induced inhibition of angiogenesis in the rat sponge granuloma is prevented by aminoguanidine. *Life Sci* **64**(8)**:** 655-662

Thangarajah H, Yao D, Chang EI, Shi Y, Jazayeri L, Vial IN, Galiano RD, Du XL, Grogan R, Galvez MG, Januszyk M, Brownlee M, Gurtner GC (2009) The molecular basis for impaired hypoxia-induced VEGF expression in diabetic tissues. *Proc Natl Acad Sci U S A*

Thieme H, Aiello LP, Takagi H, Ferrara N, King GL (1995) Comparative analysis of vascular endothelial growth factor receptors on retinal and aortic vascular endothelial cells. *Diabetes* **44**(1)**:** 98-103

Thornalley PJ (1990) The glyoxalase system: new developments towards functional characterization of a metabolic pathway fundamental to biological life. *Biochem J* **269**(1)**:** 1-11

Thornalley PJ (2008) Protein and nucleotide damage by glyoxal and methylglyoxal in physiological systems--role in ageing and disease. *Drug Metabol Drug Interact* **23**(1-2)**:** 125-150

Thornalley PJ, Langborg A, Minhas HS (1999) Formation of glyoxal, methylglyoxal and 3-deoxyglucosone in the glycation of proteins by glucose. *Biochem J* **344 Pt 1:** 109-116

Thrash-Bingham CA, Tartof KD (1999) aHIF: a natural antisense transcript overexpressed in human renal cancer and during hypoxia. *J Natl Cancer Inst* **91**(2)**:** 143-151

Thrower JS, Hoffman L, Rechsteiner M, Pickart CM (2000) Recognition of the polyubiquitin proteolytic signal. *EMBO J* **19**(1)**:** 94-102

Tian J, Ishibashi K, Reiser K, Grebe R, Biswal S, Gehlbach P, Handa JT (2005) Advanced glycation endproduct-induced aging of the retinal pigment epithelium and choroid: a comprehensive transcriptional response. *Proc Natl Acad Sci U S A* **102**(33)**:** 11846-11851

Tuo QH, Zeng H, Stinnett A, Yu H, Aschner JL, Liao DF, Chen JX (2008) Critical role of angiopoietins/Tie-2 in hyperglycemic exacerbation of myocardial infarction and impaired angiogenesis. *Am J Physiol Heart Circ Physiol* **294**(6)**:** H2547-2557

Uchida T, Rossignol F, Matthay MA, Mounier R, Couette S, Clottes E, Clerici C (2004) Prolonged hypoxia differentially regulates hypoxia-inducible factor (HIF)-1alpha and HIF-2alpha expression in lung epithelial cells: implication of natural antisense HIF-1alpha. *J Biol Chem* **279**(15)**:** 14871-14878

Verheul HM, Pinedo HM (2007) Possible molecular mechanisms involved in the toxicity of angiogenesis inhibition. *Nat Rev Cancer* **7**(6)**:** 475-485

Vernace VA, Schmidt-Glenewinkel T, Figueiredo-Pereira ME (2007) Aging and regulated protein degradation: who has the UPPer hand? *Aging Cell* **6**(5)**:** 599-606

Voellmy R (2004) On mechanisms that control heat shock transcription factor activity in metazoan cells. *Cell Stress Chaperones* **9**(2)**:** 122-133

Waltenberger J (2001) Impaired collateral vessel development in diabetes: potential cellular mechanisms and therapeutic implications. *Cardiovasc Res* **49**(3)**:** 554-560

Wang GL, Jiang BH, Rue EA, Semenza GL (1995) Hypoxia-inducible factor 1 is a basic-helix-loop-helix-PAS heterodimer regulated by cellular O2 tension. *Proc Natl Acad Sci U S A* **92**(12)**:** 5510-5514

Wang GL, Semenza GL (1993) Desferrioxamine induces erythropoietin gene expression and hypoxia-inducible factor 1 DNA-binding activity: implications for models of hypoxia signal transduction. *Blood* **82**(12)**:** 3610-3615

Weidemann A, Johnson RS (2008) Biology of HIF-1alpha. *Cell Death Differ* **15**(4)**:** 621-627

Wickner S, Maurizi MR, Gottesman S (1999) Posttranslational quality control: folding, refolding, and degrading proteins. *Science* **286**(5446)**:** 1888-1893

Willam C, Maxwell PH, Nichols L, Lygate C, Tian YM, Bernhardt W, Wiesener M, Ratcliffe PJ, Eckardt KU, Pugh CW (2006) HIF prolyl hydroxylases in the rat; organ distribution and changes in expression following hypoxia and coronary artery ligation. *J Mol Cell Cardiol* **41**(1)**:** 68-77

Williams B, Gallacher B, Patel H, Orme C (1997) Glucose-induced protein kinase C activation regulates vascular permeability factor mRNA expression and peptide production by human vascular smooth muscle cells in vitro. *Diabetes* **46**(9)**:** 1497-1503

Williamson JR, Chang K, Frangos M, Hasan KS, Ido Y, Kawamura T, Nyengaard JR, van den Enden M, Kilo C, Tilton RG (1993) Hyperglycemic pseudohypoxia and diabetic complications. *Diabetes* **42**(6)**:** 801-813

Wirostko B, Wong TY, Simo R (2008) Vascular endothelial growth factor and diabetic complications. *Prog Retin Eye Res* **27**(6)**:** 608-621

Xiang J, Chao DT, Korsmeyer SJ (1996) BAX-induced cell death may not require interleukin 1 beta-converting enzyme-like proteases. *Proc Natl Acad Sci U S A* **93**(25)**:** 14559-14563

Xu W, Marcu M, Yuan X, Mimnaugh E, Patterson C, Neckers L (2002) Chaperone-dependent E3 ubiquitin ligase CHIP mediates a degradative pathway for c-ErbB2/Neu. *Proc Natl Acad Sci U S A* **99**(20)**:** 12847-12852

Yancopoulos GD, Davis S, Gale NW, Rudge JS, Wiegand SJ, Holash J (2000) Vascular-specific growth factors and blood vessel formation. *Nature* **407**(6801)**:** 242-248

Yao D, Taguchi T, Matsumura T, Pestell R, Edelstein D, Giardino I, Suske G, Rabbani N, Thornalley PJ, Sarthy VP, Hammes HP, Brownlee M (2007) High glucose increases angiopoietin-2 transcription in microvascular endothelial cells through methylglyoxal modification of mSin3A. *J Biol Chem* **282**(42)**:** 31038-31045

Yasinska IM, Sumbayev VV (2003) S-nitrosation of Cys-800 of HIF-1alpha protein activates its interaction with p300 and stimulates its transcriptional activity. *FEBS Lett* **549**(1-3)**:** 105-109

Yoon YS, Uchida S, Masuo O, Cejna M, Park JS, Gwon HC, Kirchmair R, Bahlman F, Walter D, Curry C, Hanley A, Isner JM, Losordo DW (2005) Progressive attenuation of myocardial vascular endothelial growth factor expression is a seminal event in diabetic cardiomyopathy: restoration of microvascular homeostasis and recovery of cardiac function in diabetic cardiomyopathy after replenishment of local vascular endothelial growth factor. *Circulation* **111**(16)**:** 2073-2085

Young JC, Moarefi I, Hartl FU (2001) Hsp90: a specialized but essential protein-folding tool. *J Cell Biol* **154**(2)**:** 267-273

Yu AY, Frid MG, Shimoda LA, Wiener CM, Stenmark K, Semenza GL (1998) Temporal, spatial, and oxygen-regulated expression of hypoxia-inducible factor-1 in the lung. *Am J Physiol* **275**(4 Pt 1)**:** L818-826

Yu DY, Cringle SJ (2005) Retinal degeneration and local oxygen metabolism. *Exp Eye Res* **80**(6)**:** 745-751

Yuan LW, Giordano A (2002) Acetyltransferase machinery conserved in p300/CBP-family proteins. *Oncogene* **21**(14)**:** 2253-2260

Yuan Y, Hilliard G, Ferguson T, Millhorn DE (2003) Cobalt inhibits the interaction between hypoxia-inducible factor-alpha and von Hippel-Lindau protein by direct binding to hypoxia-inducible factor-alpha. *J Biol Chem* **278**(18)**:** 15911-15916

Zagorska A, Dulak J (2004) HIF-1: the knowns and unknowns of hypoxia sensing. *Acta Biochim Pol* **51**(3)**:** 563-585

Zagzag D, Krishnamachary B, Yee H, Okuyama H, Chiriboga L, Ali MA, Melamed J, Semenza GL (2005) Stromal cell-derived factor-1alpha and CXCR4 expression in hemangioblastoma and clear cell-renal cell carcinoma: von Hippel-Lindau loss-of-function induces expression of a ligand and its receptor. *Cancer Res* **65**(14)**:** 6178-6188

Zhang M, Windheim M, Roe SM, Peggie M, Cohen P, Prodromou C, Pearl LH (2005) Chaperoned ubiquitylation--crystal structures of the CHIP U box E3 ubiquitin ligase and a CHIP-Ubc13-Uev1a complex. *Mol Cell* **20**(4)**:** 525-538

Zhang SX, Gozal D, Sachleben LR, Jr., Rane M, Klein JB, Gozal E (2003) Hypoxia induces an autocrine-paracrine survival pathway via platelet-derived growth factor (PDGF)-B/PDGF-beta receptor/phosphatidylinositol 3-kinase/Akt signaling in RN46A neuronal cells. *FASEB J* **17**(12)**:** 1709-1711